Title

Insights Into Reionization From the Large-Scale Statistics of Lyman-α Emission and Absorption

Author

Gangolli, Nakul

Publication Date

2025

Peer reviewed|Thesis/dissertation

UNIVERSITY OF CALIFORNIA
RIVERSIDE

Insights Into Reionization From the Large-Scale Statistics of Lyman-α Emission and Absorption

A Dissertation submitted in partial satisfaction
of the requirements for the degree of

Doctor of Philosophy

in

Physics

by

Nakul S. Gangolli

March 2025

Dissertation Committee:

Anson D'Aloisio, Chairperson
George D. Becker
Simeon Bird

The Dissertation of Nakul S. Gangolli is approved:

Committee Chairperson

University of California, Riverside

Acknowledgments

I am grateful to my advisor, Anson D'Aloisio, whose help and mentorship has helped me gain and hone skills which will forever help me in future endeavors. He gave me the fundamental advice and was there during hard times and was always willing to help and listen. I also want to thank George Becker and Simeon Bird for their help and advice throughout my PhD career. I also want to extend special thanks to my research group including Christopher Cain, Garett Lopez, Bayu Wilson, and Joshua Roth.

I would like to give thanks to my undergraduate advisor Eric Gawiser with who helped set the foundations for the research that I have done during my time at UC Riverside, and for his guidance in good research practices. I want to also thank all the friends that I made here at UCR, to those who are still here and who have long since left. You all made my time here enjoyable, especially keeping me company during the COVID epidemic. I would like to give special thanks to my Dungeons and Dragons group as well for allowing me to live not only in this world, but many others as well. I also similarly want to thank my Destiny 2 friends, especially Garett, for walking me through raids and dungeons.

This thesis is especially dedicated my parents Shridhar and Seema Gangolli, my brother Kunal, my girlfriend Erica Li and her family for giving me the motivation to reach for the stars.

ABSTRACT OF THE DISSERTATION

Insights Into Reionization From the Large-Scale Statistics of Lyman-α Emission and Absorption

by

Nakul S. Gangolli

Doctor of Philosophy, Graduate Program in Physics
University of California, Riverside, March 2025
Anson D'Aloisio, Chairperson

The Epoch of Reionization is the cosmological time period during which the gas in the inter-galactic medium (IGM) underwent its last major transition from cold and neutral to hot and highly ionized, driven by the first sources of hydrogen-ionizing photons. Over the past decade, cosmic microwave background (CMB) measurements, in combination with observations of the Lyman-α (Lyα) forest of high-redshift quasars, indicate that the bulk of reionization occurred between $z \approx 5 - 12$. Relatively little is known about the sources that drove this process. In this dissertation, I use cosmological simulations to explore how observations of Lyα emissions from high-redshift galaxies, as well as Lyα forest absorption, can be used to probe the nature of reionization and its sources. In Project 1, I explore large-scale statistics of Lyα emitters (LAEs) as a probe of reionization. Curiously, SILVERRUSH, a recent LAE survey using Hyper Suprime-Cam on the Subaru telescope, displays large-scale (~ 200 comoving Mpc) intra-field fluctuations in the observed surface densities of LAEs. The fluctuations are particularly prominent at redshift $z = 5.7$, an epoch when state-of-the-art models of reionization suggest that there might have been large

patches of neutral gas in cosmological voids. I explore the nature of these fluctuations, as well as the capabilities of different LAE spatial-clustering statistics, such as the two-point correlation function, void probability function, and peak overdensity function, to detect the presence of reionization's tail end in the observed spatial distribution of LAEs. In Project 2, I explore the correlation between LAE large-scale structure and the local Lyα forest opacity as measured along nearby quasar sightlines – termed the opacity-density relation. Recent observations suggest that both highly-opaque and highly-transmissive Lyα forest sight lines are associated with local under-densities in the galaxy distribution. The association of transmissive sight lines with under-densities is difficult to reconcile with some existing models of intergalactic fluctuations. I test the consistency of these results with new radiative transfer simulations of reionization, which provide detailed modeling of the intergalactic radiation, temperature, and ionization fluctuations. I also use these simulations to explore what the opacity-density relation can (and cannot) tell us about the reionization process and its sources.

Contents

List of Figures

List of Tables

Chapter 1

Chapter 1: Main Introduction

1.1 Background

The Epoch of Reionization is the time period during which the intergalactic medium (IGM) underwent its last major transition from neutral to highly ionized hydrogen. This process began when energetic photons from the first stars and galaxies started to ionize and heat the surrounding IGM. In the standard cosmological model, the first sources formed in the highest density peaks of the universe. It is thus believed that reionization started in the densest environments and propagated outward, completing in the voids of the galaxy distribution. Over the past decade, cosmic microwave background (CMB) measurements [640], in combination with observations of the Lyman-α (Lyα) forest of high-redshift quasars [252, 52, 79, 237, 56, e.g.], have greatly sharpened our understand of reionization's timeline. They indicate that the bulk of reionization occurred at redshifts $z \approx 5 - 12$. However, in spite of extensive observational and computational resources dedicated to understanding this process, large uncertainties still remain.

Among the most pressing uncertainties undercutting our understanding of reionization is the nature of the ionizing sources. The rate at which the sources emit ionizing photons into the IGM is quantified with the ionizing emissivity, $\dot{n}_{\rm ion}$, the number of ionizing photons per unit time, per unit volume. The emissivity is often parameterized as

$$\dot{n}_{\rm ion} = \rho_{\rm UV} \xi_{\rm ion} f_{\rm esc}^{\rm LyC}, \tag{1.1}$$

where $\rho_{\rm UV}$ is the non-ionizing ultraviolet (UV) luminosity density, $\xi_{\rm ion}$ is the ionizing photon production efficiency, and $f_{\rm esc}^{\rm LyC}$ is the fraction of Lyman continuum (LyC) photons that escape into the IGM. Previous measurements from ground-based and space-based telescopes have placed constraints on $\rho_{\rm UV}$, the *observed* rest-frame UV luminosity per unit volume in the Universe. With the advent of the James Webb Space Telescope (JWST), we have begun to probe the contribution of fainter galaxies to $\rho_{\rm UV}$, and out to higher redshift [82, 276, 526, 820, 230]. The standard cosmological model, however, predicts that most galaxies are significantly fainter than current detection limits. This makes a full direct census of ionizing sources impossible for the foreseeable future. The other quantities in equation (1.1), $\xi_{\rm ion}$ and $f_{\rm esc}^{\rm LyC}$, also pose formidable challenges. Both quantities are set by complex physical processes occurring at or below galaxy length scales, including (but not limited to) interstellar and circumgalactic gas distributions, star formation and its feedback processes, galactic outflows, and interstellar dust [134, 431, 491, 521, 845]. Compounding these difficulties is the fact that direct measurements of $f_{\rm esc}^{\rm LyC}$ in the reionization epoch are impossible because intergalactic gas absorbs 100% of the ionizing photons. Together, these uncertainties have prohibited our understanding of the ionizing sources that drove reionization.

Given the possibility that many of the ionizing sources will remain undetected for the foreseeable future, constraining the ionization state of the IGM and its spatial structure as a function of time is our most promising way to learn about the nature of the sources. For example, consider a scenario in which low-mass galaxies are the main drivers of reionization owing to their abundance, high star-formation rates, and possibly high escape fractions [273, 621]. In this case, the sources reside in less biased (less clustered) dark matter halos, which leads to the ionization field consisting of smaller and more numerous ionized bubbles at the beginning and middle of reionization. Toward the end of reionization, the last remaining patches of neutral gas – termed neutral islands – are more porous and more spread out within the cosmological voids. The spatial structure of the ionization field is often termed the "morphology" of reionization, a term I will use throughout this dissertation.

Now consider a contrasting scenario in which the *observed* galaxies, the UV-brightest in the population, are the drivers of reionization. This kind of model is motivated by some recent studies which note that UV-bright LAEs at lower redshift appear to be prodigious leakers of ionizing radiation [584, 583, 521, 519] (see however [144]). In this case, the sources reside in massive, highly biased halos, and the morphology of reionization is dominated by larger and more contiguous ionized bubbles. Similarly, the neutral islands near the end of reionization will be more contiguous and clustered toward the centers of the voids. (See e.g. [532, 106] for a detailed discussion of these effects on morphology.) The different source populations have their effect on the timing of reionization too. In the standard cosmological model, structure formation proceeds in a bottom-up manner with the smallest galaxies forming first. As a consequence, scenarios in which the ionizing photons are provided by the most massive galaxies, for example, result in a later reionization process, simply because it takes time for these galaxies to assemble. This discussion highlights how constraining reionization sheds light on the nature of the first ionizing sources in the Universe.

1.2 Lyα Observables

Lyα emission or absorption corresponds to electronic transitions in neutral hydrogen between the $2P$ and $1S$ states, with a rest-frame photon wavelength $\lambda = 1216\AA$. Lyα emission from gaseous nebulae in galaxies is associated with energetic phenomena such as hot gas, star formation, and young stellar populations. The utility of Lyα transitions for studying reionization has long been recognized owing to its resonant nature; even a small neutral gas fraction (e.g. $x_{\rm HI} \sim 10^{-4}$ at $z = 5.7$) can completely absorb the Lyα flux in a background source spectrum. Hence, the observation of Lyα photons is associated with highly ionized environments.

Galaxies with strong Lyα emission lines – termed Lyα emitters (LAEs) – are a useful empirical window into reionization because they probe the local ionization state of the IGM. The visibility of LAEs requires sufficiently large ionized bubbles that allow the Lyα line to redshift out of resonance with the neutral gas so that these photons can stream relatively freely through the IGM. The detection of high redshift galaxies by HST, and more recently with JWST, with observed Lyα emission at $z \gtrsim 7$ has been interpretted to imply that these galaxies reside in large ionized bubbles, among the earliest regions to reionize in the Universe [869, 818, 514, 819, 462, 247, 101, 169, 761]. Furthermore, multiple detections of LAEs with double-peaked Lyα emission lines such as COLA1, NEPLA-4, and A370p-z1, have been used to place lower limits on the sizes of the ionized bubbles hosting these galaxies. Other examples using the detection of Lyα emission from galaxies to constrain reionization include the declining observations of Lyman-break populations with Lyman-α flux above $z > 6$ [419, 686, 613, 632, 555, 689, 515, 394, 380], and the differential evolution of the bright and faint LAE populations at $z > 7$ [113, 112, 616, 615, 750, 367, 247]. Interpreting these observations, however, requires much care; the constraints on reionization rely heavily on assumptions about the highly uncertain strength and shape of the Lyα emission lines emerging from the galaxies, i.e. before they are absorbed by intergalactic hydrogen.

Another observational tool that has come to maturity over the past decade is the Lyα forest of high-z quasar spectra. Absorption features are imprinted in the continuum spectrum of a distant quasar blue-ward of the rest-frame Lyα emission line (as this part of the continuum will redshift into the Lyα resonance as the light travels through the expanding Universe). The absorption features of the forest constitute a record of the neutral hydrogen densities encountered along the line of sight, which encodes information about the extragalactic ionizing radiation background, the temperature of the IGM, and cosmological density fluctuations. Measurements of the mean absorption of the Lyα forest, its sightline-to-sightline variations [252, 52, 237, 79, 78, 842], and statistics of absorption gaps [866, 867], have been particularly transformative because they place strong constraints on the last phases of reionization. I will discuss this further in Chapter 3.

In this dissertation, I use cosmological simulations to explore how observations of Lyα emission and absorption can be used to probe the nature of reionization and its sources. In Chapter 2, I explore large-scale statistics of LAEs as a probe of reionization. Curiously, SILVERRUSH, a recent LAE survey using Hyper Suprime-Cam on the Subaru telecope, displays large-scale ($\sim$ 200 comoving Mpc) intra-field fluctuations in the observed surface densities of LAEs [619, 719, 449, 394]. The fluctuations are particularly prominent at redshift $z = 5.7$, an epoch when state-of-the-art models of reionization suggest that there might have been large patches of neutral gas in cosmological voids. I explore the nature of these fluctuations, as well as the capabilities of different LAE spatial-clustering statistics, such as the two-point correlation function, void probability function, and peak overdensity function, to detect the presence of reionization's tail end in the observed spatial distribution of LAEs. In Chapter 3, I explore the correlation between LAE large-scale structure and the local Lyα forest opacity as measured along nearby quasar sightlines – termed the opacity-density relation. Recent observations suggest that both highly-opaque and highly-transmissive Lyα forest sight lines are associated with local under-densities in the galaxy distribution [57, 143, 142]. The association between transmissive sight lines and under-densities is hard to reconcile with some existing models of intergalactic fluctuations. I test the consistency of these results with new radiative transfer simulations of reionization, which provide detailed modeling of the intergalactic radiation, temperature, and ionization fluctuations. I also use these simulations to explore what the opacity-density relation can (and cannot) tell us about the reionization process and its sources. I offer concluding remarks in Chapter 4.

Unless otherwise stated, the simulations run for this dissertation adopt a standard flat ΛCDM cosmology with $\Omega_M = 0.305$, $\Omega_\Lambda = 1 - \Omega_M$, $\Omega_b = 0.048$, $H_0 = 100h$ km/s/Mpc, with $h = 0.68$. The simulations are initialized with a linear matter power spectrum with $\sigma_8 = 0.82$ and $n_s = 0.9667$. All distances are quoted in comoving units unless otherwise noted.

Chapter 2

Chapter 2: Constraining Reionization in Progress at z = 5.7 with LAEs: Voids, Peaks, and Cosmic Variance

2.1 Introduction

As stated in Chapter 1, observational measurements of the Lyα forest have narrowed the range of viable reionization models to those that end around $z = 5{-}5.5$. This timing is consistent with transmission measurements of the Lyα and Lyβ forests [253, 525, 812], as well as evidence of quasar damping wings in $z > 7$ quasars [577, 201, 811]. Additionally, at $z \gtrsim 5.5$, the Lyα forest exhibits large scatter in its transmission averaged over long path lengths, epitomized by the $110h^{-1}$ comoving Mpc Lyα trough reported by [52] (see also [253, 79, 237]). Some models proposed to explain this scatter place the end of reionization as late as $z = 5$ [454, 589, 426]. Although a broadly consistent picture of late reionization has emerged from all of these observations, the reionization history in detail as well as its sources remain unknown.

LAEs have long been an important probe of the EoR owing to the resonant nature of the Lyα line to neutral gas. Visible LAEs indicate the presence of ionized gas within the IGM because even small densities of neutral hydrogen nearby can attenuate LAEs significantly. Hence the observations of these galaxies indicate the presence of highly ionized gas in the localized regions in which they are observed. Given sufficiently large survey area and a statistical sample of galaxies, the angular two point correlation function (2PCF) is considered a robust probe of reionization.

One of the central questions motivating this Chapter is whether the 2PCF is the most sensitive statistic for constraining reionization during its final stages. As in Chapter 1, there is mounting evidence that existing LAE samples at $z \sim 7$ are probing deep into reionization. Even the most densely sampled data at $z = 5.7$ may be probing the tail end of reionization [589, 426]. Radiative transfer simulations indicate that neutral gas becomes increasingly relegated to the voids in the source distribution when the global neutral fraction drops below 50% [231, 454, 316, 829, e.g.]. We therefore expect LAEs located in voids to be preferentially obscured by neutral islands during the last stages of reionization. Motivated by this expectation, we reexamine the use of LAE void statistics for constraining reionization, with an eye towards recent models that place the neutral fraction at $\sim 10\%$ at $z = 5.7$. We also explore peaks in the LAE distribution as a complementary method for quantifying reionization's effect on the apparent clustering of LAEs.

LAE void statistics in the context of reionization were considered by [531]. The current Chapter adds to previous work in three ways: (1) Whereas the simulations in [531] concluded reionization well before $z = 5.7$, we focus explicitly on the possibility of constraining models in which reionization was still ongoing at $z = 5.7$. This updates previous studies with the most recent empirical developments and may be of particular interest because LAE samples are currently largest at $z = 5.7$; (2) We employ simulation volumes of $(1\ \mathrm{Gpc}/h)^3$, a factor of ≈ 470 bigger than the largest in [531], to model reionization and the LAE population. This allows us to develop statistically representative models of narrow band surveys whose individual fields of view often are comparable to, or larger than, the simulation box sizes of previous studies. The SILVERRUSH fields are striking visually because they exhibit significant field-to-field variation in surface density, as well as clear asymmetries in the LAE distribution over enormous scales ($\sim 200\ \mathrm{Mpc}/h$). Some fields are pocketed with highly-clustered regions and nearly empty holes. We exploit our large simulation volumes to address additionally whether the observed features are consistent with expected cosmic variance from large-scale structure, or whether they may be indicative of some other source of variance; (3) We contrast the constraining power of voids and peak statistics with that of the 2PCF. We will find that voids provide a more sensitive test of models than the 2PCF during the late stages of reionization.

The remainder of Chapter 2 is outlined as follows. In §2.2 we summarize our simulation methods. In §2.2.3 we describe how we derive our simulated fields, and in §3.4

we present our main results. In §3.6 we conclude.

2.2 Simulation Methodology

The visibility of LAEs is set by physical processes spanning an enormous dynamic range, from hundreds of Mpc/h to sub-galactic scales. In addition, narrow band survey fields of view span (∼hundreds of Mpc)^2. Our multi-scale approach attempts to bridge the scale gap by using several cosmological simulations in tandem. In this section we describe each component of our models.

2.2.1 The underlying LAE population

The basis for our mock LAE catalogs is the publicly available halo catalogs from the Multi-Dark Simulation (MDPL) of [434], which affords us a 1 (h^{-1} Gpc)^3 volume. The MDPL simulation is a dark-matter-only N-body simulation that was run with a modified version of the GADGET-2 code [745] using $N = 3840^3$ particles, which corresponds to a particle mass of $1.51 \times 10^9 h^{-1}$ M$_\odot$. We used the friends-of-friends (FoF) halo catalogs provided by the `CosmoSim` database[1]. The minimum halo mass in these catalogs is $M_{\rm min} = 3 \times 10^{10} h^{-1}$ M$_\odot$.

To populate the MDPL halos with galaxies, we applied an abundance matching scheme that equates the cumulative number density of halos with the integrated rest-frame UV luminosity functions of [83] (see also [275]). Following [817], we model the duty cycle of these galaxies with the method of [780]. The duty cycle is parameterized by a star formation time-scale Δt, which we take to be one of the free parameters in our models. Smaller values

[1]`https://www.cosmosim.org/`

of Δt result in UV luminous galaxies being assigned to less massive halos. In what follows, we adopt $\Delta t = 50$ Myr as our fiducial value. In §2.3 we show that this choice provides a reasonable match to statistics of the observed LAE population.

Given UV luminosities, the Lyα rest-frame equivalent widths (REWs) of galaxies were drawn randomly from the empirically calibrated model distribution of [226]. Scatterings of Lyα photons by the interstellar gas results in a complex frequency structure for the Lyα line as it emerges from source galaxies. We do not attempt to model these physical processes in detail here. Instead we assume that the structure of the line blue-ward of systemic is completely absorbed by the IGM – a good approximation at the high redshifts of interest, in most cases [378, 520, 740, see however]. We model the red-ward side with a Gaussian profile characterized by a velocity offset, Δv, and width σ_v. We set $\Delta v = \beta v_{\rm circ}$, where $v_{\rm circ}$ is the circular velocity of the halo at its boundary[2], and β is a free parameter in our model [817, e.g.]. Following [515], we fix σ_v by setting the full-width half-maximum of the Gaussian equal to $v_{\rm circ}$. These choices are motivated by radiative transfer calculations of the Lyα line structure emerging from simple models of the ISM in star-forming galaxies [864].

2.2.2 Opacity of the IGM

The attenuation of Lyα emission lines by intergalactic hydrogen comes from two sources: (1) The neutral hydrogen in yet-to-be reionized gas; (2) Self-shielding regions and residual neutral hydrogen within ionized bubbles. Sections 2.2.2 and 2.2.2, respectively, describe how we model these.

[2]Here, the "radius" of an FoF halo is defined to be that of a sphere with equal volume.

Reionization simulations

We modeled the distribution of neutral hydrogen during reionization with a numerical implementation of the excursion-set model of reionization (ESMR; [292, 559]). Following previous implementations [852, see e.g.], we smoothed the MDPL halo field onto a grid with dimension $N = 512^3$ to obtain the collapsed fraction field, $f_{\rm coll}(\mathbf{r})$. The latter was then smoothed over a hierarchy of scales with a top-hat filter in Fourier space. Cells were marked as ionized when the condition $\zeta f_{\rm coll}(\mathbf{r}) \geq 1$ was satisfied, where ζ is a free parameter quantifying the efficiency at which the sources deliver ionizing photons to the IGM. As we describe in §2.3, we adjusted ζ to obtain different global ionized fractions at $z = 5.7$ and $z = 6.6$.

It is important to account for the enhancement of the ionizing ultraviolet background (UVB) intensity around bright and/or clustered LAEs. We modelled spatial fluctuations in the UVB with a simple attenuation model, separately from the ESMR reionization simulations. We computed the hydrogen photoionization rate, $\Gamma_{\rm HI}$, on a uniform grid with $N = 512^3$ cells assuming that each source at location $\vec{x}_j$ makes a contribution $\propto L_{912} \exp(-|\vec{x}_i - \vec{x}_j|/\lambda_{912}^{\rm mfp})/|\vec{x}_i - \vec{x}_j|^2$ to the cell at $\vec{x}_i$, where L_{912} is the source's specific luminosity at 912 Å, and $\lambda_{912}^{\rm mfp}$ is the mean free path. For simplicity we adopt a uniform $\lambda_{912}^{\rm mfp} = 30(15)h^{-1}$ Mpc at $z = 5.7(6.6)$, which is motivated by extrapolating the observational measurements of [827] at $z \lesssim 5.2$. Assuming a constant $\lambda_{912}^{\rm mfp}$ affords us the ability to compute $\Gamma_{\rm HI}$ fields efficiently using Fast Fourier Transforms, at the expense of neglecting potentially large spatial variations in $\lambda_{912}^{\rm mfp}$ at these redshifts [199, 187]. Small local values of $\lambda_{912}^{\rm mfp}$ – for example, in cosmic voids with a dearth of sources – leads to more attenuation of the local LAE population by self-shielding systems [72, 675], introducing another source of fluctuation in the LAE distribution. Another effect that our method misses is the shadowing of the UVB which leads to a suppression of $\Gamma_{\rm HI}$ in the vicinity of neutral hydrogen [589].

Absorptions within ionized bubbles

Even within an ionized bubble, residual neutral hydrogen in the cosmic web can contribute significantly to the attenuation of Lyα emission [72, 555, e.g.]. We model this component of the opacity using one-dimensional skewers extracted from an Eulerian cosmological hydrodynamics simulation run with a modified version of the code of [777]. The details of our code implementation have been described elsewhere [187, 589]. Here we summarize the salient points (including updates) for the current Chapter.

Our simulation used a periodic box with side length $L_{\rm box} = 20h^{-1}$ Mpc, and 2×2048^3 gas and dark matter resolution elements. The simulation was initiailzed at $z = 300$ using first-order perturbation theory and transfer functions from the CAMB software [468]. The gas was flash ionized at redshift $z_{\rm reion} = 8.5$ by a uniform ionizing radiation background with specific intensity $J_\nu \propto \nu^{-1.5}$ (where ν is frequency) between $1 - 4$ Ry. At this time the gas was also impulsively heated to $T = 20,000$ K. The normalization of the UVB was fixed to give a global mean hydrogen photoionization rate of $\Gamma_{\rm HI} = 10^{-13}$ s^{-1}. However, to incorporate spatial fluctuations in the UVB, we re-scaled $\Gamma_{\rm HI}$ in post-processing along the skewers using the UVB models from the last section. To model self-shielding in over-dense regions, we implemented the model of [651] with parameters updated by [123]. We traced

20,000 skewers at random angles from halos[3] with masses $M \geq 10^{10}$ $M_\odot$. As we describe in the next section, we used the gas data from these skewers to model attenuation of the Lyα line by self-shielding regions along the sight lines to LAEs.

2.2.3 Construction of Mock Surveys

We piece together all the elements described above to construct mock LAE catalogs. The first step is to create $1,000$ mock fields of view (FoVs) by taking randomly located and oriented sub-volumes of the MDPL simulation – utilizing the periodic boundary conditions. Our sub-volumes have widths of 180(200) h^{-1}Mpc at $z = 5.7(6.6)$, and depths of 29 h^{-1} Mpc. The widths correspond approximately to the average FoV scale of SILVER-RUSH, and the depths represent the selection windows of the NB816 (NB921) filters [619]. We then populate the halos in these sub-volumes with LAEs using the method outlined in §2.2.1. This step produces the "intrinsic" LAE population.

The next step is to attenuate Lyα luminosities and REWs by applying the opacity of the IGM redward of systematic Lyα. We trace skewers of length 150 h^{-1}Mpc from each LAE along the line of sight. The skewers consist of uniform grid points at the resolution of the hydrodynamics simulation, $\Delta x = 9.77$ h^{-1}kpc, or $\Delta v = 1.41(1.50)$ km/s at $z = 5.7(6.6)$. Gas properties are assigned to these skewers from randomly chosen skewers through the hydrodynamics simulation. Our ESMR simulations provide the morphology of the neutral gas around the LAEs. For a given reionization model, wherever a skewer intersected neutral regions in the corresponding ESMR field, the neutral fraction of the gas was set to unity.

[3] Halos were identified with a spherical-overdensity criterion in which the mass enclosed is $M_{200} = 200\bar{\rho}_m(4\pi/3)R_{200}^3$, where $\bar{\rho}_m$ is the cosmic mean matter density and R_{200} is the radius within which the mean matter density is $200\bar{\rho}_m$.

We emphasize that the ESMR fields and the LAEs share the same underlying density field (from the MDPL box), but the $L = 20\ h^{-1}$Mpc hydrodynamics simulation does not. Similar multi-scale approaches have been employed by [555] and [201].

By integrating along the line of sight, we compute the IGM transmission fraction redward of systemic,

$$T^{\rm IGM}_{\rm Ly\alpha} = \frac{\int d\nu J(\nu) e^{-\tau(\nu)}}{\int d\nu J(\nu)}, \tag{2.1}$$

where $J(\nu)$ is the line profile normalized to intergrate to unity, and $\tau(\nu)$ is the opacity including contributions from the ionized and fully neutral regions [555, 817]. After attenuating the LAEs, we apply cuts on the Lyα luminosity ($L_{\rm Ly\alpha}$) and REW. Unless specified otherwise, we select $L_{\rm Ly\alpha} > 6.3 \times 10^{42}$ (7.9×10^{42}) ergs/s and REW $> 10(14)$ Å at $z = 5.7(6.6)$. These cuts from [817] approximate those employed by SILVERRUSH, though we note that different sample cuts are applied in the SILVERRUSH analyses depending on the application. We also note that different SILVERRUSH fields have different limiting depths.

The end result of this process is a sample of 1,000 mock survey FoVs with properties similar to the SILVERRUSH fields. We will use these mocks to explore the effect of reionization on various LAE statistics in §2.4.

2.3 Models

A summary of parameters for each of our models is provided in Table 2.1. We generated mock LAE populations for three global neutral fractions ($\bar{x}_{\rm HI}$) at $z = 5.7$, and three at $z = 6.6$. Since the neutral fraction is the key distinction between our models, we

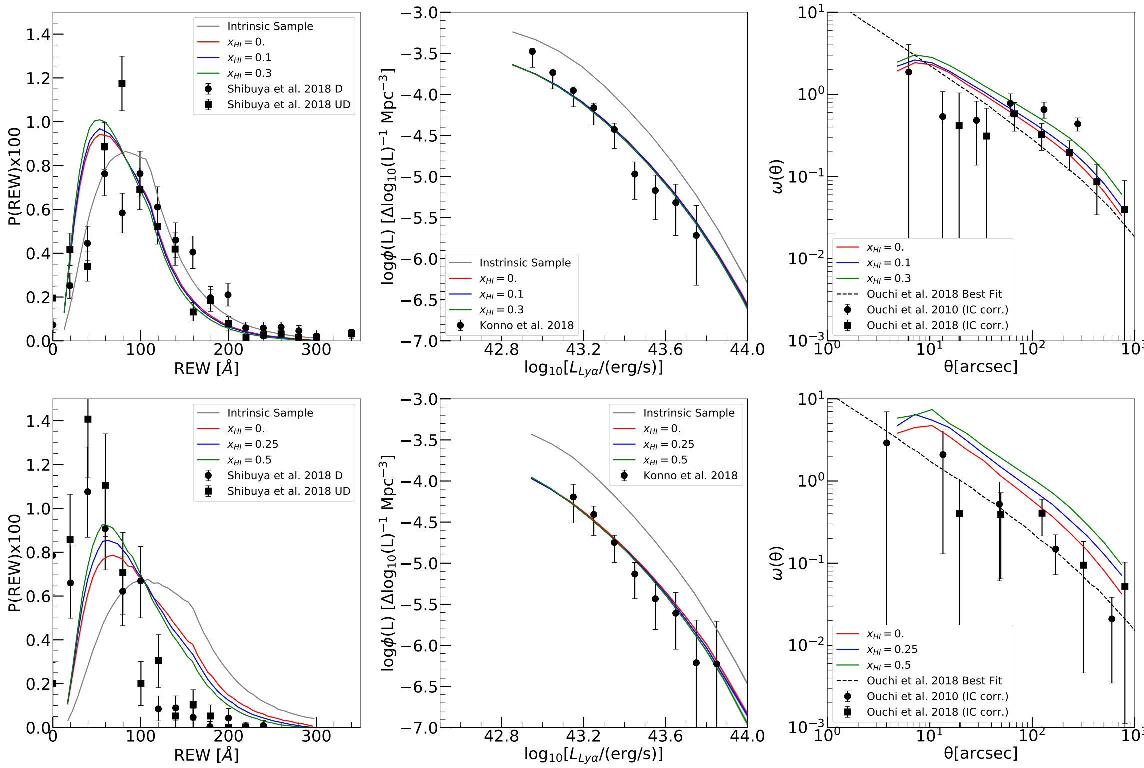

Figure 2.1: Comparison of our models to recent observational measurements. The left, middle, and right columns correspond to the REW distribution, Lyα luminosity function, and angular two-point correlation function, respectively. The top and bottom rows show results for $z = 5.7$ and 6.6, respectively. Our models are distinguished by the mean neutral fraction of the IGM, as indicated in the plot legends. In the left and middle panels, the light gray curves correspond to the "intrinsic" LAE population, before any attenuation from the IGM/neutral regions is applied. In the right panels, the dashed curves show the best fit power-law models of [619]. In the left panel legends, "D" and "UD" denote the Deep and the Ultra-Deep fields, respectively. Our models parameters have been tuned to provide reasonable agreement with these observations. In §2.4, we use these models to explore the efficacy of void and peak statistics for constraining reionization.

z	$\bar{x}_{\rm HI}$	β	$\lambda^{\rm mfp}_{912\mathring{A}}$ [cMpc/h]	$\langle\Gamma_{\rm HI}\rangle$ [$\times10^{-12}$ s^{-1}]	Δt [Myr]	$\langle\Sigma\rangle$ [deg^{-2}]
5.7	0.0	1.2	30	0.37	50	72
	0.1	1.25	30	0.50	50	72
	0.3	1.4	30	0.74	50	71
6.6	0.0	1.2	15	0.37	50	32
	0.25	1.4	15	0.50	50	32
	0.5	1.8	15	0.74	50	32

Table 2.1: Summary of our model parameters. Columns 2-6 list the five free parameters in our models. The last column shows the resulting mean LAE surface densities, $\langle\Sigma\rangle$, which have been tuned to match (approximately) the observed values in SILVERRUSH. Here, $\bar{x}_{\rm HI}$ is the mean neutral fraction of the IGM, β is the proportionality constant between halo circular velocity and Lyα line offset, $\lambda^{\rm mfp}_{912\mathring{A}}$ is the mean free path in ionized regions, $\langle\Gamma_{\rm HI}\rangle$ is the mean hydrogen photoionization rate in ionized regions, and Δt is the duty cycle star formation timescale.

will label them with $\bar{x}_{\rm HI}$ hereafter. The values of $\bar{x}_{\rm HI}$ are loosely motivated by the "late" and "early" reionization scenarios considered in [589]. We note that a neutral fraction of $\bar{x}_{\rm HI} = 0.3$ at $z = 5.7$ is in mild tension with the Lyα forest dark pixel constraints of [525]. One of the main motivations of this Chapter is to explore whether LAE measurements could provide a complementary test of such a model.

The other parameters were fixed by matching to observational constraints provided by SILVERRUSH and quasar absorption spectra measurements. To fix the LAE parameters, we considered the mean LAE surface density, REW distribution, Lyα luminosity function, and 2PCF. Most importantly for the ensuing discussions, at a given redshift, all of our models were calibrated to have approximately the same mean LAE surface density, as shown in the last column of Table 2.1. To achieve this, we adjusted the proportionality between halo circular velocity and line offset (β) to match our models approximately to SILVERRUSH surface densities. Our model surface densities are closest to those of the

"Homogeneous sample" described in [619].[4] We found that a reasonable match could be obtained for all the other LAE constraints by fixing the duty cycle to $\Delta t = 50$ Myr.

The mean ionizing intensity in our fluctuating UVB models (§2.2.2) were calibrated by Lyα forest measurements where available. At $z = 5.7$, we constructed synthetic Lyα forest sight lines through our simulations and rescaled the intensity, assuming photoionization equilibrium, to match the mean flux measurement of [79]. Currently, forest segments at $z = 6.6$ are too saturated and sparse to provide a reliable estimate of the mean flux. For simplicity, we held the mean intensities fixed with redshift between the $x_{\rm HI} = 0$ models, the $x_{\rm HI} = 0.1$ and 0.25 models, and the $x_{\rm HI} = 0.3$ and 0.5 models. This can be seen in the mean hydrogen photoionization rates in ionized regions provided in Table 2.1. We tested models in which $\langle \Gamma_{\rm HI} \rangle$ is a factor of 5 lower at $z = 6.6$ than at $z = 5.7$. We found that $\langle \Gamma_{\rm HI} \rangle$ is almost completely degenerate with β, motivating our choice to hold the former fixed with redshift. The mean free path through ionized gas, $\lambda_{912}^{\rm mfp}$, is another key parameter in our UVB model. We fixed this parameter by extrapolating to higher redshift the empirical fit of [827]. We note that $\lambda^{\rm mfp}$ during reionization could be considerably shorter than the values adopted here owing to the potentially lower $\Gamma_{\rm HI}$ as well as relaxation effects [191].

Figure 2.1 shows that our models are in reasonable agreement with measurements of the REW distribution (left), luminosity function (middle), and 2PCF (right) from SILVERRUSH observations. The top and bottom rows correspond to $z = 5.7$ and 6.6, respectively. In all top (bottom) panels, the red, blue, and green curves respectively correspond to $\bar{x}_{\rm HI} = 0.0$ (0.0), 0.1 (0.25), and 0.3 (0.5). Additionally, the grey curves show the intrinsic

[4] For reference, the Homogeneous sample from [619] has surface densities of 70 and 41 deg^{-2} at $z = 5.7$ and 6.6, respectively.

statistics before attenuation by the IGM. For comparison, the data points show some of the most recent observational measurements. IGM opacity acts to skew the REW distribution toward lower values. It also changes the normalization and shape of the luminosity function, and increases the observed clustering of LAEs. These trends are consistent with previous findings [531, 401, 817, e.g.]. Similar to the results of [817], our 2PCFs exhibit more clustering compared to the SILVERRUSH measurements at $z = 6.6$. This may owe to the relatively massive halos that our LAEs inhabit. Our models have $M_{\rm min} = 3 \times 10^{10}\ h^{-1}$ $M_\odot$ and an average mass of $\langle M \rangle = 1.5 \times 10^{11}\ h^{-1} M_\odot$. In contrast, SILVERRUSH reports $M_{\rm min} \sim 2.1 \times 10^{9} (8.8 \times 10^{8})\ h^{-1} M_\odot$, and average masses of $\sim 8.7 \times 10^{10} (4.4 \times 10^{10})\ h^{-1} M_\odot$ at z=5.7(6.6) [619]. These masses were derived by applying the halo occupation distribution (HOD) modelling of [355] to the measured 2PCF. Another effect at play could be the lower surface densities in our models compared to the Homogenous sample used to measure the 2PCF.

Figures 2.2 and 2.3 show mock survey fields of size $(500 h^{-1}{\rm Mpc})^2$ at $z = 5.7$ and 6.6, respectively. For all panels we impose the survey cuts described in §2.2.3. The top-left panels show the intrinsic distribution of LAEs in the slices, i.e. without attenuation by the IGM. The subsequent plots (moving clockwise) correspond to increasing global neutral fractions, where the shading shows the projected neutral gas density. The different dot-colors correspond to Lyα magnitude bins, as denoted in the plot legends. In the latter half of reionization, the neutral gas is increasingly confined to voids in the LAE distribution. This gas attenuates the Lyα lines of background LAEs, obscuring some of them from view. Importantly, because we fix the surface density of LAEs to be approximately the same between our models, these missing LAEs are compensated by an increased density of LAEs in the ionized regions. This effect contributes to the enhanced clustering seen in the 2PCFs (Fig. 2.1), and we will see its consequences for peak statistics later in this Chapter.

2.4 Results

2.4.1 Cosmic Variance

We begin with a broad comparison of our simulated ensembles to the SILVERRUSH fields. We have applied homogeneous luminosity and color cuts to the publicly available SILVERRUSH catalogs (see text in §2.4.1). The LAE surface density of each field is reported in Table 2.2. The data exhibits significant field-to-field variation. At $z = 5.7$, D-ELAISN1 has a surface density of just ≈ 31 deg^{-2}, whereas UD-SXDS is a factor of 3 denser with ≈ 98 deg^{-2}. Additionally, some fields, such as D-ELAISN1 at z=5.7 and D-DEEP2-3 at z=6.6, show conspicuous asymmetries over $\sim 200\ h^{-1}$Mpc scales (see e.g. Figs. 4 and 5 of [619]). Some regions remain largely empty of LAEs, while others contain significant over-densities. In this section, we explore whether the observed variations are consistent with expectations from large-scale structure formation alone, or if some other source of variance is required. We also quantify the contribution of reionization to the expected cosmic variance.

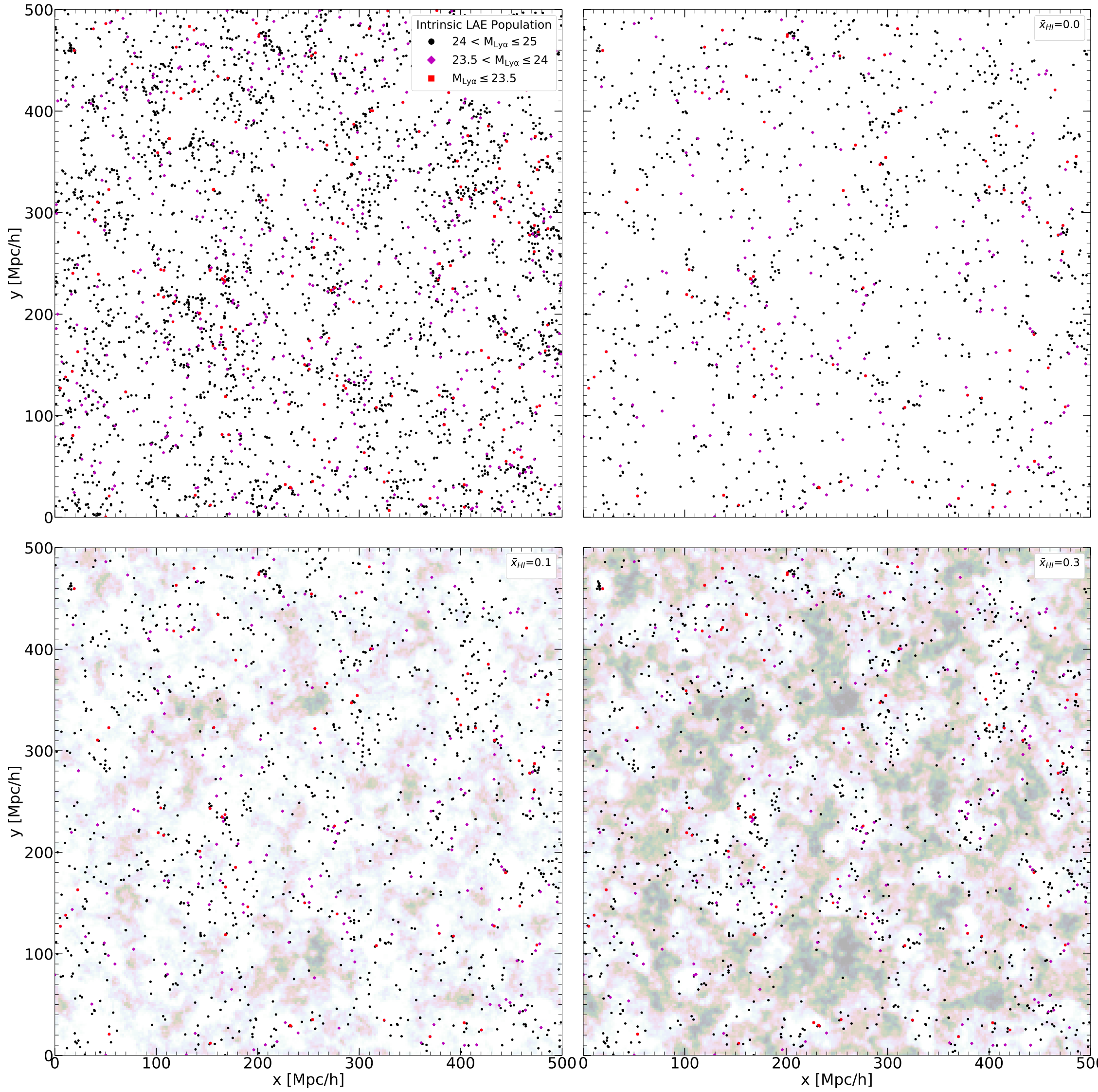

Figure 2.2: Example 500×500 $(h^{-1}\text{Mpc})^2$ slices through our simulated LAE distributions at $z = 5.7$. The different dot-colors correspond to the Lyα apparent narrow-band magnitude ($M_{\text{Ly}\alpha}$) ranges shown in the top-left panel. The top-left panel shows the intrinsic LAE sample before any attenuation by the IGM is applied. The remaining panels correspond to our models with $\bar{x}_{\text{HI}} = 0.0$ (top-right), $\bar{x}_{\text{HI}} = 0.1$ (bottom-left), and $\bar{x}_{\text{HI}} = 0.3$ (bottom-right). The shading shows the integrated neutral fraction along the line of sight, which is 30 h^{-1}Mpc deep. Darker shades indicate regions with higher neutral fractions. These three panels have approximately the same mean LAE surface density, $\langle\Sigma\rangle \approx 72$ (deg)$^{-2}$. At fixed $\langle\Sigma\rangle$, a higher neutral fraction obscures LAEs in the voids, but these must be compensated by more visible LAEs elsewhere. Hence the presence of neutral gas leads to more apparent clustering of the LAEs. Notably, the neutral gas is relegated to the voids in the tail end of reionization, suggesting that LAE void statistics may provide an informative test of models in this regime.

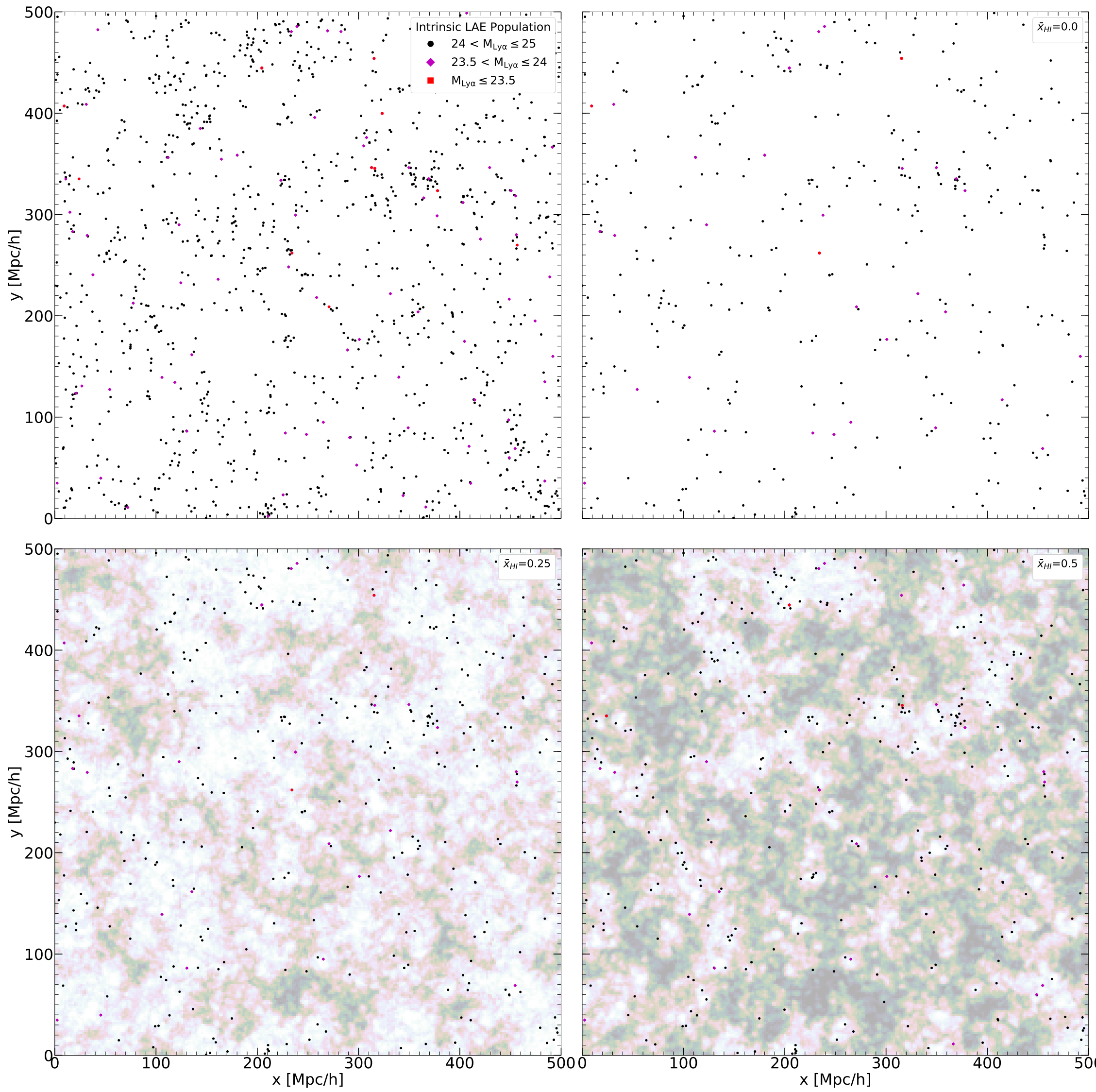

Figure 2.3: Same as Figure 2.2, except at $z = 6.6$. The top-right ($\bar{x}_{\rm HI} = 0.0$), bottom-left ($\bar{x}_{\rm HI} = 0.25$), and bottom-right ($\bar{x}_{\rm HI} = 0.5$) panels have a fixed $\langle\Sigma\rangle \approx 32$ (deg)$^{-2}$.

LAE Surface Density

In Figure 2.4 we show the LAE surface density distributions in our reionization models. The top and bottom panels correspond to $z = 5.7$ and $z = 6.6$, respectively. The red, blue and green histograms represent different neutral fractions, as denoted in the plot legends. For each model, the distributions consist of $1,000$ mock FoVs. To facilitate comparisons with the observations, we have matched the sizes of our fields to the mean sizes of the SILVERRUSH fields (see §2.2.3). This is not ideal because the SILVERRUSH fields vary in size, from 2-6 square degrees [719, ?]. However, we will find that the observed cosmic variance can be reproduced reasonably with our simplistic approach. To remove the effect of small differences in the mean surface densities in our models, we plot the surface density contrast, $\delta = (\Sigma - \langle\Sigma\rangle)/\langle\Sigma\rangle$, where $\langle\Sigma\rangle$ is the average surface density. Figure 2.4 shows that reionization increases the cosmic variance in δ quite subtly. For reference, the standard deviations of δ between our models are 0.14(0.20), 0.15(0.23), and 0.17(0.25) for neutral fractions of $\bar{x}_{\rm HI} = 0.0(0.0)$, 0.1(0.25), and 0.3(0.5) at $z = 5.7(6.6)$, respectively.

The black vertical lines in Figure 2.4 illustrate the cosmic variance in the SILVERRUSH data. Each line is annotated with its respective field name (see Table 2.2). The luminosity and color cuts applied in the published SILVERRUSH analyses vary, depending on the application. Hence, we downloaded the public SILVERRUSH catalogs[5] and applied our own cuts with the goal of matching our simulated catalogs to the extent possible. Specifically, at $z = 5.7$, we selected Lyα luminosities $> 6.3 \times 10^{42}$ erg/s and applied a color cut of $i-$NB816 > 1.2. This yields $\langle\Sigma\rangle = 72$ deg^{-2}, in agreement with our models (see Table

[5] `http://cos.icrr.u-tokyo.ac.jp/rush.html`

2.1). At $z = 6.6$, we used $> 1.41 \times 10^{43}$ erg/s and $z-$NB921> 1.8. The higher luminosity limit adopted for $z = 6.6$ ensures that a homogeneous cut can be applied across all fields in the public SILVERRUSH data. Note that this limit is much higher than in our fiducial $z = 6.6$ catalog used throughout the rest of this Chapter, and results in our models having $\langle\Sigma\rangle = 9.5$ deg^{-2} at $z = 6.6$. The color cuts, which are from [**?**], roughly match the REW cuts applied to our simulated catalogs. For comparison, the red/dashed vertical lines show the 2σ limits of the model distributions with $\bar{x}_{\rm HI} = 0$. (The 2σ limits for the other models are similar.)

We find that the observed field-to-field variation is almost entirely consistent with expectations from large scale structure alone, and that reionization is unlikely to play a significant role in increasing this variation. At $z = 5.7$, our models, however, cannot account for the dearth of LAEs observed in D-ELAISN1. However, as noted by [**?**], the deficit may owe to poor seeing for that field. Interestingly, D-ELAISN1 also shows a strong asymmetry in the LAE distribution, although there is no evidence of spatial variations in the data quality [619]. In the next section we explore the nature of such asymmetries.

Split-screen contrast

We quantify half-plane variations in the LAE fields using a statistic that we term the "split-screen contrast." The FoV is split, either vertically, horizontally, or diagonally to create regions of roughly equal area. We then calculate the contrast,

$$\frac{\Delta\Sigma}{\Sigma} = \frac{|\Sigma_1 - \Sigma_2|}{\Sigma} \tag{2.2}$$

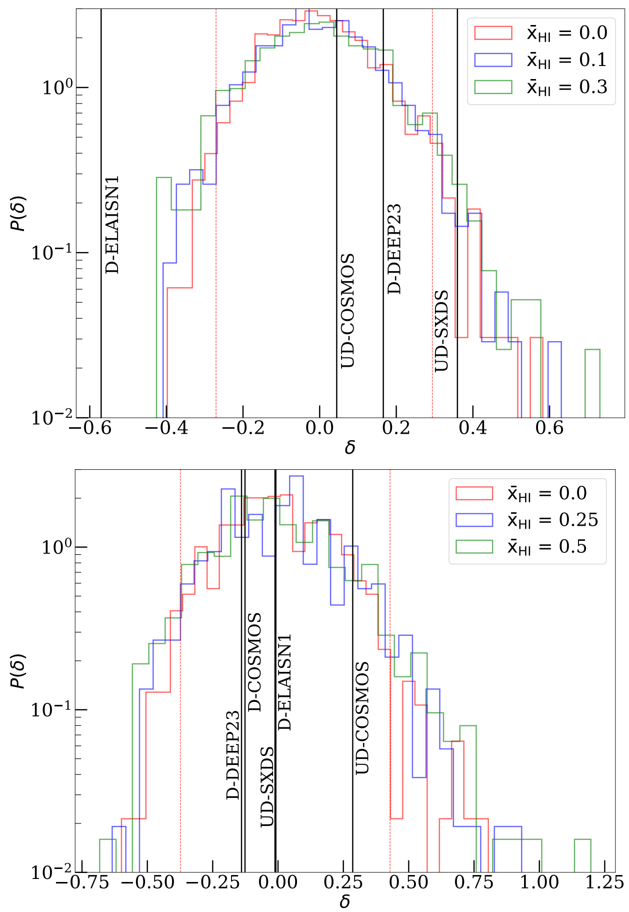

Figure 2.4: Cosmic variance in the surface density of SILVERRUSH-sized fields of view. Here we show the probability distribution of the surface density contrast, $\delta = \Sigma/\langle\Sigma\rangle - 1$. The top and bottom panels correspond to $z = 5.7$ and $z = 6.6$, respectively. The red, blue, and green histograms represent our models with different global neutral fractions. The vertical black lines represent δ measured from the publicly available SILVERRUSH catalogs [719], with uniform luminosity and color cuts applied. The red, thin-dashed lines show the 2σ range of our surface density distribution in a completely ionized scenario. Black lines are annotated with individual field names. A more neutral IGM yields only a slight increase in the cosmic variance. Our model distributions are consistent with the data, aside from D-ELAISN1, which is likely affected by poor seeing [**?**].

where Σ_1 and Σ_2 are the surface densities of the two halves (or "split screens") and Σ is the surface density of the field.

In Figure 2.5 we show the cumulative probability distribution of split-screen contrasts in our models, $P(< \Delta\Sigma/\Sigma)$, or the probability of finding $\Delta\Sigma/\Sigma$ less than a given value. Reionization widens the distribution somewhat. At $z = 5.7$, the standard deviation increases by 30% between a completely ionized IGM and $\bar{x}_{\rm HI} = 0.3$. At $z = 6.6$ the differences are more subtle, a 12% increase in width between $\bar{x}_{\rm HI} = 0.0$ and 0.5, owing to the relative dominance of shot noise from a lower mean surface density. Generally speaking, a larger neutral fraction extends the high-contrast tail of the distribution, enhancing the likelihood of finding more extreme half-plane asymmetries.

For comparison, we attempt to quantify the split-screen contrasts in the SILVERRUSH data using the same luminosity and color cuts described in the last section. We note that the fields have different sizes and non-trivial shapes. To account for this, we inspected the fields and found axes of symmetry along which to perform the bisections, maintaining roughly equal areas between the split screens. The black histograms in Figure 2.5 show the results of our crude measurements, which are reported in Table 2.2. (Individual fields have more than one split-screen configuration.) The largest contrasts are found in D-ELAISN1 at $z = 5.7$, and in D-COSMOS and UD-COSMOS at $z = 6.6$. Note that we have applied our own homogeneous luminosity and color cuts to the data, so the split screen contrasts that we report here may not be visually apparent in published visualizations of the fields [619, e.g.].

Our measurements from SILVERRUSH lie comfortably within the dispersion of

z	Field	Σ [deg^{-2}]	$\Delta\Sigma\ /\Sigma$
5.7	UD-COSMOS	75.6	0.27, 0.14
	UD-SXDS	98.4	0.33, 0.03
	D-DEEP2-3	84.4	0.28, 0.46, 0.18
	D-ELAISN1	31.1	0.20, 0.18, 0.76, 0.02, 0.55, 0.58
6.6	UD-COSMOS	12.2	0.75, 0.32
	UD-SXDS	9.41	0.11, 0.55
	D-COSMOS	8.27	0.75, 0.44, 0.31
	D-DEEP2-3	8.16	0.31, 0.15, 0.08, 0.15, 0.23, 0.08
	D-ELAISN1	9.38	0.15, 0.07, 0.44, 0.22, 0.29, 0.51

Table 2.2: Surface densities (3rd column) and split-screen contrasts (4th column) measured from our sample of the SILVERRUSH data. Our luminosity and color cuts are described in §2.4.1. This data is compared against our models in Figures 2.4 and 2.5.

our models. A Kolmogorov–Smirnov test indicates that the observed distributions are consistent with all of the models. For example, at $z = 5.7$, we find p-values of 0.8 and 0.3 for $\bar{x}_{\rm HI} = 0.3$ and 0.0, respectively. We conclude that the half-plane asymmetries present in the SILVERRUSH data are consistent with the expected large scale structure alone. Patchy reionization does, however, enhance the probability of observing larger split-screen contrasts. For example, the probabilities of finding $\Delta\Sigma/\langle\Sigma\rangle \geq 0.5$ are 4(21)%, 6(23)%, 10(27)% in our models with $\bar{x}_{\rm HI} = 0.0(0.0)$, 0.1(0.3), and 0.3(0.5) at z=5.7(6.6), respectively.

In conclusion, we have found that our ensembles of simulated fields are consistent with the cosmic variance and half-plane asymmetries observed in the SILVERRUSH data.

2.4.2 Voids

Clustering statistics of LAEs provide an important observational window into the reionization process. Previous studies have focused on using the 2PCF to constrain the

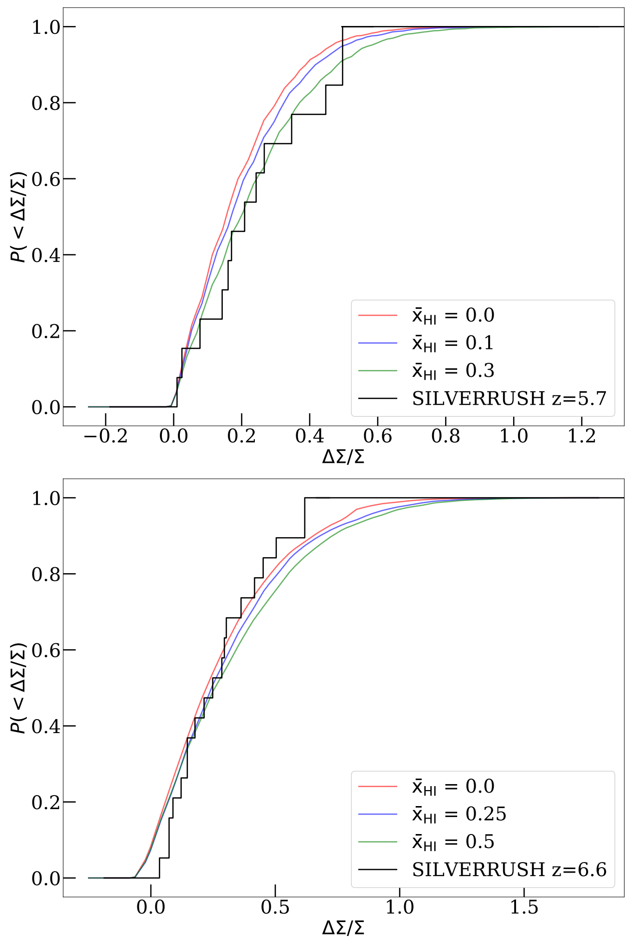

Figure 2.5: Cumulative probability distribution of the split-screen contrast, $\Delta\Sigma/\Sigma$. The split-screen contrast quantifies half-plane asymmetry in the LAE distribution (see main text for more details). The top and bottom panels correspond to $z = 5.7$ and $z = 6.6$, respectively. The colored curves correspond to our reionization models. The black histograms show measurements from the publicly available SILVERRUSH catalogs [719], with uniform luminosity and color cuts applied. The likelihood of finding a field with high $\Delta\Sigma/\Sigma$ increases slightly with neutral gas fraction. However, the visually apparent half-plane asymmetries seen in some of the SILVERRUSH fields are consistent with expectations from large-scale structure formation alone.

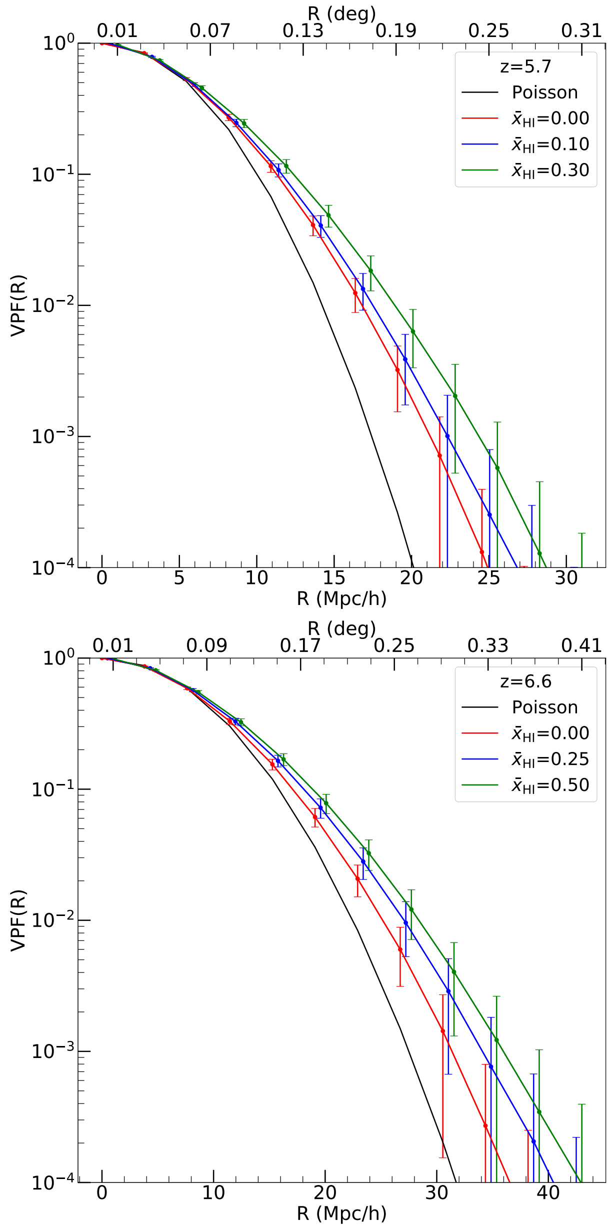

Figure 2.6: The void probability function (VPF) at $z = 5.7$ (top) and $z = 6.6$ (bottom) for our models with different global neutral fractions. The black curves show the analytic result for a uniform-random distribution of LAEs with matched surface density. The error bars show the 1σ dispersion from cosmic variance in a 10-field survey, or a SILVERRUSH-like survey with roughly double the size. A larger neutral fraction increases the probability of finding larger empty circles. This is a consequence of LAEs being obscured in the low-density regions of the IGM, which are the last places to be reionized.

neutral fraction of the IGM [531, 617, 401, 386, 737, 619]. However, Figure 2.2 illustrates that, toward the end of reionization, neutral gas is mostly relegated to voids in the LAE distribution. This suggests that void statistics could be more informative in the final stages of reionization, when the neutral gas disproportionately obscures LAEs in under-dense regions. Also working in favor of this idea is the fact that the space density of $z = 5.7$ LAEs is considerably larger than at e.g. $z = 6.6$. In what follows, we examine the prospect of constraining reionization with the statistics of voids.

We quantify reionization's effect on LAE void statistics using the void probability function (VPF), or the probability of finding a circle of radius R containing no LAEs ([771]; [770]; [531]; [633]). The VPF is complementary to the 2PCF, encoding correlations at orders beyond the two-point function. A key advantage of the VPF is that it is simple and can be applied even to sparse LAE fields, although see [633] for important caveats on its application. We compute the VPF by randomly placing down circles with radius R in our mock fields and then finding the fraction of circles that do not contain LAEs.

In Figure 2.6 we show our VPF results at $z = 5.7$ (top) and $z = 6.6$ (bottom). The red, blue, and green curves show our reionization scenarios as denoted in the plot legends. For comparison, the black curves show the VPF in the case of a uniform-random distribution of LAEs, $P(R) = \exp(-\pi R^2 \langle\Sigma\rangle)$, with the same mean surface density (see Table 2.1 for $\langle\Sigma\rangle$). A comparison between the black and red curves shows that large scale structure clearly enhances the VPF above the Poisson expectation. Consistent with previous works, we find that an ongoing reionization process further enhances the VPF. Neutral gas in the cosmic voids attenuates Lyα emission, making holes in the LAE distribution appear larger (cf. Figs. 2.2 and 2.3). A higher global neutral fraction enhances the probability of finding empty circles on larger scales. At z=6.6 we find that the probability of finding larger empty circles is enhanced significantly. (Note the different scales in the panels.) This owes to two effects. First, there are simply fewer LAEs at $z = 6.6$, which results in larger random gaps in the distribution (see [176] for a discussion). Second, the larger neutral fraction results in more LAEs being obscured.

Even on the $L \sim 200\ h^{-1}$ Mpc scales of our fields, large-scale power can lead to substantial cosmic variance in our void statistics. Such variations can pose a challenge for constraining reionization with voids. We quantify the cosmic variance by bootstrap resampling our simulated FoV ensemble. If our mock survey contains N fields, we draw N samples with replacement and calculate the VPF from these samples. The resulting VPF constitutes one realization of a mock survey, and we generate $10,000$ of these. We have checked that our results are well converged in the number of realizations. In what follows, we consider two survey configurations; (1) The current SILVERRUSH size: $N = 4$ and 5 for $z = 5.7$ and 6.6, respectively; (2) A future SILVERRUSH-like survey covering twice the area, $N = 10$. The error bars in Figure 2.6 show the 1σ dispersion from cosmic variance in the VPF assuming the futuristic $N = 10$ field survey. From here on, all cosmic variance error bars assume $N = 10$.

Can the VPF provide stronger constraints than the 2PCF on the tail end of reionization, as we have argued above? We address this question with a simple χ^2 analysis. We gauge the significance at which a statistic can rule out our model with $\bar{x}_{\rm HI} = 0.3$ (0.5) at $z = 5.7$ (6.6), assuming that the true model is $\bar{x}_{\rm HI} = 0$. To this end, we used our bootstrap samples of the $\bar{x}_{\mathrm{HI}} = 0$ model to compute the covariance matrix[6], taking into account correlations between radial bins. We then calculated $\chi^2 = \boldsymbol{P}^T C^{-1} \boldsymbol{P}$, where C is the covariance matrix and $\boldsymbol{P}$ is the difference vector between the 0.3(0.5) model and a mock survey drawn from the $\bar{x}_{\mathrm{HI}} = 0$ model. Finally, we calculated p-values to assess the rarity of the obtained χ^2. Given the non-Gaussianity exhibited in some of the radial bins, we integrated the numerical χ^2-distribution from the bootstrapping to compute the p-values.

A summary of our simple χ^2 analysis is reported in Table 2.3. There we show p-values for the 2PCF, VPF, as well as two of the peak-based statistics that we explore in the next section. To ensure that our conclusions are not biased by a random fluctuation, the p-values reported there are the average values over $1,000$ mock observations. Results are given for current and "futuristic" (10-field) survey configurations. We note that our analysis adopts cosmic variance error bars, ignoring all other observational uncertainties. The numbers in parentheses correspond to cases in which we assume that a fraction of the LAEs are actually misidentified foreground interlopers. (See discussion below.) Let us consider first the ideal case with no contamination. We find that the VPF outperforms the 2PCF at testing late reionization models in which the tail end extends below $z = 5.7$. On the other hand, for both survey configurations, the 2PCF and VPF provide similar constraining power for a model with $\bar{x}_{\mathrm{HI}} = 0.5$ at $z = 6.6$. These results have an intuitive interpretation. The neutral gas is mostly in the voids at $z = 5.7$, leaving a stronger signature in the VPF compared to the 2PCF.

In the absence of full spectroscopic confirmation, however, narrow band surveys

[6]We have checked that our calculation is well converged in number of realizations.

z	Statistic	p-value (SILVERRUSH-like)	p-value (10 fields)
5.7	2PCF	0.26	0.18
	10% contamination	(0.28)	(0.22)
	30% contamination	(0.34)	(0.32)
	VPF	0.18	0.07
	10% contamination	(0.23)	(0.12)
	30% contamination	(0.31)	(0.23)
	PTF	0.42	0.30
	PPF	0.63	0.51
6.6	2PCF	0.19	0.08
	10% contamination	(0.26)	(0.12)
	30% contamination	(0.32)	(0.21)
	VPF	0.21	0.09
	10% contamination	(0.25)	(0.14)
	30% contamination	(0.34)	(0.23)
	PTF	0.19	0.10
	PPF	0.58	0.25

Table 2.3: Simple χ^2 analysis to gauge the efficacy of void and peak statistics for testing reionization models. The reference models have $\bar{x}_{\rm HI} = 0$ and we compute the probabilities of obtaining χ^2 at least as extreme as those of the $\bar{x}_{\rm HI} = 0.3$ and 0.5 models at $z = 5.7$ and 6.6, respectively, assuming cosmic variance uncertainties. These p-values are shown for two survey configurations: (1) A SILVERRUSH-like survey with 4 and 5 fields at $z = 5.7$ and $z = 6.6$, respectively; (2) An expanded SILVERRUSH-like survey with 10 fields (roughly doubled in area). We consider the two-point correlation function (2PCF), Void Probability Function (VPF; §2.4.2), Pixel Threshold Fraction (PTF; §2.4.3), and Peak Probability Function (PPF; §2.4.3). The numbers shown in parentheses for the 2PCF and VPF assume that 10% or 30% of the LAEs are misidentified foreground sources. All other numbers assume no contamination. The VPF is particularly well-suited for probing the tail end of reionization, where LAE surface densities are highest.

are inevitably contaminated by misidentified lower redshift sources. The contamination could be particularly problematic for the VPF, which is exponentially sensitive to interlopers [533]. To gauge this effect, we selected a fraction of our LAEs and shuffled them to random locations in the field. This procedure ignores the clustering of the interlopers, which is likely to be a small effect for the low number densities that we assume here. Based on spectroscopic followups, [619] estimated contamination rates of $\approx 8\%$ and $\approx 14\%$ in their $z = 5.7$ and $z = 6.6$ samples, respectively. [619] also found that the contamination rate depends on source brightness. They reported a higher rate of $\approx 33\%$ for sources brighter than 24 magnitudes in their $z = 6.6$ sample. In Table 2.3, the p-values in parentheses assume contamination fractions of 10% and 30%. We find that the contamination significantly degrades the sensitivities of both the VPF and 2PCF. However, for the 10-field configuration, we find that the VPF maintains an advantage over the 2PCF at $z = 5.7$, even in the presence of signficant contamination.

Our results suggest that the VPF can provide information on reionization that is complementary to the 2PCF. We find that the former is a more sensitive test of the final stages of reionization in which neutral gas is contained primarily in the voids, and LAE surface densities are highest.

2.4.3 Peak Statistics

LAE peak statistics offer a complementary picture to the voids. When comparing models with $\bar{x}_{\rm HI} = 0$ and 0.3 at fixed $\langle \Sigma \rangle$, any LAEs that are obscured in the voids of the latter model must be compensated by other LAEs unveiled elsewhere. Thus, we also expect the statistics of LAE over-densities to be different between the two models (see §2.3). We quantify this effect here. We explore three different approaches, starting with the simplest statistic based on thresholding the LAE field.

Pixel Threshold Fraction

We begin by counting the fraction of pixels exceeding an over-density threshold in a smoothed map of the LAE distribution. The LAE distribution is first smoothed onto a uniform 2-dimensional grid using a Gaussian filter with a smoothing scale of $\sigma = 10\ h^{-1}$Mpc. We employ a grid with $N = 512^2$, but our conclusions are broadly robust to the exact choice. The size of the smoothing scale was adopted from previous studies of galaxy proto-clusters at $z = 5.7$ and 6.6 [131, e.g.]. It is roughly the spatial extent of over-dense regions that later collapse into clusters at $z \sim 0$. We then count the fraction of pixels above a given surface over-density $\Sigma_{10}(\mathbf{x})/\langle\Sigma\rangle$, where the subscript denotes that we have smoothed over a scale of $10\ h^{-1}$Mpc. We set the minimum threshold to be the 95th percentile in the $\bar{x}_{\rm HI} = 0$ models, since we find that differences between the models are strongest at the largest over-densities. For reference, this minimum threshold corresponds to $2\langle\Sigma\rangle$ and $2.5\langle\Sigma\rangle$ at $z = 5.7$ and 6.6, respectively.[7] We refer to this statistic, $F(> \Sigma_{10}/\langle\Sigma\rangle)$, as the Pixel Threshold Fraction (PTF).

We show our results for the PTF in Figure 2.7. Consistent with expectations, the fraction of over-dense pixels increases with the neutral fraction for fixed $\langle\Sigma\rangle$. This is particularly prominent amongst our models at $z = 6.6$. The differences in the PTF reflect

[7] Our thresholds are lower than those of previous studies which define clusters and proto-clusters with surface-densities greater than $4 - 5\sigma$ over the mean density [394, 354, e.g.]. In this section, we use the term “LAE peak” to distinguish between our liberal definition of a high-density region and the more stringent classification of proto-clusters used in those works [394, 354].

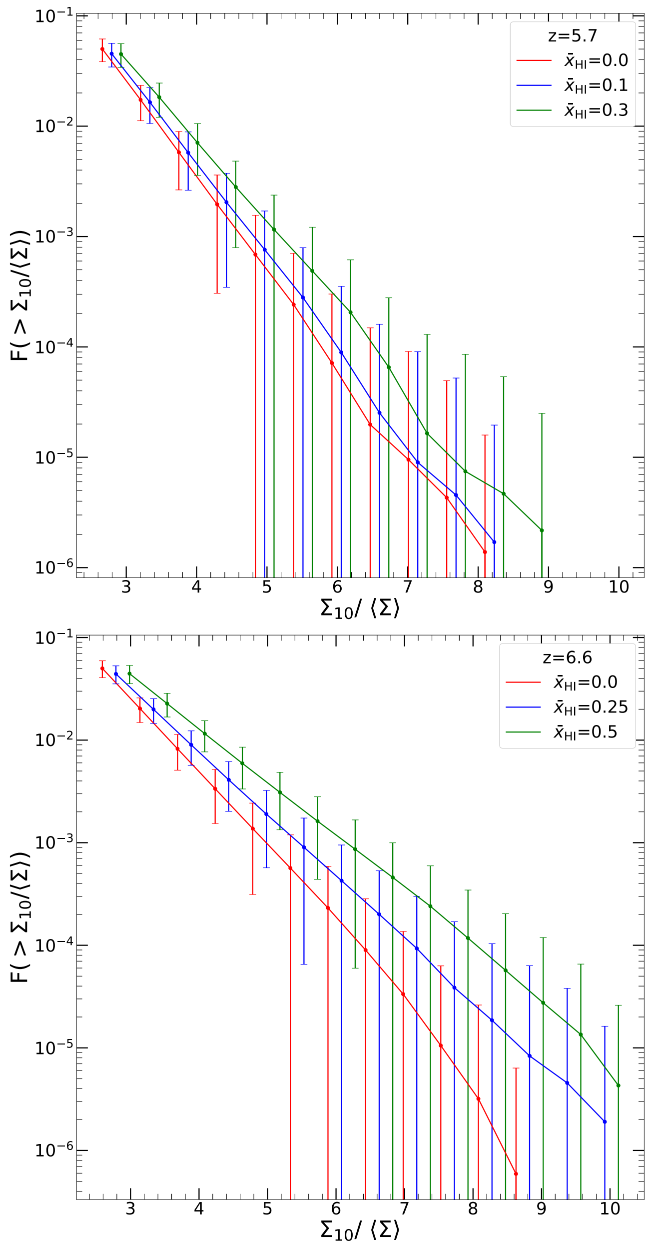

Figure 2.7: The Pixel Threshold Fraction (PTF), or fraction of pixels with LAE surface densities above $\Sigma_{10}/\langle\Sigma\rangle$. Here, Σ_{10} is the surface density smoothed over a scale of $\sigma = 10\ h^{-1}$Mpc with a Gaussian filter. The error bars show the 1σ dispersion from cosmic variance in an expanded (10-field) SILVERRUSH-like survey. At a given redshift, all models shown have a fixed $\langle\Sigma\rangle$ (see Table 2.1). In this case, a more neutral IGM leads to a larger fraction of over-dense pixels, a consequence of conservation of LAE number. LAEs that are obscured in voids are compensated by more LAEs being visible elsewhere, which leads to an apparent enhancement in clustering.

an enhancement in the apparent clustering of LAEs due to patchy reionization, offering an alternative to the 2PCF for quantifying this effect. The error bars in Figure 2.7 show the 1σ cosmic variance obtained from the bootstrap method described in §2.4.2. The results of our χ^2 analysis on the PTF is also shown in Table 2.3. At $z = 6.6$, the PTF can discriminate the $\bar{x}_{\rm HI} = 0.5$ and $\bar{x}_{\rm HI} = 0.0$ models at a similar level to the 2PCF and the VPF. However, at $z = 5.7$, the PTF is significantly weaker. This behavior may owe to the fact that the LAEs in our models are more highly biased at $z = 6.6$.

Peak Overdensity Function

Next we consider a more sophisticated approach that groups together high surface density pixels ("peak pixels"). This approach has the added benefit that we can analyze the effect of reionization on the morphology of LAE peaks. Peak pixels are identified in our smoothed surface density maps using the same threshold as in the last section. They are then grouped into connected sets that we call peaks. To avoid edge effects, we eliminate peaks whose boundaries are one pixel from any edge of the field. We count the number of LAEs contained within each peak and eliminate peaks with less than 8(5) LAEs at $z = 5.7(6.6)$, which, we find, reduces the effects of shot noise and grid resolution on our results. This procedure yields catalogs of bounded regions of the highest intensity pixels.

In Figure 2.8, we show example applications of our peak finding algorithm to mock fields at $z = 5.7$ (top row) and $z = 6.6$ (bottom row). The columns correspond to different neutral fractions as denoted in the plot labels. In each panel, the dots show the LAE distributions, while the color maps correspond to the smoothed surface density contrasts.

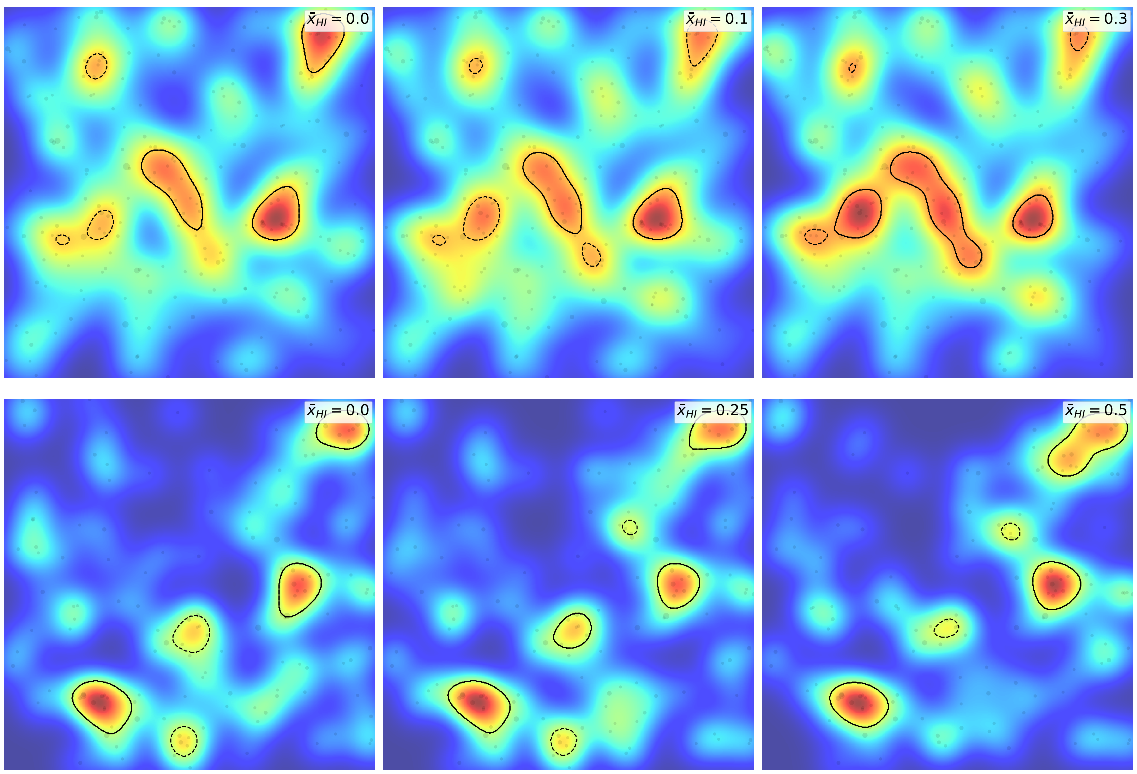

Figure 2.8: Examples of our peak finding algorithm described in §2.4.3. The color maps show the surface density contrast of the LAE field smoothed on a $\sigma = 10\ h^{-1}$Mpc scale with a Gaussian filter. The top and bottom rows correspond to $z = 5.7$ and $z = 6.6$, respectively, while the columns correspond to models with different global neutral fractions. The top panels are $180\times180\ (h^{-1}\text{Mpc})^2$ while the bottom panels are $200\times200\ (h^{-1}\text{Mpc})^2$. The solid black contours enclose regions identified as peaks in the LAE distribution. For reference, the dashed contours show over-dense regions that did not fulfill our LAE occupancy cut (see main text for details).

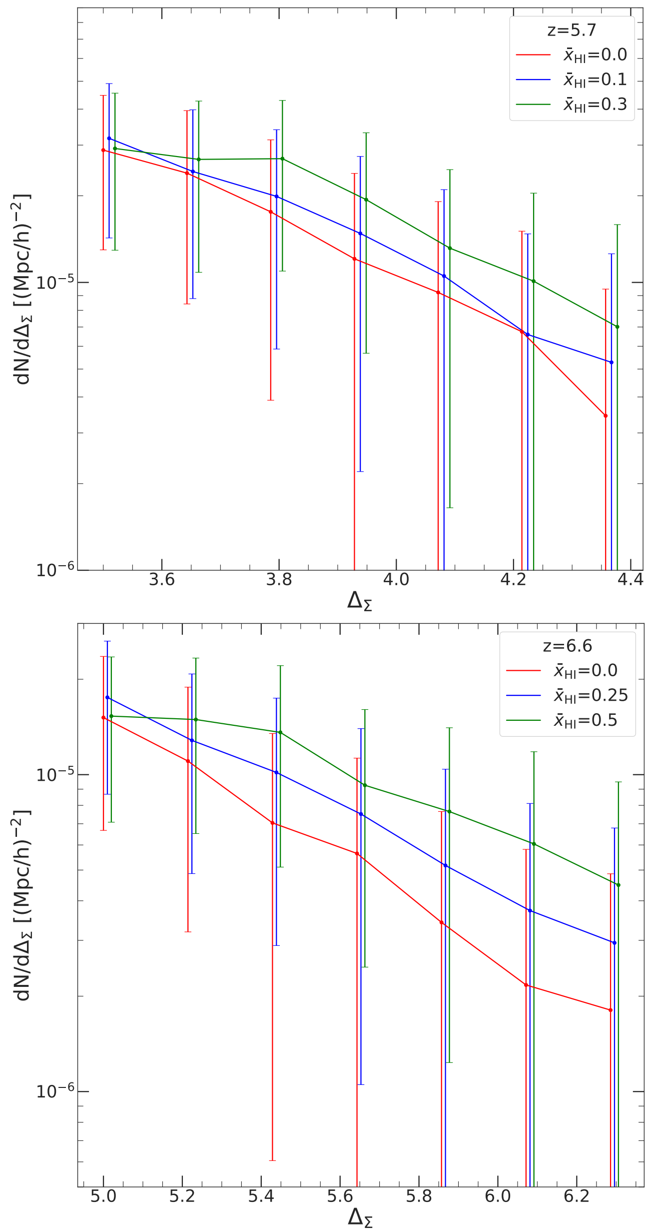

Figure 2.9: The Peak Overdensity Function (POF), $d\mathrm{N}/d\Delta_\Sigma$, or number of peaks per unit area, per unit surface over-density, $\Delta_\Sigma = \Sigma/\langle\Sigma\rangle$. For this statistic, peaks are identified as connected sets of pixels satisfying a minimum over-density threshold, as well as a minimum LAE occupancy (see main text for details). Error bars show the 1σ dispersion from cosmic variance in an expanded (10-field) SILVERRUSH-like survey. At fixed $\langle\Sigma\rangle$, the over-dense LAE peaks are more numerous in models with higher neutral fraction.

The solid curves bound the LAE peaks selected by our algorithm while the dashed curves show regions that did not make our final cut owing to low LAE occupancy (i.e. not satisfying the minimum occupancy of 8(5) at $z = 5.7$ and 6.6).

We have quantified the shapes of LAE peaks by computing moments of their surface density distributions. We found that the shapes (e.g. ellipticities) and sizes of the peaks are statistically quite similar between our models, with variations $\sim 5\%$. We do not consider these statistics further here. Instead we focus on the abundance and occupancy of peaks, which do show significant differences. At fixed $\langle\Sigma\rangle$, a more neutral IGM leads to more LAEs per peak. In particular, models with a higher neutral fraction contain more peaks with high LAE occupancy. To demonstrate this, we consider the number of peaks per unit area, per unit surface density, $dN/d\Delta_\Sigma$, where Δ_Σ is the surface density of a peak in units of the global mean. We term $dN/d\Delta_\Sigma$ the Peak Overdensity Function (POF).

Figure 2.9 shows the POF for our models at $z = 5.7$ (top) and $z = 6.6$ (bottom). We find that Δ_Σ ranges from 3-5 at $z = 5.7$ and 4-7 at $z = 6.6$, generally reflecting the stronger bias of LAEs at higher redshifts. The number of over-dense peaks clearly increases with the neutral fraction, consistent with our arguments above. However, the error bars show considerable cosmic variance in even a future 10-field SILVERRUSH-like survey. Compared to the PTF, we find that the POF offers a much weaker discriminator between our models owing to the rarity of peaks. Indeed, Figure 2.8 illustrates that only 2-3 peaks are identified per FoV. Thus we did not consider the POF in our χ^2 comparison.

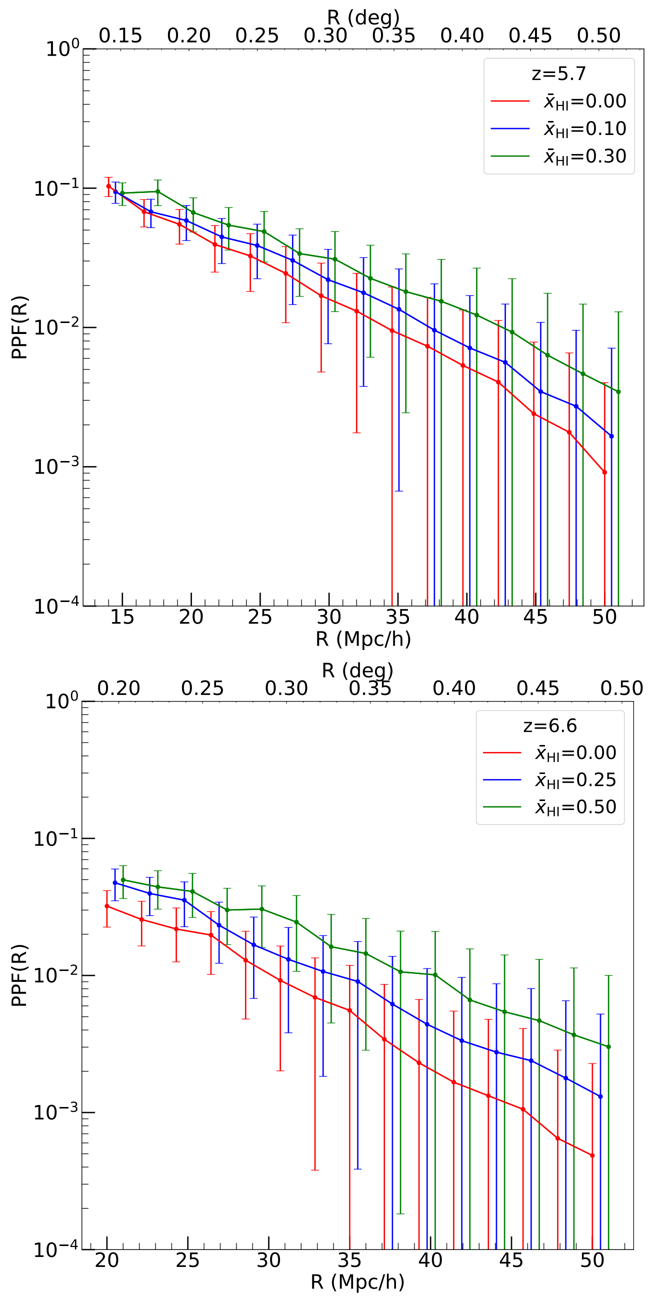

Figure 2.10: The Peak Probabiliy Function (PPF), or probability of finding an LAE overdensity greater than some threshold within a circle of radius R. We adopt a threshold of $2(2.5)\langle\Sigma\rangle$ at $z = 5.7(6.6)$ (see main text for details). Error bars show the 1σ dispersion from cosmic variance in an expanded (10-field) SILVERRUSH-like survey. At fixed $\langle\Sigma\rangle$, higher neutral fractions yield increased probabilities of finding LAE peaks.

Peak Probability Function

The last statistic that we consider is an analogue to the VPF of §2.4.2. We define the Peak Probability Function (PPF) to be the probability that a randomly placed circle of radius R has an over-density of LAEs greater than or equal to some threshold. We randomly place down circles of radius R, find the number of LAEs (N) contained within the circle, and then calculate the surface density, $\Sigma_R = N/\pi R^2$. Using the same thresholds from §2.4.3, we count only circles with $\Sigma_R > 2(2.5)\langle\Sigma\rangle$ at $z = 5.7(6.6)$. We only consider R, such that there is a minimum of 10 LAE contained within a circle. We then divide the number of circles making the cut by the total number drawn to find the probability as a function of R.

We show our results in Figure 2.10. Consistent with the previous statistics, we find that the probability of obtaining a peak increases with the neutral fraction. This further cements the conclusion that, at fixed $\langle\Sigma\rangle$, a higher neutral fraction yields a higher abundance of over-dense peaks in the LAE distribution. The results of our χ^2 analysis for the PPF are given in Table in Table 2.3. Perhaps surprisingly, the PPF is not as strong of a test of our models as the other statistics we considered, and is significantly weaker than the 2PCF. We attribute this finding to strong correlations between the radial bins, which are reflected in the highly off-diagonal structure of the covariance matrix for the PPF. The physical picture for this is as follows. Owing to the bias of LAEs, if a peak of a given radius R is found, then the probability of finding additional peaks with other values of R is enhanced significantly. On other hand, the correlations between radial bins of the VPF are weaker. Finding a random hole in the LAE distribution does not necessarily enhance the probability of finding a larger hole, for example.

2.5 Conclusion

In this Chapter we have explored the use of narrow band LAE surveys to constrain late reionization scenarios, with an eye towards recently proposed models in which reionization ends as late as $z \approx 5$ [454, 589, 426]. During the tail end of reionization, with neutral fractions $\sim 10\%$, the last remaining neutral islands in the Universe were likely relegated to voids in the galaxy distribution. The neutral islands would have preferentially obscured LAEs in under-dense regions, motivating us to explore LAE void statistics further in this . When comparing reionization models at a fixed mean surface density, LAEs obscured in the voids must be compensated by visible LAEs elsewhere in the spatial distribution. Thus, we have also explored peak statistics as a complementary discriminator of reionization models.

For several reionization scenarios spanning global neutral fractions of $\bar{x}_{\rm HI} = 0 - 0.3$ at $z = 5.7$, and $\bar{x}_{\rm HI} = 0 - 0.5$ at $z = 6.6$, we have constructed mock LAE surveys using one of the $L = (1\ h^{-1}{\rm Gpc})^3$ Multi-Dark simulations as a basis. Our models were tuned to match the LAE surface densities observed in the recently published SILVERRUSH survey, as well as a number of other observational constraints. The enormous simulation volume of Multi-Dark allowed us to capture the $\sim 10 - 100$ Mpc characteristic scales of reionization, and provided representative models for comparison against SILVERRUSH, which covers an area of $14 - 21$ deg^2 ($0.3 - 0.5$ Gpc^2). One of our primary focuses was to quantify the cosmic variance expected in a SILVERRUSH-like survey. To this end we constructed a statistical ensemble of $1,000$ mock fields of view.

The SILVERRUSH data exhibits significant field-to-field variation in surface density, and some fields have visual asymmetries in the LAE distribution over ~ 200 Mpc scales. We compared the SILVERRUSH data against our models and found that the surface density variations as well as the large-scale asymmetries of the former are well within expectations from large-scale structure formation alone. An exception to this conclusion is the field D-ELAISN1, which has $\approx 20\%$ fewer LAEs than the lowest surface density observed in our ensemble. Interestingly, D-ELAISN1 also exhibits among the largest half-plane asymmetries in its LAE distribution. However, [**?**] has attributed the exceptional features of D-ELAISN1 to poor seeing, perhaps reconciling it with our models. We generally find that patchy reionization contributes only slightly to the cosmic variance and large-scale (~ 200 Mpc) asymmetry of fields, and is an unlikely explanation for the characteristics of D-ELAISN1.

Next we considered the void probability function (VPF) as a probe of reionization models. A more neutral IGM yields a higher probability of finding large-scale empty regions in the LAE distribution. We found with a simple χ^2 calculation that the VPF is a more sensitive test of models during the last stages of reionization than the widely used angular two-point correlation function (2PCF). In spite of the VPF being exponentially sensitive to interlopers, this conclusion holds even if we assume that $10 - 30\%$ of the sources are misidentified foreground objects.

We also explored three approaches to quantifying the statistics of peaks in the LAE distribution. Using a method that groups over-dense pixels in surface density maps smoothed over 10 h^{-1}Mpc scales, we found that patchy reionization has little effect statistically on the shapes of LAE peaks. When comparing models at fixed mean surface density, the predominant effect of neutral gas is to increase the probability of finding LAE over-densities. We found that this effect can be quantified straightforwardly by thresholding smoothed LAE maps and counting the fraction of over-dense pixels. Our simplistic χ^2 analysis showed that this peak statistic offers roughly the same sensitivity as the 2PCF and VPF for discriminating between models with $\bar{x}_{\mathrm{HI}} = 0.0$ and $\bar{x}_{\mathrm{HI}} = 0.5$. However, it is generally less sensitive during the last stages of reionization.

In this Chapter, we have focused on constraining the latter half of reionization with a SILVERRUSH-like survey. However, SILVERRUSH and The Lyman Alpha Galaxies in the Epoch of Reionization (LAGER; [863]) project will continue to expand the sample of known LAEs at ≥ 7. Future work should address in further detail the efficacy for $z \sim 7$ LAEs to constrain reionization, as well as the trade-off between survey area and depth (see [633]). We note that all of our calculations have assumed that reionization proceeded in an inside-out manner, consistent with semi-numeric models and more detailed radiative transfer simulations. Future studies might further explore whether a combination of statistics could provide more fundamental insight into the connection between reionization and the underlying density field.

In recent years, the sample of known LAEs at $z \geq 5.7$ has grown to over 2,000, raising the prospects for detecting the last stages of reionization in the clustering of LAEs. Our calculations suggest that the statistics of voids and peaks offer complimentary approaches to the 2PCF, and may even be more optimal under some conditions.

Chapter 3

Chapter 3: On the correlation between Lyα forest opacity and galaxy density in late reionization models

3.1 Introduction

As mentioned in Chapter 1, quasar absorption spectra measurements have played a prominent role in sharpening our understanding of the reionization process. A widely used measurement is the large scatter in the Lyα forest effective optical depth, $\tau_{\rm eff}^{50}$, at $z \gtrsim 5.3$ [252, 52, 237, 79, 78, 842]. At these redshifts, the extended high-opacity tail of the $\tau_{\rm eff}^{50}$ distribution consists of long absorption troughs, epitomized by the extreme 110 h^{-1}cMpc-long trough in the sight light of quasar ULAS J0148+0600 [52] (J0148 hereafter). The scatter in $\tau_{\rm eff}$ and the existence of such long troughs are inconsistent with standard models of the low-redshift intergalactic medium (IGM), which adopt a uniform ionizing background (as an approximation) and a relaxed temperature-density relation – characteristics expected well after the end of reionization [78].

Early ideas to account for the $\tau_{\rm eff}^{50}$ scatter included relic temperature fluctuations from reionization [190] and large ionizing intensity fluctuations from a spatially fluctuating mean free path [199] and/or rare sources such as active galactic nuclei [124]. In the relic temperature fluctuation scenario, the most opaque regions of the $z = 5 - 6$ forest would be the cosmological density peaks that were reionized at early times, which have had a longer time to cool to lower temperatures. The most transmissive regions would be hot voids that were ionized and heated at the end of reionization. On the other hand, the intensity fluctuation scenarios generally predict the opposite; the density peaks would be the most transmissive, since the ionizing sources are clustered there, while the source-poor voids would be the most opaque.[1]

These opposing predictions led Ref. [198] to propose large-scale structure surveys centered on Lyα forest sight lines as a test of the proposed models. They showed that the models could be tested by measuring the correlation between the Lyα forest $\tau_{\rm eff}^{50}$ and the central galaxy surface density (within an impact parameter of 10 h^{-1}cMpc). In what follows, we will refer to this as the opacity-density relation. The first such survey was presented in Ref. [57]. They mapped the distribution of strong Lyα emitting galaxies (LAEs) around the

[1] The degree of correlation between cosmological density and forest transmission depends on the clustering of the sources. (Although, we will show here that the effect of clustering is degenerate with the reionization history.) The shot noise dominated AGN scenario of Ref. [124] can result in less correlation between the forest transmission and environmental density [198].

extreme Lyα trough toward J0148 and showed that it intersects a large-scale void, therefore disfavoring the possibility that the $\tau_{\rm eff}^{50}$ scatter is driven by relic temperature fluctuations alone. Subsequent studies confirmed this conclusion using Lyman Break Galaxies (LBGs) [423], as well as a different field toward another long trough in the forest of quasar SDSS J1250+3130 (J1250 hereafter) C21.

Soon after the measurement of B18, it was realized that the large scatter in $\tau_{\rm eff}^{50}$, as well as the connection between highly opaque forest segments and cosmic under-densities, could be explained more naturally by a model in which reionization ends at $z < 6$ [454, 426, 589]. As pointed out by Ref. [454], extending the tail end of reionization below $z = 6$ appears necessary for models to latch onto the observed evolution of the Lyα forest mean transmission. The model has also received support from measurements of dark gap statistics in the coeval Lyα and Lyβ forests [866, 867], and the mean free path of ionizing photons between $z = 5 - 6$ [56, 77, 868]. In the late reionization scenario, the voids contain isolated patches of neutral gas where reionization was still ongoing, which generate the long forest troughs [504]. Recently, Ref. [55] reported strong evidence for damping wing absorption at the boundary of the long trough toward J0148. Refs. [865, 743] also found evidence for damping wings in stacks of long dark gaps at $z \gtrsim 5.5$. These findings add significantly to the evidence that the long opaque segments of the forest at these redshifts are caused by neutral islands.

As a consensus was forming around the late reionization model, Ref. C23 conducted large-scale structure surveys around 2 of the most transmissive (low $\tau_{\rm eff}^{50}$) forest sight lines toward quasars SDSS J1306+0356 and PSO J359-06 (J1306 and J359), and an additional 3 quasar sight lines were surveyed in Ref. [397]. With the acquisition of these surveys, it is now possible to make a rudimentary comparison between models and measurements of the opacity-density relation. Interestingly, C23 found that the fields toward J1306 and J359 are both under-dense in LAEs within a radius of 10 h^{-1} cMpc of their respective forest sight lines. At face value, this finding is in tension with the intensity fluctuation model of Ref. [199] as well as the late reionization models of Ref. [589], which predict similarly strong anti-correlations between τ_{eff}^{50} and galaxy density.

That the models of Refs. [589] and [199] yield similar predictions should not come as a surprise, however. In Ref. [589], the ionizing backgrounds in their late reionization simulations are modeled using similar techniques and approximations to radiative transfer as those in [199]. A chief goal of this Chapter is to examine in more detail whether the C23 results are in tension with the late reionization scenario using full radiative transfer simulations of reionization. To this end, we will use several models for the sources of reionization. This allows us to address the question of whether assumptions about the sources are responsible for the tension in C23. More broadly, the opacity-density relation links the galaxies to the Lyα transmission properties of their environments. Another natural question, then, is whether the relation could tell us which galaxies sourced the high-z ionizing background. For instance, it has been recently proposed that the observed UV-bright LAEs were the sources of reionization, since, it is argued, they should have been prodigious leakers of ionizing radiation [**?**, e.g.]]Naidu19, Mathee2022v1 (see however [144]). Could a measurement of the LAE opacity-density relation test this proposal? Lastly, we will use our simulations to interpret the fields of J1306 and J359 within the context of late reionization models. We will discuss the physical conditions of the IGM that could give rise to these fields.

The remainder of Chapter 3 is outlined as follows. In §3.2 we summarize our simulation methods. In §3.3 we describe our reionization models. In §3.4 and §3.5 we present our main results. In §3.6 we conclude.

3.2 Methodology

3.2.1 Radiative transfer simulations of reionization

We ran multi-frequency radiative transfer (RT) simulations of reionization using the FlexRT code of Ref. [104] (see also[105, 106, 107]). Here we summarize the essential details for this Chapter. FlexRT is run in post-processing on density fields extracted from a cosmological simulation. The density fields used here are from the hydrodynamics simulation of [187], with a box size of $L = 200\ h^{-1}$cMpc. The original simulation was run with the Eulerian hydrodynamics code of Ref. [777] using $N = 2 \times 2048^3$ dark matter particles and gas resolution elements. A key improvement in this Chapter is that we ran a higher resolution N-body-only simulation using the same initial conditions with $N = 3600^3$ particles, allowing us to resolve halos of smaller masses. Hence, we no longer use the sub-resolution halo algorithm use in [105, 106].[2] As stated in Ref. [107], our new simulation is complete down to a mass limit of $M_{\rm min} = 3 \times 10^9\ h^{-1}{\rm M}_\odot$ at $z = 5.7$. (Here we define our simulated mass function to be complete if it agrees to within 10% with the mass function of Ref. [776], which was constructed from a suite of higher resolution simulations.) The

[2]Their sub-resolution halo algorithm was adapted from the non-linear bias method of Ref. [11].

schemes that we explore for assigning ionizing photon emissivities to halos are described in §3.3.

The RT is performed on a uniform grid with $N_{\rm rt} = 200^3$ cells. We adopt a source spectrum of $J_\nu \propto \nu^{-1.5}$ between 1 and 4 Ry, discretized in 5 frequency bins centered on [14.48,16.70,20.03,25.78,39.23] eV. The bins are chosen to contain an initially equal fraction of photons for the assumed source spectrum. FlexRT is based on the adaptive ray tracing method of Ref. [2] (see also Ref. [775]). Rays are cast from the centers of source cells and can adaptively split and merge to maintain a user-specified angular resolution in the radiation field. For the simulations in this Chapter, rays were cast and merged at HealPix level $l = 0$, corresponding to 12 directions per source cell. Merging begins for rays above a minimum number of 16 rays per cell. Generally speaking, a lower number of rays yields a noisier radiation field. In Appendix 3.7, we compare the ionizing background in our fiducial simulation to a simulation with higher angular resolution run at HealPix level $l = 1$ (48 directions). We also compare to an averaging procedure that smooths over the noise. We demonstrate that our main results are not significantly affected by ray noise.

The coarse-grained cosmological density fields for the RT are obtained by averaging with equal weights over the hydrodynamic simulation cells within a given RT cell. The RT cells are $\Delta x = 1\ h^{-1}$cMpc wide; too large to resolve directly the small-scale gas structures that set the LyC opacity. To remedy this, we apply the sub-grid model of Ref. [105] for the IGM opacity. This model is based on an extended suite of the high-resolution radiative hydrodynamics simulations of Refs. [192, 588], which track the evolution of the LyC opacity as the IGM responds to photoheating from reionization. The simulations upon which the sub-grid model is constructed have boxes sizes with $L_{\rm box} = 1\ h^{-1}$Mpc, equal to an RT cell size. The suite spans a range of environmental parameters –local photo-ionization rate ($\Gamma_{\rm HI}$), box-scale density, and reionization redshift ($z_{\rm reion}$) – to capture variations in the opacity owing to the patchiness of reionization. For each RT cell, these quantities are mapped to an opacity evolution in a way that accounts for the photoionization history of the cell (see Refs. [105, 106] for more details).

We use the full speed of light because the photoionization rate of the IGM near the end of reionization is highly sensitive to the reduced speed of light approximation [603, 107] (see also Cain in prep.). FlexRT tracks the photoionization and thermal states of each RT cell. For the latter, we use the fitting function of Ref. [188] for the peak temperatures achieved behind ionization fronts ($T_{\rm reion}$), which was calibrated to a suite of high-resolution one-dimensional RT simulations. The equilibrium photoheating in the highly ionized IGM includes spectral filtering as described in Ref. [107].

3.2.2 The Lyα Forest

To model the Lyα forest, we trace 4,000 skewers in random directions and starting at random locations in the periodic box of our hydrodynamic simulation. We compute the Lyα transmission along the skewers using the approximation to the Voigt profile of Ref. [766]. Applying the hydrogen photoionization rates ($\Gamma_{\rm HI}$) and temperatures (T) from the RT grid, the neutral hydrogen densities in reionized regions along the hydro skewers are rescaled under the assumption of photoionization equilibrium with the case-A recombination coefficient.[3] RT cells with ionized fraction $x_{\rm ion} < 0.5$ are taken to be fully neutral, but we find that the $\tau_{\rm eff}^{50}$ values of our mock Lyα forest are not sensitive to the particular choice of the $x_{\rm ion}$ threshold.

We note that the resolution of our hydro simulation ($N_{\rm gas} = 2048^3$) is much higher than that of our RT grid ($N_{\rm RT} = 200^3$). One issue with the approach outlined so far is that is misses the effects of temperature variations on scales smaller than our coarse-grained RT cells of $\Delta x = 1\ h^{-1}$cMpc. This is less of a problem shortly after a cell has been reionized, when it is approximately isothermal with temperature $\approx T_{\rm reion}$. Well afterwards, however, hydro cells with lower (higher) densities than the local RT-cell-averaged mean should have lower (higher) temperatures than the value assigned to the RT cell. This leads to an over-estimate of the temperatures in small-scale under-densities which, in turn, over-estimates the forest transmission by $\approx 10 - 15\%$.

We correct for this effect by assigning a local temperature-density relation to each RT cell as in [107]. Using the analytic solution of the temperature evolution equation from Ref. [538], we evaluate the IGM temperature on a grid of (z, $z_{\rm reion}$, Δ) values, where Δ is gas density in units of the cosmic mean. For each z and $z_{\rm reion}$, we evaluate γ by fitting densities with $\Delta < 1$ (the regime that sets the forest transmission) to a power law. We then assign a local value of γ to each RT cell by interpolating in z and $z_{\rm reion}$. The temperature of each hydro cell is then given by

$$T_{\rm hydro} = T_{\rm RT} \left(\frac{\Delta_{\rm hydro}}{\Delta_{\rm RT}} \right)^{\gamma(z, z_{\rm reion}) - 1}, \tag{3.1}$$

where $T_{\rm RT}$ and $\Delta_{\rm RT}$ are the temperature and density of the coarse-grained RT cell, $\Delta_{\rm hydro}$

[3] Photoionization equilibrium and the case-A recombination coefficient are good approximations in the highly ionized $\Delta \lesssim 1$ regions that set the forest transmission at these redshifts.

is the density along the hydro skewer intesecting the RT cell, and $\gamma(z, z_{\rm reion})$ represents the slope of the local temperature-density relation. We refer the reader to Appendix E of Ref. [107] for a more detailed discussion and testing of this procedure.

Lastly, it is well known that achieving numerical convergence in simulations of the high-z Lyα forest is difficult [**?**, see e.g.]]2009MNRAS.398L..26B, DAloisio2018. The appendix of Ref. [187] describes a convergence test for the same hydrodynamic simulation used in this chapter. We apply the correction factors provided in their Table A1 to the neutral hydrogen densities in reionized regions to correct for resolution in our Lyα forest fluxes. The correction increases the transmitted flux in our simulated forest, accounting for the fact that small-scale voids are deeper in more highly resolved simulations. For a fixed mean Lyα forest flux, this requires our simulations to end reionization somewhat later compared to a simulation without the correction (see §6.2 of [107]). We will return to point below when we discuss how the timing of reionization affects the opacity-density relation.

3.2.3 Lyα Emitters

To populate our halos with LAEs, we follow the approach outlined in Refs. [817, 304]. In summary, we first assign rest-frame UV magnitudes to the halos by abundance matching to the luminosity function of Ref. [273]. For a given UV magnitude, we then draw a Lyα rest-frame equivalent width from the empirically calibrated distribution of Ref. [227].

We generate mock LAE surveys as described in Ref. [589]. We first select LAEs within cylinders of radii 100 h^{-1}cMpc and depths 60 h^{-1}cMpc, centered on each of the 4,000 Lyα forest sight lines traced through our box. (In the end, LAEs are selected by magnitude and color cuts as described below; here the depth of 60 h^{-1}cMpc ensures that the preliminary selection spans the width of the filter.) Following Refs. [426, 589], we model the continuum as a power law, $F_\lambda \propto \lambda^{-2}$, and the Ly$\alpha$ line as two Gaussian peaks blue-ward and red-ward of systemic, with the former completely attenuated. The red-ward peak is characterized by two parameters: the velocity offset ($v_{\rm off}$) and the line width (σ_v). We map the UV magnitude of a galaxy to a $v_{\rm off}$ value using the scaling relation in Equation 3 of Ref. [515]. For simplicity, we follow Ref. [515] in setting $\sigma_v = v_{\rm off}$, reflecting the expectation that a line's width is correlated with its offset. Skewers are then traced along the line of sight from each LAE. The spectrum of a given LAE is attenuated according to the gas properties along the corresponding skewer, derived from the hydro and FlexRT simulations, with the rest-frame defined as the halo's frame.[4] We note that our hydro simulation does not include prescriptions for star-formation and feedback processes, and the resolution is not high enough to model the interstellar and circumgalactic gases which shape the emerging Lyα line. Instead, the approach taken here is to roll their effects into our parameterization of the line profile assigned to each halo, i.e. we assume that the red-side Gaussian is the emerging line profile. To avoid "double counting" attenuation from the gas close to the halo, we skip the first 3 hydro cells of each skewer, which corresponds to a comoving distance of 0.3 h^{-1}cMpc.

After attenuation, we calculate the NB816 and $i2$ magnitudes of the LAEs using publicly available transmission curves of these filters on the Subaru Hyper Suprime-Cam.

[4] In computing the transmitted fraction for each LAE spectrum, we use a bin size of $\Delta v = 3.5$ km/s, linearly interpolating between our hydro cells (which have a native $\Delta v = 14$ km/s). We find that the interpolation to higher resolution is necessary to avoid spurious transmission spikes in regions with large velocity gradients, owing to the lower native resolution of our hydro skewers. We have tested for convergence of the transmitted fraction with respect to Δv.

Finally, we apply magnitude and color cuts of NB816 ≤ 25.5 and $i2-$NB816 ≥ 1.2, the same as those applied in C23. C23 defined the mean surface density of a given LAE field, $\langle\Sigma_{\rm LAE}\rangle$, to be the surface density measured within an annulus of inner and outer radii 15 and 40 arcminutes, respectively. We will do the same here. The mean value of $\langle\Sigma_{\rm LAE}\rangle$ among the 4 fields in C23 is 0.022 $(h^{-1}{\rm cMpc})^{-2}$. (We emphasize that the $\langle\ldots\rangle$ denotes the average value in one field as defined above.) The LAE fields in all of our models are calibrated to match approximately this mean value. To achieve this, we perturb $v_{\rm off}$ by a constant value for all fields in a given model. After these adjustments, the average values of $\langle\Sigma_{\rm LAE}\rangle$ are in the range $0.021 - 0.022$ $(h^{-1}$ Mpc$)^{-2}$ in all of the models presented below.

3.3 Reionization Models

In this section we describe our source models (§3.3.1) and how they are calibrated to satisfy the empirical boundary conditions for reionization provided by quasar absorption spectra measurements (§3.3.2).

3.3.1 Source models

In what follows we will compare results from the following source models.

- $\dot{N}_{\rm ion} \propto L_{\rm UV}$ (green): This model adopts the standard assumption that the rate of ionizing photon production of a galaxy is proportional to its UV luminosity, $\dot{N}_{\rm ion} \propto L_{\rm UV}$. The constant of proportionality relating $L_{\rm UV}$ to $\dot{n}_{\rm ion}$ is a redshift-dependent free parameter that we tune to achieve agreement with quasar absorption spectra measurements at $z = 4.8 - 6$ (primarily the mean Lyα forest flux), as we show in the

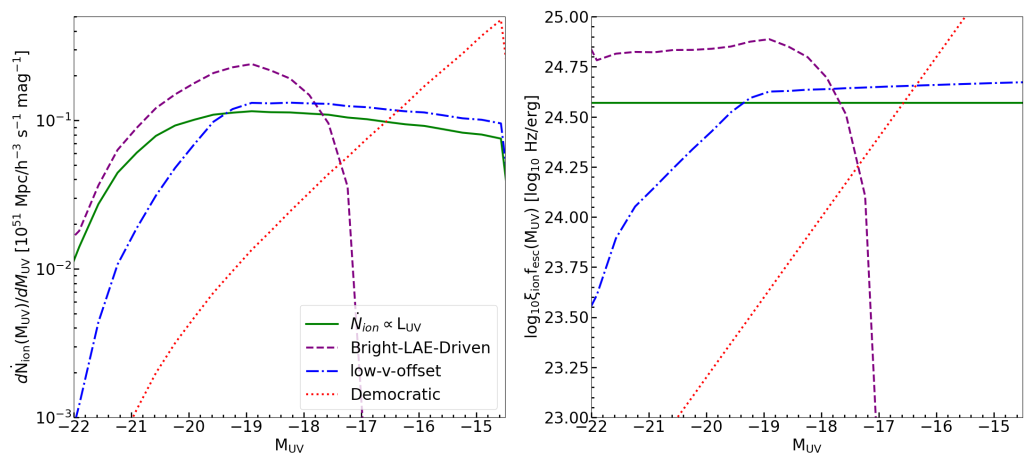

Figure 3.1: Ionizing photon output at $z = 5.7$ in our four source models. *Left:* Contribution to the ionizing emissivity per unit UV magnitude. *Right:* product of effective ionizing photon production efficiency and LyC escape fraction, $\xi_{\rm ion} f_{\rm esc}$, defined to be the ratio of the ionizing emissivity to the UV luminosity density. The models span a wide range of possibilities for the sources of reionization. For instance, in the BRIGHT-LAE-DRIVEN model, the observed UV-bright LAEs are the sole leakers of ionizing radiation. In the DEMOCRATIC model, the sources are predominantly the faintest galaxies in the UV luminosity function, well below current detection limits. We use these models to explore how different assumptions about reionization's sources affect the opacity-density relation.

next section. The left panel of Figure 3.1 shows how the ionizing emissivity varies across the source population for all of our models at $z = 5.7$, as a function of absolute UV magnitude, $M_{\rm UV}$. The right panel shows the ratio of the emissivity to the UV luminosity density, which we defined to be $\xi_{\rm ion} f_{\rm esc}$, the product of the effective ionizing photon production efficiency and escape fraction for the model. Notably, $\xi_{\rm ion} f_{\rm esc}$ is independent of the UV magnitude for this model. (We emphasize that $\xi_{\rm ion} f_{\rm esc}$ does evolve with redshift.)

- BRIGHT-LAE-DRIVEN (purple): This model assumes that the LyC leakers are the observed UV-bright LAEs. In contrast to the $\dot{N}_{\rm ion} \propto L_{\rm UV}$ model, the ionizing emissivity of a galaxy is assumed proportional to its Lyα luminosity, $\dot{N}_{\rm ion} \propto L_{\rm Ly\alpha}$. Following Ref. [519], we assume that only LAEs with $L_{\rm Ly\alpha} \geq 10^{42.2}$ erg/s contribute, and we randomly exclude 50% of the galaxies in this subset. The latter exclusion is motivated by the findings of Ref. [583] that roughly half of their sample from the $z \approx 2$ X-SHOOTER survey have a median LyC escape fraction of $f_{\rm esc}^{\rm LyC} \approx 50\%$, with the other half being non-leakers. Again, the proportionality between $\dot{N}_{\rm ion}$ and $L_{\rm Ly\alpha}$ is a redshift-dependent free parameter that we tune to achieve agreement with $z = 4.8 - 6$ quasar absorption spectra measurements.

- LOW-V-OFFSET (blue): This model also assumes $\dot{\rm N}_{\rm ion} \propto L_{\rm Ly\alpha}$. The distinguishing feature is the assumption that the LyC escape fraction is anti-correlated with the Lyα line velocity offset, $v_{\rm off}$. Again, we use the empirically calibrated $\rm M_{UV} - v_{\rm off}$ relation given by equation (3) from Ref. [515], which assigns larger $v_{\rm off}$ to more UV luminous galaxies. We then map the $v_{\rm off}$ to a LyC escape fraction using equation (2) from

Ref. [398].[5] This prescription associates high LyC leakage with strong Lyα emission at low velocity offsets from systematic. Figure 3.1 shows that this model contrasts with the BRIGHT-LAE-DRIVEN model in that many of the ionizing photons come from UV-fainter LAEs.

- DEMOCRATIC (red): In this model, we assume that every galaxy contributes the same emissivity, i.e. $\dot{N}_{\rm ion}$ is independent of $L_{\rm UV}$ and $L_{\rm Ly\alpha}$. The main purpose of this simplistic model is to provide an extreme example where the faintest galaxies dominate the ionizing photon budget (see Figure 3.1), contrasting against the models above.

The above models are used to test how different assumptions about the sources affect the opacity-density relation.

3.3.2 Model Calibration

To ensure that each reionization model satisfies the empirical boundary conditions provided by quasar absorption spectra measurements, we have calibrated the ionizing emissivity history, $\dot{N}_{\rm ion}(z)$, for each source model to match the measured evolution of the mean Lyα forest flux from $z = 5 - 6$ [78]. Figure 3.2 shows the results of these calibrations. Starting in the upper left corner, and moving clockwise, we show the: 1) ionizing emissivity; 2) reionization history; 3) mean fraction of transmitted flux in the Lyα forest; 4) IGM temperature at mean density; 5) mean free path at wavelength 912 Å; and 6) CMB electron scattering optical depth, τ_{es}. We find that by calibrating our models to match the mean

[5] As noted in Ref. [398], their relation results in $f_{esc} > 1$ for $v_{off} \lesssim 140$km/s, so we impose the limit $f_{esc} = [0, 1]$.

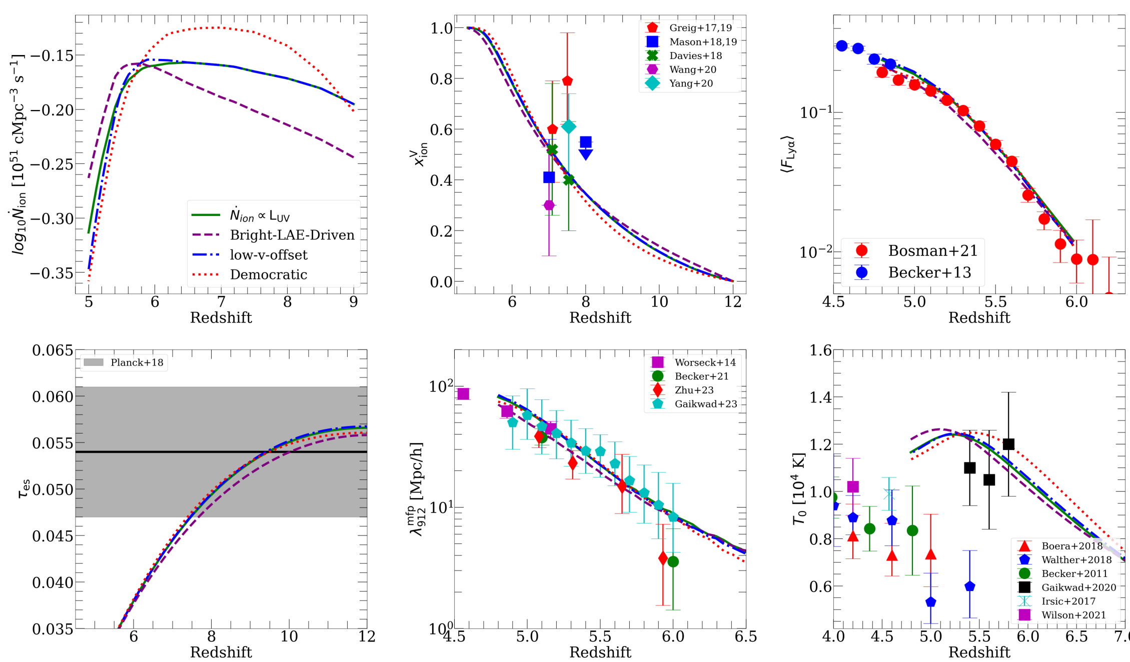

Figure 3.2: Calibration of our reionization models to match the boundary conditions provided by the Lyα forest. Starting in the upper left and moving clockwise, we show the: 1) ionizing emissivity; 2) reionization history [335, 336, 201, 811, 515, 512, 842]; 3) mean fraction of transmitted flux in the Lyα forest [59, 78]; 4) IGM temperature at mean density [54, 806, 68, 298, 822] ; 5) mean free path at wavelength 912 Å[827, 56, 297, 868]; 6) CMB electron scattering optical depth [640]. The ionizing emissivity (top-left) is adjusted as a function of redshift to match the Lyα forest mean flux evolution. Matching the mean flux yields reasonable agreement with the other observables.

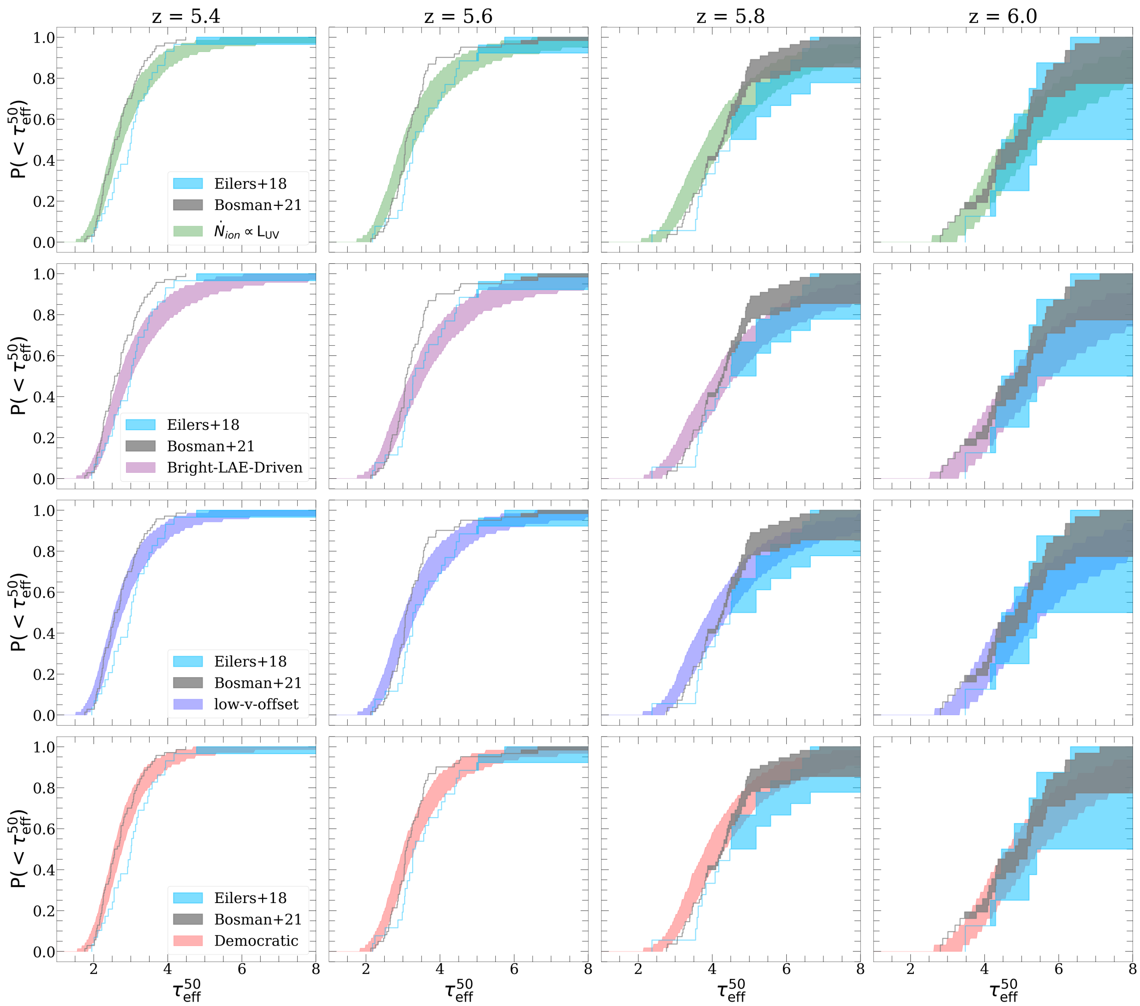

Figure 3.3: Opacity fluctuations in the Lyα forest. The panels show the CDFs of the effective optical depth, $\tau_{\rm eff}^{50}$, at redshifts annotated at the top of each panel. The cyan and gray shading shows the observational measurements of Refs. [237] and [78]. The model CDFs were obtained by bootstrap sampling using the number of sight lines in each redshift bin from [78], so are most directly comparable to the gray observational results. For each model, the colored shading encompasses 80% of the simulated CDFs.

Lyα forest flux, we consequentially recover reasonably well the other observables as well. Notably, in all models the calibration requires a steep drop in the ionizing emissivity below $z = 6$. This is qualitatively consistent with almost all other RT simulations in the literature that similarly latch onto the forest boundary conditions (see Ref. [107] for a detailed discussion).

In Figure 3.3, we compare the cumulative distribution functions (CDFs) of $\tau_{\rm eff}^{50}$ in our calibrated models against the measured distributions at $z = 5.4 - 6$ from Ref. [78], which are shown as the gray shading. For reference, we also show the measurements of Ref. [237] in cyan. The model CDFs were obtained by sampling with replacement N forest lines from our initial set of 4,000 sightlines, 500 times, where N is the number of sight lines in a given redshift bin from the measurements of Ref. [78]. The model CDFs are therefore most directly comparable to the gray observational results. The shaded regions in Figure 3.3 for the models encompass 80% of the simulated CDFs. Models in which the emissivity is sourced by brighter/rarer galaxies generally exhibit more scatter in $\tau_{\rm eff}^{50}$. This owes largely to the higher neutral fraction in those models. (For reference, the $\dot{N}_{\rm ion} \propto L_{\rm UV}$, Bright-LAE-driven, Low-v-offset, and Democratic models have $z = 5.7$ global neutral fractions of $x_{\rm HI} = 0.13$, 0.17, 0.13, and 0.1, respectively.) We note that the model CDFs are somewhat wider than the measurements of Ref. [78] across redshift. This may result from reionization ending slightly later in our simulations than the data suggests. We will return to this possibility in §3.5.

3.4 Results

3.4.1 Opacity-Density Relation

Figure 3.4 shows the LAE surface density as a function of radius from the opaque quasar sight lines with $\tau_{\rm eff}^{50} \geq 7$. This cut, which yields $200-400$ fields (depending on the model), was chosen to select analogues of the fields toward J0148 and J1250. Following C23, the surface densities for each field are normalized by their respective values of $\langle \Sigma_{\rm LAE} \rangle$. The curves show the median surface density profiles, while the dark and light shadings represent the 68% and 98% regions. The filled circles and open triangles show the measurements from J0148 and J1250, respectively, from C23. As expected, all models exhibit a strong under-density of LAEs toward the center of the field. This owes to the voids at $z = 5.7$ containing neutral islands in all of our reionization models; the most opaque segments of the Lyα forest are those that intersect the voids. The results are highly similar between the models, despite their very different ionizing source populations, highlighting the insensitivity of this statistic to the characteristics of the reionization sources.

In Figure 3.5 we show the surface density profiles around the most transmissive sight lines, which we define to be those with $2.42 \leq \tau_{\rm eff}^{50} \leq 2.92$. These bounds were chosen to have a central value of $\tau_{\rm eff}^{50} = 2.67$, similar to the mean value between J1306 and J359. The selected sample contains ~ 600 fields. In all models, the fields toward transmissive sight lines typically exhibit mild over-densities, although the scatter is large. The BRIGHT-LAE-DRIVEN model tends to exhibit stronger LAE over-densities around highly transmissive sight lines. Otherwise, the results are strikingly similar considering the large differences in the

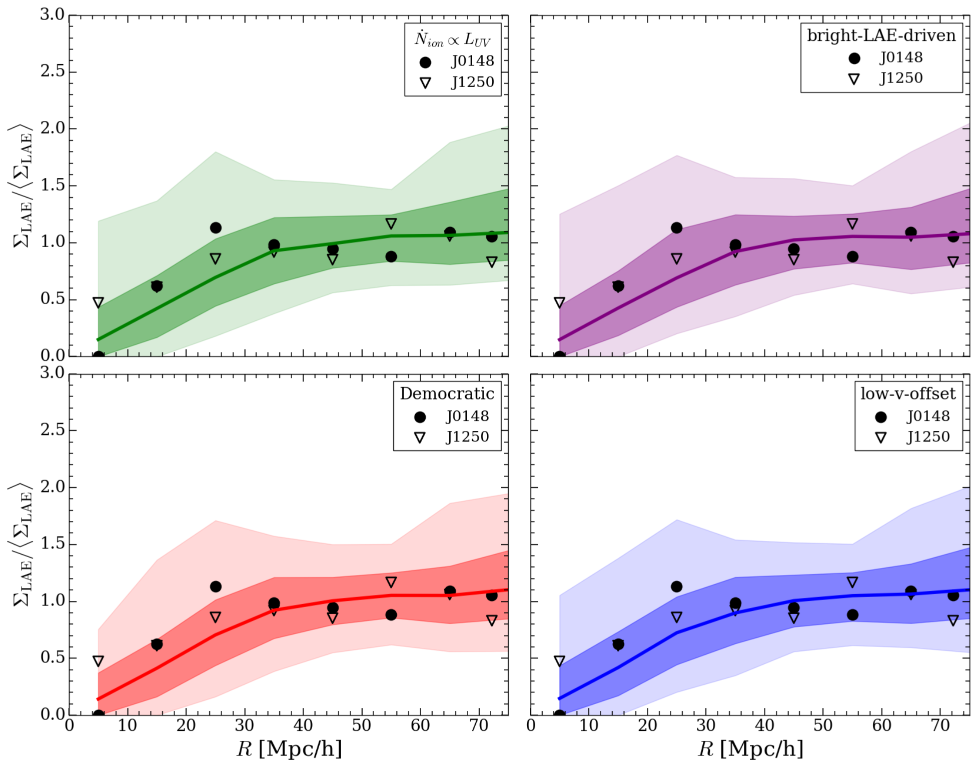

Figure 3.4: LAE surface density as a function of radius, R, from the opaque quasar sight lines ($\tau_{\rm eff}^{50} \geq 7$) in our simulated samples. The surface densities for each field are normalized by their respective values of $\langle\Sigma_{\rm LAE}\rangle$. The curves show the median profile, while the dark and light shaded regions represent the 68% and 98% ranges. The observational measurements of C23 are shown as filled circles (J0148) and open triangles (J1250). The model results are similar despite their very different assumptions about the ionizing source population. The strong under-density of LAEs near highly opaque forest segments reflects the fact that the voids contain neutral islands, which suppress the forest transmission.

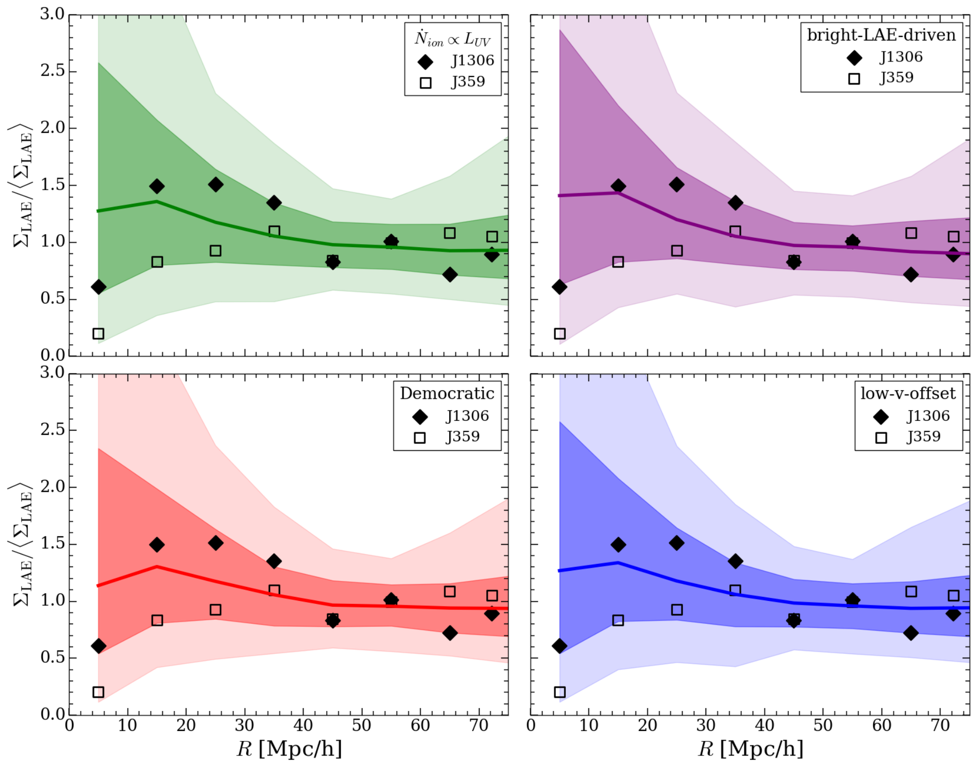

Figure 3.5: Similar to Figure 3.4, except for highly transmissive sight lines ($2.42 \leq \tau_{\rm eff} \leq 2.92$). Again, the model results are similar despite their very different assumptions about the ionizing source population.

source modeling. For instance, in the BRIGHT-LAE-DRIVEN model, it is the *observed* LAEs that provide all of the ionizing photons, whereas in the DEMOCRATIC model the photons come from galaxies well below current detection limits.

The large scatter in central LAE surface density reflects the fact that the physical conditions leading to high transmission in the forest are varied. On the one hand, the intense ionizing radiation around galaxy over-densities can lead to enhanced forest transmission. On the other hand, hot, recently reionized regions inside of the voids can be highly transmissive. More typically the transmission in average regions of the IGM is enhanced by some combination of these physical effects. Both J1306 and J359 are statistically compatible with the models given the large scatter. Notably, however, fields with the central under-density of J359 are rare in our simulations. (More about the rarity of J359 below.)

Figure 3.6 compares the opacity-density relations in our models to the four fields in C23. The surface densities are measured within a circular aperture of radius 10 cMpc/h. Again, for each field in the sample, $\Sigma_{\rm LAE}$ is normalized by its corresponding value of $\langle\Sigma_{\rm LAE}\rangle$. As expected from the previous discussion, there are only modest differences in the opacity-density relations between the models. (We note that the somewhat stronger association between low-$\tau_{\rm eff}^{50}$ sight lines and over-densities in the BRIGHT-LAE-DRIVEN model is evident in the top-right panel). These results lead us to conclude that, *for models that have been calibrated to have the same Lyα forest mean transmission*, the opacity-density relation is broadly insensitive to assumptions about which galaxies sourced the high-z ionizing background. We emphasize, however, that much of this insensitivity owes to: (1) a degeneracy between the morphology of neutral islands (which is set by the source clustering)

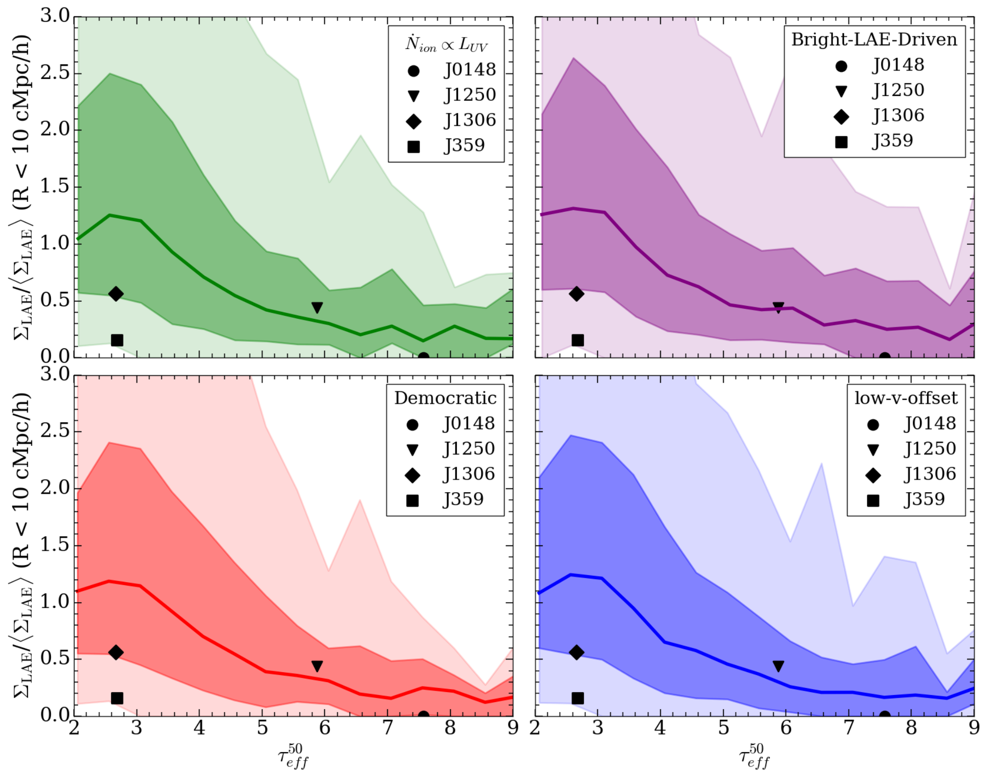

Figure 3.6: Opacity-density relation in four empirically calibrated reionization models. The curves represents the median central LAE surface density (measured within a circle of radius 10 cMpc/h) versus the $\tau_{\rm eff}^{50}$ value of the forest sight line. Dark and light shaded regions represent the 68% and 98% ranges, respectively. In the Bright-LAE-Driven model, the highly clustered nature of the sources strengthens the association between low $\tau_{\rm eff}^{50}$ sight lines and galaxy over-densities. Otherwise, the opacity-density relations are quite similar. Strongly under-dense but highly transmissive fields such as the one toward J359 are rare in all of the models, but their probability increases substantially if reionization ends slightly earlier (see §3.5).

and the global neutral fraction; (2) the models being calibrated to have the same Lyα forest mean transmission. As mentioned above, this calibration forces the $\dot{N}_{\rm ion} \propto L_{\rm UV}$, Bright-LAE-driven, Low-v-offset, and Democratic models to have $z = 5.7$ global neutral fractions of $x_{\rm HI} = 0.13$, 0.17, 0.13, and 0.1, respectively. But these differences in $x_{\rm HI}$ largely cancel differences that would otherwise arise from the different morphologies of neutral islands in the models. We demonstrate this in Appendix 3.8, by comparing the Democratic and Bright-LAE-driven models at fixed $x_{\rm HI}$. We find that the neutral islands are more clustered in the latter such that, at fixed $x_{\rm HI}$, there are significant differences in the opacity-density relation at the low-$\tau_{\rm eff}^{50}$ end. This highlights the strong degeneracy between the effects of source clustering and the global neutral fraction. It would be difficult to constrain the source clustering from the opacity-density relation alone, without tight (better than a few percent in $x_{\rm HI}$) constraints on the global neutral fraction.

We return to the question of the rarity of J359 (square data point), whose central LAE surface density falls near the lower boundaries of the expected ranges from our models. C23 report 1 LAE within a circle of radius of 10 cMpc/h, although there is another LAE just outside of this circle (see their Figure 6). To quantify how rare this sight line is, we compute the probabilities of finding ≤ 1 (2) LAEs within a circle of this radius in our models. We find probabilities of ≈ 4 (9)% in all of our models. These probabilities are likely to be sensitive to the reionization history. For instance, if reionization ended somewhat earlier than in our models, there would be fewer neutral islands in the voids and more patches of hot, recently reionized gas there. In this case, we would expect a higher probablity of observing a field like the one toward J359. We will demonstrate this point explicitly in §3.5.

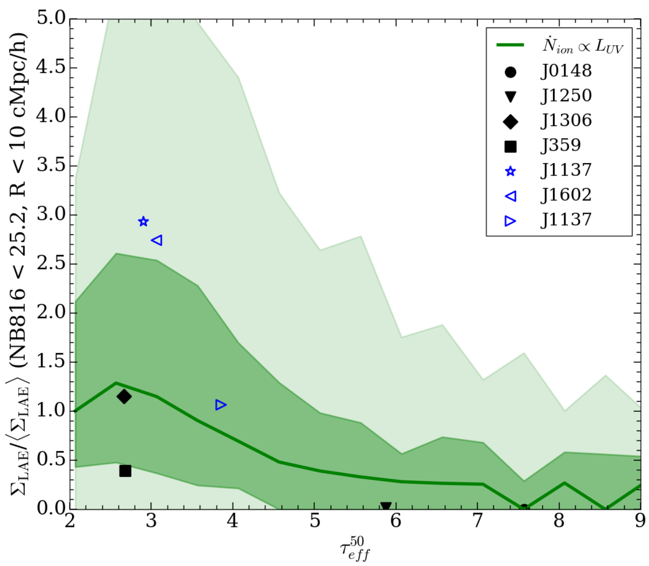

Figure 3.7: Opacity-density relation compared to an expanded set of measurements including the fields observed in Ref. [397]. For this comparison, we apply the limiting magnitude of NB816 $\leq$ 25.2 from Ref. [397] for all simulated and observed fields. (All other comparisons in this Chapter use NB816 $\leq$ 25.5 from C23.) For the fields of Ref. [397], we use the τ_{eff}^{50} reported in C23. For brevity we show only our our $\dot{\mathrm{N}}_{\mathrm{ion}} \propto \mathrm{L}_{\mathrm{UV}}$ model. The results are broadly similar in the other models.

So far we have restricted our comparisons to the fields observed in C23. Figure 3.7 adds the three fields observed by Ref. [397]. For this comparison, we apply their shallower magnitude cut of NB816 ≤ 25.2 to both our model fields and to the C23 observations. We use the $\tau_{\rm eff}^{50}$ values reported in C23 for the sight lines of Ref. [397]. Since the results are so similar across our source models, Figure 3.7 shows only our $\dot{N}_{\rm ion} \propto L_{\rm UV}$ model. The figure further demonstrates consistency between the measured sample and the model, but also highlights how deeper imaging of the fields toward transmissive sight lines in particular could help expose possible tension. For instance, the observation of more fields like that of J359 would put tension on the models.

Lastly, we note that the opacity-density relations in Figure 3.6 are markedly different from the models of Refs. [199] and [589], which are shown in C23 (see their Figure 10). In those models, the low $\tau_{\rm eff}^{50}$ sight lines are more strongly associated with over-densities. Their median $\Sigma_{\rm LAE}(R < 10~{\rm cMpc}/h)/\langle\Sigma_{\rm LAE}\rangle$ reach values around 2 for $\tau_{\rm eff} \sim 2$, and the field toward J359 falls well outside of their 98% regions. The discrepancy likely arises from differences in the structure of the ionizing radiation backgrounds in those models. Indeed, compared to our simulations, the ionizing backgrounds from the models of Ref. [589] exhibit larger fluctuations; the photoionization rate tends to be significantly higher in over-dense regions, accounting for their stronger association with low $\tau_{\rm eff}^{50}$ sight lines. In this case, the ionizing intensity fluctuations always dominate over the temperature and density fluctuations in setting the Lyα forest opacity. Fields like those of J359 and J1306, however, suggest that reionization temperature fluctuations may also play an important role. We will discuss this further in §3.4.3.

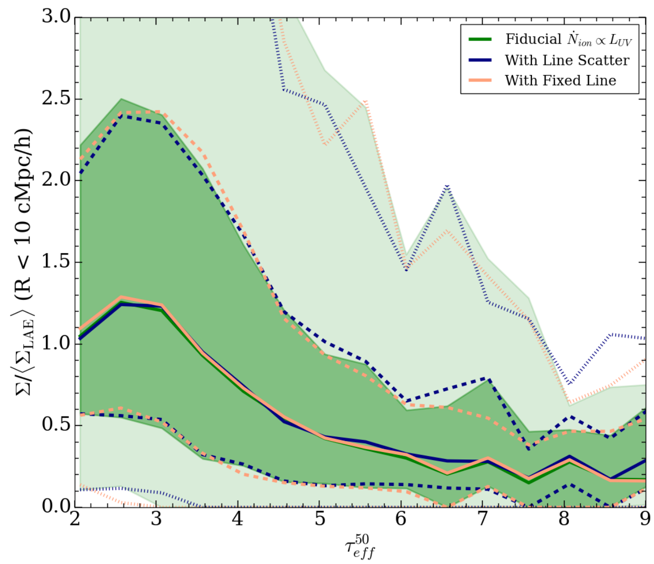

Figure 3.8: Testing how sensitive the opacity-density relation is to assumptions about the Lyα emission lines of narrow-band-selected LAEs. As in Figure 3.6, the green curve and shaded regions correspond to the median and 68/98% regions for our fiducial $\dot{N}_{ion} \propto \mathrm{L}_{\mathrm{UV}}$ model. We overlay two variations of this model. The blue curves correspond to a variation that adds scatter to the line offset (v_{off}) and width (σ_v) according to an empirically calibrated distribution of Ref. [515]. The yellow curves show a variation in which we hold $v_{\rm off}$ = 160 km/s and σ_v = 100 km/s fixed. The opacity-density relation as measured in narrow band LAE surveys is largely insensitive to the highly uncertain modelling of the Lyα line.

3.4.2 Effect of Lyα Line Properties

In this section, we address the question of how the Lyα emission line properties affect the opacity-density relation. For instance, could scatter in the line properties increase the scatter in the opacity-density relation, perhaps making sight lines like J359 less rare?

Recall that all of the models considered in the last section assume that a galaxy's rest-frame UV magnitude uniquely determines both the offset and width of its Lyα emission line (see §3.2). Here we construct two test models varying this relationship. The first variation adds scatter to the relationship. For a given $M_{\rm UV}$, we draw $v_{\rm off}$ from the distribution in equation (1) of Ref. [515], which is motivated by a collection of observational measurements of $v_{\rm off}$ from the literature (see their Fig. 2). Since we set $\sigma_v = v_{\rm off}$, this procedure also implements scatter in the line width. In the second test model, we keep $v_{\rm off}$ (and therefore also σ_v) constant for all galaxies to draw an extreme contrast with the first test model. Note that the different assumptions about the line affects the visibilities of the LAEs. LAEs for which the line offset is scattered to lower values become less likely to be visible because of IGM attenuation and inflows in the neighborhoods of galaxies. We emphasize that the physical properties of the IGM (neutral island distribution, $\Gamma_{\rm HI}$ and T fields) in these tests remain the same as before.

Figure 3.8 shows the opacity-density relations in these variations. For brevity we consider only the $\dot{\rm N}_{\rm ion} \propto {\rm L}_{\rm UV}$ reionization model. As in Figure 3.6, the green curve and contours correspond to the median and 68/98% regions for our fiducial $\dot{\rm N}_{\rm ion} \propto {\rm L}_{\rm UV}$ model. The blue and yellow solid, dashed, and dotted curves show the median and 68/98% regions for the two model variations, as indicated in the plot legend. The opacity-density relations are remarkably similar between the variations despite very different assumptions about the line properties. Indeed, introducing significant scatter to the line offset and width does not substantially add to the scatter in the relation, and under-densities around transmissive sight lines such as the one toward J359 do not become more likely.[6] In the model with line scatter we find that the probability of observing ≤ 1 (2) LAEs within a circle of radius 10 cMpc/h is 3 (8) %, compared to 4 (9) % in the fiducial model. We conclude that the opacity-density relation as measured from narrow band LAE surveys is broadly insensitive

[6] We have tested this conclusion with a model implementing more extreme scatter in the line properties as well.

	$\tau^{50}_{\rm eff,min}, \tau^{50}_{\rm eff,max}$	$\Sigma^{R<10}_{\rm LAE,min}, \Sigma^{R<10}_{\rm LAE,max}$	$N^{R<10}_{\rm LAE,min}, N^{R<10}_{\rm LAE,min}$	$\rm N_{sample}$
HIGH-$\tau_{\rm eff}$, LOW-Σ	7, ∞	0, 0.007	0, 2	212
LOW-$\tau_{\rm eff}$, LOW-Σ	2.42, 2.92	0, 0.007	0, 2	50
LOW-$\tau_{\rm eff}$, MEAN-Σ	2.42, 2.92	0.018, 0.024	6, 8	89
LOW-$\tau_{\rm eff}$, HIGH-Σ	2.42, 2.92	0.06, ∞	20, ∞	42

Table 3.1: Summary of categories for Lyα forest sight lines used in §3.4.3. The 2nd and 3rd columns give the ranges of Lyα forest effective optical depths, $\tau^{50}_{\rm eff}$, and central LAE surface densities, $\Sigma_{\rm LAE}(R < 10$ cMpc$/h)$, in units of $(\rm cMpc/h)^{-2}$, defining the categories. The 4th column provides the corresponding range in number of LAEs within $R < 10$ cMpc$/h$. The last column gives the number of sight lines in the corresponding category for the $\dot{N}_{\rm ion} \propto L_{\rm UV}$ model.

to the details of how the Lyα emission line is modeled. On the one hand, it is reassuring that the simulation predictions are so insensitive to what we assume about the sources and the Lyα emission lines. On the other hand, these results again support the conclusion that it would be difficult to use the opacity-density relation alone to learn about reionization's sources.

3.4.3 Cosmological environments of Lyα forest sight lines

We turn our attention to the physical conditions that give rise to the low and high $\tau^{50}_{\rm eff}$ sight lines in our simulations. To this end, we find it useful to define four categories detailed in Table 3.1. The field toward J0148 fits into the HIGH-$\tau_{\rm eff}$, LOW-Σ category, while J359 fits into the LOW-$\tau_{\rm eff}$, LOW-Σ category. We also introduce the LOW-$\tau_{\rm eff}$, MEAN-Σ and LOW-$\tau_{\rm eff}$, HIGH-Σ categories to span the variation in low-$\tau^{50}_{\rm eff}$ sight lines. The 2nd and 3rd columns give the ranges of $\tau^{50}_{\rm eff}$ and $\Sigma_{\rm LAE}(R < 10$ cMpc$/h)$ used to define the categories. For reference, the 4th column gives the corresponding number of LAEs within $R < 10$ cMpc$/h$, and the last column gives the number of fields in each category. In this section we show results from the $\dot{N}_{\rm ion} \propto L_{\rm UV}$ model, but the qualitative discussion applies to all of the models.

Let us begin with Figure 3.9, which visualizes a HIGH-τ_{eff}, LOW-Σ field. Starting at the top left and moving clockwise, we show the gas temperature, redshift of reionization (z_{reion}), ionized fraction (x_{ion}), and hydrogen photoionization rate (Γ_{HI}). The slices are 80×80 (cMpc/h)^2 and are averaged over a depth of 12 cMpc/h. All maps are taken at $z = 5.7$. The concentric circles represent radial increments of 10 cMpc/h. In each panel, the smaller dots show galaxies/ionizing sources while the larger stars show "observed" LAEs in the field, i.e. those that make the magnitude and color cuts described in §3.2. The large "X" denotes the centers of the fields. This field is characterized by a dearth of galaxies and LAEs within a radius of ~ 20 cMpc/h, and neutral island structure covering much of the inner field, depicted in black in the x_{ion} map, as well as in white in the Γ_{HI} map. Indeed, in general we find that HIGH-τ_{eff}, LOW-Σ sight lines are almost always centered near large neutral structures. Note that much of the Γ_{HI} field adjacent to the neutral islands reaches values as low as $\sim 10^{-14}$ s^{-1} owing to the lack of sources and the effects of shadowing by the islands (see Ref. [589] for more discussion on this shadowing effect). The gas at the boundaries of the neutral islands have $T \sim 20,000$ K, consistent with the hot temperatures behind ionization fronts [188].

Next we examine the LOW-τ_{eff}, LOW-Σ field shown in Figure 3.10. This field contains more LAEs than the one in Figure 3.9, but the center of the field is also under-dense in sources/LAEs. Together, the maps reveal what gives rise to the high Lyα forest transmission at the center of the map. The center intersects a cosmological under-density that was recently reionized, as indicated by the adjacent neutral island and the hot $\sim$

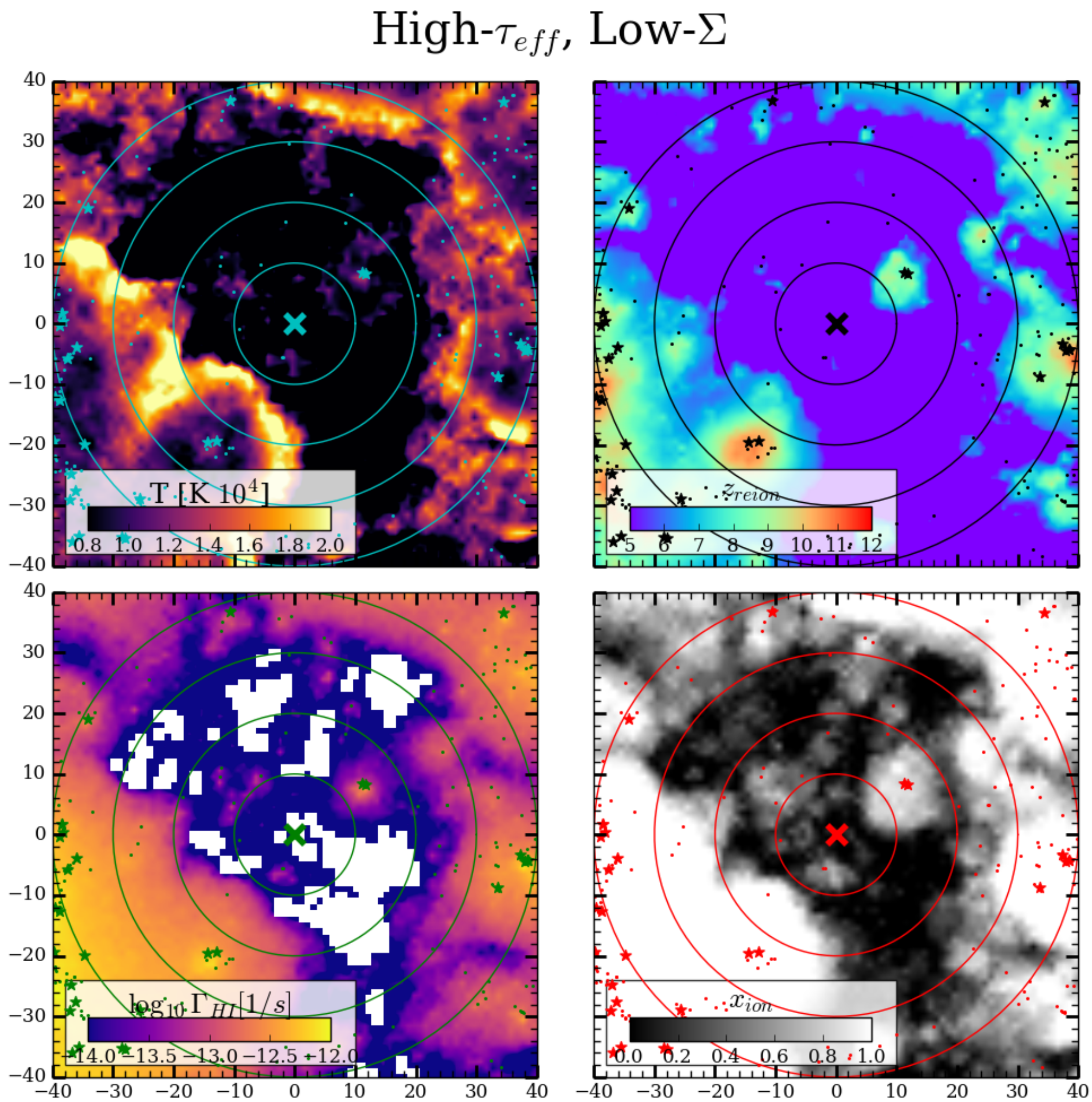

Figure 3.9: Physical environment of a HIGH-$\tau_{\rm eff}$, LOW-Σ field, such as the one toward J0148. All plots in this section use the $\dot{N}_{\rm ion} \propto L_{\rm UV}$ model, but the qualitative discussion applies to all of the models. Starting in the upper left and moving clockwise, the maps show temperature (T), redshift of reionization ($z_{\rm reion}$), ionized fraction ($x_{\rm ion}$), and hydrogen photoionization rate ($\Gamma_{\rm HI}$). Distances on the axes are in cMpc/h and slices have been averaged over a depth of 12 cMpc/h. The small dots show galaxies (ionizing sources), while the stars show "observed" LAEs in our mock surveys, i.e. those passing the magnitude and color cuts. The large "X" denotes the centers of the fields. Concentric circles correspond to radial increments of 10 cMpc/h. HIGH-$\tau_{\rm eff}$, LOW-Σ fields are characterized by large neutral structures near the center of the field and low $\Gamma_{\rm HI}$values.

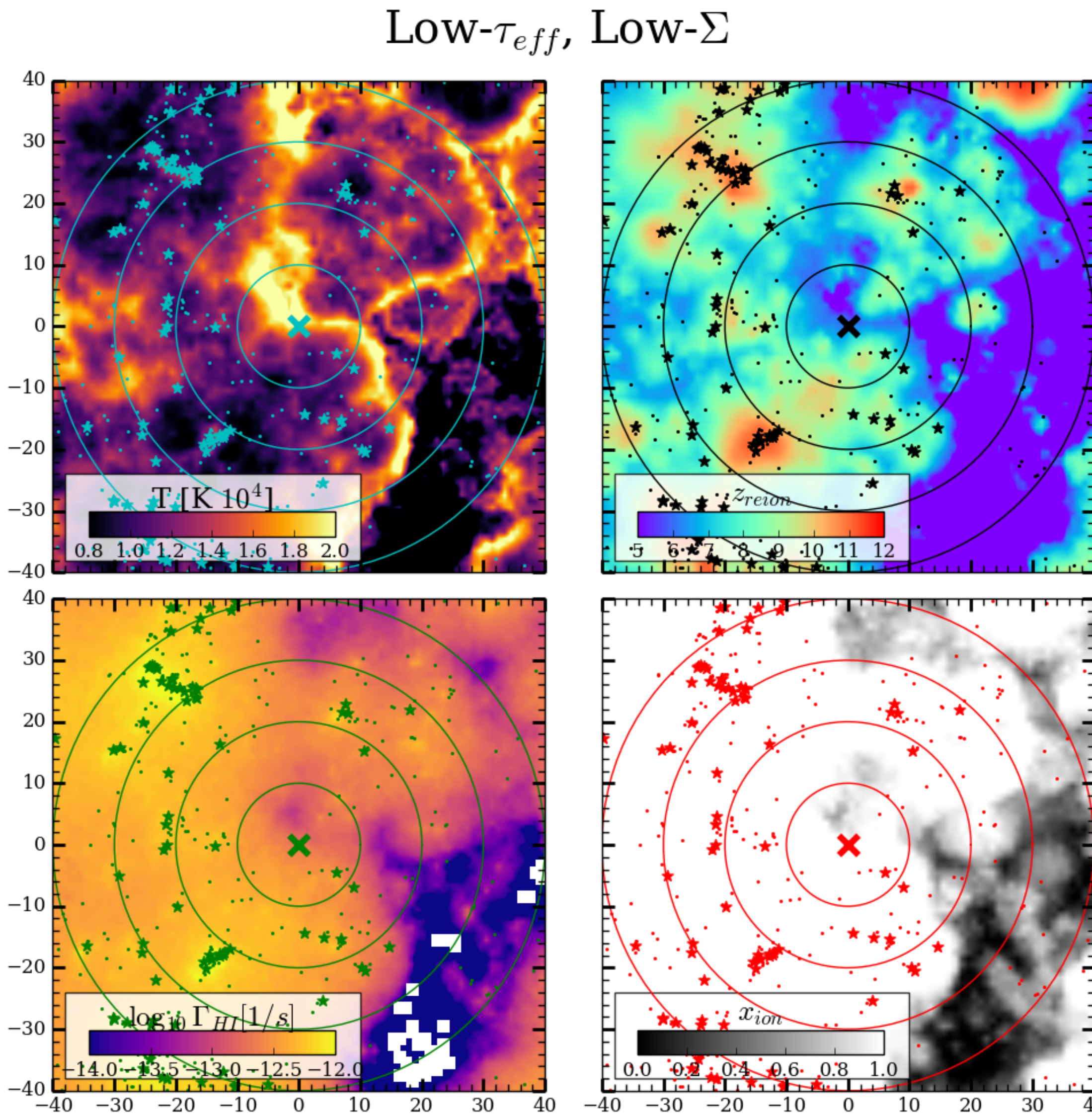

Figure 3.10: Same as in Figure 3.9, but for a Low-$\tau_{\rm eff}$, Low-Σ field. The field around J359 fits into this category. These fields are characterized by hot ($T \sim 20,000$ K), recently reionized, under-dense gas in their centers. Another important characteristic is that there are clear lines of sight from the center to over-densities of sources, such that $\Gamma_{\rm HI}$ is not suppressed there.

$20,000$K temperatures of the gas. In fact, as we will demonstrate below, most sight lines in the LOW-$\tau_{\rm eff}$, LOW-Σ category exhibit enhanced central temperatures from recently reionized gas. Another important characteristic is that there are clear lines of sight from the center to over-densities of sources (in this case to the upper and lower left), such that $\Gamma_{\rm HI}$ is not suppressed by shadowing effects. The combination of these factors leads to enhanced forest transmission at the center of the field.

The majority of fields around low-$\tau_{\rm eff}^{50}$ sight lines have $\Sigma_{\rm LAE}(R < 10$ cMpc/$h)$ close to the mean value (see Fig. 3.6). Figure 3.11 visualizes an example of a LOW-$\tau_{\rm eff}$, MEAN-Σ field. The most distinct feature is the large over-density of sources 20 cMpc/h northwest of the center. Compared to the LOW-$\tau_{\rm eff}$, LOW-Σ field in Figure 3.10, $\Gamma_{\rm HI}$ plays a larger role in enhancing the Lyα forest transmission. The central region is situated between the source over-density and the reionizing neutral island in the southwest quadrant. Examining other fields in our LOW-$\tau_{\rm eff}$, MEAN-Σ category, we find some like the one in Figure 3.11, but others in which the hotter temperatures from recently reionized gas has a more prominent effect. The diversity of this category highlights that both $\Gamma_{\rm HI}$ and T can play important roles.

Lastly, we consider a LOW-$\tau_{\rm eff}$, HIGH-Σ field in Figure 3.12. The center of the field exhibits a strong over-density of sources and correspondingly enhanced $\Gamma_{\rm HI} \sim 10^{-12}$ s^{-1}. The $z_{\rm reion}$ field indicates that the center was one of the first regions to be reionized in the simulation at around $z = 10 - 12$. As such, this region has cooled to temperatures of $T \sim 8,000$ K by $z = 5.7$. However, the high $\Gamma_{\rm HI}$ values overcome the cosmological over-density and colder temperatures to produce enhanced Lyα forest transmission at the

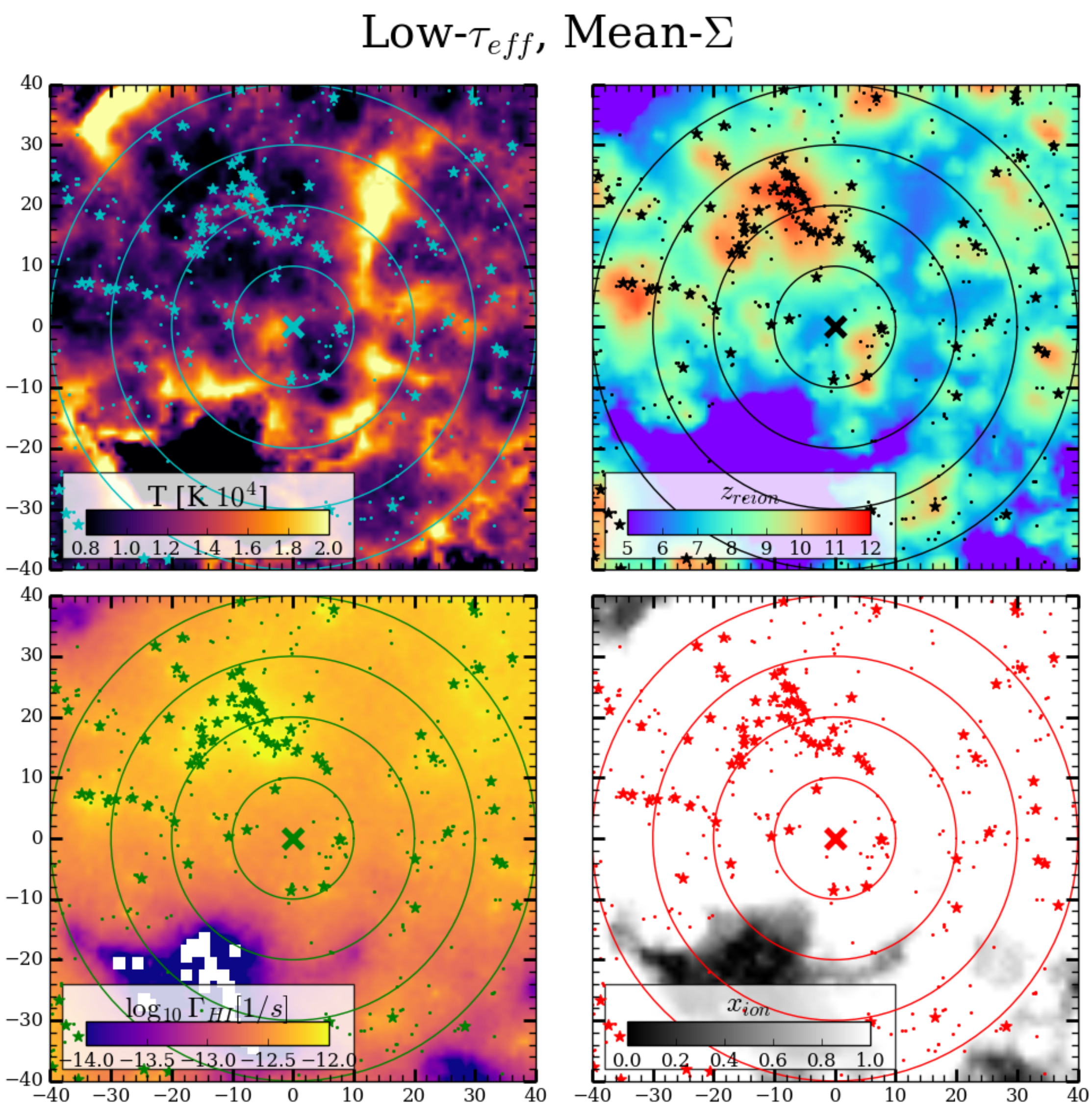

Figure 3.11: Same as in Figure 3.9, but for a Low-$\tau_{\rm eff}$, Mean-Σ field. The fields in this category are more mixed in the effects of $\Gamma_{\rm HI}$ versus T. In some fields, the proximity to an over-density of sources (and hence higher values of $\Gamma_{\rm HI}$) is the larger effect for enhancing the forest transmission. In other cases, the hotter temperatures from recently reionized gas is the larger effect. In this figure we show an example of the former.

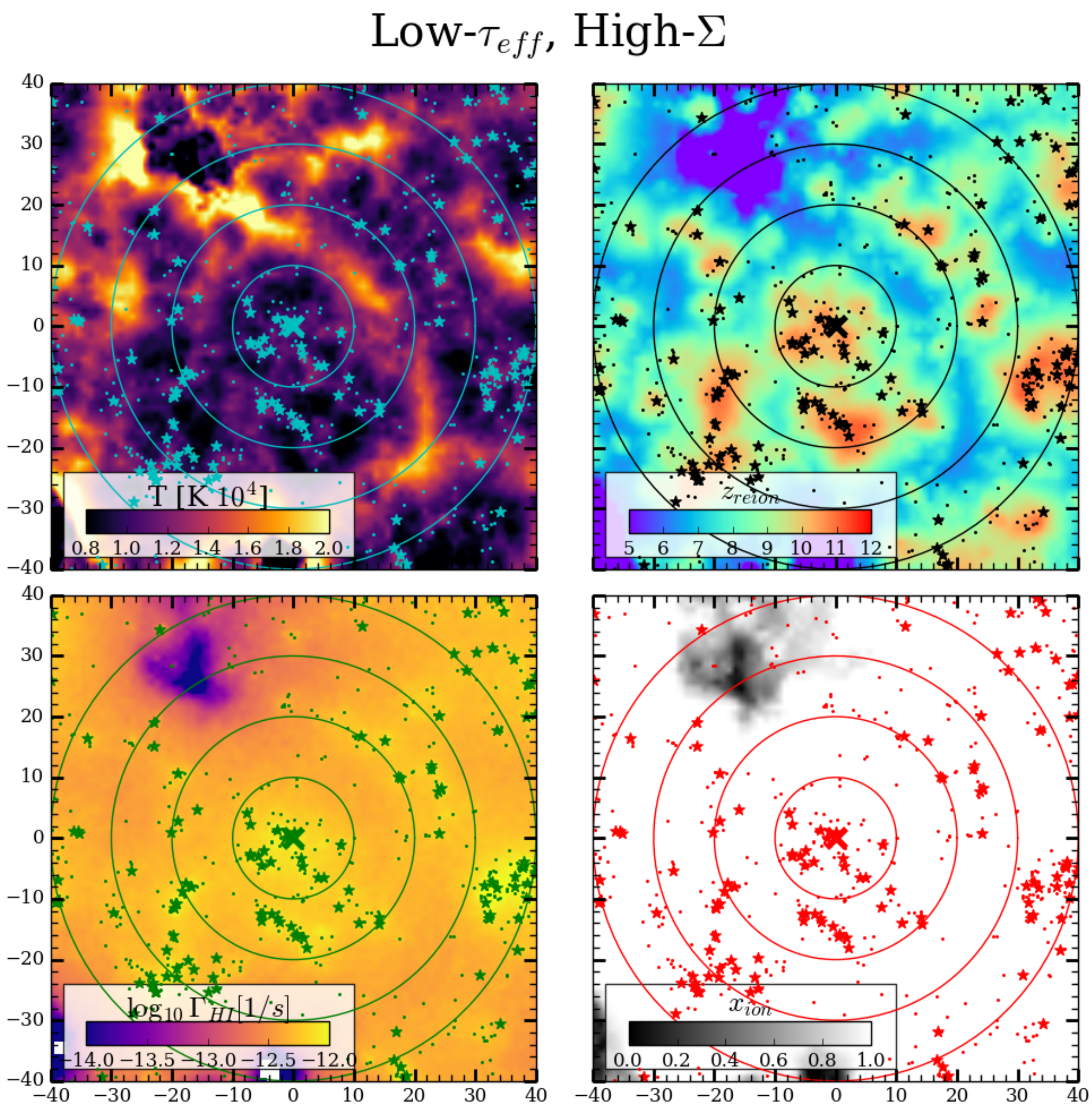

Figure 3.12: Same as in Figure 3.9, but for a Low-$\tau_{\rm eff}$, High-Σ field. The intense ionizing radiation in an over-density of sources is what drives the forest transmission in these fields. Such over-densities were reionized earlier, and therefor exhibit cooler gas temperatures.

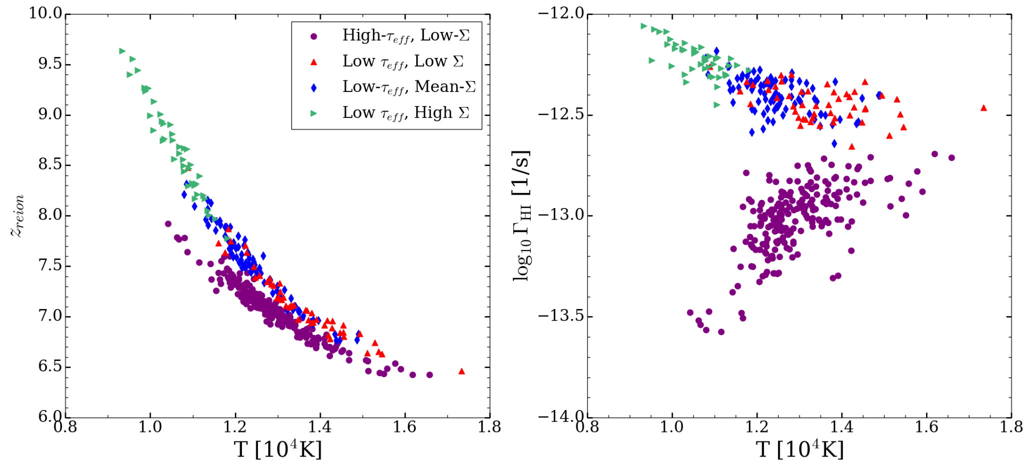

Figure 3.13: Physical properties at the centers of fields in our four categories (defined in Table 3.1). We average the temperature (T), redshift of reionization ($z_{\rm reion}$), and hydrogen photoionization rate ($\Gamma_{\rm HI}$) in fully ionized cells within a cylinder of radius 10 cMpc/h and depth of 30cMpc/h, centered on the simulated Lyα forest sight line. The depth roughly corresponds to the narrow band filter NB816 width. Each data point corresponds to a single field. The left panel displays the $z_{\rm reion}$-T plane and the right panel displays the $\Gamma_{\rm HI}$-T plane. Fields from the different categories occupy different regions of these planes, depending on the physical conditions giving rise to the Lyα forest transmission or absorption.

center of the map. We note that these types of fields dominate the transmissive end of the opacity-density relation in the strong intensity fluctuation models of Refs. [199, 589].

Figure 3.13 attempts to show more quantitatively the physical conditions giving rise to the fields in our four categories. Here we consider the central values of T, $z_{\rm reion}$, and $\Gamma_{\rm HI}$. We average these quantities in fully ionized cells within a cylinder of radius 10 cMpc/h and depth of 30cMpc/h, centered on the simulated Lyα forest sight line. The depth was chosen to span roughly the full width at half maximum (FWHM) of the narrow band filter, NB816. The data points in Figure 3.13 show each field within the four categories in the $z_{\rm reion} - T$ and $\Gamma_{\rm HI} - T$ planes.

Consider first the HIGH-$\tau_{\rm eff}$, LOW-Σ fields shown as the purple circles in Figure

3.13. As expected from our previous discussion, their central regions contain gas that was reionized more recently, with average values $z_{\rm reion} \lesssim 8$. Naturally the average central T is on the hotter side of the range. (Recall that our averaging procedure excludes the neutral islands.) On the other hand, the right panel shows that the average $\Gamma_{\rm HI}$ in this gas is lower than in the other categories. These characteristics are consistent with our previous discussion that the HIGH-$\tau_{\rm eff}$, LOW-Σ fields contain neutral islands. The gas bordering the neutral islands are recently reionized and hot, but the $\Gamma_{\rm HI}$ is suppressed in regions between the neutral islands because of shadowing effects. Next, consider the LOW-$\tau_{\rm eff}$, LOW-Σ fields (red triangles). These are also among the hot, more recently reionized regions. Note, however, that the average central $\Gamma_{\rm HI}$ values are on the higher side of the range. Again, this is consistent with our previous discussion on how the low densities, hot temperatures, and higher values of $\Gamma_{\rm HI}$ combine to produce enhanced Lyα forest transmission. Similar remarks apply to the LOW-$\tau_{\rm eff}$, MEAN-Σ fields (blue diamonds), although $\Gamma_{\rm HI}$ is likely to play a larger role in producing the forest transmission for these sight lines. Lastly, the LOW-$\tau_{\rm eff}$, HIGH-Σ fields (green triangles) clearly correspond to the colder regions with enhanced $\Gamma_{\rm HI}$ that were reionized earliest. The ionizing background in those regions is strong enough to overcome the local over-density and colder temperatures to produce enhanced transmission. These results shed light into the physical conditions giving rise to the fields in our samples.

3.5 Sensitivity to the Reionization History

In §3.4.1, we alluded to the idea that the opacity-density relation could be sensitive to the reionization history. We demonstrate this here. For this task we use three additional

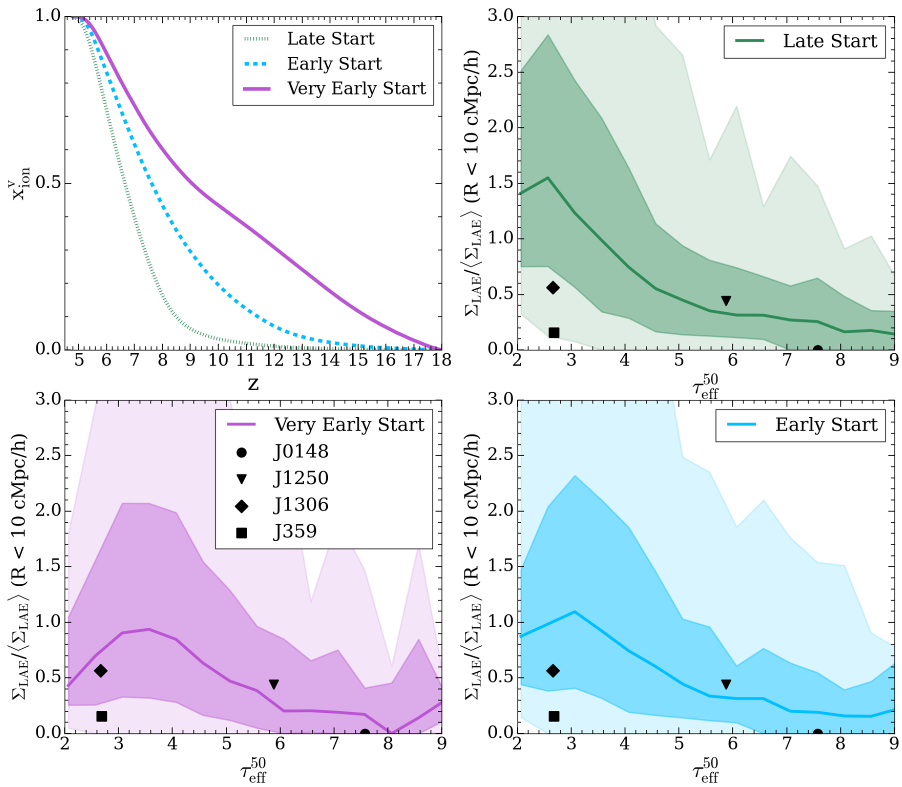

Figure 3.14: Effect of the reionization history on the opacity-density relation. The top-left panel shows the reionization histories for the three additional simulations considered in §3.5, as annotated in the legend. All three models have been calibrated to match measurements of the mean Lyα forest transmission at $z \leq 6$, but they have very different reionization histories overall. At $z = 5.7$, the Late Start, Early Start, and Very Early Start models have global neutral fractions of $x_{\rm HI} = 17$, 10, and 6 %, respectively. When the neutral fraction is lower, the larger physical cross section of hot, recently reionized gas in the voids increases the likelihood that the most transmissive forest sight lines intersect galaxy under-densities. Hence the low-$\tau_{\rm eff}^{50}$ end of the opacity-density relation is particularly sensitive to the timing of reionization's ending phases.

reionization simulations with varied reionization histories. To save computational time, the simulations used in this section were run with monochromatic RT. Photons were assigned an energy of $E_\gamma = 19$ eV to match the frequency-averaged H photoionization cross section of a power-law spectrum with $J_\nu \propto \nu^{-1.5}$ between 1 and 4 Ry. We adopt a source model similar to the $\dot{N}_{\rm ion} \propto L_{\rm UV}$ used in previous sections.[7] The top-left panel of Figure 3.14 shows the reionization histories of the three simulations. As before, the simulations have been calibrated to agree with the observed mean Lyα forest transmission at $z < 6$. (We do not show a plot here for brevity.) Note that the reionization histories differ significantly between the models, particularly in the earlier phases at $z > 7$. From here on we adopt the following names for the models shown with the green/dotted, cyan/dashed, and purple/solid curves: Late Start, Early Start, and Very Early Start, respectively. Importantly for this discussion, the variations in the $z > 7$ reionization histories result in different neutral fractions at $z = 5.7$ at roughly fixed Lyα forest transmission. The Late Start, Early Start, and Very Early Start models have global neutral fractions at $z = 5.7$ of $x_{\rm HI} = 17$, 10, and 6 %, respectively. We emphasize that these models have a fixed source clustering since they all adopt the $\dot{N}_{\rm ion} \propto L_{\rm UV}$ model.

The remaining panels in Figure 3.14 compare the opacity-density relations between the three models. As anticipated, there are significant differences in the opacity-density relations at the low-$\tau_{\rm eff}^{50}$ end. Under-densities around highly transmissive sight lines at $z = 5.7$ (such as in J1306 and J359) become significantly more likely if the global neutral

[7]There is one significant difference in the source modeling. Here we will explore models in which reionization begins significantly earlier than in our fidicial simulations. To maximize the number of halos in the box at these high redshifts ($z > 15$), we use halos down to a minimum halo mass of $M_{\rm min} = 1 \times 10^9\ h^{-1}\ {\rm M}_\odot$ in this section. Our halo mass function is only 50% complete at this lower minimum mass. We note, however, that in reality the drop-off in star formation efficiency cannot be perfectly sharp in halo mass anyways.

fraction is lower, in better agreement with the data. For instance, in the Late Start model, we find a probability of just 3% for observing ≤ 1 LAE within a circle of radius $R = 10$ cMpc/h (such as in J359). This probability increases to 9% in the Early Start model, and to 15% in the Very Early Start model. The increase in probability occurs because the likelihood of intersecting hot, recently reionized gas in the voids increases if the neutral islands are smaller, i.e. when the global neutral fraction is lower. It follows from our discussion in §3.4.3 that the likelihood of observing sight lines like J359 increases under these conditions.

Aside from the poor statistics of the current opacity-density measurements, some significant caveats prevent us from drawing the conclusion that the Very Early Start model is favored. There are other things besides the early ionization in this model that could also result in a lower neutral fraction at $z = 5.7$ for a fixed Lyα forest flux. For instance, one effect likely at play is the numerical convergence of the Lyα forest in our simulations. As mentioned in §3.2, we have applied the convergence correction factors in Table A1 of Ref. [187] to our simulated Lyα forests. As shown in Ref. [107], for a fixed Lyα forest flux, this procedure has the effect of requiring a larger neutral fraction; reionization has to end later than a simulation without the correction procedure. While it is clear that some correction for resolution is needed, it is possible that we have over-corrected our simulations. Table A1 of Ref. [187] suggests that, if anything, our correction factors may not be large enough. But those factors were obtained from a suite of convergence tests in smaller boxes with $L = 25$ cMpc/h, and it is unclear how the correction factors would change in a larger box. Other effects that could lower the $z = 5.7$ neutral fraction at fixed Lyα forest flux include the spectra and clustering of the ionizing sources. Ref. [107] found that, for a fixed Lyα forest flux evolution, reionization can end by as much as $\Delta z_{\rm end} \sim 0.5$ earlier in models with a harder ionizing spectrum and less biased sources. It is possible that some combination of these effects would remove the requirement of significant ionization at $z > 10$ that our models suggest. This discussion highlights some of the key uncertainties and degeneracies that would need to be addressed before one could draw robust inferences on reionization.

In summary, we have shown that the frequency of sight lines like J359 is sensitive to the global neutral fraction at $z = 5.7$. Indeed, if more under-dense fields are observed around the most transmissive Lyα forest sight lines, the frequency of these sight lines could be used to put model-dependent upper limits on the neutral fraction.

3.6 Conclusion

Observations of quasar absorption spectra provide strong evidence that the ending phases of reionization extended below $z = 6$. The opacity-density relation is a key observational test of this scenario. Using narrow-band surveys of $z \approx 5.7$ LAEs centered on quasar sight lines, C23 found that two of the most transmissive forest segments at this redshift intersect under-densities in the galaxy distribution. For example, the field of quasar J359 has just one LAE within a radius of 10 cMpc/h. These findings appear to be tension with the late reionization models of Ref. [589], which predict that the vast majority of the most transmissive forest segments should intersect galaxy over-densities, where the ionizing background is strongest. In this Chapter, we have used RT simulations to explore in more detail the opacity-density relation predicted by late reionization models.

We found that the opacity-density relation's transmissive end is sensitive to the amount of neutral gas in the voids, as well as its morphology, where the latter is set by the clustering of reionization sources. These effects are, however, largely degenerate with each other. We demonstrated this with four models that make very different assumptions about reionization's sources. For instance, in one model, the *observed* LAEs are the sole leakers of ionizing radiation. In another model, the sources are predominantly the faintest galaxies in the UV luminosity function, well below current detection limits. We found that the four models yield very similar opacity-density relations when their reionization histories have been calibrated to match Lyα forest mean flux measurements at $z < 6$. At fixed mean flux, the models have different neutral fractions, which largely offsets the differences in neutral island morphologies caused by source clustering.

We examined the ionization and thermal states of intergalactic gas in the fields of the most transmissive and opaque forest segments in our simulations. As anticipated, the fields of highly opaque segments with $\tau_{\rm eff} \geq 7$ are likely to be centered on a cluster of neutral islands. Highly transmissive forest segments that intersect galaxy under-densities (like J359) are typically associated with regions that were recently reionized. In this case, the Lyα forest transmission is boosted by the low cosmological density and hot temperature of the recently reionized gas. On the other hand, highly transmissive forest segments that intersect galaxy over-densities are typically associated with the earliest regions to re-ionize. There, the forest transmission owes to the strong ionizing radiation background from the over-density of sources. Lastly, highly transmissive sight lines that intersect average galaxy densities (the majority of transmissive sight lines in our simulations) originate from a range of environments. Sometimes the hot temperatures of recently reionized gas boost the transmission; other times, it is the enhanced $\Gamma_{\rm HI}$ from proximity to an over-density of ionizing sources.

Highly transmissive $z \approx 5.7$ forest segments that intersect galaxy under-densities are more common in our RT simulations than in the models of Ref. [589]. To quantify the prevalence of such fields, we calculated the probability of observing a sight line like that of J359. We found that the probability of observing ≤ 1 (2) LAEs within a radius of 10 cMpc/h from a forest segment with $\tau_{\rm eff}^{50} \approx 2.67$ is ≈ 4 (9)% in the four source models mentioned above. (Again, that the probabilities are the same for these models owes to the degeneracy between neutral fraction and neutral island morphology, and the calibration to the observed mean forest flux.) We conclude that fields like the one toward J359 are rare in our late reionization simulations, but nonetheless compatible with them. Interestingly, we found that the frequency of such fields is sensitive to the exact timing of reionization for fixed source clustering. For instance, we constructed two models with different neutral fractions at $z = 5.7$, but adopting the same source clustering model. Both models have nearly identical Lyα forest mean flux evolutions at $z < 6$, in agreement with measurements. The probability of observing a field like J359 is 15% in one model with neutral fraction $x_{\rm HI} = 5\%$ at $z = 5.7$, three times more likely than in the other model with $x_{\rm HI} = 15\%$. The frequency of fields like J359 could in principle be a useful complementary probe of the global neutral fraction in the tail of reionization.

Lastly, we tested whether the opacity-density relation measured in narrow-band LAE surveys depends on assumptions about the Lyα emission lines of the LAEs (e.g. scatter in the line offsets and widths). We found that the relation is insensitive to wide variations in the line properties. This demonstrates that the predicted narrow-band opacity-density relations from simulations are robust to some of the most uncertain modeling choices.

3.7 Appendix: Insensitivity to Ray Tracing Noise

In this appendix we demonstrate that ray tracing discreteness noise does not affect our main conclusions on the opacity-density relation. For the simulations in this paper, FlexRT has been configured to merge rays at HealPix level $l = 0$, which corresponds to tracking the radiation field with 12 unique directions in each cell. The finite number of rays leads inevitably to discreteness noise which can be seen as the graininess in the left panel of Figure 3.15. (The random rotations of the unit sphere performed at each time step translates into noise what would otherwise be spurious patterns in the RT fields.) There we show a cross section of the $z = 5.7$ $\Gamma_{\rm HI}$ field in our $\dot{N}_{\rm ion} \propto L_{\rm UV}$ model. The cross section is RT cell thick ($\Delta x = 1$ cMpc/h), and spans the entire box in width. In FlexRT, the level of this noise depends on the HealPix level of the ray merging, as well as the number of rays per cell that are "exempt" from merging. In our runs, the latter is 16, such that the maximum number of rays per cell is $12 + 16 = 28$.

To test the effect of ray tracing noise on our main results, we construct two other versions of the $\Gamma_{\rm HI}$ field: 1) we average $\Gamma_{\rm HI}$ from multiple RT steps over a time window shorter than the typical cell-crossing time of ionization fronts. Specifically, we average over 16 RT time steps corresponding to $\delta z \approx 0.05$ around $z = 5.7$. Note that in this case we still merge at HealPix level $l = 0$ (12 directions); 2) We have run version of the $\dot{N}_{\rm ion} \propto L_{\rm UV}$

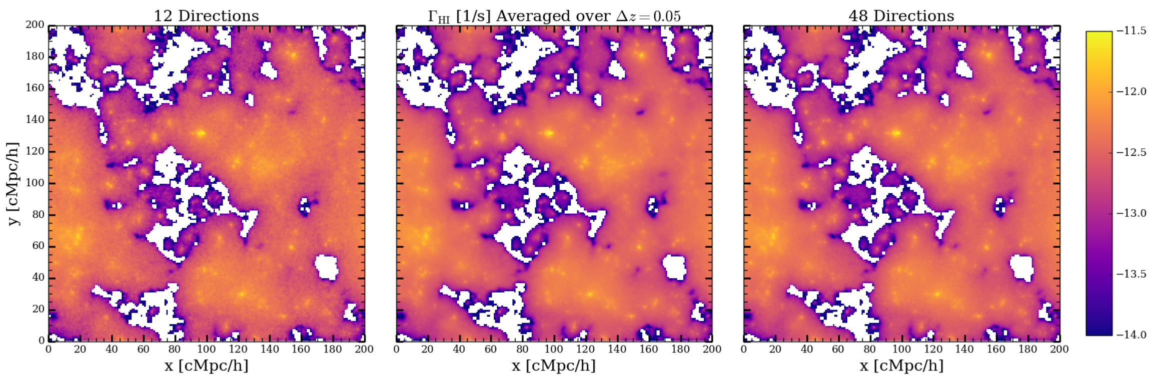

Figure 3.15: Ray tracing noise in RT simulations of reionization. *Left :* cross section through the $z = 5.7$ $\Gamma_{\rm HI}$ field in our $\dot{N}_{\rm ion} \propto L_{\rm UV}$ model. The cross section is one RT cell thick ($\Delta x = 1$ Mpc$/h$), and spans the width of the box. The RT simulation used here was run at HealPix level $l = 0$ for ray merging, corresponding to 12 independent directions per cell. Ray noise can be seen as the graininess in this panel. *Middle:* The $\Gamma_{\rm HI}$ field from the same simulation used in the left panel, but averaged over 16 adjacent RT snapshots corresponding to a $\delta z \approx 0.05$ around $z = 5.7$. *Right:* A version of the $\dot{N}_{\rm ion} \propto L_{\rm UV}$ simulation run at HealPix level $l = 1$, corresponding to 48 directions per cell. Compared to the left panel, the ray noise is reduced in the middle and right panels, but large-scale features, e.g. peaks in the $\Gamma_{\rm HI}$ field and neutral island morphology, are broadly the same.

simulation that merges rays at HealPix level $l = 1$, corresponding to 48 directions per cell. These $\Gamma_{\rm HI}$ fields are shown in the middle and right panels of Figure 3.15, respectively. In both cases, the graininess in the map is clearly reduced, but the large-scale features, e.g. intensity peaks and the morphology of neutral regions, remain largely the same.

Figure 3.16 compares the derived opacity-density relations for the three variations depicted in Figure 3.15. The green curves and contours correspond to the fiducial $\dot{\rm N}_{\rm ion} \propto {\rm L}_{\rm UV}$ simulation. As before, the curve shows the median $\Sigma_{\rm LAE}/\langle\Sigma_{\rm LAE}\rangle$ versus $\tau_{\rm eff}^{50}$, while the dark and light shadings give the 68% and 98% regions, respectively. The blue and red sets of curves show the same for two variations introduced above. We find that the fiducial simulation may under estimate the 68% and 98% upper limits by ≈ 5 %, but the opacity-density relations are otherwise quite similar. Importantly for the discussion in the main

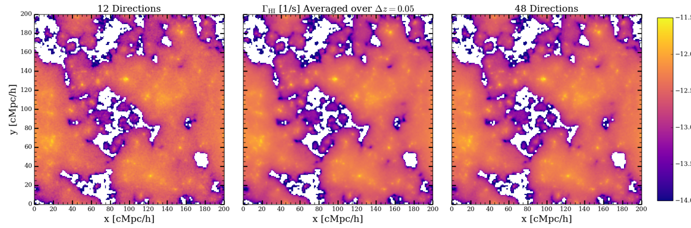

Figure 3.16: Effect of ray noise on the opacity-density relation. The opacity-density relation of the fiducial $\dot{\rm N}_{\rm ion} \propto {\rm L}_{\rm UV}$ simulation (12 directions) is represented by the green curve and shaded regions, which show the median $\Sigma_{\rm LAE}/\langle\Sigma_{\rm LAE}\rangle$ versus $\tau_{\rm eff}^{50}$ and 68/98% regions (c.f. Figure 3.6). The blue and red sets of curves show the same for the two variations of the $\Gamma_{\rm HI}$ field in Figure 3.15. The opacity-density relation is robust to our choice of merging rays at HealPix level $l = 0$, which saves a significant amount of computational time.

text, the probability of observing under-dense fields toward highly transmissive sight lines is not significantly affected by the ray noise. We conclude that our main results are robust to our choice of merging rays at level $l = 0$. It is worth noting that this choice (rather than $l = 1$) greatly reduced the computational cost of the RT simulations run for this paper.

3.8 Appendix: Effect of neutral island morphology on the opacity-density relation

In this section we show that the insensitivity of the opacity-density relation to the source model that we found in §3.4.1 owes largely to the fact that all of our models have been calibrated to have the same mean Lyα forest transmission at $z \leq 6$. For models with a fixed neutral fraction at $z = 5.7$, the morphology of neutral islands – their sizes, shapes, and clustering properties – has an important effect on the opacity-density relation. Generally speaking, neutral islands tend to be larger and more clustered when the ionizing photon

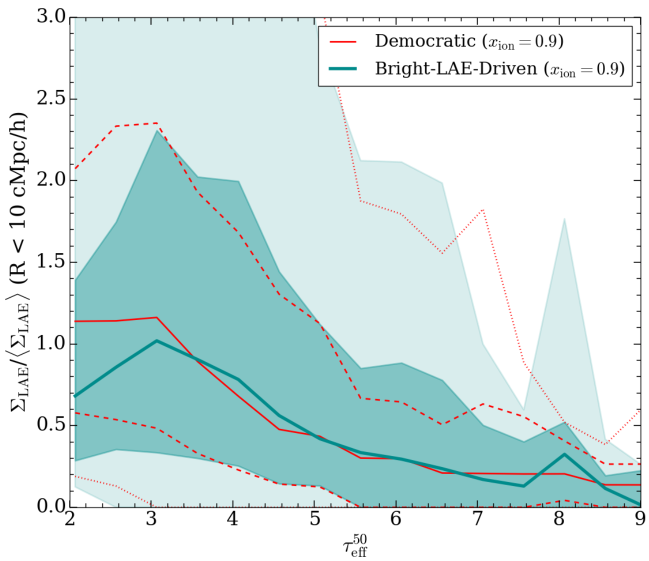

Figure 3.17: Effect of neutral island morphology on the opacity-density relation at fixed global neutral fraction of $x_{\rm HI} = 0.1$. The red solid, dashed, and dotted curves show the median and 68/98% regions from our fidicucial DEMOCRATIC model. The turquoise curve and shaded regions corresponds to a variation of our BRIGHT-LAE-DRIVEN model that has been re-scaled to have $x_{\rm HI} = 0.1$ at $z = 5.7$ (see text for details). Owing to the more clustered sources, the neutral islands in this model are more clustered at the centers of the voids compared to the DEMOCRATIC model at fixed neutral fraction. This increases the physical cross section of hot, recently reionized gas in the voids, thereby increasing the likelihood that highly transmissive sight lines are associated with galaxy under-densities.

budget is dominated by more biased sources [107], and this can have a particularly strong affect on the low-$\tau_{\rm eff}^{50}$ end of the opacity-density relation.

To illustrate this, we compare two models with the same global neutral fraction at $z = 5.7$, but with very different source populations. For one case we use our Democratic model from §3.4.1, which has $x_{\rm HI}(z = 5.7) = 0.1$. For the other model, we re-scale the $z = 5.4$ snapshot from the Bright-LAE-driven simulation, which also has $x_{\rm HI} = 0.1$. Specifically, we apply the neutral island, temperature, and $\Gamma_{\rm HI}$ fields from this later snapshot to construct our mock Lyα forest segments, re-scaling $\Gamma_{\rm HI}$ in ionized regions to match the mean forest transmission at $z = 5.7$. This approximates a simulation in which the tail end of reionization proceeds more rapidly than in our fiducial Bright-LAE-driven model, such that the $x_{\rm HI}$ is lower at $z = 5.7$.

Figure 3.17 compares the opacity-density relations between these two test models. The red curves show the median and 68/98% limits from the Democratic model, while the turquoise curve and shaded regions correspond to the re-scaled Bright-LAE-driven model. We emphasize that this comparison is at fixed $x_{\rm HI} = 0.1$. Here we see important differences on the low-$\tau_{\rm eff}^{50}$ end of the relation. Under-densities around highly transmissive sight lines are more likely in the Bright-LAE-driven model. Indeed, the probability of observing ≤ 1 LAE within a radius of $R = 10$ cMpc/h is 10% in that model, compared to the 4% probability in the Democratic model. The increased probability in the former occurs because the neutral islands are more clustered, i.e. they are less spread out throughout the voids compared to the Democratic model. Hence, even at fixed global neutral fraction, the likelihood of intersecting hot, recently reionized gas in the voids is higher in the Bright-

LAE-DRIVEN model. This highlights the role that neutral island morphology plays in setting the frequency of sight lines like J359.

Chapter 4

Conclusions

In this dissertation, I have examined multiple large-scale statistics that quantify the impact of neutral gas from the end stages of reionization on the large-scale distribution of LAEs. I have also shown how correlating Lyα forest opacities with the surrounding LAE surface densities, obtained from targeted narrowband surveys, can further provide evidence for the reionization process.

In Chapter 1, I analyzed different spatial statistics of narrowband LAE surveys to detect the presence of neutral gas in late-ending reionization models. This work included simulating the reionizing IGM with neutral fractions of $x_{\rm ion} = 0 - 0.3$ at $z = 5.7$ and $x_{\rm ion} = 0 - 0.5$ at $z = 6.6$. Our examination of LAE clustering statistics was motivated by the significant large-scale fluctuations and visual asymmetries seen on ~ 200 Mpc scales in the LAE surface densities observed in the SILVERRUSH fields. After modeling the IGM using numerical methods, we observed that neutral islands remaining during the tail-end of reionization were relegated to the voids of the large-scale structure. The obscuration of

LAEs in under-dense regions consequentially increased the sizes of the large-scale under-densities, and motivated the exploration of LAE void statistics, like the void probability functions. Furthermore, since our models were calibrated to maintain the observed mean LAE surface densities found in the SILVERRUSH fields, the over-dense and biased regions consequentially became more transmissive to Lyα photons, increasing the LAE surface densities in these regions. This motivated the exploration of LAE clustering and peak statistics, including the TPCF, pixel threshold fraction, and peak probability functions, all of which were aimed at quantifying the expected enhancement of the LAE surface density fluctuations and clustering.

We found that the presence of neutral islands from an ongoing reionization process increases the probability of observing large-scale field asymmetries in the spatial distributions of LAEs. However, the observed asymmetries observed in some of the SILVERRUSH fields are consistent with those expected from cosmic variance and large-structure evolution alone, and do not require neutral islands for their explanation. With an eye toward future surveys, we found that the VPF is better-suited than the TPCF in detecting neutral gas left at the tail end of the reionization process at $z \approx 5.7$. Hence, the prospects for detecting the last stages of reionization with the spatial distribution of LAEs are promising in futuristic surveys, and measurements of the statistics of voids and peaks offer complementary approaches to the TPCF.

In Chapter 2, we discussed another powerful large-scale statistic synergizing quasar absorption spectra with the LAE spatial distribution through the opacity-density relation. Our initial motivation was to address the findings in C23, where two of the most opaque, as well as two of the most transmissive, sight lines intersect under-densities in the LAE distribution. The association of highly opaque sight lines with under-densities is consistent with models in which large-scale fluctuations in the ionizing radiation background, and/or the presence of neutral islands, drive the observed scatter in $\tau_{\rm eff}$. On the other hand, the association between highly-transmissive sight lines and under-densities is more consistent with models in which relic temperature fluctuations from reionization drive the observed scatter in $\tau_{\rm eff}$. We found that both sets of observations can be explained by an ongoing reionization process in which there are large fluctuations in the ionizing radiation background and in the IGM temperature, as well as neutral islands in the cosmological voids. This owes to the fact that Lyα forest transmission in the voids can be both enhanced by hot, low-density, recently reionized gas, as well as suppressed by the presence of neutral islands. Our findings suggest a more nuanced interpretation of the observed spatial fluctuations in $\tau_{\rm eff}$ than has been applied in previous studies.

We found that the opacity-density relation is insensitive to the exact nature of the source and emission line modeling at fixed mean Lyα forest transmission, demonstrating the robustness of the models to some of the most uncertain modeling choices. We also found that the transmissive end of the opacity-density relation is sensitive ultimately to the volume of hot, recently reionized gas contained in the voids, making it a possible probe of the exact timing of reionization's end. In models where reionization ends earlier, the increased volume of such recently reionized gas significantly increases the correlation between highly transmissive Lyα forest sight lines and under-densities in the galaxy distribution. At the time of writing this dissertation, ongoing spectroscopic surveys with JWST by the EIGER

[422] and ASPIRE [813] collaborations are mapping the large-scale structure around a combined total of 31 high-z quasar sight lines. This will provide an unprecedented view into the relationship between the galaxy population and IGM transmission near the epoch of reionization. Our work informs their analyses by exploring how the interplay between the ionizing radiation background, IGM temperature, cosmological densities, and neutral islands, all work in concert to set the relationship between the galaxy distribution and Lyα forest transmission.

Bibliography

[1] T. Abel, O. Hahn, and R. Kaehler. Tracing the dark matter sheet in phase space. *Monthly Notices of the RAS*, 427:61–76, November 2012.

[2] Tom Abel and Benjamin D. Wandelt. Adaptive ray tracing for radiative transfer around point sources. *Monthly Notices of the RAS*, 330(3):L53–L56, March 2002.

[3] L. Ackerman, M. R. Buckley, S. M. Carroll, and M. Kamionkowski. Dark Matter and Dark Radiation. *ArXiv e-prints*, October 2008.

[4] V. Acquaviva, N. Bartolo, S. Matarrese, and A. Riotto. Gauge-invariant second-order perturbations and non-Gaussianity from inflation. *Nuclear Physics B*, 667:119–148, September 2003.

[5] P. A. R. Ade, N. Aghanim, C. Armitage-Caplan, M. Arnaud, M. Ashdown, F. Atrio-Barandela, J. Aumont, C. Baccigalupi, A. J. Banday, and et al. Planck 2013 Results. XXIV. Constraints on primordial non-Gaussianity. *ArXiv e-prints*, March 2013.

[6] P. Adshead, E. J. Baxter, S. Dodelson, and A. Lidz. Non-Gaussianity and excursion set theory: Halo bias. *Physical Review D.*, 86(6):063526, September 2012.

[7] N. Afshordi and A. J. Tolley. Primordial non-Gaussianity, statistics of collapsed objects, and the integrated Sachs-Wolfe effect. *Physical Review D.*, 78(12):123507, December 2008.

[8] I. Agullo and L. Parker. Non-Gaussianities and the stimulated creation of quanta in the inflationary universe. *Physical Review D.*, 83(6):063526, March 2011.

[9] I. Agullo and S. Shandera. Large non-Gaussian halo bias from single field inflation. *Journal of Cosmology and Astroparticle Physics*, 9:7, September 2012.

[10] K. Ahn, I. T. Iliev, P. R. Shapiro, G. Mellema, J. Koda, and Y. Mao. Detecting the Rise and Fall of the First Stars by Their Impact on Cosmic Reionization. *Astrophysical Journal*, 756:L16, September 2012.

[11] Kyungjin Ahn, Ilian T. Iliev, Paul R. Shapiro, and Chaichalit Srisawat. Non-linear bias of cosmological halo formation in the early universe. *Monthly Notices of the RAS*, 450(2):1486–1502, June 2015.

[12] A. Albrecht, G. Bernstein, R. Cahn, W. L. Freedman, J. Hewitt, W. Hu, J. Huth, M. Kamionkowski, E. W. Kolb, L. Knox, J. C. Mather, S. Staggs, and N. B. Suntzeff. Report of the Dark Energy Task Force. *ArXiv Astrophysics e-prints*, September 2006.

[13] S. W. Allen, R. W. Schmidt, H. Ebeling, A. C. Fabian, and L. van Speybroeck. Constraints on dark energy from Chandra observations of the largest relaxed galaxy clusters. *Monthly Notices of the RAS*, 353:457–467, September 2004.

[14] Gabriel Altay, Tom Theuns, Joop Schaye, Neil H. M. Crighton, and Claudio Dalla Vecchia. Through Thick and Thin—H I Absorption in Cosmological Simulations. *Astrophysical Journal*, 737(2):L37, Aug 2011.

[15] M. A. Alvarez and T. Abel. The Effect of Absorption Systems on Cosmic Reionization. *Astrophysical Journal*, 747:126, March 2012.

[16] M. A. Alvarez, M. Busha, T. Abel, and R. H. Wechsler. Connecting Reionization to the Local Universe. *Astrophysical Journal*, 703:L167–L171, October 2009.

[17] M. A. Alvarez, E. Komatsu, O. Doré, and P. R. Shapiro. The Cosmic Reionization History as Revealed by the Cosmic Microwave Background Doppler-21 cm Correlation. *Astrophysical Journal*, 647:840–852, August 2006.

[18] L. Amendola, J. A. Frieman, and I. Waga. Weak gravitational lensing by voids. *Monthly Notices of the RAS*, 309:465–473, October 1999.

[19] L. Anderson, F. Governato, M. Karcher, T. Quinn, and J. Wadsley. The Little Galaxies that Could (Reionize the Universe): Faint End Slopes & Escape Fractions at z ¿ 4. *ArXiv e-prints*, June 2016.

[20] R. E. Angulo, R. Chen, S. Hilbert, and T. Abel. Noiseless Gravitational Lensing Simulations. *ArXiv e-prints*, September 2013.

[21] R. E. Angulo, C. G. Lacey, C. M. Baugh, and C. S Frenk. The Fate of Substructures in Cold Dark Matter Haloes. *ArXiv e-prints*, October 2008.

[22] K. Arun, C. Mishra, C. Van Den Broeck, B. Iyer, B. Sathyaprakash, and S. Sinha. LISA as a dark energy probe. *ArXiv e-prints*, October 2008.

[23] Astropy Collaboration, Thomas P. Robitaille, Erik J. Tollerud, Perry Greenfield, Michael Droettboom, Erik Bray, Tom Aldcroft, Matt Davis, Adam Ginsburg, Adrian M. Price-Whelan, Wolfgang E. Kerzendorf, Alexander Conley, Neil Crighton, Kyle Barbary, Demitri Muna, Henry Ferguson, Frédéric Grollier, Madhura M. Parikh, Prasanth H. Nair, Hans M. Unther, Christoph Deil, Julien Woillez, Simon Conseil, Roban Kramer, James E. H. Turner, Leo Singer, Ryan Fox, Benjamin A. Weaver, Victor Zabalza, Zachary I. Edwards, K. Azalee Bostroem, D. J. Burke, Andrew R. Casey, Steven M. Crawford, Nadia Dencheva, Justin Ely, Tim Jenness, Kathleen Labrie, Pey Lian Lim, Francesco Pierfederici, Andrew Pontzen, Andy Ptak, Brian Refsdal, Mathieu Servillat, and Ole Streicher. Astropy: A community Python package for astronomy. *Astronomy and Astrophysics*, 558:A33, Oct 2013.

[24] Hakim Atek, Ivo Labbé, Lukas J. Furtak, Iryna Chemerynska, Seiji Fujimoto, David J. Setton, Tim B. Miller, Pascal Oesch, Rachel Bezanson, Sedona H. Price, Pratika Dayal, Adi Zitrin, Vasily Kokorev, John R. Weaver, Gabriel Brammer, Pieter van Dokkum, Christina C. Williams, Sam E. Cutler, Robert Feldmann, Yoshinobu Fudamoto, Jenny E. Greene, Joel Leja, Michael V. Maseda, Adam Muzzin, Richard Pan, Casey Papovich, Erica J. Nelson, Themiya Nanayakkara, Daniel P. Stark, Mauro Stefanon, Katherine A. Suess, Bingjie Wang, and Katherine E. Whitaker. First spectroscopic observations of the galaxies that reionized the Universe. *arXiv e-prints*, page arXiv:2308.08540, August 2023.

[25] D. Aubert and R. Teyssier. Reionization Simulations Powered by Graphics Processing Units. I. On the Structure of the Ultraviolet Radiation Field. *Astrophysical Journal*, 724:244–266, November 2010.

[26] V. Avila-Reese, P. Colín, G. Piccinelli, and C. Firmani. The Effects of Non-Gaussian Initial Conditions on the Structure and Substructure of Cold Dark Matter Halos. *Astrophysical Journal*, 598:36–48, November 2003.

[27] E. Bañados, B. P. Venemans, C. Mazzucchelli, E. P. Farina, F. Walter, F. Wang, R. Decarli, D. Stern, X. Fan, F. B. Davies, J. F. Hennawi, R. A. Simcoe, M. L. Turner, H.-W. Rix, J. Yang, D. D. Kelson, G. C. Rudie, and J. M. Winters. An 800-million-solar-mass black hole in a significantly neutral Universe at a redshift of 7.5. *Nature*, 553:473–476, January 2018.

[28] D. Babich, P. Creminelli, and M. Zaldarriaga. The shape of non-Gaussianities. *Journal of Cosmology and Astroparticle Physics*, 8:9, August 2004.

[29] D. Babich and M. Zaldarriaga. Primordial bispectrum information from CMB polarization. *Physical Review D.*, 70(8):083005, October 2004.

[30] D. J. Bacon, A. R. Refregier, and R. S. Ellis. Detection of weak gravitational lensing by large-scale structure. *Monthly Notices of the RAS*, 318:625–640, October 2000.

[31] Y. M. Bahé, I. G. McCarthy, and L. J. King. Mock weak lensing analysis of simulated galaxy clusters: bias and scatter in mass and concentration. *Monthly Notices of the RAS*, 421:1073–1088, April 2012.

[32] T. Baldauf, U. Seljak, and L. Senatore. Primordial non-Gaussianity in the bispectrum of the halo density field. *Journal of Cosmology and Astroparticle Physics*, 4:6, April 2011.

[33] T. Baldauf, U. Seljak, L. Senatore, and M. Zaldarriaga. Galaxy bias and non-linear structure formation in general relativity. *Journal of Cosmology and Astroparticle Physics*, 10:31, October 2011.

[34] E. A. Baltz, P. Marshall, and M. Oguri. Analytic models of plausible gravitational lens potentials. *ArXiv e-prints*, May 2007.

[35] R. Barkana. Effect of Large-Scale Structure on Multiply Imaged Sources. *Astrophysical Journal*, 468:17–+, September 1996.

[36] R. Barkana and A. Loeb. High-Redshift Galaxies: Their Predicted Size and Surface Brightness Distributions and Their Gravitational Lensing Probability. *Astrophysical Journal*, 531:613–623, March 2000.

[37] R. Barkana and A. Loeb. A Method for Separating the Physics from the Astrophysics of High-Redshift 21 Centimeter Fluctuations. *Astrophysical Journal*, 624:L65–L68, May 2005.

[38] M. Barnabè, O. Czoske, L. V. E. Koopmans, T. Treu, A. S. Bolton, and R. Gavazzi. Two-dimensional kinematics of SLACS lenses - II. Combined lensing and dynamics analysis of early-type galaxies at z = 0.08-0.33. *Monthly Notices of the RAS*, 399:21–36, October 2009.

[39] M. Bartelmann. Arcs from a universal dark-matter halo profile. *Astronomy and Astrophysics*, 313:697–702, September 1996.

[40] M. Bartelmann, A. Huss, J. M. Colberg, A. Jenkins, and F. R. Pearce. Arc statistics with realistic cluster potentials. IV. Clusters in different cosmologies. *Astronomy and Astrophysics*, 330:1–9, February 1998.

[41] M. Bartelmann, M. Meneghetti, F. Perrotta, C. Baccigalupi, and L. Moscardini. Arc statistics in cosmological models with dark energy. *Astronomy and Astrophysics*, 409:449–457, October 2003.

[42] M. Bartelmann and P. Schneider. Weak gravitational lensing. *Physics Reports*, 340:291–472, January 2001.

[43] M. Bartelmann, M. Steinmetz, and A. Weiss. Arc statistics with realistic cluster potentials. 2: Influence of cluster asymmetry and substructure. *Astronomy and Astrophysics*, 297:1–12, May 1995.

[44] M. Bartelmann and A. Weiss. Arc statistics with realistic cluster potentials. 1: Method and first results. *Astronomy and Astrophysics*, 287:1–14, July 1994.

[45] N. Bartolo, S. Matarrese, and A. Riotto. Relativistic effects and primordial non-Gaussianity in the galaxy bias. *Journal of Cosmology and Astroparticle Physics*, 4:11, April 2011.

[46] N. Battaglia, H. Trac, R. Cen, and A. Loeb. Reionization on Large Scales. I. A Parametric Model Constructed from Radiation-hydrodynamic Simulations. *Astrophysical Journal*, 776:81, October 2013.

[47] M. B. Bayliss, M. D. Gladders, M. Oguri, J. F. Hennawi, K. Sharon, B. P. Koester, and H. Dahle. The Redshift Distribution of Giant Arcs in the Sloan Giant Arcs Survey. *Astrophysical Journal*, 727:L26+, January 2011.

[48] M. B. Bayliss, T. Johnson, M. D. Gladders, K. Sharon, and M. Oguri. Line-of-sight Structure toward Strong Lensing Galaxy Clusters. *Astrophysical Journal*, 783:41, March 2014.

[49] M. B. Bayliss, E. Wuyts, K. Sharon, M. D. Gladders, J. F. Hennawi, B. P. Koester, and H. Dahle. Two Lensed Lyman-α Emitting Galaxies at z˜ 5. *Astrophysical Journal*, 720:1559–1568, September 2010.

[50] G. D. Becker and J. S. Bolton. New measurements of the ionizing ultraviolet background over 2 ¡ z ¡ 5 and implications for hydrogen reionization. *Monthly Notices of the RAS*, 436:1023–1039, December 2013.

[51] G. D. Becker, J. S. Bolton, M. G. Haehnelt, and W. L. W. Sargent. Detection of extended He II reionization in the temperature evolution of the intergalactic medium. *Monthly Notices of the RAS*, 410:1096–1112, January 2011.

[52] G. D. Becker, J. S. Bolton, P. Madau, M. Pettini, E. V. Ryan-Weber, and B. P. Venemans. Evidence of patchy hydrogen reionization from an extreme Lyα trough below redshift six. *Monthly Notices of the RAS*, 447:3402–3419, March 2015.

[53] G. D. Becker, J. S. Bolton, P. Madau, M. Pettini, E. V. Ryan-Weber, and B. P. Venemans. Evidence of patchy hydrogen reionization from an extreme Lyα trough below redshift six. *Monthly Notices of the RAS*, 447:3402–3419, March 2015.

[54] George D. Becker, James S. Bolton, Martin G. Haehnelt, and Wallace L. W. Sargent. Detection of extended He II reionization in the temperature evolution of the intergalactic medium. *Monthly Notices of the RAS*, 410(2):1096–1112, January 2011.

[55] George D. Becker, James S. Bolton, Yongda Zhu, and Seyedazim Hashemi. Damping wing absorption associated with a giant Lyα trough at $z < 6$: direct evidence for late-ending reionization. *arXiv e-prints*, page arXiv:2405.08885, May 2024.

[56] George D. Becker, Anson D'Aloisio, Holly M. Christenson, Yongda Zhu, Gábor Worseck, and James S. Bolton. The mean free path of ionizing photons at 5 ¡ z ¡ 6: evidence for rapid evolution near reionization. *Monthly Notices of the RAS*, 508(2):1853–1869, December 2021.

[57] George D. Becker, Frederick B. Davies, Steven R. Furlanetto, Matthew A. Malkan, Elisa Boera, and Craig Douglass. Evidence for Large-scale Fluctuations in the Metagalactic Ionizing Background Near Redshift Six. *Astrophysical Journal*, 863(1):92, August 2018.

[58] George D. Becker, Frederick B. Davies, Steven R. Furlanetto, Matthew A. Malkan, Elisa Boera, and Craig Douglass. Evidence for Large-scale Fluctuations in the Metagalactic Ionizing Background Near Redshift Six. *Astrophysical Journal*, 863(1):92, August 2018.

[59] George D. Becker, Paul C. Hewett, Gábor Worseck, and J. Xavier Prochaska. A refined measurement of the mean transmitted flux in the Lyα forest over 2 ¡ z ¡ 5 using composite quasar spectra. *Monthly Notices of the RAS*, 430(3):2067–2081, April 2013.

[60] M. R. Becker and A. V. Kravtsov. On the Accuracy of Weak-lensing Cluster Mass Reconstructions. *Astrophysical Journal*, 740:25, October 2011.

[61] N. F. Bell and T. D. Jacques. Gamma-ray Constraints on Dark Matter Annihilation into Charged Particles. *ArXiv e-prints*, November 2008.

[62] J. Beltran Jimenez and A. L. Maroto. Avoiding the dark energy coincidence problem with a cosmic vector. *ArXiv e-prints*, December 2008.

[63] J. Benjamin, C. Heymans, E. Semboloni, L. van Waerbeke, H. Hoekstra, T. Erben, M. D. Gladders, M. Hetterscheidt, Y. Mellier, and H. K. C. Yee. Cosmological constraints from the 100-deg^2 weak-lensing survey. *Monthly Notices of the RAS*, 381:702–712, October 2007.

[64] C. L. Bennett, D. Larson, J. L. Weiland, N. Jarosik, G. Hinshaw, N. Odegard, K. M. Smith, R. S. Hill, and et al. Nine-Year Wilkinson Microwave Anisotropy Probe (WMAP) Observations: Final Maps and Results. *ArXiv e-prints*, December 2012.

[65] M. Bernardi, J. B. Hyde, R. K. Sheth, C. J. Miller, and R. C. Nichol. The Luminosities, Sizes, and Velocity Dispersions of Brightest Cluster Galaxies: Implications for Formation History. *Astronomical Journal*, 133:1741–1755, April 2007.

[66] E. Bertin and S. Arnouts. SExtractor: Software for source extraction. *Astronomy and Astrophysicss*, 117:393–404, Jun 1996.

[67] E. Boera, M. T. Murphy, G. D. Becker, and J. S. Bolton. The thermal history of the intergalactic medium down to redshift z = 1.5: a new curvature measurement. *Monthly Notices of the RAS*, 441:1916–1933, July 2014.

[68] Elisa Boera, George D. Becker, James S. Bolton, and Fahad Nasir. Revealing Reionization with the Thermal History of the Intergalactic Medium: New Constraints from the Lyα Flux Power Spectrum. *Astrophysical Journal*, 872(1):101, February 2019.

[69] A. S. Bolton, T. Treu, L. V. E. Koopmans, R. Gavazzi, L. A. Moustakas, S. Burles, D. J. Schlegel, and R. Wayth. The Sloan Lens ACS Survey. VII. Elliptical Galaxy Scaling Laws from Direct Observational Mass Measurements. *Astrophysical Journal*, 684:248–259, September 2008.

[70] J. S. Bolton and G. D. Becker. Resolving the high redshift Lyα forest in smoothed particle hydrodynamics simulations. *Monthly Notices of the RAS*, 398:L26–L30, September 2009.

[71] J. S. Bolton and M. G. Haehnelt. The observed ionization rate of the intergalactic medium and the ionizing emissivity at z ¿= 5: evidence for a photon-starved and extended epoch of reionization. *Monthly Notices of the RAS*, 382:325–341, November 2007.

[72] J. S. Bolton and M. G. Haehnelt. On the rapid demise of Ly α emitters at redshift z $\gtrsim$ 7 due to the increasing incidence of optically thick absorption systems. *Monthly Notices of the RAS*, 429:1695–1704, February 2013.

[73] J. R. Bond, S. Cole, G. Efstathiou, and N. Kaiser. Excursion set mass functions for hierarchical Gaussian fluctuations. *Astrophysical Journal*, 379:440–460, October 1991.

[74] A. Bongiorno, G. Zamorani, I. Gavignaud, B. Marano, S. Paltani, G. Mathez, P. Møller, J. P. Picat, and et al. The VVDS type-1 AGN sample: the faint end of the luminosity function. *Astronomy and Astrophysics*, 472:443–454, September 2007.

[75] S. Bonoli, F. Shankar, S. D. M. White, V. Springel, and J. S. B. Wyithe. On merger bias and the clustering of quasars. *Monthly Notices of the RAS*, 404:399–408, May 2010.

[76] C. Bonvin and R. Durrer. What galaxy surveys really measure. *Physical Review D.*, 84(6):063505, September 2011.

[77] Sarah E. I. Bosman. Constraints on the mean free path of ionising photons at $z \sim 6$ using limits on individual free paths. *arXiv e-prints*, page arXiv:2108.12446, August 2021.

[78] Sarah E. I. Bosman, Frederick B. Davies, George D. Becker, Laura C. Keating, Rebecca L. Davies, Yongda Zhu, Anna-Christina Eilers, Valentina D'Odorico, Fuyan Bian, Manuela Bischetti, Stefano V. Cristiani, Xiaohui Fan, Emanuele P. Farina, Martin G. Haehnelt, Joseph F. Hennawi, Girish Kulkarni, Andrei Mesinger, Romain A. Meyer, Masafusa Onoue, Andrea Pallottini, Yuxiang Qin, Emma Ryan-Weber, Jan-Torge Schindler, Fabian Walter, Feige Wang, and Jinyi Yang. Hydrogen reionization ends by z = 5.3: Lyman-α optical depth measured by the XQR-30 sample. *Monthly Notices of the RAS*, 514(1):55–76, July 2022.

[79] Sarah E. I. Bosman, Xiaohui Fan, Linhua Jiang, Sophie Reed, Yoshiki Matsuoka, George Becker, and Martin Haehnelt. New constraints on Lyman-α opacity with a sample of 62 quasarsat z ¿ 5.7. *Monthly Notices of the RAS*, 479(1):1055–1076, September 2018.

[80] R. Bouwens, L. Bradley, A. Zitrin, D. Coe, M. Franx, W. Zheng, R. Smit, O. Host, and et. al. A Census of Star-Forming Galaxies in the z˜9-10 Universe based on HST+Spitzer Observations Over 19 CLASH clusters: Three Candidate z˜9-10 Galaxies and Improved Constraints on the Star Formation Rate Density at z˜9.2. *ArXiv e-prints*, November 2012.

[81] R. J. Bouwens, G. D. Illingworth, L. D. Bradley, H. Ford, M. Franx, W. Zheng, T. Broadhurst, D. Coe, and M. J. Jee. z ˜ 7-10 Galaxies Behind Lensing Clusters: Contrast with Field Search Results. *Astrophysical Journal*, 690:1764–1771, January 2009.

[82] R. J. Bouwens, G. D. Illingworth, P. A. Oesch, I. Labbé, P. G. van Dokkum, M. Trenti, M. Franx, R. Smit, V. Gonzalez, and D. Magee. UV-continuum Slopes of ¿4000 z ˜4-8 Galaxies from the HUDF/XDF, HUDF09, ERS, CANDELS-South, and CANDELS-North Fields. *Astrophysical Journal*, 793(2):115, October 2014.

[83] R. J. Bouwens, G. D. Illingworth, P. A. Oesch, M. Trenti, I. Labbé, L. Bradley, M. Carollo, P. G. van Dokkum, V. Gonzalez, B. Holwerda, M. Franx, L. Spitler, R. Smit, and D. Magee. UV Luminosity Functions at Redshifts z $\sim$ 4 to z $\sim$ 10: 10,000 Galaxies from HST Legacy Fields. *Astrophysical Journal*, 803(1):34, April 2015.

[84] R. J. Bouwens, G. D. Illingworth, P. A. Oesch, M. Trenti, I. Labbé, M. Franx, M. Stiavelli, C. M. Carollo, P. van Dokkum, and D. Magee. Lower-luminosity Galaxies Could Reionize the Universe: Very Steep Faint-end Slopes to the UV Luminosity Functions at z ¿= 5-8 from the HUDF09 WFC3/IR Observations. *Astrophysical Journal*, 752:L5, June 2012.

[85] R. J. Bouwens, P. A. Oesch, G. D. Illingworth, R. S. Ellis, and M. Stefanon. The z $\sim$ 6 Luminosity Function Fainter than -15 mag from the Hubble Frontier Fields: The Impact of Magnification Uncertainties. *Astrophysical Journal*, 843(2):129, July 2017.

[86] A. Boyarsky and O. Ruchayskiy. Bounds on Light Dark Matter. *ArXiv e-prints*, November 2008.

[87] M. Boylan-Kolchin, J. S. Bullock, and S. Garrison-Kimmel. Near-field limits on the role of faint galaxies in cosmic reionization. *Monthly Notices of the RAS*, 443:L44–L48, September 2014.

[88] V. Bozza. A comparison of approximate gravitational lens equations and a proposal for an improved new one. *ArXiv e-prints*, July 2008.

[89] M. Bradač, D. Clowe, A. H. Gonzalez, P. Marshall, W. Forman, C. Jones, M. Markevitch, S. Randall, T. Schrabback, and D. Zaritsky. Strong and Weak Lensing United. III. Measuring the Mass Distribution of the Merging Galaxy Cluster 1ES 0657-558. *Astrophysical Journal*, 652:937–947, December 2006.

[90] M. Bradač, T. Erben, P. Schneider, H. Hildebrandt, M. Lombardi, M. Schirmer, J.-M. Miralles, D. Clowe, and S. Schindler. Strong and weak lensing united. *Astronomy and Astrophysics*, 437:49–60, July 2005.

[91] M. Bradač, P. Schneider, M. Lombardi, and T. Erben. Strong and weak lensing united. *Astronomy and Astrophysics*, 437:39–48, July 2005.

[92] M. Bradač, P. Schneider, M. Lombardi, M. Steinmetz, L. V. E. Koopmans, and J. F. Navarro. The signature of substructure on gravitational lensing in the ΛCDM cosmological model. *Astronomy and Astrophysics*, 423:797–809, September 2004.

[93] L. D. Bradley, R. J. Bouwens, H. C. Ford, G. D. Illingworth, M. J. Jee, N. Benítez, T. J. Broadhurst, M. Franx, B. L. Frye, L. Infante, V. Motta, P. Rosati, R. L. White, and W. Zheng. Discovery of a Very Bright Strongly Lensed Galaxy Candidate at z ˜ 7.6. *Astrophysical Journal*, 678:647–654, May 2008.

[94] L. D. Bradley, M. Trenti, P. A. Oesch, M. Stiavelli, T. Treu, R. J. Bouwens, J. M. Shull, B. W. Holwerda, and N. Pirzkal. The Brightest of Reionizing Galaxies Survey: Constraints on the Bright End of the z ˜ 8 Luminosity Function. *Astrophysical Journal*, 760:108, December 2012.

[95] L. D. Bradley, A. Zitrin, D. Coe, R. Bouwens, M. Postman, I. Balestra, C. Grillo, A. Monna, and et. al. CLASH: A Census of Magnified Star-Forming Galaxies at z ˜ 6-8. *ArXiv e-prints*, August 2013.

[96] T. Broadhurst, N. Benítez, D. Coe, and et al. Strong-Lensing Analysis of A1689 from Deep Advanced Camera Images. *Astrophysical Journal*, 621:53–88, March 2005.

[97] M. Bruni, R. Crittenden, K. Koyama, R. Maartens, C. Pitrou, and D. Wands. Disentangling non-Gaussianity, bias, and general relativistic effects in the galaxy distribution. *Physical Review D.*, 85(4):041301, February 2012.

[98] G. Bruzual and S. Charlot. Stellar population synthesis at the resolution of 2003. *Monthly Notices of the RAS*, 344:1000–1028, October 2003.

[99] J. S. Bullock, T. S. Kolatt, Y. Sigad, R. S. Somerville, A. V. Kravtsov, A. A. Klypin, J. R. Primack, and A. Dekel. Profiles of dark haloes: evolution, scatter and environment. *Monthly Notices of the RAS*, 321:559–575, March 2001.

[100] J. S. Bullock, K. R. Stewart, and C. W. Purcell. Mergers and Disk Survival in LCDM. *ArXiv e-prints*, November 2008.

[101] Andrew J. Bunker, Aayush Saxena, Alex J. Cameron, Chris J. Willott, Emma Curtis-Lake, Peter Jakobsen, Stefano Carniani, Renske Smit, Roberto Maiolino, Joris Witstok, Mirko Curti, Francesco D'Eugenio, Gareth C. Jones, Pierre Ferruit, Santiago Arribas, Stephane Charlot, Jacopo Chevallard, Giovanna Giardino, Anna de Graaff, Tobias J. Looser, Nora Lützgendorf, Michael V. Maseda, Tim Rawle, Hans-Walter Rix, Bruno Rodríguez Del Pino, Stacey Alberts, Eiichi Egami, Daniel J. Eisenstein, Ryan Endsley, Kevin Hainline, Ryan Hausen, Benjamin D. Johnson, George Rieke, Marcia Rieke, Brant E. Robertson, Irene Shivaei, Daniel P. Stark, Fengwu Sun, Sandro Tacchella, Mengtao Tang, Christina C. Williams, Christopher N. A. Willmer, William M. Baker, Stefi Baum, Rachana Bhatawdekar, Rebecca Bowler, Kristan Boyett, Zuyi Chen, Chiara Circosta, Jakob M. Helton, Zhiyuan Ji, Nimisha Kumari, Jianwei Lyu, Erica Nelson, Eleonora Parlanti, Michele Perna, Lester Sandles, Jan Scholtz, Katherine A. Suess, Michael W. Topping, Hannah Übler, Imaan E. B. Wallace, and Lily

Whitler. JADES NIRSpec Spectroscopy of GN-z11: Lyman-α emission and possible enhanced nitrogen abundance in a z = 10.60 luminous galaxy. *Astronomy and Astrophysics*, 677:A88, September 2023.

[102] M. T. Busha, M. A. Alvarez, R. H. Wechsler, T. Abel, and L. E. Strigari. The Impact of Inhomogeneous Reionization on the Satellite Galaxy Population of the Milky Way. *ArXiv e-prints*, January 2009.

[103] M. Cacciato, M. Bartelmann, M. Meneghetti, and L. Moscardini. Combining weak and strong lensing in cluster potential reconstruction. *Astronomy and Astrophysics*, 458:349–356, November 2006.

[104] Christopher Cain and Anson D'Aloisio. FLEXRT — A fast and flexible cosmological radiative transfer code for reionization studies. Part I. Code validation. *Journal of Cosmology and Astroparticle Physics*, 2024(12):025, December 2024.

[105] Christopher Cain, Anson D'Aloisio, Nakul Gangolli, and George D. Becker. A Short Mean Free Path at z = 6 Favors Late and Rapid Reionization by Faint Galaxies. *Astrophysical Journal*, 917(2):L37, August 2021.

[106] Christopher Cain, Anson D'Aloisio, Nakul Gangolli, and Matthew McQuinn. The Morphology of Reionization in a Dynamically Clumpy Universe. *arXiv e-prints*, page arXiv:2207.11266, July 2022.

[107] Christopher Cain, Anson D'Aloisio, Garett Lopez, Nakul Gangolli, and Joshua T. Roth. On the rise and fall of galactic ionizing output at the end of reionization. *arXiv e-prints*, page arXiv:2311.13638, November 2023.

[108] Christopher Cain, Anson D'Aloisio, Garett Lopez, Nakul Gangolli, and Joshua T. Roth. On the rise and fall of galactic ionizing output at the end of reionization. *Monthly Notices of the RAS*, 531(1):1951–1970, June 2024.

[109] A. P. Calverley, G. D. Becker, M. G. Haehnelt, and J. S. Bolton. Measurements of the ultraviolet background at $4.6 < z < 6.4$ using the quasar proximity effect. *Monthly Notices of the RAS*, 412:2543–2562, April 2011.

[110] C. Carbone, L. Verde, and S. Matarrese. Non-Gaussian Halo Bias and Future Galaxy Surveys. *Astrophysical Journal*, 684:L1–L4, September 2008.

[111] D. Carney, W. Fischler, S. Paban, and N. Sivanandam. The inflationary wavefunction and its initial conditions. *Journal of Cosmology and Astroparticle Physics*, 12:12, December 2012.

[112] J. Caruana, A. J. Bunker, S. M. Wilkins, E. R. Stanway, S. Lorenzoni, M. J. Jarvis, and H. Ebert. Spectroscopy of $z \sim 7$ candidate galaxies: using Lyman α to constrain the neutral fraction of hydrogen in the high-redshift universe. *Monthly Notices of the RAS*, 443:2831–2842, October 2014.

[113] Joseph Caruana, Andrew J. Bunker, Stephen M. Wilkins, Elizabeth R. Stanway, Mark Lacy, Matt J. Jarvis, Silvio Lorenzoni, and Samantha Hickey. No evidence for Lyman α emission in spectroscopy of z ¿ 7 candidate galaxies. *Monthly Notices of the RAS*, 427(4):3055–3070, December 2012.

[114] M. Castellano, P. Dayal, L. Pentericci, A. Fontana, A. Hutter, G. Brammer, E. Merlin, A. Grazian, S. Pilo, R. Amorin, S. Cristiani, M. Dickinson, A. Ferrara, S. Gallerani, E. Giallongo, M. Giavalisco, L. Guaita, A. Koekemoer, R. Maiolino, D. Paris, P. Santini, L. Vallini, E. Vanzella, and J. Wagg. First Observational Support for Overlapping Reionized Bubbles Generated by a Galaxy Overdensity. *Astrophysical Journal*, 818(1):L3, February 2016.

[115] M. Castellano, L. Pentericci, G. Cupani, E. Curtis-Lake, E. Vanzella, R. Amorín, D. Belfiori, A. Calabrò, S. Carniani, S. Charlot, J. Chevallard, P. Dayal, M. Dickinson, A. Ferrara, A. Fontana, E. Giallongo, A. Hutter, E. Merlin, D. Paris, and P. Santini. The ionizing properties of two bright Lyα emitters in the Bremer Deep Field reionized bubble at z = 7. *Astronomy and Astrophysics*, 662:A115, June 2022.

[116] M. Castellano, L. Pentericci, E. Vanzella, F. Marchi, A. Fontana, P. Dayal, A. Ferrara, A. Hutter, S. Carniani, S. Cristiani, M. Dickinson, S. Gallerani, E. Giallongo, M. Giavalisco, A. Grazian, R. Maiolino, E. Merlin, D. Paris, S. Pilo, and P. Santini. Spectroscopic Investigation of a Reionized Galaxy Overdensity at z = 7. *Astrophysical Journal*, 863(1):L3, August 2018.

[117] R. Cen, P. McDonald, H. Trac, and A. Loeb. Probing the Epoch of Reionization with the Lyα Forest at z ˜ 4-5. *Astrophysical Journal*, 706:L164–L167, November 2009.

[118] R. Cen, J. Miralda-Escudé, J. P. Ostriker, and M. Rauch. Gravitational collapse of small-scale structure as the origin of the Lyman-alpha forest. *Astrophysical Journal*, 437:L9–L12, December 1994.

[119] Renyue Cen and Zoltan Haiman. Quasar Strömgren Spheres Before Cosmological Reionization. *Astrophysical Journal*, 542(2):L75–L78, October 2000.

[120] A. Challinor and A. Lewis. Linear power spectrum of observed source number counts. *Physical Review D.*, 84(4):043516, August 2011.

[121] S. Chandrasekhar. Stochastic Problems in Physics and Astronomy. *Reviews of Modern Physics*, 15:1–89, January 1943.

[122] J. Chardin, M. G. Haehnelt, D. Aubert, and E. Puchwein. Calibrating cosmological radiative transfer simulations with Ly α forest data: evidence for large spatial UV background fluctuations at z ˜ 5.6-5.8 due to rare bright sources. *Monthly Notices of the RAS*, 453:2943–2964, November 2015.

[123] Jonathan Chardin, Girish Kulkarni, and Martin G. Haehnelt. Self-shielding of hydrogen in the IGM during the epoch of reionization. *Monthly Notices of the RAS*, 478(1):1065–1076, July 2018.

[124] Jonathan Chardin, Ewald Puchwein, and Martin G. Haehnelt. Large-scale opacity fluctuations in the Lyα forest: evidence for QSOs dominating the ionizing UV background at z $\sim$ 5.5-6? *Monthly Notices of the RAS*, 465(3):3429–3445, March 2017.

[125] J. Chen, A. V. Kravtsov, and C. R. Keeton. Lensing Optical Depths for Substructure and Isolated Dark Matter Halos. *Astrophysical Journal*, 592:24–31, July 2003.

[126] X. Chen, H. Firouzjahi, M. H. Namjoo, and M. Sasaki. A Single Field Inflation Model with Large Local Non-Gaussianity. *ArXiv e-prints*, January 2013.

[127] X. Chen, M.-x. Huang, S. Kachru, and G. Shiu. Observational signatures and non-Gaussianities of general single-field inflation. *Journal of Cosmology and Astroparticle Physics*, 1:2, January 2007.

[128] C. Cheung, A. L. Fitzpatrick, J. Kaplan, and L. Senatore. On the consistency relation of the three-point function in single-field inflation. *Journal of Cosmology and Astroparticle Physics*, 2:21, February 2008.

[129] Jacopo Chevallard, Stéphane Charlot, Peter Senchyna, Daniel P. Stark, Alba Vidal-García, Anna Feltre, Julia Gutkin, Tucker Jones, Ramesh Mainali, and Aida Wofford. Physical properties and H-ionizing-photon production rates of extreme nearby star-forming regions. *Monthly Notices of the RAS*, 479(3):3264–3273, September 2018.

[130] M. Chevallier and D. Polarski. Accelerating universes with scaling dark matter. *IJMPD*, 10(2):213–223, 2001.

[131] Yi-Kuan Chiang, Roderik A. Overzier, Karl Gebhardt, and Bruno Henriques. Galaxy Protoclusters as Drivers of Cosmic Star Formation History in the First 2 Gyr. *Astrophysical Journal*, 844(2):L23, August 2017.

[132] M. Chiba. Probing Dark Matter Substructure in Lens Galaxies. *Astrophysical Journal*, 565:17–23, January 2002.

[133] M. Chiba, T. Minezaki, N. Kashikawa, H. Kataza, and K. T. Inoue. Subaru Mid-Infrared Imaging of the Quadruple Lenses PG 1115+080 and B1422+231: Limits on Substructure Lensing. *Astrophysical Journal*, 627:53–61, July 2005.

[134] J. Chisholm, S. Gazagnes, D. Schaerer, A. Verhamme, J. R. Rigby, M. Bayliss, K. Sharon, M. Gladders, and H. Dahle. Accurately predicting the escape fraction of ionizing photons using rest-frame ultraviolet absorption lines. *Astronomy and Astrophysics*, 616:A30, August 2018.

[135] W. A. Chiu and J. P. Ostriker. A Semianalytic Model for Cosmological Reheating and Reionization Due to the Gravitational Collapse of Structure. *Astrophysical Journal*, 534:507–532, May 2000.

[136] S. Chongchitnan. The 21cm power spectrum and the shapes of non-Gaussianity. *Journal of Cosmology and Astroparticle Physics*, 3:37, March 2013.

[137] S. Chongchitnan and J. Silk. The 21-cm radiation from minihaloes as a probe of small primordial non-Gaussianity. *Monthly Notices of the RAS*, 426:L21–L25, October 2012.

[138] R. Chornock, E. Berger, D. B. Fox, W. Fong, T. Laskar, and K. C. Roth. GRB 140515A at z=6.33: Constraints on the End of Reionization From a Gamma-ray Burst in a Low Hydrogen Column Density Environment. *ArXiv e-prints*, May 2014.

[139] R. Chornock, E. Berger, D. B. Fox, R. Lunnan, M. R. Drout, W.-f. Fong, T. Laskar, and K. C. Roth. GRB 130606A as a Probe of the Intergalactic Medium and the Interstellar Medium in a Star-forming Galaxy in the First Gyr after the Big Bang. *Astrophysical Journal*, 774:26, September 2013.

[140] T. R. Choudhury, E. Puchwein, M. G. Haehnelt, and J. S. Bolton. Lyman-alpha emitters gone missing: evidence for late reionization? *ArXiv e-prints*, December 2014.

[141] Tirthankar Roy Choudhury, Martin G. Haehnelt, and John Regan. Inside-out or outside-in: the topology of reionization in the photon-starved regime suggested by Lyα forest data. *Monthly Notices of the RAS*, 394(2):960–977, Apr 2009.

[142] Holly M. Christenson, George D. Becker, Anson D'Aloisio, Frederick B. Davies, Yongda Zhu, Elisa Boera, Fahad Nasir, Steven R. Furlanetto, and Matthew A. Malkan. The relationship between IGM Lyman-alpha opacity and galaxy density near the end of reionization. *arXiv e-prints*, page arXiv:2308.13064, August 2023.

[143] Holly M. Christenson, George D. Becker, Steven R. Furlanetto, Frederick B. Davies, Matthew A. Malkan, Yongda Zhu, Elisa Boera, and Adam Trapp. Constraints on the End of Reionization from the Density Fields Surrounding Two Highly Opaque Quasar Sightlines. *Astrophysical Journal*, 923(1):87, December 2021.

[144] Annalisa Citro, Claudia M. Scarlata, Kameswara B. Mantha, Liliya R. Williams, Marc Rafelski, Mitchell Revalski, Matthew J. Hayes, Alaina Henry, Michael J. Rutkowski, and Harry I. Teplitz. Challenging the LyC-Lyα relation: strong Lyα emitters without LyC leakage at z $\sim$ 2.3. *arXiv e-prints*, page arXiv:2406.07618, June 2024.

[145] Ryan Cloutier, René Doyon, Francois Bouchy, and Guillaume Hébrard. Quantifying the Observational Effort Required for the Radial Velocity Characterization of TESS Planets. *Astronomical Journal*, 156(2):82, Aug 2018.

[146] D. Coe, N. Benitez, T. Broadhurst, L. Moustakas, and H. Ford. The Highest Resolution Mass Map of Galaxy Cluster Substructure To Date Without Assuming Light Traces Mass: LensPerfect Analysis of Abell 1689. *ArXiv e-prints*, May 2010.

[147] D. Coe, E. Fuselier, N. Benítez, T. Broadhurst, B. Frye, and H. Ford. LensPerfect: Gravitational Lens Mass Map Reconstructions Yielding Exact Reproduction of All Multiple Images. *Astrophysical Journal*, 681:814–830, July 2008.

[148] D. Coe, A. Zitrin, M. Carrasco, X. Shu, W. Zheng, M. Postman, L. Bradley, A. Koekemoer, and et. al. CLASH: Three Strongly Lensed Images of a Candidate z $\approx$ 11 Galaxy. *Astrophysical Journal*, 762:32, January 2013.

[149] G. Cognola, E. Elizalde, S. D. Odintsov, P. Tretyakov, and S. Zerbini. Initial and final de Sitter universes from modified $f(R)$ gravity. *ArXiv e-prints*, October 2008.

[150] J. D. Cohn and T.-C. Chang. Source mergers and bubble growth during reionization. *Monthly Notices of the RAS*, 374:72–94, January 2007.

[151] J. M. Comerford and P. Natarajan. The observed concentration-mass relation for galaxy clusters. *Monthly Notices of the RAS*, 379:190–200, July 2007.

[152] M. Compostella, S. Cantalupo, and C. Porciani. The imprint of inhomogeneous He II reionization on the H I and He II Lyα forest. *Monthly Notices of the RAS*, 435:3169–3190, November 2013.

[153] A. Cooney, S. DeDeo, and D. Psaltis. Gravity with Perturbative Constraints: Dark Energy Without New Degrees of Freedom. *ArXiv e-prints*, November 2008.

[154] A. Cooray and R. Sheth. Halo models of large scale structure. *Physics Reports*, 372:1–129, December 2002.

[155] A. R. Cooray. An Upper Limit on Ω_m Using Lensed Arcs. *Astrophysical Journal*, 524:504–509, October 1999.

[156] E. J. Copeland, M. Sami, and S. Tsujikawa. Dynamics of Dark Energy. *International Journal of Modern Physics D*, 15:1753–1935, 2006.

[157] P. S. Corasaniti and I. Achitouv. Excursion set halo mass function and bias in a stochastic barrier model of ellipsoidal collapse. *Physical Review D.*, 84(2):023009, July 2011.

[158] V. L. Corless, L. J. King, and D. Clowe. A New Look at Massive Clusters: weak lensing constraints on the triaxial dark matter halos of Abell 1689, Abell 1835, & Abell 2204. *ArXiv e-prints*, December 2008.

[159] Lia Corrales. X-Ray Scattering Echoes and Ghost Halos from the Intergalactic Medium: Relation to the Nature of AGN Variability. *Astrophysical Journal*, 805(1):23, May 2015.

[160] L. L. Cowie, A. J. Barger, and L. Trouille. Measuring the Sources of the Intergalactic Ionizing Flux. *Astrophysical Journal*, 692:1476–1488, February 2009.

[161] P. Creminelli, G. D'Amico, J. Noreña, and F. Vernizzi. The Effective Theory of Quintessence: the w¡-1 Side Unveiled. *ArXiv e-prints*, November 2008.

[162] P. Creminelli, A. Nicolis, L. Senatore, M. Tegmark, and M. Zaldarriaga. Limits on non-Gaussianities from WMAP data. *Journal of Cosmology and Astroparticle Physics*, 5:4, May 2006.

[163] P. Creminelli and M. Zaldarriaga. A single-field consistency relation for the three-point function. *Journal of Cosmology and Astroparticle Physics*, 10:6, October 2004.

[164] D. Crociani, A. Mesinger, L. Moscardini, and S. Furlanetto. The distribution of Lyman-limit absorption systems during and after reionization. *Monthly Notices of the RAS*, 411(1):289–300, Feb 2011.

[165] D. Crociani, L. Moscardini, M. Viel, and S. Matarrese. The effects of primordial non-Gaussianity on the cosmological reionization. *Monthly Notices of the RAS*, 394:133–141, March 2009.

[166] D. J. Croton, L. Gao, and S. D. M. White. Halo assembly bias and its effects on galaxy clustering. *Monthly Notices of the RAS*, 374:1303–1309, February 2007.

[167] C. Cunha, D. Huterer, and O. Doré. Primordial non-Gaussianity from the covariance of galaxy cluster counts. *Physical Review D.*, 82(2):023004–+, July 2010.

[168] J. V. Cunha. Kinematic Constraints to the Transition Redshift from SNe Ia Union Data. *ArXiv e-prints*, November 2008.

[169] Emma Curtis-Lake, Stefano Carniani, Alex Cameron, Stephane Charlot, Peter Jakobsen, Roberto Maiolino, Andrew Bunker, Joris Witstok, Renske Smit, Jacopo Chevallard, Chris Willott, Pierre Ferruit, Santiago Arribas, Nina Bonaventura, Mirko Curti, Francesco D'Eugenio, Marijn Franx, Giovanna Giardino, Tobias J. Looser, Nora Lützgendorf, Michael V. Maseda, Tim Rawle, Hans-Walter Rix, Bruno Rodríguez del Pino, Hannah Übler, Marco Sirianni, Alan Dressler, Eiichi Egami, Daniel J. Eisenstein, Ryan Endsley, Kevin Hainline, Ryan Hausen, Benjamin D. Johnson, Marcia Rieke, Brant Robertson, Irene Shivaei, Daniel P. Stark, Sandro Tacchella, Christina C. Williams, Christopher N. A. Willmer, Rachana Bhatawdekar, Rebecca Bowler, Kristan Boyett, Zuyi Chen, Anna de Graaff, Jakob M. Helton, Raphael E. Hviding, Gareth C. Jones, Nimisha Kumari, Jianwei Lyu, Erica Nelson, Michele Perna, Lester Sandles, Aayush Saxena, Katherine A. Suess, Fengwu Sun, Michael W. Topping, Imaan E. B. Wallace, and Lily Whitler. Spectroscopic confirmation of four metal-poor galaxies at z = 10.3-13.2. *Nature Astronomy*, 7:622–632, May 2023.

[170] N. Dalal, O. Doré, D. Huterer, and A. Shirokov. Imprints of primordial non-Gaussianities on large-scale structure: Scale-dependent bias and abundance of virialized objects. *Physical Review D.*, 77(12):123514–+, June 2008.

[171] N. Dalal, J. F. Hennawi, and P. Bode. Noise in Strong Lensing Cosmography. *Astrophysical Journal*, 622:99–105, March 2005.

[172] N. Dalal, G. Holder, and J. F. Hennawi. Statistics of Giant Arcs in Galaxy Clusters. *Astrophysical Journal*, 609:50–60, July 2004.

[173] N. Dalal, D. E. Holz, X. Chen, and J. A. Frieman. Corrective Lenses for High-Redshift Supernovae. *Astrophysical Journal*, 585:L11–L14, March 2003.

[174] N. Dalal and C. S. Kochanek. Direct Detection of Cold Dark Matter Substructure. *Astrophysical Journal*, 572:25–33, June 2002.

[175] A. Dall'Aglio, L. Wisotzki, and G. Worseck. An unbiased measurement of the UV background and its evolution via the proximity effect in quasar spectra. *Astronomy and Astrophysics*, 491:465–481, November 2008.

[176] A. D'Aloisio and S. R. Furlanetto. High-redshift voids in the excursion set formalism. *Monthly Notices of the RAS*, 382:860–870, December 2007.

[177] A. D'Aloisio, M. McQuinn, and H. Trac. Large Opacity Variations in the High-redshift Lyα Forest: The Signature of Relic Temperature Fluctuations from Patchy Reionization. *Astrophysical Journal*, 813:L38, November 2015.

[178] A. D'Aloisio and P. Natarajan. Cosmography with cluster strong lenses: the influence of substructure and line-of-sight haloes. *Monthly Notices of the RAS*, 411:1628–1640, March 2011.

[179] A. D'Aloisio and P. Natarajan. The effects of primordial non-Gaussianity on giant-arc statistics. *Monthly Notices of the RAS*, 415:1913–1927, August 2011.

[180] A. D'Aloisio and P. Natarajan. The Effects of Primordial Non-Gaussianity on Giant-Arc Statistics: A Scale Dependent Example. *Proceedings of the 2011 Frank N. Bash New Horizons in Astronomy Symposium*, February 2012.

[181] A. D'Aloisio, P. Natarajan, and P. R. Shapiro. The Effect of Large-Scale Structure on the Magnification of High-Redshift Sources by Cluster-Lenses. *Monthly Notices of the RAS*, submitted (arXiv:1311.1614), 2013.

[182] A. D'Aloisio, P. R. Upton Sanderbeck, M. McQuinn, H. Trac, and P. R. Shapiro. On the Contribution of Active Galactic Nuclei to the High-Redshift Metagalactic Ionizing Background. *ArXiv e-prints*, 468:4691, July 2016.

[183] A. D'Aloisio, J. Zhang, D. Jeong, and P. R. Shapiro. Halo statistics in non-Gaussian cosmologies: the collapsed fraction, conditional mass function, and halo bias from the path-integral excursion set method. *ArXiv e-prints*, June 2012.

[184] A. D'Aloisio, J. Zhang, D. Jeong, and P. R. Shapiro. Halo statistics in non-Gaussian cosmologies: the collapsed fraction, conditional mass function and halo bias from the path-integral excursion set method. *Monthly Notices of the RAS*, 428:2765–2788, January 2013.

[185] A. D'Aloisio, J. Zhang, P. R. Shapiro, and Y. Mao. The scale-dependent signature of primordial non-Gaussianity in the large-scale structure of cosmic reionization. *Monthly Notices of the RAS*, 433:2900–2919, August 2013.

[186] Anson D'Aloisio, Steven R. Furlanetto, and Priyamvada Natarajan. The abundance of lensing protoclusters. *MNRAS*, 394(3):1469–1486, 09 2008.

[187] Anson D'Aloisio, Matthew McQuinn, Frederick B. Davies, and Steven R. Furlanetto. Large fluctuations in the high-redshift metagalactic ionizing background. *Monthly Notices of the RAS*, 473(1):560–575, January 2018.

[188] Anson D'Aloisio, Matthew McQuinn, Oliver Maupin, Frederick B. Davies, Hy Trac, Spencer Fuller, and Phoebe R. Upton Sanderbeck. Heating of the Intergalactic Medium by Hydrogen Reionization. *Astrophysical Journal*, 874(2):154, April 2019.

[189] Anson D'Aloisio, Matthew McQuinn, Oliver Maupin, Frederick B. Davies, Hy Trac, Spencer Fuller, and Phoebe R. Upton Sanderbeck. Heating of the Intergalactic Medium by Hydrogen Reionization. *Astrophysical Journal*, 874(2):154, Apr 2019.

[190] Anson D'Aloisio, Matthew McQuinn, and Hy Trac. Large Opacity Variations in the High-redshift Lyα Forest: The Signature of Relic Temperature Fluctuations from Patchy Reionization. *Astrophysical Journal*, 813(2):L38, November 2015.

[191] Anson D'Aloisio, Matthew McQuinn, Hy Trac, Christopher Cain, and Andrei Mesinger. Hydrodynamic Response of the Intergalactic Medium to Reionization. *Astrophysical Journal*, 898(2):149, August 2020.

[192] Anson D'Aloisio, Matthew McQuinn, Hy Trac, Christopher Cain, and Andrei Mesinger. Hydrodynamic response of the intergalactic medium to reionization. *The Astrophysical Journal*, 898(2):149, aug 2020.

[193] Anson D'Aloisio, Phoebe R. Upton Sanderbeck, Matthew McQuinn, Hy Trac, and Paul R. Shapiro. On the contribution of active galactic nuclei to the high-redshift metagalactic ionizing background. *Monthly Notices of the RAS*, 468(4):4691–4701, Jul 2017.

[194] G. D'Amico, M. Musso, J. Noreña, and A. Paranjape. An improved calculation of the non-Gaussian halo mass function. *Journal of Cosmology and Astroparticle Physics*, 2:1, February 2011.

[195] G. D'Amico, M. Musso, J. Noreña, and A. Paranjape. Excursion sets and non-Gaussian void statistics. *Physical Review D.*, 83(2):023521, January 2011.

[196] S. Das and D. N. Spergel. CMB Lensing and the WMAP Cold Spot. *ArXiv e-prints*, September 2008.

[197] F. B. Davies and S. R. Furlanetto. Large fluctuations in the hydrogen-ionizing background and mean free path following the epoch of reionization. *Monthly Notices of the RAS*, 460:1328, April 2016.

[198] Frederick B. Davies, George D. Becker, and Steven R. Furlanetto. Determining the Nature of Late Gunn-Peterson Troughs with Galaxy Surveys. *Astrophysical Journal*, 860(2):155, June 2018.

[199] Frederick B. Davies and Steven R. Furlanetto. Large fluctuations in the hydrogen-ionizing background and mean free path following the epoch of reionization. *Monthly Notices of the RAS*, 460(2):1328–1339, August 2016.

[200] Frederick B. Davies and Steven R. Furlanetto. Large fluctuations in the hydrogen-ionizing background and mean free path following the epoch of reionization. *Monthly Notices of the RAS*, 460(2):1328–1339, August 2016.

[201] Frederick B. Davies, Joseph F. Hennawi, Eduardo Bañados, Zarija Lukić, Roberto Decarli, Xiaohui Fan, Emanuele P. Farina, Chiara Mazzucchelli, Hans-Walter Rix, Bram P. Venemans, Fabian Walter, Feige Wang, and Jinyi Yang. Quantitative Constraints on the Reionization History from the IGM Damping Wing Signature in Two Quasars at z > 7. *Astrophysical Journal*, 864(2):142, September 2018.

[202] Frederick B. Davies, Joseph F. Hennawi, and Anna-Christina Eilers. Evidence for Low Radiative Efficiency or Highly Obscured Growth of z > 7 Quasars. *Astrophysical Journal*, 884(1):L19, Oct 2019.

[203] A. J. Davis, A. D'Aloisio, and P. Natarajan. Virialization of high-redshift dark matter haloes. *Monthly Notices of the RAS*, 416:242–247, September 2011.

[204] G. De Lucia, G. Kauffmann, V. Springel, S. D. M. White, B. Lanzoni, F. Stoehr, G. Tormen, and N. Yoshida. Substructures in cold dark matter haloes. *Monthly Notices of the RAS*, 348:333–344, February 2004.

[205] A. De Simone, M. Maggiore, and A. Riotto. Excursion Set Theory for generic moving barriers and non-Gaussian initial conditions. *ArXiv e-prints*, July 2010.

[206] A. de Simone, M. Maggiore, and A. Riotto. Conditional probabilities in the excursion set theory: generic barriers and non-Gaussian initial conditions. *Monthly Notices of the RAS*, 418:2403–2421, December 2011.

[207] A. de Simone, M. Maggiore, and A. Riotto. Excursion set theory for generic moving barriers and non-Gaussian initial conditions. *Monthly Notices of the RAS*, 412:2587–2602, April 2011.

[208] Nicolas Deparis, Dominique Aubert, Pierre Ocvirk, Jonathan Chardin, and Joseph Lewis. Impact of the reduced speed of light approximation on ionization front velocities in cosmological simulations of the epoch of reionization. *Astronomy and Astrophysics*, 622:A142, Feb 2019.

[209] V. Desjacques, M. Crocce, R. Scoccimarro, and R. K. Sheth. Modeling scale-dependent bias on the baryonic acoustic scale with the statistics of peaks of Gaussian random fields. *Physical Review D.*, 82(10):103529, November 2010.

[210] V. Desjacques, D. Jeong, and F. Schmidt. Accurate predictions for the scale-dependent galaxy bias from primordial non-Gaussianity. *Physical Review D.*, 84(6):061301, September 2011.

[211] V. Desjacques, D. Jeong, and F. Schmidt. Non-Gaussian Halo Bias Re-examined: Mass-dependent Amplitude from the Peak-Background Split and Thresholding. *Physical Review D.*, 84(6):063512, September 2011.

[212] V. Desjacques and U. Seljak. Primordial non-Gaussianity from the large-scale structure. *Classical and Quantum Gravity*, 27(12):124011, June 2010.

[213] V. Desjacques and U. Seljak. Primordial Non-Gaussianity in the Large-Scale Structure of the Universe. *Advances in Astronomy*, 2010, 2010.

[214] V. Desjacques and U. Seljak. Signature of primordial non-Gaussianity of φ^3 type in the mass function and bias of dark matter haloes. *Physical Review D.*, 81(2):023006, January 2010.

[215] V. Desjacques, U. Seljak, and I. T. Iliev. Scale-dependent bias induced by local non-Gaussianity: a comparison to N-body simulations. *Monthly Notices of the RAS*, 396:85–96, June 2009.

[216] L.-B. Desroches, E. Quataert, C.-P. Ma, and A. A. West. Luminosity dependence in the Fundamental Plane projections of elliptical galaxies. *Monthly Notices of the RAS*, 377:402–414, May 2007.

[217] A. Dey, E. Kovetz, and S. Paban. Non-Gaussianities in the cosmological perturbation spectrum due to primordial anisotropy II. *Journal of Cosmology and Astroparticle Physics*, 10:55, October 2012.

[218] A. Dey and S. Paban. Non-gaussianities in the cosmological perturbation spectrum due to primordial anisotropy. *Journal of Cosmology and Astroparticle Physics*, 4:39, April 2012.

[219] J. M. Diego, P. Protopapas, H. B. Sandvik, and M. Tegmark. Non-parametric inversion of strong lensing systems. *Monthly Notices of the RAS*, 360:477–491, June 2005.

[220] J. M. Diego, H. B. Sandvik, P. Protopapas, M. Tegmark, N. Benítez, and T. Broadhurst. Non-parametric mass reconstruction of A1689 from strong lensing data with the Strong Lensing Analysis Package. *Monthly Notices of the RAS*, 362:1247–1258, October 2005.

[221] J. Diemand, M. Kuhlen, and P. Madau. Dark Matter Substructure and Gamma-Ray Annihilation in the Milky Way Halo. *Astrophysical Journal*, 657:262–270, March 2007.

[222] J. Diemand, M. Kuhlen, and P. Madau. Formation and Evolution of Galaxy Dark Matter Halos and Their Substructure. *Astrophysical Journal*, 667:859–877, October 2007.

[223] M. Dijkstra, Z. Haiman, M. J. Rees, and D. H. Weinberg. Photoionization Feedback in Low-Mass Galaxies at High Redshift. *Astrophysical Journal*, 601:666–675, February 2004.

[224] Mark Dijkstra. Lyα Emitting Galaxies as a Probe of Reionisation. *Publications of the Astron. Soc. of Australia*, 31:e040, October 2014.

[225] Mark Dijkstra. Lyα Emitting Galaxies as a Probe of Reionisation. *Publications of the Astron. Soc. of Australia*, 31:e040, October 2014.

[226] Mark Dijkstra and J. Stuart B. Wyithe. An empirical study of the relationship between Lyα and UV-selected galaxies: do theorists and observers 'select' the same objects? *Monthly Notices of the RAS*, 419(4):3181–3193, February 2012.

[227] Mark Dijkstra and J. Stuart B. Wyithe. An empirical study of the relationship between Lyα and UV-selected galaxies: do theorists and observers 'select' the same objects? *Monthly Notices of the RAS*, 419(4):3181–3193, February 2012.

[228] S. G. Djorgovski, S. Castro, D. Stern, and A. A. Mahabal. On the Threshold of the Reionization Epoch. *Astrophysical Journal*, 560:L5–L8, October 2001.

[229] S. Dodelson. Cluster masses: Accounting for structure along the line of sight. *Physical Review D.*, 70(2):023008, July 2004.

[230] C. T. Donnan, R. J. McLure, J. S. Dunlop, D. J. McLeod, D. Magee, K. Z. Arellano-Córdova, L. Barrufet, R. Begley, R. A. A. Bowler, A. C. Carnall, F. Cullen, R. S. Ellis, A. Fontana, G. D. Illingworth, N. A. Grogin, M. L. Hamadouche, A. M. Koekemoer, F. Y. Liu, C. Mason, P. Santini, and T. M. Stanton. JWST PRIMER: a new multifield determination of the evolving galaxy UV luminosity function at redshifts z $\sim$ 9 - 15. *Monthly Notices of the RAS*, 533(3):3222–3237, September 2024.

[231] Aristide Doussot, Hy Trac, and Renyue Cen. SCORCH. II. Radiation-hydrodynamic Simulations of Reionization with Varying Radiation Escape Fractions. *Astrophysical Journal*, 870(1):18, Jan 2019.

[232] A. R. Duffy, J. Schaye, S. T. Kay, and C. Dalla Vecchia. Dark matter halo concentrations in the Wilkinson Microwave Anisotropy Probe year 5 cosmology. *Monthly Notices of the RAS*, 390:L64–L68, October 2008.

[233] J. S. Dunlop, A. B. Rogers, R. J. McLure, R. S. Ellis, B. E. Robertson, A. Koekemoer, P. Dayal, E. Curtis-Lake, and et. al. The UV continua and inferred stellar populations of galaxies at z $\approx$ 7-9 revealed by the Hubble Ultra-Deep Field 2012 campaign. *Monthly Notices of the RAS*, 432:3520–3533, July 2013.

[234] S. Dutta, S. D. H. Hsu, D. Reeb, and R. J. Scherrer. Dark radiation as a signature of dark energy. *ArXiv e-prints*, February 2009.

[235] H. Ebeling, A. C. Edge, and J. P. Henry. MACS: A Quest for the Most Massive Galaxy Clusters in the Universe. *Astrophysical Journal*, 553:668–676, June 2001.

[236] G. Efstathiou, S. Moody, J. A. Peacock, and et al. Evidence for a non-zero Λ and a low matter density from a combined analysis of the 2dF Galaxy Redshift Survey and cosmic microwave background anisotropies. *Monthly Notices of the RAS*, 330:L29–L35, February 2002.

[237] Anna-Christina Eilers, Frederick B. Davies, and Joseph F. Hennawi. The Opacity of the Intergalactic Medium Measured along Quasar Sightlines at z $\sim$ 6. *Astrophysical Journal*, 864(1):53, September 2018.

[238] Anna-Christina Eilers, Frederick B. Davies, Joseph F. Hennawi, J. Xavier Prochaska, Zarija Lukić, and Chiara Mazzucchelli. Implications of z $\sim$6 Quasar Proximity Zones for the Epoch of Reionization and Quasar Lifetimes. *Astrophysical Journal*, 840(1):24, May 2017.

[239] D. J. Eisenstein and W. Hu. Power Spectra for Cold Dark Matter and Its Variants. *Astrophysical Journal*, 511:5–15, January 1999.

[240] D. J. Eisenstein, I. Zehavi, D. W. Hogg, and et al. Detection of the Baryon Acoustic Peak in the Large-Scale Correlation Function of SDSS Luminous Red Galaxies. *Astrophysical Journal*, 633:560–574, November 2005.

[241] V. R. Eke, J. F. Navarro, and M. Steinmetz. The Power Spectrum Dependence of Dark Matter Halo Concentrations. *Astrophysical Journal*, 554:114–125, June 2001.

[242] J. J. Eldridge and E. R. Stanway. The effect of stellar evolution uncertainties on the rest-frame ultraviolet stellar lines of C IV and He II in high-redshift Lyman-break galaxies. *Monthly Notices of the RAS*, 419:479–489, January 2012.

[243] Á. Elíasdóttir, M. Limousin, J. Richard, J. Hjorth, J.-P. Kneib, P. Natarajan, K. Pedersen, E. Jullo, and D. Paraficz. Where is the matter in the Merging Cluster Abell 2218? *ArXiv e-prints*, October 2007.

[244] R. S. Ellis, R. J. McLure, J. S. Dunlop, B. E. Robertson, Y. Ono, M. A. Schenker, A. Koekemoer, R. A. A. Bowler, M. Ouchi, A. B. Rogers, E. Curtis-Lake, E. Schneider, S. Charlot, D. P. Stark, S. R. Furlanetto, and M. Cirasuolo. The Abundance of Star-forming Galaxies in the Redshift Range 8.5-12: New Results from the 2012 Hubble Ultra Deep Field Campaign. *Astrophysical Journal*, 763:L7, January 2013.

[245] J. D. Emberson, Rajat M. Thomas, and Marcelo A. Alvarez. The Opacity of the Intergalactic Medium during Reionization: Resolving Small-scale Structure. *Astrophysical Journal*, 763(2):146, Feb 2013.

[246] Ryan Endsley and Daniel P. Stark. Strong Lyα Emission in an Overdense Region at $z = 6.8$: A Very Large ($R \sim 3$ physical Mpc) Ionized Bubble in COSMOS? *arXiv e-prints*, page arXiv:2112.14779, December 2021.

[247] Ryan Endsley, Daniel P. Stark, Stéphane Charlot, Jacopo Chevallard, Brant Robertson, Rychard J. Bouwens, and Mauro Stefanon. MMT spectroscopy of Lyman-alpha at z $\simeq$ 7: evidence for accelerated reionization around massive galaxies. *Monthly Notices of the RAS*, 502(4):6044–6063, April 2021.

[248] T. Erben, L. van Waerbeke, Y. Mellier, P. Schneider, J.-C. Cuillandre, F. J. Castander, and M. Dantel-Fort. Mass-detection of a matter concentration projected near the

cluster Abell 1942: Dark clump or high-redshift cluster? *Astronomy and Astrophysics*, 355:23–36, March 2000.

[249] X. Fan, C. L. Carilli, and B. Keating. Observational Constraints on Cosmic Reionization. *Annual Review of Astronomy and Astrophysics*, 44:415–462, September 2006.

[250] X. Fan, V. K. Narayanan, R. H. Lupton, M. A. Strauss, G. R. Knapp, R. H. Becker, R. L. White, L. Pentericci, and et. al. A Survey of z¿5.8 Quasars in the Sloan Digital Sky Survey. I. Discovery of Three New Quasars and the Spatial Density of Luminous Quasars at z˜6. *Astronomical Journal*, 122:2833–2849, December 2001.

[251] X. Fan, V. K. Narayanan, M. A. Strauss, R. L. White, R. H. Becker, L. Pentericci, and H.-W. Rix. Evolution of the Ionizing Background and the Epoch of Reionization from the Spectra of z˜6 Quasars. *Astronomical Journal*, 123:1247–1257, March 2002.

[252] X. Fan, M. A. Strauss, R. H. Becker, R. L. White, J. E. Gunn, G. R. Knapp, G. T. Richards, D. P. Schneider, J. Brinkmann, and M. Fukugita. Constraining the Evolution of the Ionizing Background and the Epoch of Reionization with z˜6 Quasars. II. A Sample of 19 Quasars. *Astronomical Journal*, 132:117–136, July 2006.

[253] X. Fan, M. A. Strauss, R. H. Becker, R. L. White, J. E. Gunn, G. R. Knapp, G. T. Richards, D. P. Schneider, J. Brinkmann, and M. Fukugita. Constraining the Evolution of the Ionizing Background and the Epoch of Reionization with z˜6 Quasars. II. A Sample of 19 Quasars. *Astronomical Journal*, 132:117–136, July 2006.

[254] X. Fan, M. A. Strauss, R. H. Becker, R. L. White, J. E. Gunn, G. R. Knapp, G. T. Richards, D. P. Schneider, J. Brinkmann, and M. Fukugita. Constraining the Evolution of the Ionizing Background and the Epoch of Reionization with z˜6 Quasars. II. A Sample of 19 Quasars. *Astronomical Journal*, 132:117–136, July 2006.

[255] X. Fan, M. A. Strauss, D. P. Schneider, J. E. Gunn, R. H. Lupton, R. H. Becker, M. Davis, J. A. Newman, and et al. High-Redshift Quasars Found in Sloan Digital Sky Survey Commissioning Data. IV. Luminosity Function from the Fall Equatorial Stripe Sample. *Astronomical Journal*, 121:54–65, January 2001.

[256] C.-A. Faucher-Giguère, A. Lidz, M. Zaldarriaga, and L. Hernquist. A New Calculation of the Ionizing Background Spectrum and the Effects of He II Reionization. *Astrophysical Journal*, 703:1416–1443, October 2009.

[257] C. Faure, J.-P. Kneib, S. Hilbert, R. Massey, G. Covone, A. Finoguenov, A. Leauthaud, J. E. Taylor, S. Pires, N. Scoville, and A. M. Koekemoer. On the Contribution of Large-Scale Structure to Strong Gravitational Lensing. *Astrophysical Journal*, 695:1233–1243, April 2009.

[258] C. Fedeli and M. Bartelmann. Effects of early dark energy on strong cluster lensing. *Astronomy and Astrophysics*, 461:49–57, January 2007.

[259] C. Fedeli, M. Bartelmann, M. Meneghetti, and L. Moscardini. Strong lensing statistics and the power spectrum normalisation. *Astronomy and Astrophysics*, 486:35–44, July 2008.

[260] C. Fedeli, M. Meneghetti, M. Bartelmann, K. Dolag, and L. Moscardini. A fast method for computing strong-lensing cross sections: application to merging clusters. *Astronomy and Astrophysics*, 447:419–430, February 2006.

[261] C. Fedeli, M. Meneghetti, S. Gottlöber, and G. Yepes. Strong lensing in the MARENOSTRUM UNIVERSE. II. Scaling relations and optical depths. *Astronomy and Astrophysics*, 519:A91+, September 2010.

[262] C. Fedeli and L. Moscardini. Cosmic shear statistics in cosmologies with non-Gaussian initial conditions. *Monthly Notices of the RAS*, 405:681–694, June 2010.

[263] C. Fedeli, L. Moscardini, and S. Matarrese. The clustering of galaxy clusters in cosmological models with non-Gaussian initial conditions: predictions for future surveys. *Monthly Notices of the RAS*, 397:1125–1137, August 2009.

[264] G. J. Ferland, R. L. Porter, P. A. M. van Hoof, R. J. R. Williams, N. P. Abel, M. L. Lykins, G. Shaw, W. J. Henney, and P. C. Stancil. The 2013 Release of Cloudy. *Revista Mexicana de Astronomia y Astrofisica*, 49:137–163, Apr 2013.

[265] E. R. Fernandez, I. T. Iliev, E. Komatsu, and P. R. Shapiro. The Cosmic near Infrared Background. III. Fluctuations, Reionization, and the Effects of Minimum Mass and Self-regulation. *Astrophysical Journal*, 750:20, May 2012.

[266] E. R. Fernandez and E. Komatsu. The Cosmic Near-Infrared Background: Remnant Light from Early Stars. *Astrophysical Journal*, 646:703–718, August 2006.

[267] E. R. Fernandez, E. Komatsu, I. T. Iliev, and P. R. Shapiro. The Cosmic Near-Infrared Background. II. Fluctuations. *Astrophysical Journal*, 710:1089–1110, February 2010.

[268] A. Fernández-Soto, K. M. Lanzetta, and A. Yahil. A New Catalog of Photometric Redshifts in the Hubble Deep Field. *Astrophysical Journal*, 513:34–50, March 1999.

[269] Anastasia Fialkov, Rennan Barkana, and Eli Visbal. The observable signature of late heating of the Universe during cosmic reionization. *Nature*, 506(7487):197–199, Feb 2014.

[270] S. L. Finkelstein, C. Papovich, M. Dickinson, M. Song, V. Tilvi, A. M. Koekemoer, K. D. Finkelstein, B. Mobasher, H. C. Ferguson, M. Giavalisco, N. Reddy, M. L. N. Ashby, A. Dekel, G. G. Fazio, A. Fontana, N. A. Grogin, J. S. Huang, D. Kocevski, M. Rafelski, B. J. Weiner, and S. P. Willner. A galaxy rapidly forming stars 700 million years after the Big Bang at redshift 7.51. *Nature*, 502(7472):524–527, October 2013.

[271] S. L. Finkelstein, C. Papovich, R. E. Ryan, A. H. Pawlik, M. Dickinson, H. C. Ferguson, K. Finlator, A. M. Koekemoer, M. Giavalisco, A. Cooray, J. S. Dunlop, S. M. Faber, N. A. Grogin, D. D. Kocevski, and J. A. Newman. CANDELS: The Contribution of the Observed Galaxy Population to Cosmic Reionization. *Astrophysical Journal*, 758:93, October 2012.

[272] Steven L. Finkelstein, Micaela Bagley, Mimi Song, Rebecca Larson, Casey Papovich, Mark Dickinson, Keely Finkelstein, Anton M. Koekemoer, Norbert Pirzkal, Rachel S. Somerville, L. Y. Aaron Yung, Peter Behroozi, Harry Ferguson, Mauro Giavalisco, Norman Grogin, Nimish Hathi, Taylor Hutchison, Intae Jung, Dale Kocevski, Lalitwadee Kawinwanichakij, Sofia Rojas-Ruiz, Jr. Ryan, Russell, Gregory F. Snyder, and Sandro Tacchella. A Census of the Bright z=8.5-11 Universe with the Hubble and Spitzer Space Telescopes in the CANDELS Fields. *arXiv e-prints*, page arXiv:2106.13813, June 2021.

[273] Steven L. Finkelstein, Anson D'Aloisio, Jan-Pieter Paardekooper, Jr. Ryan, Russell, Peter Behroozi, Kristian Finlator, Rachael Livermore, Phoebe R. Upton Sanderbeck, Claudio Dalla Vecchia, and Sadegh Khochfar. Conditions for Reionizing the Universe with a Low Galaxy Ionizing Photon Escape Fraction. *Astrophysical Journal*, 879(1):36, July 2019.

[274] Steven L. Finkelstein, Anson D'Aloisio, Jan-Pieter Paardekooper, Jr. Ryan, Russell, Peter Behroozi, Kristian Finlator, Rachael Livermore, Phoebe R. Upton Sanderbeck, Claudio Dalla Vecchia, and Sadegh Khochfar. Conditions for Reionizing the Universe with a Low Galaxy Ionizing Photon Escape Fraction. *Astrophysical Journal*, 879(1):36, Jul 2019.

[275] Steven L. Finkelstein, Jr. Ryan, Russell E., Casey Papovich, Mark Dickinson, Mimi Song, Rachel S. Somerville, Henry C. Ferguson, Brett Salmon, Mauro Giavalisco, Anton M. Koekemoer, Matthew L. N. Ashby, Peter Behroozi, Marco Castellano, James S. Dunlop, Sandy M. Faber, Giovanni G. Fazio, Adriano Fontana, Norman A. Grogin, Nimish Hathi, Jason Jaacks, Dale D. Kocevski, Rachael Livermore, Ross J. McLure, Emiliano Merlin, Bahram Mobasher, Jeffrey A. Newman, Marc Rafelski, Vithal Tilvi, and S. P. Willner. The Evolution of the Galaxy Rest-frame Ultraviolet Luminosity Function over the First Two Billion Years. *Astrophysical Journal*, 810(1):71, September 2015.

[276] Steven L. Finkelstein, Russell E. Ryan, Jr., Casey Papovich, Mark Dickinson, Mimi Song, Rachel S. Somerville, Henry C. Ferguson, Brett Salmon, Mauro Giavalisco, Anton M. Koekemoer, Matthew L. N. Ashby, Peter Behroozi, Marco Castellano, James S. Dunlop, Sandy M. Faber, Giovanni G. Fazio, Adriano Fontana, Norman A. Grogin, Nimish Hathi, Jason Jaacks, Dale D. Kocevski, Rachael Livermore, Ross J. McLure, Emiliano Merlin, Bahram Mobasher, Jeffrey A. Newman, Marc Rafelski, Vithal Tilvi, and S. P. Willner. The Evolution of the Galaxy Rest-frame Ultraviolet Luminosity Function over the First Two Billion Years. *Astrophysical Journal*, 810(1):71, September 2015.

[277] K. Finlator, S. P. Oh, F. Özel, and R. Davé. Gas Clumping in Self-Consistent Reionisation Models. *ArXiv e-prints*, September 2012.

[278] K. Finlator, F. Özel, R. Davé, and B. D. Oppenheimer. The late reionization of filaments. *Monthly Notices of the RAS*, 400:1049–1061, December 2009.

[279] R. A. Flores, A. H. Maller, and J. R. Primack. Arc Statistics in Clusters: Galaxy Contribution. *Astrophysical Journal*, 535:555–560, June 2000.

[280] A. Fontana, E. Vanzella, L. Pentericci, M. Castellano, M. Giavalisco, A. Grazian, K. Boutsia, S. Cristiani, M. Dickinson, E. Giallongo, R. Maiolino, A. Moorwood, and P. Santini. The Lack of Intense Lyα in Ultradeep Spectra of z = 7 Candidates in GOODS-S: Imprint of Reionization? *Astrophysical Journal*, 725(2):L205–L209, December 2010.

[281] F. Fontanot, S. Cristiani, and E. Vanzella. On the relative contribution of high-redshift galaxies and active galactic nuclei to reionization. *Monthly Notices of the RAS*, 425:1413–1420, September 2012.

[282] M. M. Friedrich, G. Mellema, M. A. Alvarez, P. R. Shapiro, and I. T. Iliev. Topology and sizes of H II regions during cosmic reionization. *Monthly Notices of the RAS*, 413:1353–1372, May 2011.

[283] J. A. Frieman, M. S. Turner, and D. Huterer. Dark Energy and the Accelerating Universe. *Annual Review of Astronomy and Astrophysics*, 46:385–432, September 2008.

[284] A. Fritz, B. L. Ziegler, R. G. Bower, I. Smail, and R. L. Davies. On the evolutionary status of early-type galaxies in clusters at z˜ 0.2 - I. The Fundamental Plane. *Monthly Notices of the RAS*, 358:233–255, March 2005.

[285] L. Fu, E. Semboloni, H. Hoekstra, and et al. Very weak lensing in the CFHTLS wide: cosmology from cosmic shear in the linear regime. *Astronomy and Astrophysics*, 479:9–25, February 2008.

[286] S. R. Furlanetto and A. Loeb. Is Double Reionization Physically Plausible? *Astrophysical Journal*, 634:1–13, November 2005.

[287] S. R. Furlanetto, M. McQuinn, and L. Hernquist. Characteristic scales during reionization. *Monthly Notices of the RAS*, 365:115–126, January 2006.

[288] S. R. Furlanetto and S. P. Oh. Taxing the rich: recombinations and bubble growth during reionization. *Monthly Notices of the RAS*, 363:1031–1048, November 2005.

[289] S. R. Furlanetto and S. P. Oh. The Temperature-Density Relation of the Intergalactic Medium after Hydrogen Reionization. *Astrophysical Journal*, 701:94–104, August 2009.

[290] S. R. Furlanetto, S. P. Oh, and F. H. Briggs. Cosmology at low frequencies: The 21 cm transition and the high-redshift Universe. *Physics Reports*, 433:181–301, October 2006.

[291] S. R. Furlanetto and T. Piran. The evidence of absence: galaxy voids in the excursion set formalism. *Monthly Notices of the RAS*, 366:467–479, February 2006.

[292] S. R. Furlanetto, M. Zaldarriaga, and L. Hernquist. The Growth of H II Regions During Reionization. *Astrophysical Journal*, 613:1–15, September 2004.

[293] Steven R. Furlanetto. The global 21-centimeter background from high redshifts. *Monthly Notices of the RAS*, 371(2):867–878, Sep 2006.

[294] Steven R. Furlanetto and S. Peng Oh. Taxing the rich: recombinations and bubble growth during reionization. *Monthly Notices of the Royal Astronomical Society*, 363(3):1031–1048, 11 2005.

[295] Steven R. Furlanetto, Matias Zaldarriaga, and Lars Hernquist. The effects of reionization on Lyα galaxy surveys. *Monthly Notices of the RAS*, 365(3):1012–1020, January 2006.

[296] Steven R. Furlanetto, Matias Zaldarriaga, and Lars Hernquist. The effects of reionization on Lyα galaxy surveys. *Monthly Notices of the RAS*, 365(3):1012–1020, January 2006.

[297] Prakash Gaikwad, Martin G. Haehnelt, Fredrick B. Davies, Sarah E. I. Bosman, Margherita Molaro, Girish Kulkarni, Valentina D'Odorico, George D. Becker, Rebecca L. Davies, Fahad Nasir, James S. Bolton, Laura C. Keating, Vid Iršič, Ewald Puchwein, Yongda Zhu, Shikhar Asthana, Jinyi Yang, Samuel Lai, and Anna-Christina Eilers. Measuring the photoionization rate, neutral fraction, and mean free path of H I ionizing photons at $4.9 \leq z \leq 6.0$ from a large sample of XShooter and ESI spectra. *Monthly Notices of the RAS*, 525(3):4093–4120, November 2023.

[298] Prakash Gaikwad, Michael Rauch, Martin G. Haehnelt, Ewald Puchwein, James S. Bolton, Laura C. Keating, Girish Kulkarni, Vid Iršič, Eduardo Bañados, George D. Becker, Elisa Boera, Fakhri S. Zahedy, Hsiao-Wen Chen, Robert F. Carswell, Jonathan Chardin, and Alberto Rorai. Probing the thermal state of the intergalactic medium at z ¿ 5 with the transmission spikes in high-resolution Ly α forest spectra. *Monthly Notices of the RAS*, 494(4):5091–5109, June 2020.

[299] S. Gallerani, T. R. Choudhury, and A. Ferrara. Constraining the reionization history with QSO absorption spectra. *Monthly Notices of the RAS*, 370:1401–1421, August 2006.

[300] S. Gallerani, A. Ferrara, X. Fan, and T. R. Choudhury. Glimpsing through the high-redshift neutral hydrogen fog. *Monthly Notices of the RAS*, 386:359–369, May 2008.

[301] J. Ganc. Calculating the local-type f_{NL} for slow-roll inflation with a nonvacuum initial state. *Physical Review D.*, 84(6):063514, September 2011.

[302] J. Ganc and E. Komatsu. Scale-dependent bias of galaxies and μ-type distortion of the cosmic microwave background spectrum from single-field inflation with a modified initial state. *Physical Review D.*, 86(2):023518, July 2012.

[303] Nakul Gangolli, Anson D'Aloisio, Christopher Cain, George D. Becker, and Holly Christenson. On the correlation between Lyα forest opacity and galaxy density in late reionization models. *arXiv e-prints*, page arXiv:2408.08358, August 2024.

[304] Nakul Gangolli, Anson D'Aloisio, Fahad Nasir, and Zheng Zheng. Constraining reionization in progress at z = 5.7 with Lyman-α emitters: voids, peaks, and cosmic variance. *Monthly Notices of the RAS*, 501(4):5294–5308, March 2021.

[305] A. Gangui, F. Lucchin, S. Matarrese, and S. Mollerach. The three-point correlation function of the cosmic microwave background in inflationary models. *Astrophysical Journal*, 430:447–457, August 1994.

[306] G. J. Gao, Y. P. Jing, S. Mao, G. L. Li, and X. Kong. Impacts of Source Properties on Strong Lensing by Rich Galaxy Clusters. *Astrophysical Journal*, 707:472–481, December 2009.

[307] L. Gao, J. F. Navarro, S. Cole, C. S. Frenk, S. D. M. White, V. Springel, A. Jenkins, and A. F. Neto. The redshift dependence of the structure of massive Λ cold dark matter haloes. *Monthly Notices of the RAS*, 387:536–544, June 2008.

[308] J. Garcia-Bellido and T. Haugboelle. The radial BAO scale and Cosmic Shear, a new observable for Inhomogeneous Cosmologies. *ArXiv e-prints*, October 2008.

[309] A. Georgakakis, J. Aird, J. Buchner, M. Salvato, M.-L. Menzel, W. N. Brandt, I. D. McGreer, T. Dwelly, G. Mountrichas, C. Koki, I. Georgantopoulos, L.-T. Hsu, A. Merloni, Z. Liu, K. Nandra, and N. P. Ross. The X-ray luminosity function of active galactic nuclei in the redshift interval z=3-5. *Monthly Notices of the RAS*, 453:1946–1964, October 2015.

[310] E. M. George, C. L. Reichardt, K. A. Aird, B. A. Benson, L. E. Bleem, J. E. Carlstrom, C. L. Chang, H.-M. Cho, T. M. Crawford, A. T. Crites, T. de Haan, M. A. Dobbs, J. Dudley, N. W. Halverson, N. L. Harrington, G. P. Holder, W. L. Holzapfel, Z. Hou, J. D. Hrubes, R. Keisler, L. Knox, A. T. Lee, E. M. Leitch, M. Lueker, D. Luong-Van, J. J. McMahon, J. Mehl, S. S. Meyer, M. Millea, L. M. Mocanu, J. J. Mohr, T. E. Montroy, S. Padin, T. Plagge, C. Pryke, J. E. Ruhl, K. K. Schaffer, L. Shaw, E. Shirokoff, H. G. Spieler, Z. Staniszewski, A. A. Stark, K. T. Story, A. van Engelen, K. Vanderlinde, J. D. Vieira, R. Williamson, and O. Zahn. A Measurement of Secondary Cosmic Microwave Background Anisotropies from the 2500 Square-degree SPT-SZ Survey. *Astrophysical Journal*, 799:177, February 2015.

[311] E. Giallongo, A. Grazian, F. Fiore, A. Fontana, L. Pentericci, E. Vanzella, M. Dickinson, D. Kocevski, and et al. Faint AGNs at z ¿ 4 in the CANDELS GOODS-S field: looking for contributors to the reionization of the Universe. *Astronomy and Astrophysics*, 578:A83, June 2015.

[312] T. Giannantonio and C. Porciani. Structure formation from non-Gaussian initial conditions: Multivariate biasing, statistics, and comparison with N-body simulations. *Physical Review D.*, 81(6):063530, March 2010.

[313] T. Giannantonio, C. Porciani, J. Carron, A. Amara, and A. Pillepich. Constraining primordial non-Gaussianity with future galaxy surveys. *Monthly Notices of the RAS*, 422:2854–2877, June 2012.

[314] T. Giannantonio, A. J. Ross, W. J. Percival, R. Crittenden, D. Bacher, M. Kilbinger, R. Nichol, and J. Weller. Improved Primordial Non-Gaussianity Constraints from Measurements of Galaxy Clustering and the Integrated Sachs-Wolfe Effect. *ArXiv e-prints*, March 2013.

[315] J. Gilmore and P. Natarajan. Cosmography with cluster strong lensing. *Monthly Notices of the RAS*, 396:354–364, June 2009.

[316] Sambit K. Giri, Garrelt Mellema, Thomas Aldheimer, Keri L. Dixon, and Ilian T. Iliev. Neutral island statistics during reionization from 21-cm tomography. *Monthly Notices of the RAS*, 489(2):1590–1605, October 2019.

[317] Sambit K. Giri, Garrelt Mellema, and Raghunath Ghara. Optimal identification of H II regions during reionization in 21-cm observations. *Monthly Notices of the RAS*, 479(4):5596–5611, October 2018.

[318] M. L. Giroux and P. R. Shapiro. The Reionization of the Intergalactic Medium and Its Observational Consequences. *Astrophysical Journals*, 102:191, February 1996.

[319] M. D. Gladders. Strong Lensing by High-Redshift Red-Sequence Selected Galaxy Clusters. In Y. Mellier & G. Meylan, editor, *Gravitational Lensing Impact on Cosmology*, volume 225 of *IAU Symposium*, pages 149–154, June 2005.

[320] M. D. Gladders, H. Hoekstra, H. K. C. Yee, P. B. Hall, and L. F. Barrientos. The Incidence of Strong-Lensing Clusters in the Red-Sequence Cluster Survey. *Astrophysical Journal*, 593:48–55, August 2003.

[321] E. Glikman, S. G. Djorgovski, D. Stern, A. Dey, B. T. Jannuzi, and K.-S. Lee. The Faint End of the Quasar Luminosity Function at z ˜ 4: Implications for Ionization of the Intergalactic Medium and Cosmic Downsizing. *Astrophysical Journal*, 728:L26, February 2011.

[322] N. Y. Gnedin. Cosmological Reionization by Stellar Sources. *Astrophysical Journal*, 535:530–554, June 2000.

[323] N. Y. Gnedin. Effect of Reionization on Structure Formation in the Universe. *Astrophysical Journal*, 542:535–541, October 2000.

[324] N. Y. Gnedin, G. D. Becker, and X. Fan. Cosmic Reionization On Computers. Properties of the Post-reionization IGM. *ArXiv e-prints*, May 2016.

[325] N. Y. Gnedin and A. A. Kaurov. Cosmic Reionization on Computers. II. Reionization History and Its Back-reaction on Early Galaxies. *Astrophysical Journal*, 793:30, September 2014.

[326] N. Y. Gnedin, A. V. Kravtsov, and D. H. Rudd. Implementing the DC Mode in Cosmological Simulations with Supercomoving Variables. *Astrophysical Journals*, 194:46, June 2011.

[327] N. Y. Gnedin and J. P. Ostriker. Reionization of the Universe and the Early Production of Metals. *Astrophysical Journal*, 486:581, September 1997.

[328] Nickolay Y. Gnedin. Cosmic Reionization on Computers. I. Design and Calibration of Simulations. *Astrophysical Journal*, 793(1):29, Sep 2014.

[329] G. Golse and J.-P. Kneib. Pseudo elliptical lensing mass model: Application to the NFW mass distribution. *Astronomy and Astrophysics*, 390:821–827, August 2002.

[330] G. Golse, J.-P. Kneib, and G. Soucail. Constraining the cosmological parameters using strong lensing. *Astronomy and Astrophysics*, 387:788–803, June 2002.

[331] K. M. Górski, E. Hivon, A. J. Banday, B. D. Wandelt, F. K. Hansen, M. Reinecke, and M. Bartelmann. HEALPix: A Framework for High-Resolution Discretization and Fast Analysis of Data Distributed on the Sphere. *Astrophysical Journal*, 622:759–771, April 2005.

[332] A. Grazian, E. Giallongo, K. Boutsia, S. Cristiani, E. Vanzella, C. Scarlata, P. Santini, L. Pentericci, E. Merlin, N. Menci, F. Fontanot, A. Fontana, F. Fiore, F. Civano, M. Castellano, M. Brusa, A. Bonchi, R. Carini, F. Cusano, M. Faccini, B. Garilli, A. Marchetti, A. Rossi, and R. Speziali. The contribution of faint AGNs to the ionizing background at z $\sim$ 4. *Astronomy and Astrophysics*, 613:A44, May 2018.

[333] A. Grazian, E. Giallongo, F. Fiore, K. Boutsia, F. Civano, S. Cristiani, G. Cupani, M. Dickinson, F. Fontanot, N. Menci, and M. Romano. On the AGN Nature of Two UV-bright Sources at $z_{spec} \sim 5.5$ in the CANDELS Fields: An Update on the AGN Space Density at $M_{1450} \sim$ -22.5. *Astrophysical Journal*, 897(1):94, July 2020.

[334] A. Grazian, E. Giallongo, R. Gerbasi, F. Fiore, A. Fontana, O. Le Fèvre, L. Pentericci, E. Vanzella, G. Zamorani, P. Cassata, B. Garilli, V. Le Brun, D. Maccagni, L. A. M. Tasca, R. Thomas, E. Zucca, R. Amorín, S. Bardelli, L. P. Cassarà, M. Castellano, A. Cimatti, O. Cucciati, A. Durkalec, M. Giavalisco, N. P. Hathi, O. Ilbert, B. C. Lemaux, S. Paltani, B. Ribeiro, D. Schaerer, M. Scodeggio, V. Sommariva, M. Talia, L. Tresse, D. Vergani, A. Bonchi, K. Boutsia, P. Capak, S. Charlot, T. Contini, S. de la Torre, J. Dunlop, S. Fotopoulou, L. Guaita, A. Koekemoer, C. López-Sanjuan, Y. Mellier, E. Merlin, D. Paris, J. Pforr, S. Pilo, P. Santini, N. Scoville, Y. Taniguchi, and P. W. Wang. The Lyman continuum escape fraction of galaxies at z = 3.3 in the VUDS-LBC/COSMOS field. *Astronomy and Astrophysics*, 585:A48, January 2016.

[335] Bradley Greig and Andrei Mesinger. The global history of reionization. *Monthly Notices of the RAS*, 465(4):4838–4852, March 2017.

[336] Bradley Greig, Andrei Mesinger, and Eduardo Bañados. Constraints on reionization from the z = 7.5 QSO ULASJ1342+0928. *Monthly Notices of the RAS*, 484(4):5094–5101, April 2019.

[337] Bradley Greig, Andrei Mesinger, Eduardo Bañados, George D. Becker, Sarah E. I. Bosman, Huanqing Chen, Frederick B. Davies, Valentina D'Odorico, Anna-Christina Eilers, Simona Gallerani, Martin G. Haehnelt, Laura Keating, Samuel Lai, Yuxiang Qin, Emma Ryan-Weber, Sindhu Satyavolu, Feige Wang, Jinyi Yang, and Yongda Zhu. IGM damping wing constraints on the tail end of reionisation from the enlarged XQR-30 sample. *arXiv e-prints*, page arXiv:2404.12585, April 2024.

[338] Bradley Greig, Andrei Mesinger, Zoltán Haiman, and Robert A. Simcoe. Are we witnessing the epoch of reionisation at z = 7.1 from the spectrum of J1120+0641? *Monthly Notices of the RAS*, 466(4):4239–4249, Apr 2017.

[339] Max Gronke, Pierre Ocvirk, Charlotte Mason, Jorryt Matthee, Sarah E. I. Bosman, Jenny G. Sorce, Joseph Lewis, Kyungjin Ahn, Dominique Aubert, Taha Dawoodbhoy, Ilian T. Iliev, Paul R. Shapiro, and Gustavo Yepes. Lyman-α transmission properties of the intergalactic medium in the CoDaII simulation. *Monthly Notices of the RAS*, 508(3):3697–3709, December 2021.

[340] M. Grossi, K. Dolag, E. Branchini, S. Matarrese, and L. Moscardini. Evolution of massive haloes in non-Gaussian scenarios. *Monthly Notices of the RAS*, 382:1261–1267, December 2007.

[341] M. Grossi and V. Springel. The impact of early dark energy on non-linear structure formation. *Monthly Notices of the RAS*, 394:1559–1574, April 2009.

[342] M. Grossi, L. Verde, C. Carbone, K. Dolag, E. Branchini, F. Iannuzzi, S. Matarrese, and L. Moscardini. Large-scale non-Gaussian mass function and halo bias: tests on N-body simulations. *Monthly Notices of the RAS*, 398:321–332, September 2009.

[343] A. Gruzinov and W. Hu. Secondary Cosmic Microwave Background Anisotropies in a Universe Reionized in Patches. *Astrophysical Journal*, 508:435–439, December 1998.

[344] J. E. Gunn and B. A. Peterson. On the Density of Neutral Hydrogen in Intergalactic Space. *Astrophysical Journal*, 142:1633–1641, November 1965.

[345] F. Haardt and P. Madau. Radiative Transfer in a Clumpy Universe. IV. New Synthesis Models of the Cosmic UV/X-Ray Background. *Astrophysical Journal*, 746:125, February 2012.

[346] O. Hahn and T. Abel. Multi-scale initial conditions for cosmological simulations. *Monthly Notices of the RAS*, 415:2101–2121, August 2011.

[347] Z. Haiman, T. Abel, and M. J. Rees. The Radiative Feedback of the First Cosmological Objects. *Astrophysical Journal*, 534:11–24, May 2000.

[348] Z. Haiman and G. P. Holder. The Reionization History at High Redshifts. I. Physical Models and New Constraints from Cosmic Microwave Background Polarization. *Astrophysical Journal*, 595:1–12, September 2003.

[349] A. Halkola, S. Seitz, and M. Pannella. Parametric strong gravitational lensing analysis of Abell 1689. *Monthly Notices of the RAS*, 372:1425–1462, November 2006.

[350] N. Hall, M. Bradač, A. H. Gonzalez, T. Treu, D. Clowe, C. Jones, M. Stiavelli, D. Zaritsky, J.-G. Cuby, and B. Clément. Using the Bullet Cluster as a Gravitational Telescope to Study z ¿˜ 7 Lyman Break Galaxies. *Astrophysical Journal*, 745:155, February 2012.

[351] T. Hamana, H. Martel, and T. Futamase. Statistics of Weak Gravitational Lensing in Cold Dark Matter Models: Magnification Bias on Quasar Luminosity Functions. *Astrophysical Journal*, 529:56–68, January 2000.

[352] A. J. S. Hamilton, P. Kumar, E. Lu, and A. Matthews. Reconstructing the primordial spectrum of fluctuations of the universe from the observed nonlinear clustering of galaxies. *Astrophysical Journal*, 374:L1–L4, June 1991.

[353] R. J. Hanisch and C. D. Biemesderfer. T_EX and LAT_EX Macro Definition Files for Astronomical Publications. In *Bulletin of the American Astronomical Society*, page 780, Mar 1989.

[354] Yuichi Harikane, Masami Ouchi, Yoshiaki Ono, Seiji Fujimoto, Darko Donevski, Takatoshi Shibuya, Andreas L. Faisst, Tomotsugu Goto, Bunyo Hatsukade, Nobunari Kashikawa, Kotaro Kohno, Takuya Hashimoto, Ryo Higuchi, Akio K. Inoue, Yen-Ting Lin, Crystal L. Martin, Roderik Overzier, Ian Smail, Jun Toshikawa, Hideki Umehata, Yiping Ao, Scott Chapman, David L. Clements, Myungshin Im, Yipeng Jing, Toshihiro Kawaguchi, Chien-Hsiu Lee, Minju M. Lee, Lihwai Lin, Yoshiki Matsuoka, Murilo Marinello, Tohru Nagao, Masato Onodera, Sune Toft, and Wei-Hao Wang. SILVERRUSH. VIII. Spectroscopic Identifications of Early Large-scale Structures with Protoclusters over 200 Mpc at z ∼6-7: Strong Associations of Dusty Star-forming Galaxies. *Astrophysical Journal*, 883(2):142, October 2019.

[355] Yuichi Harikane, Masami Ouchi, Yoshiaki Ono, Surhud More, Shun Saito, Yen-Ting Lin, Jean Coupon, Kazuhiro Shimasaku, Takatoshi Shibuya, Paul A. Price, Lihwai Lin, Bau-Ching Hsieh, Masafumi Ishigaki, Yutaka Komiyama, John Silverman, Tadafumi Takata, Hiroko Tamazawa, and Jun Toshikawa. Evolution of Stellar-to-Halo Mass Ratio at z = 0 - 7 Identified by Clustering Analysis with the Hubble Legacy Imaging and Early Subaru/Hyper Suprime-Cam Survey Data. *Astrophysical Journal*, 821(2):123, April 2016.

[356] Charles R. Harris, K. Jarrod Millman, St'efan J. van der Walt, Ralf Gommers, Pauli Virtanen, David Cournapeau, Eric Wieser, Julian Taylor, Sebastian Berg, Nathaniel J. Smith, Robert Kern, Matti Picus, Stephan Hoyer, Marten H. van Kerkwijk, Matthew Brett, Allan Haldane, Jaime Fern'andez del R'ıo, Mark Wiebe, Pearu Peterson, Pierre

G'erard-Marchant, Kevin Sheppard, Tyler Reddy, Warren Weckesser, Hameer Abbasi, Christoph Gohlke, and Travis E. Oliphant. Array programming with NumPy. *Nature*, 585(7825):357–362, September 2020.

[357] D. Harsono and R. De Propris. The Luminosity Function of Galaxies to $M_{BgVriz} \sim$ -14 in $z \sim 0.3$ Clusters. *Astronomical Journal*, 137:3091–3099, February 2009.

[358] Sultan Hassan, Romeel Davé, Matthew McQuinn, Rachel S. Somerville, Laura C. Keating, Daniel Anglés-Alcázar, Francisco Villaescusa-Navarro, and David N. Spergel. Reionization with SIMBA: How Much Does Astrophysics Matter in Modeling Cosmic Reionization? *Astrophysical Journal*, 931(1):62, May 2022.

[359] Sultan Hassan and Max Gronke. Can galaxy evolution mimic cosmic reionization? *arXiv e-prints*, page arXiv:2010.00023, September 2020.

[360] Sultan Hassan and Max Gronke. Can Galaxy Evolution Mimic Cosmic Reionization? *Astrophysical Journal*, 908(2):219, February 2021.

[361] J. F. Hennawi, N. Dalal, P. Bode, and J. P. Ostriker. Characterizing the Cluster Lens Population. *Astrophysical Journal*, 654:714–730, January 2007.

[362] L. Hernquist, N. Katz, D. H. Weinberg, and J. Miralda-Escudé. The Lyman-Alpha Forest in the Cold Dark Matter Model. *Astrophysical Journal*, 457:L51+, February 1996.

[363] S. Hilbert, J. Hartlap, S. D. M. White, and P. Schneider. Ray-tracing through the Millennium Simulation: Born corrections and lens-lens coupling in cosmic shear and galaxy-galaxy lensing. *Astronomy and Astrophysics*, 499:31–43, September 2009.

[364] S. Hilbert, S. D. M. White, J. Hartlap, and P. Schneider. Strong lensing optical depths in a ΛCDM universe. *Monthly Notices of the RAS*, 382:121–132, November 2007.

[365] G. Hinshaw, D. Larson, E. Komatsu, D. N. Spergel, C. L. Bennett, J. Dunkley, M. R. Nolta, M. Halpern, and et. al. Nine-Year Wilkinson Microwave Anisotropy Probe (WMAP) Observations: Cosmological Parameter Results. *ArXiv e-prints*, December 2012.

[366] S. Ho and M. White. Cluster arc statistics. *Astroparticle Physics*, 24:257–272, October 2005.

[367] A. Hoag, M. Bradač, K. Huang, C. Mason, T. Treu, K. B. Schmidt, M. Trenti, V. Strait, B. C. Lemaux, E. Q. Finney, and M. Paddock. Constraining the Neutral Fraction of Hydrogen in the IGM at Redshift 7.5. *Astrophysical Journal*, 878(1):12, June 2019.

[368] H. M. Hodges, G. R. Blumenthal, L. A. Kofman, and J. R. Primack. Nonstandard primordial fluctuations from a polynomial inflation potential. *Nuclear Physics B*, 335:197–220, April 1990.

[369] M. Hoeft, G. Yepes, S. Gottlöber, and V. Springel. Dwarf galaxies in voids: suppressing star formation with photoheating. *Monthly Notices of the RAS*, 371:401–414, September 2006.

[370] H. Hoekstra. The effect of distant large scale structure on weak lensing mass estimates. *Astronomy and Astrophysics*, 370:743–753, May 2001.

[371] H. Hoekstra, M. Franx, K. Kuijken, R. G. Carlberg, and H. K. C. Yee. Lensing by galaxies in CNOC2 fields. *Monthly Notices of the RAS*, 340:609–622, April 2003.

[372] H. Hoekstra, J. Hartlap, S. Hilbert, and E. van Uitert. Effects of distant large-scale structure on the precision of weak lensing mass measurements. *Monthly Notices of the RAS*, 412:2095–2103, April 2011.

[373] P. F. Hopkins, L. Hernquist, T. J. Cox, T. Di Matteo, B. Robertson, and V. Springel. A Unified, Merger-driven Model of the Origin of Starbursts, Quasars, the Cosmic X-Ray Background, Supermassive Black Holes, and Galaxy Spheroids. *Astrophysical Journals*, 163:1–49, March 2006.

[374] A. Horesh, D. Maoz, S. Hilbert, and M. Bartelmann. Lensed arc statistics: comparison of Millennium-simulation galaxy clusters to Hubble Space Telescope observations of an X-ray selected sample. *ArXiv e-prints*, January 2011.

[375] A. Horesh, E. O. Ofek, D. Maoz, M. Bartelmann, M. Meneghetti, and H.-W. Rix. The Lensed Arc Production Efficiency of Galaxy Clusters: A Comparison of Matched Observed and Simulated Samples. *Astrophysical Journal*, 633:768–780, November 2005.

[376] O. Host. Galaxy cluster strong lensing: image deflections from density fluctuations along the line of sight. *Monthly Notices of the RAS*, 420:L18–L22, February 2012.

[377] E. M. Hu, L. L. Cowie, A. J. Barger, P. Capak, Y. Kakazu, and L. Trouille. An Atlas of z = 5.7 and z = 6.5 Lyα Emitters. *Astrophysical Journal*, 725(1):394–423, December 2010.

[378] E. M. Hu, L. L. Cowie, A. Songaila, A. J. Barger, B. Rosenwasser, and I. G. B. Wold. An Ultraluminous Lyα Emitter with a Blue Wing at z = 6.6. *Astrophysical Journal*, 825(1):L7, July 2016.

[379] W. Hu. Power Spectrum Tomography with Weak Lensing. *Astrophysical Journal*, 522:L21–L24, September 1999.

[380] Weida Hu, Junxian Wang, Zhen-Ya Zheng, Sangeeta Malhotra, James E. Rhoads, Leopoldo Infante, L. Felipe Barrientos, Huan Yang, Chunyan Jiang, Wenyong Kang, Lucia A. Perez, Isak Wold, Pascale Hibon, Linhua Jiang, Ali Ahmad Khostovan, Francisco Valdes, Alistair R. Walker, Gaspar Galaz, Alicia Coughlin, Santosh Harish, Xu Kong, John Pharo, and XianZhong Zheng. The Lyα Luminosity Function and Cosmic Reionization at z $\sim$ 7.0: A Tale of Two LAGER Fields. *Astrophysical Journal*, 886(2):90, December 2019.

[381] Weida Hu, Junxian Wang, Zhen-Ya Zheng, Sangeeta Malhotra, James E. Rhoads, Leopoldo Infante, L. Felipe Barrientos, Huan Yang, Chunyan Jiang, Wenyong Kang, Lucia A. Perez, Isak Wold, Pascale Hibon, Linhua Jiang, Ali Ahmad Khostovan, Francisco Valdes, Alistair R. Walker, Gaspar Galaz, Alicia Coughlin, Santosh Harish, Xu Kong, John Pharo, and XianZhong Zheng. The Lyα Luminosity Function and Cosmic Reionization at z $\sim$ 7.0: A Tale of Two LAGER Fields. *Astrophysical Journal*, 886(2):90, December 2019.

[382] Weida Hu, Junxian Wang, Zhen-Ya Zheng, Sangeeta Malhotra, James E. Rhoads, Leopoldo Infante, L. Felipe Barrientos, Huan Yang, Chunyan Jiang, Wenyong Kang, Lucia A. Perez, Isak Wold, Pascale Hibon, Linhua Jiang, Ali Ahmad Khostovan, Francisco Valdes, Alistair R. Walker, Gaspar Galaz, Alicia Coughlin, Santosh Harish, Xu Kong, John Pharo, and XianZhong Zheng. The Lyα Luminosity Function and Cosmic Reionization at z $\sim$ 7.0: A Tale of Two LAGER Fields. *Astrophysical Journal*, 886(2):90, December 2019.

[383] L. Hui and N. Y. Gnedin. Equation of state of the photoionized intergalactic medium. *Monthly Notices of the RAS*, 292:27, November 1997.

[384] L. Hui and Z. Haiman. The Thermal Memory of Reionization History. *Astrophysical Journal*, 596:9–18, October 2003.

[385] J. D. Hunter. Matplotlib: A 2d graphics environment. *Computing in Science & Engineering*, 9(3):90–95, 2007.

[386] Anne Hutter, Pratika Dayal, and Volker Müller. Clustering and lifetime of Lyman Alpha Emitters in the Epoch of Reionization. *Monthly Notices of the RAS*, 450(4):4025–4034, July 2015.

[387] Anne Hutter, Pratika Dayal, and Volker Müller. Clustering and lifetime of Lyman Alpha Emitters in the Epoch of Reionization. *Monthly Notices of the RAS*, 450(4):4025–4034, July 2015.

[388] H. Ikeda, T. Nagao, K. Matsuoka, Y. Taniguchi, Y. Shioya, M. Kajisawa, M. Enoki, P. Capak, F. Civano, A. M. Koekemoer, D. Masters, T. Morokuma, M. Salvato, E. Schinnerer, and N. Z. Scoville. Constraints on the Faint End of the Quasar Luminosity Function at z ˜ 5 in the COSMOS Field. *Astrophysical Journal*, 756:160, September 2012.

[389] H. Ikeda, T. Nagao, K. Matsuoka, Y. Taniguchi, Y. Shioya, J. R. Trump, P. Capak, A. Comastri, M. Enoki, Y. Ideue, Y. Kakazu, A. M. Koekemoer, T. Morokuma, T. Murayama, T. Saito, M. Salvato, E. Schinnerer, N. Z. Scoville, and J. D. Silverman. Probing the Faint End of the Quasar Luminosity Function at z˜ 4 in the COSMOS Field. *Astrophysical Journal*, 728:L25, February 2011.

[390] I. T. Iliev, G. Mellema, P. R. Shapiro, and U.-L. Pen. Self-regulated reionization. *Monthly Notices of the RAS*, 376:534–548, April 2007.

[391] I. T. Iliev, U.-L. Pen, J. Richard Bond, G. Mellema, and P. R. Shapiro. kSZ from patchy reionization: The view from the simulations. *New Astronomy Review*, 50:909–917, December 2006.

[392] Ilian T. Iliev, Garrelt Mellema, Kyungjin Ahn, Paul R. Shapiro, Yi Mao, and Ue-Li Pen. Simulating cosmic reionization: how large a volume is large enough? *Monthly Notices of the RAS*, 439(1):725–743, Mar 2014.

[393] Ilian T. Iliev, Paul R. Shapiro, and Alejandro C. Raga. Minihalo photoevaporation during cosmic reionization: evaporation times and photon consumption rates. *Monthly Notices of the RAS*, 361(2):405–414, Aug 2005.

[394] Akio K Inoue, Kenji Hasegawa, Tomoaki Ishiyama, Hidenobu Yajima, Ikkoh Shimizu, Masayuki Umemura, Akira Konno, Yuichi Harikane, Takatoshi Shibuya, Masami Ouchi, and et al. Silverrush. vi. a simulation of lyα emitters in the reionization epoch and a comparison with subaru hyper suprime-cam survey early data. *Publications of the Astronomical Society of Japan*, 70(3), May 2018.

[395] K. T. Inoue and J. Silk. Local Voids as the Origin of Large-Angle Cosmic Microwave Background Anomalies. I. *Astrophysical Journal*, 648:23–30, September 2006.

[396] Vid Iršič, Matteo Viel, Martin G. Haehnelt, James S. Bolton, Stefano Cristiani, George D. Becker, Valentina D'Odorico, Guido Cupani, Tae-Sun Kim, Trystyn A. M. Berg, Sebastian López, Sara Ellison, Lise Christensen, Kelly D. Denney, and Gábor Worseck. New constraints on the free-streaming of warm dark matter from intermediate and small scale Lyman-α forest data. *Physical Review D.*, 96(2):023522, Jul 2017.

[397] Rikako Ishimoto, Nobunari Kashikawa, Daichi Kashino, Kei Ito, Yongming Liang, Zheng Cai, Takehiro Yoshioka, Katsuya Okoshi, Toru Misawa, Masafusa Onoue, Yoshihiro Takeda, and Hisakazu Uchiyama. The physical origin for spatially large scatter of IGM opacity at the end of reionization: The IGM Lyα opacity-galaxy density relation. *Monthly Notices of the RAS*, 515(4):5914–5926, October 2022.

[398] Y I Izotov, G Worseck, D Schaerer, N G Guseva, T X Thuan, Fricke, A Verhamme, and I Orlitová. Low-redshift Lyman continuum leaking galaxies with high [O iii]/[O ii] ratios. *Monthly Notices of the Royal Astronomical Society*, 478(4):4851–4865, 05 2018.

[399] B. Jain and M. Lima. Magnification effects on source counts and fluxes. *Monthly Notices of the RAS*, 411:2113–2117, March 2011.

[400] M. Jaroszynski and Z. Kostrzewa-Rutkowska. Background, foreground and nearby matter influence on strong gravitational lenses. *Monthly Notices of the RAS*, 424:325–332, July 2012.

[401] H. Jensen, M. Hayes, I. T. Iliev, P. Laursen, G. Mellema, and E. Zackrisson. Studying reionization with the next generation of Lyα emitter surveys. *Monthly Notices of the RAS*, 444(3):2114–2127, November 2014.

[402] H. Jensen, M. Hayes, I. T. Iliev, P. Laursen, G. Mellema, and E. Zackrisson. Studying reionization with the next generation of Lyα emitter surveys. *Monthly Notices of the RAS*, 444(3):2114–2127, November 2014.

[403] D. Jeong and E. Komatsu. Primordial Non-Gaussianity, Scale-dependent Bias, and the Bispectrum of Galaxies. *Astrophysical Journal*, 703:1230–1248, October 2009.

[404] D. Jeong, F. Schmidt, and C. M. Hirata. Large-scale clustering of galaxies in general relativity. *Physical Review D.*, 85(2):023504, January 2012.

[405] L. Jiang, X. Fan, F. Bian, J. Annis, K. Chiu, S. Jester, H. Lin, R. H. Lupton, G. T. Richards, M. A. Strauss, V. Malanushenko, E. Malanushenko, and D. P. Schneider. A Survey of z ˜ 6 Quasars in the Sloan Digital Sky Survey Deep Stripe. II. Discovery of Six Quasars at z $_{AB}$¿21. *Astronomical Journal*, 138:305–311, July 2009.

[406] S. Joudaki, O. Doré, L. Ferramacho, M. Kaplinghat, and M. G. Santos. Primordial Non-Gaussianity from the 21 cm Power Spectrum during the Epoch of Reionization. *Physical Review Letters*, 107(13):131304, September 2011.

[407] E. Jullo and J.-P. Kneib. Multiscale cluster lens mass mapping - I. Strong lensing modelling. *Monthly Notices of the RAS*, 395:1319–1332, May 2009.

[408] E. Jullo, J.-P. Kneib, M. Limousin, Á. Elíasdóttir, P. J. Marshall, and T. Verdugo. A Bayesian approach to strong lensing modelling of galaxy clusters. *New Journal of Physics*, 9:447–+, December 2007.

[409] E. Jullo, P. Natarajan, J.-P. Kneib, A. D'Aloisio, M. Limousin, J. Richard, and C. Schimd. Cosmological constraints from strong gravitational lensing in clusters of galaxies. *Science*, 329:924–927, 2010.

[410] Intae Jung, Steven L. Finkelstein, Mark Dickinson, Taylor A. Hutchison, Rebecca L. Larson, Casey Papovich, Laura Pentericci, Amber N. Straughn, Yicheng Guo, Sangeeta Malhotra, James Rhoads, Mimi Song, Vithal Tilvi, and Isak Wold. Texas Spectroscopic Search for Lyα Emission at the End of Reionization III. the Lyα Equivalent-width Distribution and Ionized Structures at $z > 7$. *arXiv e-prints*, page arXiv:2009.10092, September 2020.

[411] Intae Jung, Steven L. Finkelstein, Rebecca L. Larson, Taylor A. Hutchison, Amber N. Straughn, Micaela B. Bagley, Marco Castellano, Nikko J. Cleri, M. C. Cooper, Mark Dickinson, Henry C. Ferguson, Benne W. Holwerda, Jeyhan S. Kartaltepe, Seonwoo Kim, Anton M. Koekemoer, Casey Papovich, Hyunbae Park, Laura Pentericci, Pablo G. Perez-Gonzalez, Mimi Song, Sandro Tacchella, Benjamin J. Weiner, Christopher N. A. Willmer, and Jorge A. Zavala. New $z > 7$ Lyman-alpha Emitters in EGS: Evidence of an Extended Ionized Structure at $z \sim 7.7$. *arXiv e-prints*, page arXiv:2212.09850, December 2022.

[412] R. Kaehler, O. Hahn, and T. Abel. A Novel Approach to Visualizing Dark Matter Simulations. *ArXiv e-prints*, August 2012.

[413] N. Kaiser. On the spatial correlations of Abell clusters. *Astrophysical Journal*, 284:L9–L12, September 1984.

[414] N. Kaiser, G. Wilson, and G. A. Luppino. Large-Scale Cosmic Shear Measurements. *ArXiv Astrophysics e-prints*, March 2000.

[415] Koki Kakiichi, Richard S. Ellis, Nicolas Laporte, Adi Zitrin, Anna-Christina Eilers, Emma Ryan-Weber, Romain A. Meyer, Brant Robertson, Daniel P. Stark, and Sarah E. I. Bosman. The role of galaxies and AGN in reionizing the IGM - I. Keck spectroscopy of 5 ¡ z ¡ 7 galaxies in the QSO field J1148+5251. *Monthly Notices of the RAS*, 479(1):43–63, September 2018.

[416] M. Kamionkowski, L. Verde, and R. Jimenez. The Void Abundance with Non-Gaussian Primordial Perturbations. *ArXiv e-prints*, September 2008.

[417] M. Kamionkowski, L. Verde, and R. Jimenez. The void abundance with non-gaussian primordial perturbations. *Journal of Cosmology and Astroparticle Physics*, 1:10, January 2009.

[418] N. Kashikawa, Y. Ishizaki, C. J. Willott, M. Onoue, M. Im, H. Furusawa, J. Toshikawa, S. Ishikawa, Y. Niino, K. Shimasaku, M. Ouchi, and P. Hibon. The Subaru High-z Quasar Survey: Discovery of Faint z ˜ 6 Quasars. *Astrophysical Journal*, 798:28, January 2015.

[419] N. Kashikawa, K. Shimasaku, M. A. Malkan, M. Doi, Y. Matsuda, M. Ouchi, Y. Taniguchi, C. Ly, T. Nagao, M. Iye, K. Motohara, T. Murayama, K. Murozono, K. Nariai, K. Ohta, S. Okamura, T. Sasaki, Y. Shioya, and M. Umemura. The End of the Reionization Epoch Probed by Lyα Emitters at z = 6.5 in the Subaru Deep Field. *Astrophysical Journal*, 648:7–22, September 2006.

[420] Nobunari Kashikawa, Kazuhiro Shimasaku, Matthew A. Malkan, Mamoru Doi, Yuichi Matsuda, Masami Ouchi, Yoshiaki Taniguchi, Chun Ly, Tohru Nagao, Masanori Iye, Kentaro Motohara, Takashi Murayama, Kouji Murozono, Kyoji Nariai, Kouji Ohta, Sadanori Okamura, Toshiyuki Sasaki, Yasuhiro Shioya, and Masayuki Umemura. The End of the Reionization Epoch Probed by Lyα Emitters at z = 6.5 in the Subaru Deep Field. *Astrophysical Journal*, 648(1):7–22, September 2006.

[421] Nobunari Kashikawa, Kazuhiro Shimasaku, Yuichi Matsuda, Eiichi Egami, Linhua Jiang, Tohru Nagao, Masami Ouchi, Matthew A. Malkan, Takashi Hattori, Kazuaki Ota, Yoshiaki Taniguchi, Sadanori Okamura, Chun Ly, Masanori Iye, Hisanori Furusawa, Yasuhiro Shioya, Takatoshi Shibuya, Yoshifumi Ishizaki, and Jun Toshikawa. Completing the Census of Lyα Emitters at the Reionization Epoch. *Astrophysical Journal*, 734(2):119, June 2011.

[422] Daichi Kashino, Simon J. Lilly, Jorryt Matthee, Anna-Christina Eilers, Ruari Mackenzie, Rongmon Bordoloi, and Robert A. Simcoe. EIGER. I. A Large Sample of [O III]-emitting Galaxies at 5.3 ¡ z ¡ 6.9 and Direct Evidence for Local Reionization by Galaxies. *Astrophysical Journal*, 950(1):66, June 2023.

[423] Daichi Kashino, Simon J. Lilly, Takatoshi Shibuya, Masami Ouchi, and Nobunari Kashikawa. Evidence for a Highly Opaque Large-scale Galaxy Void at the End of Reionization. *Astrophysical Journal*, 888(1):6, January 2020.

[424] A. Kassiola and I. Kovner. Elliptic Mass Distributions versus Elliptic Potentials in Gravitational Lenses. *Astrophysical Journal*, 417:450–+, November 1993.

[425] A. A. Kaurov and N. Y. Gnedin. Cosmic Reionization on Computers. III. The Clumping Factor. *Astrophysical Journal*, 810:154, September 2015.

[426] Laura C. Keating, Lewis H. Weinberger, Girish Kulkarni, Martin G. Haehnelt, Jonathan Chardin, and Dominique Aubert. Long troughs in the Lyman-α forest below redshift 6 due to islands of neutral hydrogen. *Monthly Notices of the RAS*, 491(2):1736–1745, Jan 2020.

[427] C. R. Keeton. Source Ellipticity and the Statistics of Lensed Arcs. *Astrophysical Journal*, 562:160–163, November 2001.

[428] C. R. Keeton, C. S. Kochanek, and U. Seljak. Shear and Ellipticity in Gravitational Lenses. *Astrophysical Journal*, 482:604, June 1997.

[429] I. S. Khrykin, J. F. Hennawi, M. McQuinn, and G. Worseck. He II Proximity Effect and the Lifetime of Quasars. *ArXiv e-prints*, November 2015.

[430] M. Kilbinger, K. Benabed, J. Guy, P. Astier, I. Tereno, L. Fu, D. Wraith, J. Coupon, Y. Mellier, C. Balland, F. R. Bouchet, T. Hamana, D. Hardin, H. J. McCracken, R. Pain, N. Regnault, M. Schultheiss, and H. Yahagi. Dark energy constraints and correlations with systematics from CFHTLS weak lensing, SNLS supernovae Ia and WMAP5. *ArXiv e-prints*, October 2008.

[431] Taysun Kimm, Jérémy Blaizot, Thibault Garel, Léo Michel-Dansac, Harley Katz, Joakim Rosdahl, Anne Verhamme, and Martin Haehnelt. Understanding the escape of LyC and Lyα photons from turbulent clouds. *Monthly Notices of the RAS*, 486(2):2215–2237, June 2019.

[432] T. D. Kitching, A. F. Heavens, A. N. Taylor, M. L. Brown, K. Meisenheimer, C. Wolf, M. E. Gray, and D. J. Bacon. Cosmological constraints from COMBO-17 using 3D weak lensing. *Monthly Notices of the RAS*, 376:771–778, April 2007.

[433] A. Klypin, G. Yepes, S. Gottlober, F. Prada, and S. Hess. MultiDark simulations: the story of dark matter halo concentrations and density profiles. *ArXiv e-prints*, November 2014.

[434] Anatoly Klypin, Gustavo Yepes, Stefan Gottlöber, Francisco Prada, and Steffen Heß. MultiDark simulations: the story of dark matter halo concentrations and density profiles. *Monthly Notices of the RAS*, 457(4):4340–4359, April 2016.

[435] J.-P. Kneib, R. S. Ellis, I. Smail, W. J. Couch, and R. M. Sharples. Hubble Space Telescope Observations of the Lensing Cluster Abell 2218. *Astrophysical Journal*, 471:643, November 1996.

[436] J.-P. Kneib, P. Hudelot, R. S. Ellis, T. Treu, G. P. Smith, P. Marshall, O. Czoske, I. Smail, and P. Natarajan. A Wide-Field Hubble Space Telescope Study of the Cluster Cl 0024+1654 at z=0.4. II. The Cluster Mass Distribution. *Astrophysical Journal*, 598:804–817, December 2003.

[437] J.-P. Kneib and P. Natarajan. Cluster lenses. *Astronomy and Astrophysicsr*, 19:47, November 2011.

[438] L. Knox, R. Scoccimarro, and S. Dodelson. Impact of Inhomogeneous Reionization on Cosmic Microwave Background Anisotropy. *Physical Review Letters*, 81:2004–2007, September 1998.

[439] C. S. Kochanek and N. Dalal. Tests for Substructure in Gravitational Lenses. *Astrophysical Journal*, 610:69–79, July 2004.

[440] L. Kofman, G. R. Blumenthal, H. Hodges, and J. R. Primack. Generation of Non-Flat and Non-Gaussian Perturbations from Inflation. In D. W. Latham and L. A. N. da Costa, editors, *Large-scale Structures and Peculiar Motions in the Universe*, volume 15 of *Astronomical Society of the Pacific Conference Series*, page 339, 1991.

[441] K. Kohler, N. Y. Gnedin, and A. J. S. Hamilton. Large-Scale Simulations of Reionization. *Astrophysical Journal*, 657:15–29, March 2007.

[442] E. W. Kolb, V. Marra, and S. Matarrese. Description of our cosmological spacetime as a perturbed conformal Newtonian metric and implications for the backreaction proposal for the accelerating universe. *ArXiv e-prints*, July 2008.

[443] E. Komatsu. Hunting for primordial non-Gaussianity in the cosmic microwave background. *Classical and Quantum Gravity*, 27(12):124010, June 2010.

[444] E. Komatsu, J. Dunkley, M. R. Nolta, C. L. Bennett, B. Gold, G. Hinshaw, N. Jarosik, D. Larson, M. Limon, L. Page, D. N. Spergel, M. Halpern, R. S. Hill, A. Kogut, S. S. Meyer, G. S. Tucker, J. L. Weiland, E. Wollack, and E. L. Wright. Five-Year Wilkinson Microwave Anisotropy Probe Observations: Cosmological Interpretation. *Astrophysical Journals*, 180:330–376, February 2009.

[445] E. Komatsu, K. M. Smith, J. Dunkley, C. L. Bennett, B. Gold, G. Hinshaw, N. Jarosik, D. Larson, and et al. Seven-year Wilkinson Microwave Anisotropy Probe (WMAP) Observations: Cosmological Interpretation. *Astrophysical Journals*, 192:18–+, February 2011.

[446] E. Komatsu and D. N. Spergel. Acoustic signatures in the primary microwave background bispectrum. *Physical Review D.*, 63(6):063002, March 2001.

[447] Akira Konno, Masami Ouchi, Yoshiaki Ono, Kazuhiro Shimasaku, Takatoshi Shibuya, Hisanori Furusawa, Kimihiko Nakajima, Yoshiaki Naito, Rieko Momose, Suraphong Yuma, and Masanori Iye. Accelerated Evolution of the Lyα Luminosity Function at z >~7 Revealed by the Subaru Ultra-deep Survey for Lyα Emitters at z = 7.3. *Astrophysical Journal*, 797(1):16, December 2014.

[448] Akira Konno, Masami Ouchi, Yoshiaki Ono, Kazuhiro Shimasaku, Takatoshi Shibuya, Hisanori Furusawa, Kimihiko Nakajima, Yoshiaki Naito, Rieko Momose, Suraphong Yuma, and Masanori Iye. Accelerated Evolution of the Lyα Luminosity Function at z ¿~7 Revealed by the Subaru Ultra-deep Survey for Lyα Emitters at z = 7.3. *Astrophysical Journal*, 797(1):16, December 2014.

[449] Akira Konno, Masami Ouchi, Takatoshi Shibuya, Yoshiaki Ono, Kazuhiro Shimasaku, Yoshiaki Taniguchi, Tohru Nagao, Masakazu A. R. Kobayashi, Masaru Kajisawa, Nobunari Kashikawa, Akio K. Inoue, Masamune Oguri, Hisanori Furusawa, Tomotsugu Goto, Yuichi Harikane, Ryo Higuchi, Yutaka Komiyama, Haruka Kusakabe, Satoshi Miyazaki, Kimihiko Nakajima, and Shiang-Yu Wang. SILVERRUSH. IV. Lyα luminosity functions at z = 5.7 and 6.6 studied with $\sim$1300 Lyα emitters on the 14-21 deg^2 sky. *Publications of the ASJ*, 70:S16, January 2018.

[450] M. Kowalski, D. Rubin, G. Aldering, and et al. Improved Cosmological Constraints from New, Old, and Combined Supernova Data Sets. *Astrophysical Journal*, 686:749–778, October 2008.

[451] R. H. Kramer, Z. Haiman, and S. P. Oh. Feedback from Clustered Sources during Reionization. *Astrophysical Journal*, 649:570–578, October 2006.

[452] M. Kuhlen and P. Madau. The first miniquasar. *Monthly Notices of the RAS*, 363:1069–1082, November 2005.

[453] G. Kulkarni and T. R. Choudhury. Reionization and feedback in overdense regions at high redshift. *Monthly Notices of the RAS*, 412:2781–2789, April 2011.

[454] Girish Kulkarni, Laura C. Keating, Martin G. Haehnelt, Sarah E. I. Bosman, Ewald Puchwein, Jonathan Chardin, and Dominique Aubert. Large Ly α opacity fluctuations and low CMB τ in models of late reionization with large islands of neutral hydrogen extending to z < 5.5. *Monthly Notices of the RAS*, 485(1):L24–L28, May 2019.

[455] Girish Kulkarni, Gábor Worseck, and Joseph F. Hennawi. Evolution of the AGN UV luminosity function from redshift 7.5. *Monthly Notices of the RAS*, 488(1):1035–1065, Sep 2019.

[456] C. Lacey and S. Cole. Merger rates in hierarchical models of galaxy formation. *Monthly Notices of the RAS*, 262:627–649, June 1993.

[457] T. Y. Lam and R. K. Sheth. The nonlinear probability distribution function in models with local primordial non-Gaussianity. *ArXiv e-prints*, December 2008.

[458] A. Lamastra, N. Menci, F. Fiore, and P. Santini. The interaction-driven starburst contribution to the cosmic star formation rate density. *ArXiv e-prints*, February 2013.

[459] L. Lamport. *LaTeX: A Document Preparation System.* Addison-Wesley Professional, 2 edition, 1994.

[460] Stephen D. Landy and Alexander S. Szalay. Bias and Variance of Angular Correlation Functions. *Astrophysical Journal*, 412:64, July 1993.

[461] N. Laporte, R. A. Meyer, R. S. Ellis, B. E. Robertson, J. Chisholm, and G. W. Roberts-Borsani. Probing cosmic dawn: Ages and star formation histories of candidate $z \geq 9$ galaxies. *Monthly Notices of the RAS*, 505(3):3336–3346, August 2021.

[462] Rebecca L. Larson, Steven L. Finkelstein, Taylor A. Hutchison, Casey Papovich, Micaela Bagley, Mark Dickinson, Sofía Rojas-Ruiz, Harry C. Ferguson, Intae Jung, Mauro Giavalisco, Andrea Grazian, Laura Pentericci, and Sandro Tacchella. Searching for Islands of Reionization: A Potential Ionized Bubble Powered by a Spectroscopic Overdensity at $z = 8.7$. *Astrophysical Journal*, 930(2):104, May 2022.

[463] O. Le Fevre, F. Hammer, M. C. Angonin, I. M. Gioia, and G. A. Luppino. Imaging of 16 distant EMSS clusters with Z greater than or equal to 0.2 and L(subx,44) greater than or equal to 4: New arcs and first consequences. *Astrophysical Journal*, 422:L5–L8, February 1994.

[464] J. Lee, X. Kang, and Y. P. Jing. The Intrinsic Alignment of Dark Halo Substructures. *Astrophysical Journal*, 629:L5–L8, August 2005.

[465] C. Leitherer, D. Schaerer, J. D. Goldader, R. M. G. Delgado, C. Robert, D. F. Kune, D. F. de Mello, D. Devost, and T. M. Heckman. Starburst99: Synthesis Models for Galaxies with Active Star Formation. *Astrophysical Journals*, 123:3–40, July 1999.

[466] D. Lemze, R. Barkana, T. J. Broadhurst, and Y. Rephaeli. Mass and gas profiles in A1689: joint X-ray and lensing analysis. *Monthly Notices of the RAS*, 386:1092–1106, May 2008.

[467] E. Leonova, P. A. Oesch, Y. Qin, R. P. Naidu, J. S. B. Wyithe, S. de Barros, R. J. Bouwens, R. S. Ellis, R. M. Endsley, A. Hutter, G. D. Illingworth, J. Kerutt, I. Labbe, N. Laporte, D. Magee, S. J. Mutch, G. W. Roberts-Borsani, R. Smit, D. P. Stark, M. Stefanon, S. Tacchella, and A. Zitrin. The Prevalence of Galaxy Overdensities Around UV-Luminous Lyman α Emitters in the Epoch of Reionization. *arXiv e-prints*, page arXiv:2112.07675, December 2021.

[468] Antony Lewis, Anthony Challinor, and Anthony Lasenby. Efficient computation of CMB anisotropies in closed FRW models. *Astrophys. J.*, 538:473–476, 2000.

[469] G.-L. Li, S. Mao, Y. P. Jing, M. Bartelmann, X. Kang, and M. Meneghetti. Is the Number of Giant Arcs in ΛCDM Consistent with Observations? *Astrophysical Journal*, 635:795–805, December 2005.

[470] G.-L. Li, S. Mao, Y. P. Jing, X. Kang, and M. Bartelmann. Smoothing Algorithms and High-Order Singularities in Gravitational Lensing. *Astrophysical Journal*, 652:43–55, November 2006.

[471] G. L. Li, S. Mao, Y. P. Jing, H. J. Mo, L. Gao, and W. P. Lin. The giant arc statistics in the three-year Wilkinson Microwave Anisotropy Probe cosmological model. *Monthly Notices of the RAS*, 372:L73–L77, October 2006.

[472] Leping Li, Jun Zhang, Hardi Peter, Lakshmi Pradeep Chitta, Jiangtao Su, Hongqiang Song, Chun Xia, and Yijun Hou. Quasi-periodic Fast Propagating Magnetoacoustic Waves during the Magnetic Reconnection Between Solar Coronal Loops. *Astrophysical Journal*, 868(2):L33, Dec 2018.

[473] A. Lidz, E. J. Baxter, P. Adshead, and S. Dodelson. Primordial non-Gaussianity and reionization. *Physical Review D.*, 88(2):023534, July 2013.

[474] A. Lidz, E. J. Baxter, P. Adshead, and S. Dodelson. Primordial Non-Gaussianity and Reionization. *ArXiv e-prints*, April 2013.

[475] A. Lidz, C.-A. Faucher-Giguère, A. Dall'Aglio, M. McQuinn, C. Fechner, M. Zaldarriaga, L. Hernquist, and S. Dutta. A Measurement of Small-scale Structure in the 2.2 <= z <= 4.2 Lyα Forest. *Astrophysical Journal*, 718:199–230, July 2010.

[476] A. Lidz and M. Malloy. On Modeling and Measuring the Temperature of the z ˜ 5 Intergalactic Medium. *Astrophysical Journal*, 788:175, June 2014.

[477] A. Lidz, S. P. Oh, and S. R. Furlanetto. Have We Detected Patchy Reionization in Quasar Spectra? *Astrophysical Journal*, 639:L47–L50, March 2006.

[478] M. Lima, B. Jain, and M. Devlin. Lensing magnification: implications for counts of submillimetre galaxies and SZ clusters. *Monthly Notices of the RAS*, 406:2352–2372, August 2010.

[479] M. Limousin, J.-P. Kneib, and P. Natarajan. Constraining the mass distribution of galaxies using galaxy-galaxy lensing in clusters and in the field. *Monthly Notices of the RAS*, 356:309–322, January 2005.

[480] M. Limousin, J. Richard, E. Jullo, J.-P. Kneib, B. Fort, G. Soucail, Á. Elíasdóttir, P. Natarajan, R. S. Ellis, I. Smail, O. Czoske, G. P. Smith, P. Hudelot, S. Bardeau, H. Ebeling, E. Egami, and K. K. Knudsen. Combining Strong and Weak Gravitational Lensing in Abell 1689. *Astrophysical Journal*, 668:643–666, October 2007.

[481] M. Limousin, J. Richard, J.-P. Kneib, H. Brink, R. Pelló, E. Jullo, H. Tu, J. Sommer-Larsen, E. Egami, M. J. Michałowski, R. Cabanac, and D. P. Stark. Strong lensing in Abell 1703: constraints on the slope of the inner dark matter distribution. *Astronomy and Astrophysics*, 489:23–35, October 2008.

[482] S. Linden and J.-M. Virey. Test of the Chevallier-Polarski-Linder parametrization for rapid dark energy equation of state transitions. *Physical Review D.*, 78(2):023526–+, July 2008.

[483] E. V. Linder. Exploring the Expansion History of the Universe. *Physical Review Letters*, 90(9):091301–+, March 2003.

[484] R. Link and M. J. Pierce. Cosmological Parameters from Multiple-Arc Gravitational Lensing Systems. I. Smooth Lensing Potentials. *Astrophysical Journal*, 502:63–+, July 1998.

[485] M. Lo Verde, A. Miller, S. Shandera, and L. Verde. Effects of scale-dependent non-Gaussianity on cosmological structures. *Journal of Cosmology and Astro-Particle Physics*, 4:14–+, April 2008.

[486] M. LoVerde and K. M. Smith. The non-Gaussian halo mass function with f_{NL}, g_{NL} and τ_{NL}. *Journal of Cosmology and Astroparticle Physics*, 8:3, August 2011.

[487] J. Lu, L. Xu, M. Liu, and Y. Gui. Constraints on accelerating universe using ESSENCE and Gold supernovae data combined with other cosmological probes. *ArXiv e-prints*, December 2008.

[488] E. Lusso, G. Worseck, J. F. Hennawi, J. X. Prochaska, C. Vignali, J. Stern, and J. M. O'Meara. The first ultraviolet quasar-stacked spectrum at $z \approx 2.4$ from WFC3. *Monthly Notices of the RAS*, 449:4204–4220, June 2015.

[489] C.-P. Ma and J. N. Fry. Deriving the Nonlinear Cosmological Power Spectrum and Bispectrum from Analytic Dark Matter Halo Profiles and Mass Functions. *Astrophysical Journal*, 543:503–513, November 2000.

[490] C.-P. Ma, M. Maggiore, A. Riotto, and J. Zhang. The bias and mass function of dark matter haloes in non-Markovian extension of the excursion set theory. *Monthly Notices of the RAS*, 411:2644–2652, March 2011.

[491] Xiangcheng Ma, Eliot Quataert, Andrew Wetzel, Philip F. Hopkins, Claude-André Faucher-Giguère, and Dušan Kereš. No missing photons for reionization: moderate ionizing photon escape fractions from the FIRE-2 simulations. *Monthly Notices of the RAS*, 498(2):2001–2017, October 2020.

[492] A. V. Macciò. Strong gravitational lensing and dynamical dark energy. *Monthly Notices of the RAS*, 361:1250–1256, August 2005.

[493] P. Madau and F. Haardt. Cosmic Reionization after Planck: Could Quasars Do It All? *Astrophysical Journal*, 813:L8, November 2015.

[494] Piero Madau. Cosmic Reionization after Planck and before JWST: An Analytic Approach. *Astrophysical Journal*, 851(1):50, Dec 2017.

[495] Piero Madau, Francesco Haardt, and Martin J. Rees. Radiative Transfer in a Clumpy Universe. III. The Nature of Cosmological Ionizing Sources. *Astrophysical Journal*, 514(2):648–659, Apr 1999.

[496] M. Maggiore and A. Riotto. The Halo Mass Function from Excursion Set Theory. I. Gaussian Fluctuations with Non-Markovian Dependence on the Smoothing Scale. *Astrophysical Journal*, 711:907–927, March 2010.

[497] M. Maggiore and A. Riotto. The Halo mass function from Excursion Set Theory. II. The Diffusing Barrier. *Astrophysical Journal*, 717:515–525, July 2010.

[498] M. Maggiore and A. Riotto. The Halo Mass Function from Excursion Set Theory. III. Non-Gaussian Fluctuations. *Astrophysical Journal*, 717:526–541, July 2010.

[499] A. Mahdavi, H. Hoekstra, A. Babul, J. Sievers, S. T. Myers, and J. P. Henry. Joint Analysis of Cluster Observations. I. Mass Profile of Abell 478 from Combined X-Ray, Sunyaev-Zel'dovich, and Weak-Lensing Data. *Astrophysical Journal*, 664:162–180, July 2007.

[500] A. Maizy, J. Richard, M. A. de Leo, R. Pelló, and J. P. Kneib. Looking for the first galaxies: lensing or blank fields? *Astronomy and Astrophysics*, 509:A105, January 2010.

[501] S. Majumdar, G. Mellema, K. K. Datta, H. Jensen, T. R. Choudhury, S. Bharadwaj, and M. M. Friedrich. On the use of seminumerical simulations in the 21-cm signal from the epoch of reionization. *Monthly Notices of the RAS*, 443:2843–2861, October 2014.

[502] J. Maldacena. Non-gaussian features of primordial fluctuations in single field inflationary models. *Journal of High Energy Physics*, 5:13, May 2003.

[503] Sangeeta Malhotra and James E. Rhoads. Luminosity Functions of Lyα Emitters at Redshifts z=6.5 and z=5.7: Evidence against Reionization at z¡=6.5. *Astrophysical Journal*, 617(1):L5–L8, December 2004.

[504] Matthew Malloy and Adam Lidz. How to Search for Islands of Neutral Hydrogen in the z ~5.5 IGM. *Astrophysical Journal*, 799(2):179, February 2015.

[505] S. Mao and P. Schneider. Evidence for substructure in lens galaxies? *Monthly Notices of the RAS*, 295:587, April 1998.

[506] Y. Mao, A. D'Aloisio, J. Zhang, and P. R. Shapiro. Primordial non-Gaussianity estimation using 21 cm tomography from the epoch of reionization. *Physical Review D.*, 88(8):081303, October 2013.

[507] Y. Mao, M. Tegmark, M. McQuinn, M. Zaldarriaga, and O. Zahn. How accurately can 21cm tomography constrain cosmology? *Physical Review D.*, 78(2):023529, July 2008.

[508] F. Marchi, L. Pentericci, L. Guaita, D. Schaerer, A. Verhamme, M. Castellano, B. Ribeiro, B. Garilli, O. Le Fèvre, R. Amorin, S. Bardelli, P. Cassata, A. Durkalec, A. Grazian, N. P. Hathi, B. C. Lemaux, D. Maccagni, E. Vanzella, and E. Zucca. Lyα-Lyman continuum connection in 3.5 $\leq$ z $\leq$ 4.3 star-forming galaxies from the VUDS survey. *Astronomy and Astrophysics*, 614:A11, June 2018.

[509] L. Marian, R. E. Smith, and G. M. Bernstein. The Impact of Correlated Projections on Weak Lensing Cluster Counts. *Astrophysical Journal*, 709:286–300, January 2010.

[510] V. J. Martinez, P. Arnalte-Mur, E. Saar, P. de la Cruz, M. J. Pons-Borderia, S. Paredes, A. Fernandez-Soto, and E. Tempel. Reliability of the detection of the Baryonic Acoustic Peak. *ArXiv e-prints*, December 2008.

[511] N. Mashian and A. Loeb. Constraining the Minimum Luminosity of High Redshift Galaxies through Gravitational Lensing. *ArXiv e-prints*, May 2013.

[512] Charlotte A. Mason, Adriano Fontana, Tommaso Treu, Kasper B. Schmidt, Austin Hoag, Louis Abramson, Ricardo Amorin, Maruša Bradač, Lucia Guaita, Tucker Jones, Alaina Henry, Matthew A. Malkan, Laura Pentericci, Michele Trenti, and Eros Vanzella. Inferences on the timeline of reionization at z $\sim$ 8 from the KMOS Lens-Amplified Spectroscopic Survey. *Monthly Notices of the RAS*, 485(3):3947–3969, May 2019.

[513] Charlotte A. Mason and Max Gronke. Measuring the properties of reionised bubbleswith resolved Lyman alpha spectra. *Monthly Notices of the RAS*, September 2020.

[514] Charlotte A. Mason, Tommaso Treu, Stephane de Barros, Mark Dijkstra, Adriano Fontana, Andrei Mesinger, Laura Pentericci, Michele Trenti, and Eros Vanzella. Beacons into the Cosmic Dark Ages: Boosted Transmission of Lyα from UV Bright Galaxies at z $\gtrsim$ 7. *Astrophysical Journal*, 857(2):L11, April 2018.

[515] Charlotte A. Mason, Tommaso Treu, Mark Dijkstra, Andrei Mesinger, Michele Trenti, Laura Pentericci, Stephane de Barros, and Eros Vanzella. The Universe Is Reionizing at z ˜7: Bayesian Inference of the IGM Neutral Fraction Using Lyα Emission from Galaxies. *Astrophysical Journal*, 856(1):2, March 2018.

[516] D. Masters, P. Capak, M. Salvato, F. Civano, B. Mobasher, B. Siana, G. Hasinger, C. D. Impey, T. Nagao, J. R. Trump, H. Ikeda, M. Elvis, and N. Scoville. Evolution of the Quasar Luminosity Function over 3 $<$ z $<$ 5 in the COSMOS Survey Field. *Astrophysical Journal*, 755:169, August 2012.

[517] S. Matarrese and L. Verde. The Effect of Primordial Non-Gaussianity on Halo Bias. *Astrophysical Journal*, 677:L77–L80, April 2008.

[518] S. Matarrese, L. Verde, and R. Jimenez. The Abundance of High-Redshift Objects as a Probe of Non-Gaussian Initial Conditions. *Astrophysical Journal*, 541:10–24, September 2000.

[519] Jorryt Matthee, Rohan P. Naidu, Gabriele Pezzulli, Max Gronke, David Sobral, Pascal A. Oesch, Matthew Hayes, Dawn Erb, Daniel Schaerer, Ricardo Amorín, Sandro Tacchella, Ana Paulino-Afonso, Mario Llerena, João Calhau, and Huub Röttgering. (Re)Solving reionization with Lyα: how bright Lyα Emitters account for the z $\approx$ 2-8 cosmic ionizing background. *Monthly Notices of the RAS*, 512(4):5960–5977, June 2022.

[520] Jorryt Matthee, David Sobral, Max Gronke, Ana Paulino-Afonso, Mauro Stefanon, and Huub Röttgering. Confirmation of double peaked Lyα emission at z = 6.593. Witnessing a galaxy directly contributing to the reionisation of the Universe. *Astronomy and Astrophysics*, 619:A136, November 2018.

[521] Jorryt Matthee, David Sobral, Matthew Hayes, Gabriele Pezzulli, Max Gronke, Daniel Schaerer, Rohan P. Naidu, Huub Röttgering, João Calhau, Ana Paulino-Afonso, Sérgio Santos, and Ricardo Amorín. The X-SHOOTER Lyman α survey at z = 2 (XLS-z2) I: what makes a galaxy a Lyman α emitter? *Monthly Notices of the RAS*, 505(1):1382–1412, July 2021.

[522] P. McDonald. Primordial non-Gaussianity: Large-scale structure signature in the perturbative bias model. *Physical Review D.*, 78(12):123519–+, December 2008.

[523] P. McDonald, J. Miralda-Escudé, M. Rauch, W. L. W. Sargent, T. A. Barlow, and R. Cen. A Measurement of the Temperature-Density Relation in the Intergalactic Medium Using a New Lyα Absorption-Line Fitting Method. *Astrophysical Journal*, 562:52–75, November 2001.

[524] I. D. McGreer, L. Jiang, X. Fan, G. T. Richards, M. A. Strauss, N. P. Ross, M. White, Y. Shen, D. P. Schneider, A. D. Myers, W. N. Brandt, C. DeGraf, E. Glikman, J. Ge, and A. Streblyanska. The z = 5 Quasar Luminosity Function from SDSS Stripe 82. *Astrophysical Journal*, 768:105, May 2013.

[525] I. D. McGreer, A. Mesinger, and V. D'Odorico. Model-independent evidence in favour of an end to reionization by z $\approx$ 6. *Monthly Notices of the RAS*, 447:499–505, February 2015.

[526] D. J. McLeod, C. T. Donnan, R. J. McLure, J. S. Dunlop, D. Magee, R. Begley, A. C. Carnall, F. Cullen, R. S. Ellis, M. L. Hamadouche, and T. M. Stanton. The galaxy UV luminosity function at z $\approx$ 11 from a suite of public JWST ERS, ERO, and Cycle-1 programs. *Monthly Notices of the RAS*, 527(3):5004–5022, January 2024.

[527] R. J. McLure, J. S. Dunlop, R. A. A. Bowler, E. Curtis-Lake, M. Schenker, R. S. Ellis, B. E. Robertson, A. M. Koekemoer, A. B. Rogers, Y. Ono, M. Ouchi, S. Charlot, V. Wild, D. P. Stark, S. R. Furlanetto, M. Cirasuolo, and T. A. Targett. A new multifield determination of the galaxy luminosity function at z = 7-9 incorporating the 2012 Hubble Ultra-Deep Field imaging. *Monthly Notices of the RAS*, 432:2696–2716, July 2013.

[528] M. McQuinn. The Implications of Gunn-Peterson Troughs in the He II Lyα Forest. *Astrophysical Journal*, 704:L89–L92, October 2009.

[529] M. McQuinn. Constraints on X-ray emissions from the reionization era. *Monthly Notices of the RAS*, 426:1349–1360, October 2012.

[530] M. McQuinn, S. R. Furlanetto, L. Hernquist, O. Zahn, and M. Zaldarriaga. The Kinetic Sunyaev-Zel'dovich Effect from Reionization. *Astrophysical Journal*, 630:643–656, September 2005.

[531] M. McQuinn, L. Hernquist, M. Zaldarriaga, and S. Dutta. Studying reionization with Lyα emitters. *Monthly Notices of the RAS*, 381:75–96, October 2007.

[532] M. McQuinn, A. Lidz, O. Zahn, S. Dutta, L. Hernquist, and M. Zaldarriaga. The morphology of HII regions during reionization. *Monthly Notices of the RAS*, 377:1043–1063, May 2007.

[533] M. McQuinn, A. Lidz, M. Zaldarriaga, L. Hernquist, and S. Dutta. Probing the neutral fraction of the IGM with GRBs during the epoch of reionization. *Monthly Notices of the RAS*, 388:1101–1110, August 2008.

[534] M. McQuinn, A. Lidz, M. Zaldarriaga, L. Hernquist, P. F. Hopkins, S. Dutta, and C.-A. Faucher-Giguère. He II Reionization and its Effect on the Intergalactic Medium. *Astrophysical Journal*, 694:842–866, April 2009.

[535] M. McQuinn, S. P. Oh, and C.-A. Faucher-Giguère. On Lyman-limit Systems and the Evolution of the Intergalactic Ionizing Background. *Astrophysical Journal*, 743:82, December 2011.

[536] Matthew McQuinn. The Evolution of the Intergalactic Medium. *Annual Review of Astronomy and Astrophysics*, 54:313–362, Sep 2016.

[537] Matthew McQuinn, S. Peng Oh, and Claude-André Faucher-Giguère. ON LYMAN-LIMIT SYSTEMS AND THE EVOLUTION OF THE INTERGALACTIC IONIZING BACKGROUND. *The Astrophysical Journal*, 743(1):82, nov 2011.

[538] Matthew McQuinn and Phoebe R. Upton Sanderbeck. On the intergalactic temperature-density relation. *Monthly Notices of the RAS*, 456(1):47–54, February 2016.

[539] Matthew McQuinn and Phoebe R. Upton Sanderbeck. On the intergalactic temperature-density relation. *Monthly Notices of the RAS*, 456(1):47–54, Feb 2016.

[540] J. M. G. Mead, L. J. King, D. Sijacki, A. Leonard, E. Puchwein, and I. G. McCarthy. The impact of AGN feedback and baryonic cooling on galaxy clusters as gravitational lenses. *Monthly Notices of the RAS*, 406:434–444, July 2010.

[541] A. Meiksin. Constraints on the ionization sources of the high-redshift intergalactic medium. *Monthly Notices of the RAS*, 356:596–606, January 2005.

[542] Avery Meiksin. The influence of metagalactic ultraviolet background fluctuations on the high-redshift Lyα forest. *Monthly Notices of the RAS*, 491(4):4884–4893, Feb 2020.

[543] B. Ménard, T. Hamana, M. Bartelmann, and N. Yoshida. Improving the accuracy of cosmic magnification statistics. *Astronomy and Astrophysics*, 403:817–828, June 2003.

[544] M. Meneghetti, R. Argazzi, F. Pace, L. Moscardini, K. Dolag, M. Bartelmann, G. Li, and M. Oguri. Arc sensitivity to cluster ellipticity, asymmetries, and substructures. *Astronomy and Astrophysics*, 461:25–38, January 2007.

[545] M. Meneghetti, M. Bartelmann, K. Dolag, L. Moscardini, F. Perrotta, C. Baccigalupi, and G. Tormen. Strong lensing efficiency of galaxy clusters in dark energy cosmologies. *Astronomy and Astrophysics*, 442:413–422, November 2005.

[546] M. Meneghetti, M. Bartelmann, K. Dolag, F. Perrotta, C. Baccigalupi, L. Moscardini, and G. Tormen. Strong lensing by cluster-sized halos in dark energy cosmologies. *New Astronomy Review*, 49:111–114, May 2005.

[547] M. Meneghetti, M. Bartelmann, and L. Moscardini. cD galaxy contribution to the strong lensing cross-sections of galaxy clusters. *Monthly Notices of the RAS*, 346:67–77, November 2003.

[548] M. Meneghetti, M. Bolzonella, M. Bartelmann, L. Moscardini, and G. Tormen. Effects of cluster galaxies on arc statistics. *Monthly Notices of the RAS*, 314:338–347, May 2000.

[549] M. Meneghetti, C. Fedeli, F. Pace, S. Gottlöber, and G. Yepes. Strong lensing in the MARENOSTRUM UNIVERSE. I. Biases in the cluster lens population. *Astronomy and Astrophysics*, 519:A90+, September 2010.

[550] M. Meneghetti, C. Fedeli, A. Zitrin, M. Bartelmann, T. Broadhurst, S. Gottloeber, L. Moscardini, and G. Yepes. Comparison of an X-ray selected sample of massive lensing clusters with the MareNostrum Universe LCDM simulation. *ArXiv e-prints*, February 2011.

[551] M. Meneghetti, B. Jain, M. Bartelmann, and K. Dolag. Constraints on dark energy models from galaxy clusters with multiple arcs. *Monthly Notices of the RAS*, 362:1301–1310, October 2005.

[552] M. Meneghetti, P. Melchior, A. Grazian, G. De Lucia, K. Dolag, M. Bartelmann, C. Heymans, L. Moscardini, and M. Radovich. Realistic simulations of gravitational lensing by galaxy clusters: extracting arc parameters from mock DUNE images. *Astronomy and Astrophysics*, 482:403–418, May 2008.

[553] M. Meneghetti, E. Rasia, J. Merten, F. Bellagamba, S. Ettori, P. Mazzotta, K. Dolag, and S. Marri. Weighing simulated galaxy clusters using lensing and X-ray. *Astronomy and Astrophysics*, 514:A93+, May 2010.

[554] J. Merten, M. Cacciato, M. Meneghetti, C. Mignone, and M. Bartelmann. Combining weak and strong cluster lensing: applications to simulations and MS 2137. *Astronomy and Astrophysics*, 500:681–691, June 2009.

[555] A. Mesinger, A. Aykutalp, E. Vanzella, L. Pentericci, A. Ferrara, and M. Dijkstra. Can the intergalactic medium cause a rapid drop in Lyα emission at z ¿ 6? *Monthly Notices of the RAS*, 446:566–577, January 2015.

[556] A. Mesinger and M. Dijkstra. Ultraviolet radiative feedback during the advanced stages of reionization. *Monthly Notices of the RAS*, 390:1071–1080, November 2008.

[557] A. Mesinger and S. Furlanetto. Efficient Simulations of Early Structure Formation and Reionization. *Astrophysical Journal*, 669:663–675, November 2007.

[558] A. Mesinger and S. Furlanetto. The inhomogeneous ionizing background following reionization. *Monthly Notices of the RAS*, 400:1461–1471, December 2009.

[559] A. Mesinger, S. Furlanetto, and R. Cen. 21CMFAST: a fast, seminumerical simulation of the high-redshift 21-cm signal. *Monthly Notices of the RAS*, 411:955–972, February 2011.

[560] Andrei Mesinger. Was reionization complete by z ~5-6? *Monthly Notices of the RAS*, 407(2):1328–1337, September 2010.

[561] R. B. Metcalf. Gravitational lensing of high-redshift Type IA supernovae: a probe of medium-scale structure. *Monthly Notices of the RAS*, 305:746–754, May 1999.

[562] R. B. Metcalf and P. Madau. Compound Gravitational Lensing as a Probe of Dark Matter Substructure within Galaxy Halos. *Astrophysical Journal*, 563:9–20, December 2001.

[563] R. B. Metcalf and H. Zhao. Flux Ratios as a Probe of Dark Substructures in Quadruple-Image Gravitational Lenses. *Astrophysical Journal*, 567:L5–L8, March 2002.

[564] C. A. Metzler, M. White, and C. Loken. The Effect of the Cosmic Web on Cluster Weak Lensing Mass Estimates. *Astrophysical Journal*, 547:560–573, February 2001.

[565] Romain A. Meyer, Koki Kakiichi, Sarah E. I. Bosman, Richard S. Ellis, Nicolas Laporte, Brant E. Robertson, Emma V. Ryan-Weber, Ken Mawatari, and Adi Zitrin. The role of galaxies and AGN in reionizing the IGM - III. IGM-galaxy cross-correlations at z $\sim$ 6 from eight quasar fields with DEIMOS and MUSE. *Monthly Notices of the RAS*, 494(2):1560–1578, May 2020.

[566] Romain A. Meyer, Koki Kakiichi, Sarah E. I. Bosman, Richard S. Ellis, Nicolas Laporte, Brant E. Robertson, Emma V. Ryan-Weber, Ken Mawatari, and Adi Zitrin. The role of galaxies and AGN in reionizing the IGM - III. IGM-galaxy cross-correlations at z $\sim$ 6 from eight quasar fields with DEIMOS and MUSE. *Monthly Notices of the RAS*, 494(2):1560–1578, March 2020.

[567] J. Miralda-Escude. Statistics of Highly Magnified Gravitational Images in Clusters of Galaxies. II. Implications for the Sources. *Astrophysical Journal*, 403:509–+, February 1993.

[568] J. Miralda-Escudé, R. Cen, J. P. Ostriker, and M. Rauch. The Ly alpha Forest from Gravitational Collapse in the Cold Dark Matter + Lambda Model. *Astrophysical Journal*, 471:582–+, November 1996.

[569] J. Miralda-Escudé, M. Haehnelt, and M. J. Rees. Reionization of the Inhomogeneous Universe. *Astrophysical Journal*, 530:1–16, February 2000.

[570] J. Miralda-Escude and J. P. Ostriker. What produces the ionizing background at large redshift? *Astrophysical Journal*, 350:1–22, February 1990.

[571] J. Miralda-Escudé and M. J. Rees. Reionization and thermal evolution of a photoionized intergalactic medium. *Monthly Notices of the RAS*, 266:343–352, January 1994.

[572] H. J. Mo and S. D. M. White. An analytic model for the spatial clustering of dark matter haloes. *Monthly Notices of the RAS*, 282:347–361, September 1996.

[573] K. Molikawa and M. Hattori. Radial Arc Statistics: A Powerful New Probe of the Central Density Profile of Galaxy Clusters. *Astrophysical Journal*, 559:544–551, October 2001.

[574] M. F. Morales. HI Structure Observations of Reionization and Dark Energy. In R. Minchin and E. Momjian, editors, *The Evolution of Galaxies Through the Neutral Hydrogen Window*, volume 1035 of *American Institute of Physics Conference Series*, pages 82–86, August 2008.

[575] A. More, J. P. McKean, S. More, R. W. Porcas, L. V. E. Koopmans, and M. A. Garrett. The role of luminous substructure in the gravitational lens system MG 2016+112. *ArXiv e-prints*, October 2008.

[576] D. J. Mortlock and E. L. Turner. Empirical constraints on alternative gravity theories from gravitational lensing. *Monthly Notices of the RAS*, 327:552–556, October 2001.

[577] D. J. Mortlock, S. J. Warren, B. P. Venemans, M. Patel, P. C. Hewett, R. G. McMahon, C. Simpson, T. Theuns, E. A. Gonzáles-Solares, A. Adamson, S. Dye, N. C. Hambly, P. Hirst, M. J. Irwin, E. Kuiper, A. Lawrence, and H. J. A. Röttgering. A luminous quasar at a redshift of z = 7.085. *Nature*, 474:616–619, June 2011.

[578] R. E. Mostardi, A. E. Shapley, C. C. Steidel, R. F. Trainor, N. A. Reddy, and B. Siana. A High-Resolution Hubble Space Telescope Study of Apparent Lyman Continuum Leakers at z˜3. *Astrophysical Journal*, 810:107, September 2015.

[579] J. A. Muñoz, S. P. Oh, F. B. Davies, and S. R. Furlanetto. The Flatness and Sudden Evolution of the Intergalactic Ionizing Background. *ArXiv:1410.2249*, October 2014.

[580] M. Musso and A. Paranjape. Non-Gaussian halo abundances in the excursion set approach with correlated steps. *Monthly Notices of the RAS*, 420:369–378, February 2012.

[581] M. Musso, A. Paranjape, and R. K. Sheth. Scale dependent halo bias in the excursion set approach. *ArXiv e-prints*, May 2012.

[582] M. Musso and R. K. Sheth. One step beyond: the excursion set approach with correlated steps. *Monthly Notices of the RAS*, 423:L102–L106, June 2012.

[583] Rohan P. Naidu, Jorryt Matthee, Pascal A. Oesch, Charlie Conroy, David Sobral, Gabriele Pezzulli, Matthew Hayes, Dawn Erb, Ricardo Amorín, Max Gronke, Daniel Schaerer, Sandro Tacchella, Josephine Kerutt, Ana Paulino-Afonso, João Calhau, Mario Llerena, and Huub Röttgering. The synchrony of production and escape: half the bright Lyα emitters at z $\approx$ 2 have Lyman continuum escape fractions $\approx$50 per cent. *Monthly Notices of the RAS*, 510(3):4582–4607, March 2022.

[584] Rohan P. Naidu, Sandro Tacchella, Charlotte A. Mason, Sownak Bose, Pascal A. Oesch, and Charlie Conroy. Rapid Reionization by the Oligarchs: The Case for Massive, UV-bright, Star-forming Galaxies with High Escape Fractions. *Astrophysical Journal*, 892(2):109, April 2020.

[585] Minami Nakane, Masami Ouchi, Kimihiko Nakajima, Yuichi Harikane, Yoshiaki Ono, Hiroya Umeda, Yuki Isobe, Yechi Zhang, and Yi Xu. Lyα Emission at z = 7–13: Clear Evolution of Lyα Equivalent Width Indicating a Late Cosmic Reionization History. *Astrophysical Journal*, 967(1):28, May 2024.

[586] M. H. Namjoo, H. Firouzjahi, and M. Sasaki. Violation of non-Gaussianity consistency relation in a single-field inflationary model. *EPL (Europhysics Letters)*, 101:39001, February 2013.

[587] R. Narayan and M. Bartelmann. Lectures on Gravitational Lensing. *ArXiv Astrophysics e-prints*, June 1996.

[588] Fahad Nasir, Christopher Cain, Anson D'Aloisio, Nakul Gangolli, and Matthew McQuinn. Hydrodynamic Response of the Intergalactic Medium to Reionization. II. Physical Characteristics and Dynamics of Ionizing Photon Sinks. *Astrophysical Journal*, 923(2):161, December 2021.

[589] Fahad Nasir and Anson D'Aloisio. Observing the tail of reionization: neutral islands in the z = 5.5 Lyman-α forest. *Monthly Notices of the RAS*, 494(3):3080–3094, April 2020.

[590] P. Natarajan and J.-P. Kneib. Lensing by galaxy haloes in clusters of galaxies. *Monthly Notices of the RAS*, 287:833–847, June 1997.

[591] P. Natarajan, J.-P. Kneib, and I. Smail. Evidence for Tidal Stripping of Dark Matter Halos in Massive Cluster Lenses. *Astrophysical Journal*, 580:L11–L15, November 2002.

[592] P. Natarajan, J.-P. Kneib, I. Smail, and R. S. Ellis. The Mass-to-Light Ratio of Early-Type Galaxies: Constraints from Gravitational Lensing in the Rich Cluster AC 114. *Astrophysical Journal*, 499:600–+, May 1998.

[593] P. Natarajan, J.-P. Kneib, I. Smail, T. Treu, R. Ellis, S. Moran, M. Limousin, and O. Czoske. The Survival of Dark Matter Halos in the Cluster Cl 0024+16. *Astrophysical Journal*, 693:970–983, March 2009.

[594] P. Natarajan and V. Springel. Abundance of Substructure in Clusters of Galaxies. *Astrophysical Journal*, 617:L13–L16, December 2004.

[595] J. F. Navarro, C. S. Frenk, and S. D. M. White. The assembly of galaxies in a hierarchically clustering universe. *Monthly Notices of the RAS*, 275:56–66, July 1995.

[596] J. F. Navarro, C. S. Frenk, and S. D. M. White. The Structure of Cold Dark Matter Halos. *Astrophysical Journal*, 462:563–+, May 1996.

[597] J. F. Navarro, C. S. Frenk, and S. D. M. White. A Universal Density Profile from Hierarchical Clustering. *Astrophysical Journal*, 490:493–+, December 1997.

[598] A. F. Neto, L. Gao, P. Bett, S. Cole, J. F. Navarro, C. S. Frenk, S. D. M. White, V. Springel, and A. Jenkins. The statistics of Λ CDM halo concentrations. *Monthly Notices of the RAS*, 381:1450–1462, November 2007.

[599] A. B. Newman, T. Treu, R. S. Ellis, D. J. Sand, J. Richard, P. J. Marshall, P. Capak, and S. Miyazaki. The Distribution of Dark Matter Over Three Decades in Radius in the Lensing Cluster Abell 611. *Astrophysical Journal*, 706:1078–1094, December 2009.

[600] T. Nishimichi, A. Taruya, K. Koyama, and C. Sabiu. Scale dependence of halo bispectrum from non-Gaussian initial conditions in cosmological N-body simulations. *Journal of Cosmology and Astroparticle Physics*, 7:2, July 2010.

[601] Y. Noh and M. McQuinn. A physical understanding of how reionization suppresses accretion on to dwarf haloes. *Monthly Notices of the RAS*, 444:503–514, October 2014.

[602] Jose Oñorbe, Joseph F. Hennawi, and Zarija Lukić. Self-consistent Modeling of Reionization in Cosmological Hydrodynamical Simulations. *Astrophysical Journal*, 837(2):106, March 2017.

[603] P. Ocvirk, D. Aubert, J. Chardin, N. Deparis, and J. Lewis. Impact of the reduced speed of light approximation on the post-overlap neutral hydrogen fraction in numerical simulations of the epoch of reionization. *Astronomy and Astrophysics*, 626:A77, June 2019.

[604] Pierre Ocvirk, Nicolas Gillet, Paul R. Shapiro, Dominique Aubert, Ilian T. Iliev, Romain Teyssier, Gustavo Yepes, Jun-Hwan Choi, David Sullivan, Alexander Knebe, Stefan Gottlöber, Anson D'Aloisio, Hyunbae Park, Yehuda Hoffman, and Timothy Stranex. Cosmic Dawn (CoDa): the First Radiation-Hydrodynamics Simulation of Reionization and Galaxy Formation in the Local Universe. *Monthly Notices of the RAS*, 463(2):1462–1485, Dec 2016.

[605] Pierre Ocvirk, Joseph S. W. Lewis, Nicolas Gillet, Jonathan Chardin, Dominique Aubert, Nicolas Deparis, and Émilie Thélie. Lyman-alpha opacities at z = 4-6 require low mass, radiatively-suppressed galaxies to drive cosmic reionization. *Monthly Notices of the RAS*, 507(4):6108–6117, November 2021.

[606] P. A. Oesch, P. G. van Dokkum, G. D. Illingworth, R. J. Bouwens, I. Momcheva, B. Holden, G. W. Roberts-Borsani, R. Smit, M. Franx, I. Labbé, V. González, and

D. Magee. A Spectroscopic Redshift Measurement for a Luminous Lyman Break Galaxy at z = 7.730 Using Keck/MOSFIRE. *Astrophysical Journal*, 804(2):L30, May 2015.

[607] M. Oguri. Systematic Effects on Tangential and Radial Arc Statistics: The Finite Source Size and Ellipticities of the Lens and Source. *Astrophysical Journal*, 573:51–59, July 2002.

[608] M. Oguri and R. D. Blandford. What is the largest Einstein radius in the universe? *Monthly Notices of the RAS*, 392:930–944, January 2009.

[609] M. Oguri, J. Lee, and Y. Suto. Arc Statistics in Triaxial Dark Matter Halos: Testing the Collisionless Cold Dark Matter Paradigm. *Astrophysical Journal*, 599:7–23, December 2003.

[610] T. Okamoto, L. Gao, and T. Theuns. Mass loss of galaxies due to an ultraviolet background. *Monthly Notices of the RAS*, 390:920–928, November 2008.

[611] C. A. Onken and J. Miralda-Escudé. History of Hydrogen Reionization in the Cold Dark Matter Model. *Astrophysical Journal*, 610:1–8, July 2004.

[612] Y. Ono, M. Ouchi, E. Curtis-Lake, M. A. Schenker, R. S. Ellis, R. J. McLure, J. S. Dunlop, B. E. Robertson, A. M. Koekemoer, R. A. A. Bowler, A. B. Rogers, E. Schneider, S. Charlot, D. P. Stark, K. Shimasaku, S. R. Furlanetto, and M. Cirasuolo. Evolution of the Sizes of Galaxies over 7¡z¡12 Revealed by the 2012 Hubble Ultra Deep Field Campaign. *ArXiv e-prints*, December 2012.

[613] Y. Ono, M. Ouchi, B. Mobasher, M. Dickinson, K. Penner, K. Shimasaku, B. J. Weiner, J. S. Kartaltepe, K. Nakajima, H. Nayyeri, D. Stern, N. Kashikawa, and H. Spinrad. Spectroscopic Confirmation of Three z-dropout Galaxies at z = 6.844-7.213: Demographics of Lyα Emission in z ˜ 7 Galaxies. *Astrophysical Journal*, 744:83, January 2012.

[614] Y. Ono, M. Ouchi, B. Mobasher, M. Dickinson, K. Penner, K. Shimasaku, B. J. Weiner, J. S. Kartaltepe, K. Nakajima, H. Nayyeri, D. Stern, N. Kashikawa, and H. Spinrad. Spectroscopic Confirmation of Three z-dropout Galaxies at z = 6.844-7.213: Demographics of Lyα Emission in z ˜ 7 Galaxies. *Astrophysical Journal*, 744:83, January 2012.

[615] Kazuaki Ota, Masanori Iye, Nobunari Kashikawa, Kazuhiro Shimasaku, Masakazu Kobayashi, Tomonori Totani, Masahiro Nagashima, Tomoki Morokuma, Hisanori Furusawa, Takashi Hattori, Yuichi Matsuda, Tetsuya Hashimoto, and Masami Ouchi. Reionization and Galaxy Evolution Probed by z = 7 Lyα Emitters. *Astrophysical Journal*, 677(1):12–26, April 2008.

[616] Kazuaki Ota, Masanori Iye, Nobunari Kashikawa, Kazuhiro Shimasaku, Masami Ouchi, Tomonori Totani, Masakazu A. R. Kobayashi, Masahiro Nagashima, Atsushi Harayama, Natsuki Kodaka, Tomoki Morokuma, Hisanori Furusawa, Akito Tajitsu,

and Takashi Hattori. Lyα Emitters at z = 7 in the Subaru/XMM-Newton Deep Survey Field: Photometric Candidates and Luminosity Functions. *Astrophysical Journal*, 722(1):803–811, October 2010.

[617] M. Ouchi, K. Shimasaku, H. Furusawa, T. Saito, M. Yoshida, M. Akiyama, Y. Ono, T. Yamada, K. Ota, N. Kashikawa, M. Iye, T. Kodama, S. Okamura, C. Simpson, and M. Yoshida. Statistics of 207 Lyα Emitters at a Redshift Near 7: Constraints on Reionization and Galaxy Formation Models. *Astrophysical Journal*, 723:869–894, November 2010.

[618] M. Ouchi, K. Shimasaku, H. Furusawa, T. Saito, M. Yoshida, M. Akiyama, Y. Ono, T. Yamada, K. Ota, N. Kashikawa, M. Iye, T. Kodama, S. Okamura, C. Simpson, and M. Yoshida. Statistics of 207 Lyα Emitters at a Redshift Near 7: Constraints on Reionization and Galaxy Formation Models. *Astrophysical Journal*, 723:869–894, November 2010.

[619] Masami Ouchi, Yuichi Harikane, Takatoshi Shibuya, Kazuhiro Shimasaku, Yoshiaki Taniguchi, Akira Konno, Masakazu Kobayashi, Masaru Kajisawa, Tohru Nagao, Yoshiaki Ono, Akio K. Inoue, Masayuki Umemura, Masao Mori, Kenji Hasegawa, Ryo Higuchi, Yutaka Komiyama, Yuichi Matsuda, Kimihiko Nakajima, Tomoki Saito, and Shiang-Yu Wang. Systematic Identification of LAEs for Visible Exploration and Reionization Research Using Subaru HSC (SILVERRUSH). I. Program strategy and clustering properties of $\sim$2000 Lyα emitters at z = 6-7 over the 0.3-0.5 Gpc^2 survey area. *Publications of the ASJ*, 70:S13, January 2018.

[620] J.-P. Paardekooper, S. Khochfar, and C. Dalla Vecchia. The First Billion Years project: the escape fraction of ionizing photons in the epoch of reionization. *Monthly Notices of the RAS*, 451:2544–2563, August 2015.

[621] Jan-Pieter Paardekooper, Sadegh Khochfar, and Claudio Dalla Vecchia. The First Billion Years project: the escape fraction of ionizing photons in the epoch of reionization. *Monthly Notices of the RAS*, 451(3):2544–2563, August 2015.

[622] B. Paczynski and K. Gorski. Another possible case of a gravitational lens. *Astrophysical Journal*, 248:L101–L104, September 1981.

[623] N. Palanque-Delabrouille, C. Magneville, C. Yèche, S. Eftekharzadeh, A. D. Myers, P. Petitjean, I. Pâris, E. Aubourg, and et al. Luminosity function from dedicated SDSS-III and MMT data of quasars in $0.7 < z < 4.0$ selected with a new approach. *Astronomy and Astrophysics*, 551:A29, March 2013.

[624] A. Paranjape, T. Y. Lam, and R. K. Sheth. Halo abundances and counts-in-cells: the excursion set approach with correlated steps. *Monthly Notices of the RAS*, 420:1429–1441, February 2012.

[625] A. Paranjape and R. K. Sheth. Halo bias in the excursion set approach with correlated steps. *Monthly Notices of the RAS*, 419:132–137, January 2012.

[626] H. Park, P. R. Shapiro, E. Komatsu, I. T. Iliev, K. Ahn, and G. Mellema. The Kinetic Sunyaev-Zel'dovich Effect as a Probe of the Physics of Cosmic Reionization: The Effect of Self-regulated Reionization. *Astrophysical Journal*, 769:93, June 2013.

[627] Hyunbae Park, Paul R. Shapiro, Jun-hwan Choi, Naoki Yoshida, Shingo Hirano, and Kyungjin Ahn. The Hydrodynamic Feedback of Cosmic Reionization on Small-scale Structures and Its Impact on Photon Consumption During the Epoch of Reionization. *Astrophysical Journal*, 831(1):86, Nov 2016.

[628] A. H. Pawlik, J. Schaye, and E. van Scherpenzeel. Keeping the Universe ionized: photoheating and the clumping factor of the high-redshift intergalactic medium. *Monthly Notices of the RAS*, 394:1812–1824, April 2009.

[629] Andreas H. Pawlik, Joop Schaye, and Claudio Dalla Vecchia. Spatially adaptive radiation-hydrodynamical simulations of galaxy formation during cosmological reionization. *Monthly Notices of the RAS*, 451(2):1586–1605, Aug 2015.

[630] J. A. Peacock and S. J. Dodds. Non-linear evolution of cosmological power spectra. *Monthly Notices of the RAS*, 280:L19–L26, June 1996.

[631] L. Pentericci, A. Fontana, E. Vanzella, M. Castellano, A. Grazian, M. Dijkstra, K. Boutsia, S. Cristiani, M. Dickinson, E. Giallongo, M. Giavalisco, R. Maiolino, A. Moorwood, D. Paris, and P. Santini. Spectroscopic Confirmation of z ˜ 7 Lyman Break Galaxies: Probing the Earliest Galaxies and the Epoch of Reionization. *Astrophysical Journal*, 743:132, December 2011.

[632] L. Pentericci, E. Vanzella, A. Fontana, M. Castellano, T. Treu, A. Mesinger, M. Dijkstra, A. Grazian, M. Bradač, C. Conselice, S. Cristiani, J. Dunlop, A. Galametz, M. Giavalisco, E. Giallongo, A. Koekemoer, R. McLure, R. Maiolino, D. Paris, and P. Santini. New Observations of z ˜ 7 Galaxies: Evidence for a Patchy Reionization. *Astrophysical Journal*, 793:113, October 2014.

[633] Lucia A. Perez, Sangeeta Malhotra, James E. Rhoads, and Vithal Tilvi. Void Probability Function of Simulated Surveys of high-redshift Lyman-Alpha Emitters. *arXiv e-prints*, page arXiv:2011.03556, November 2020.

[634] S. Perlmutter, G. Aldering, M. della Valle, and et al. Discovery of a supernova explosion at half the age of the universe. *Nature*, 391:51–+, January 1998.

[635] S. Perlmutter, G. Aldering, G. Goldhaber, and et al. Measurements of Omega and Lambda from 42 High-Redshift Supernovae. *Astrophysical Journal*, 517:565–586, June 1999.

[636] L. Philpott, F. Dowker, and R. Sorkin. Energy-momentum diffusion from spacetime discreteness. *ArXiv e-prints*, October 2008.

[637] A. Pillepich, C. Porciani, and O. Hahn. Halo mass function and scale-dependent bias from N-body simulations with non-Gaussian initial conditions. *Monthly Notices of the RAS*, 402:191–206, February 2010.

[638] Planck Collaboration, P. A. R. Ade, N. Aghanim, C. Armitage-Caplan, M. Arnaud, M. Ashdown, F. Atrio-Barandela, J. Aumont, C. Baccigalupi, A. J. Banday, and et al. Planck 2013 results. XVI. Cosmological parameters. *ArXiv e-prints*, March 2013.

[639] Planck Collaboration, P. A. R. Ade, N. Aghanim, M. Arnaud, M. Ashdown, J. Aumont, C. Baccigalupi, A. J. Banday, R. B. Barreiro, J. G. Bartlett, and et al. Planck 2015 results. XIII. Cosmological parameters. *ArXiv e-prints*, February 2015.

[640] Planck Collaboration, N. Aghanim, Y. Akrami, M. Ashdown, J. Aumont, C. Baccigalupi, M. Ballardini, A. J. Banday, R. B. Barreiro, N. Bartolo, S. Basak, R. Battye, K. Benabed, J. P. Bernard, M. Bersanelli, P. Bielewicz, J. J. Bock, J. R. Bond, J. Borrill, F. R. Bouchet, F. Boulanger, M. Bucher, C. Burigana, R. C. Butler, E. Calabrese, J. F. Cardoso, J. Carron, A. Challinor, H. C. Chiang, J. Chluba, L. P. L. Colombo, C. Combet, D. Contreras, B. P. Crill, F. Cuttaia, P. de Bernardis, G. de Zotti, J. Delabrouille, J. M. Delouis, E. Di Valentino, J. M. Diego, O. Doré, M. Douspis, A. Ducout, X. Dupac, S. Dusini, G. Efstathiou, F. Elsner, T. A. Enßlin, H. K. Eriksen, Y. Fantaye, M. Farhang, J. Fergusson, R. Fernandez-Cobos, F. Finelli, F. Forastieri, M. Frailis, A. A. Fraisse, E. Franceschi, A. Frolov, S. Galeotta, S. Galli, K. Ganga, R. T. Génova-Santos, M. Gerbino, T. Ghosh, J. González-Nuevo, K. M. Górski, S. Gratton, A. Gruppuso, J. E. Gudmundsson, J. Hamann, W. Handley, F. K. Hansen, D. Herranz, S. R. Hildebrandt, E. Hivon, Z. Huang, A. H. Jaffe, W. C. Jones, A. Karakci, E. Keihänen, R. Keskitalo, K. Kiiveri, J. Kim, T. S. Kisner, L. Knox, N. Krachmalnicoff, M. Kunz, H. Kurki-Suonio, G. Lagache, J. M. Lamarre, A. Lasenby, M. Lattanzi, C. R. Lawrence, M. Le Jeune, P. Lemos, J. Lesgourgues, F. Levrier, A. Lewis, M. Liguori, P. B. Lilje, M. Lilley, V. Lindholm, M. López-Caniego, P. M. Lubin, Y. Z. Ma, J. F. Macías-Pérez, G. Maggio, D. Maino, N. Mandolesi, A. Mangilli, A. Marcos-Caballero, M. Maris, P. G. Martin, M. Martinelli, E. Martínez-González, S. Matarrese, N. Mauri, J. D. McEwen, P. R. Meinhold, A. Melchiorri, A. Mennella, M. Migliaccio, M. Millea, S. Mitra, M. A. Miville-Deschênes, D. Molinari, L. Montier, G. Morgante, A. Moss, P. Natoli, H. U. Nørgaard-Nielsen, L. Pagano, D. Paoletti, B. Partridge, G. Patanchon, H. V. Peiris, F. Perrotta, V. Pettorino, F. Piacentini, L. Polastri, G. Polenta, J. L. Puget, J. P. Rachen, M. Reinecke, M. Remazeilles, A. Renzi, G. Rocha, C. Rosset, G. Roudier, J. A. Rubiño-Martín, B. Ruiz-Granados, L. Salvati, M. Sandri, M. Savelainen, D. Scott, E. P. S. Shellard, C. Sirignano, G. Sirri, L. D. Spencer, R. Sunyaev, A. S. Suur-Uski, J. A. Tauber, D. Tavagnacco, M. Tenti, L. Toffolatti, M. Tomasi, T. Trombetti, L. Valenziano, J. Valiviita, B. Van Tent, L. Vibert, P. Vielva, F. Villa, N. Vittorio, B. D. Wand elt, I. K. Wehus, M. White, S. D. M. White, A. Zacchei, and A. Zonca. Planck 2018 results. VI. Cosmological parameters. *Astronomy and Astrophysics*, 641:A6, September 2020.

[641] Planck Collaboration, N. Aghanim, Y. Akrami, M. Ashdown, J. Aumont, C. Baccigalupi, M. Ballardini, A. J. Banday, R. B. Barreiro, N. Bartolo, S. Basak, R. Battye, K. Benabed, J. P. Bernard, M. Bersanelli, P. Bielewicz, J. J. Bock, J. R. Bond, J. Borrill, F. R. Bouchet, F. Boulanger, M. Bucher, C. Burigana, R. C. Butler, E. Calabrese, J. F. Cardoso, J. Carron, A. Challinor, H. C. Chiang, J. Chluba,

L. P. L. Colombo, C. Combet, D. Contreras, B. P. Crill, F. Cuttaia, P. de Bernardis, G. de Zotti, J. Delabrouille, J. M. Delouis, E. Di Valentino, J. M. Diego, O. Doré, M. Douspis, A. Ducout, X. Dupac, S. Dusini, G. Efstathiou, F. Elsner, T. A. Enßlin, H. K. Eriksen, Y. Fantaye, M. Farhang, J. Fergusson, R. Fernandez-Cobos, F. Finelli, F. Forastieri, M. Frailis, A. A. Fraisse, E. Franceschi, A. Frolov, S. Galeotta, S. Galli, K. Ganga, R. T. Génova-Santos, M. Gerbino, T. Ghosh, J. González-Nuevo, K. M. Górski, S. Gratton, A. Gruppuso, J. E. Gudmundsson, J. Hamann, W. Handley, F. K. Hansen, D. Herranz, S. R. Hildebrandt, E. Hivon, Z. Huang, A. H. Jaffe, W. C. Jones, A. Karakci, E. Keihänen, R. Keskitalo, K. Kiiveri, J. Kim, T. S. Kisner, L. Knox, N. Krachmalnicoff, M. Kunz, H. Kurki-Suonio, G. Lagache, J. M. Lamarre, A. Lasenby, M. Lattanzi, C. R. Lawrence, M. Le Jeune, P. Lemos, J. Lesgourgues, F. Levrier, A. Lewis, M. Liguori, P. B. Lilje, M. Lilley, V. Lindholm, M. López-Caniego, P. M. Lubin, Y. Z. Ma, J. F. Macías-Pérez, G. Maggio, D. Maino, N. Mandolesi, A. Mangilli, A. Marcos-Caballero, M. Maris, P. G. Martin, M. Martinelli, E. Martínez-González, S. Matarrese, N. Mauri, J. D. McEwen, P. R. Meinhold, A. Melchiorri, A. Mennella, M. Migliaccio, M. Millea, S. Mitra, M. A. Miville-Deschênes, D. Molinari, L. Montier, G. Morgante, A. Moss, P. Natoli, H. U. Nørgaard-Nielsen, L. Pagano, D. Paoletti, B. Partridge, G. Patanchon, H. V. Peiris, F. Perrotta, V. Pettorino, F. Piacentini, L. Polastri, G. Polenta, J. L. Puget, J. P. Rachen, M. Reinecke, M. Remazeilles, A. Renzi, G. Rocha, C. Rosset, G. Roudier, J. A. Rubiño-Martín, B. Ruiz-Granados, L. Salvati, M. Sandri, M. Savelainen, D. Scott, E. P. S. Shellard, C. Sirignano, G. Sirri, L. D. Spencer, R. Sunyaev, A. S. Suur-Uski, J. A. Tauber, D. Tavagnacco, M. Tenti, L. Toffolatti, M. Tomasi, T. Trombetti, L. Valenziano, J. Valiviita, B. Van Tent, L. Vibert, P. Vielva, F. Villa, N. Vittorio, B. D. Wand elt, I. K. Wehus, M. White, S. D. M. White, A. Zacchei, and A. Zonca. Planck 2018 results. VI. Cosmological parameters. *Astronomy and Astrophysics*, 641:A6, September 2020.

[642] M. Postman, D. Coe, N. Benítez, L. Bradley, T. Broadhurst, M. Donahue, H. Ford, O. Graur, and et. al. The Cluster Lensing and Supernova Survey with Hubble: An Overview. *Astrophysical Journals*, 199:25, April 2012.

[643] F. Prada, A. A. Klypin, A. J. Cuesta, J. E. Betancort-Rijo, and J. Primack. Halo concentrations in the standard Λ cold dark matter cosmology. *Monthly Notices of the RAS*, 423:3018–3030, July 2012.

[644] W. H. Press and P. Schechter. Formation of Galaxies and Clusters of Galaxies by Self-Similar Gravitational Condensation. *Astrophysical Journal*, 187:425–438, February 1974.

[645] J. X. Prochaska, G. Worseck, and J. M. O'Meara. A Direct Measurement of the Intergalactic Medium Opacity to H I Ionizing Photons. *Astrophysical Journal*, 705:L113–L117, November 2009.

[646] Andrej Prša, Petr Harmanec, Guillermo Torres, Eric Mamajek, Martin Asplund, Nicole Capitaine, Jørgen Christensen-Dalsgaard, Éric Depagne, Margit Haberreiter,

and Saskia Hekker. Nominal Values for Selected Solar and Planetary Quantities: IAU 2015 Resolution B3. *Astronomical Journal*, 152(2):41, Aug 2016.

[647] E. Puchwein, M. Bartelmann, K. Dolag, and M. Meneghetti. The impact of gas physics on strong cluster lensing. *Astronomy and Astrophysics*, 442:405–412, November 2005.

[648] E. Puchwein, J. S. Bolton, M. G. Haehnelt, P. Madau, G. D. Becker, and F. Haardt. The photoheating of the intergalactic medium in synthesis models of the UV background. *Monthly Notices of the RAS*, 450:4081–4097, July 2015.

[649] E. Puchwein and S. Hilbert. Cluster strong lensing in the Millennium simulation: the effect of galaxies and structures along the line-of-sight. *Monthly Notices of the RAS*, 398:1298–1308, September 2009.

[650] A. R. Pullen, O. Doré, and J. Bock. Intensity Mapping across Cosmic Times with the Lyα Line. *Astrophysical Journal*, 786:111, May 2014.

[651] Alireza Rahmati, Andreas H. Pawlik, Milan Raičević, and Joop Schaye. On the evolution of the H I column density distribution in cosmological simulations. *Monthly Notices of the RAS*, 430(3):2427–2445, April 2013.

[652] Alireza Rahmati and Joop Schaye. The mean free path of hydrogen ionizing photons during the epoch of reionization. *Monthly Notices of the RAS*, 478(4):5123–5134, Aug 2018.

[653] M. Raičević and T. Theuns. Modelling recombinations during cosmological reionization. *Monthly Notices of the RAS*, 412:L16–L19, March 2011.

[654] S. Rasanen. Structure formation as an alternative to dark energy and modified gravity. *ArXiv e-prints*, November 2008.

[655] S. Rau, S. Vegetti, and S. D. M. White. The effect of particle noise in N-body simulations of gravitational lensing. *Monthly Notices of the RAS*, 430:2232–2248, April 2013.

[656] B. A. Reid, L. Verde, K. Dolag, S. Matarrese, and L. Moscardini. Non-Gaussian halo assembly bias. *Journal of Cosmology and Astroparticle Physics*, 7:13, July 2010.

[657] J. Richard, J.-P. Kneib, H. Ebeling, D. P. Stark, E. Egami, and A. K. Fiedler. Discovery of a possibly old galaxy at z= 6.027, multiply imaged by the massive cluster Abell 383. *Monthly Notices of the RAS*, 414:L31–L35, June 2011.

[658] J. Richard, J.-P. Kneib, M. Limousin, A. Edge, and E. Jullo. Abell 370 revisited: refurbished Hubble imaging of the first strong lensing cluster. *Monthly Notices of the RAS*, 402:L44–L48, February 2010.

[659] J. Richard, L. Pei, M. Limousin, E. Jullo, and J. P. Kneib. Keck spectroscopic survey of strongly lensed galaxies in Abell 1703: further evidence of a relaxed, unimodal cluster. *Astronomy and Astrophysics*, 498:37–47, April 2009.

[660] J. Richard, G. P. Smith, J.-P. Kneib, R. S. Ellis, A. J. R. Sanderson, L. Pei, T. A. Targett, D. J. Sand, A. M. Swinbank, H. Dannerbauer, P. Mazzotta, M. Limousin, E. Egami, E. Jullo, V. Hamilton-Morris, and S. M. Moran. LoCuSS: first results from strong-lensing analysis of 20 massive galaxy clusters at z = 0.2. *Monthly Notices of the RAS*, 404:325–349, May 2010.

[661] J. Richard, D. P. Stark, R. S. Ellis, M. R. George, E. Egami, J.-P. Kneib, and G. P. Smith. A Hubble and Spitzer Space Telescope Survey for Gravitationally Lensed Galaxies: Further Evidence for a Significant Population of Low-Luminosity Galaxies beyond z=7. *Astrophysical Journal*, 685:705–724, October 2008.

[662] G. T. Richards, M. A. Strauss, X. Fan, P. B. Hall, S. Jester, D. P. Schneider, D. E. Vanden Berk, C. Stoughton, S. F. Anderson, R. J. Brunner, J. Gray, J. E. Gunn, Ž. Ivezić, M. K. Kirkland, G. R. Knapp, J. Loveday, A. Meiksin, A. Pope, A. S. Szalay, A. R. Thakar, B. Yanny, D. G. York, J. C. Barentine, H. J. Brewington, J. Brinkmann, M. Fukugita, M. Harvanek, S. M. Kent, S. J. Kleinman, J. Krzesiński, D. C. Long, R. H. Lupton, T. Nash, E. H. Neilsen, Jr., A. Nitta, D. J. Schlegel, and S. A. Snedden. The Sloan Digital Sky Survey Quasar Survey: Quasar Luminosity Function from Data Release 3. *Astronomical Journal*, 131:2766–2787, June 2006.

[663] M. Ricotti, N. Y. Gnedin, and J. M. Shull. The Evolution of the Effective Equation of State of the Intergalactic Medium. *Astrophysical Journal*, 534:41–56, May 2000.

[664] M. Ricotti, N. Y. Gnedin, and J. M. Shull. The Fate of the First Galaxies. II. Effects of Radiative Feedback. *Astrophysical Journal*, 575:49–67, August 2002.

[665] K. Riebe, A. M. Partl, H. Enke, J. Forero-Romero, S. Gottlöber, A. Klypin, G. Lemson, F. Prada, J. R. Primack, M. Steinmetz, and V. Turchaninov. The MultiDark Database: Release of the Bolshoi and MultiDark cosmological simulations. *Astronomische Nachrichten*, 334:691–708, August 2013.

[666] A. G. Riess, A. V. Filippenko, P. Challis, and et al. Observational Evidence from Supernovae for an Accelerating Universe and a Cosmological Constant. *Astronomical Journal*, 116:1009–1038, September 1998.

[667] G. W. Roberts-Borsani, R. J. Bouwens, P. A. Oesch, I. Labbe, R. Smit, G. D. Illingworth, P. van Dokkum, B. Holden, V. Gonzalez, M. Stefanon, B. Holwerda, and S. Wilkins. z $\gtrsim$ 7 Galaxies with Red Spitzer/IRAC [3.6]-[4.5] Colors in the Full CANDELS Data Set: The Brightest-Known Galaxies at z ~7-9 and a Probable Spectroscopic Confirmation at z = 7.48. *Astrophysical Journal*, 823(2):143, June 2016.

[668] Guido Roberts-Borsani, Tommaso Treu, Charlotte Mason, Richard S. Ellis, Nicolas Laporte, Thomas Schmidt, Maruša Bradač, Adriano Fontana, Takahiro Morishita, and Paola Santini. Nature and Nurture? Comparing Lyα Detections in UV Bright and Fainter [O III]+Hβ Emitters at $z \sim 8$ With Keck/MOSFIRE. *arXiv e-prints*, page arXiv:2207.01629, July 2022.

[669] B. E. Robertson, R. S. Ellis, S. R. Furlanetto, and J. S. Dunlop. Cosmic Reionization and Early Star-forming Galaxies: A Joint Analysis of New Constraints from Planck and the Hubble Space Telescope. *Astrophysical Journal*, 802:L19, April 2015.

[670] B. E. Robertson, S. R. Furlanetto, E. Schneider, S. Charlot, R. S. Ellis, D. P. Stark, R. J. McLure, J. S. Dunlop, A. Koekemoer, M. A. Schenker, M. Ouchi, Y. Ono, E. Curtis-Lake, A. B. Rogers, R. A. A. Bowler, and M. Cirasuolo. New Constraints on Cosmic Reionization from the 2012 Hubble Ultra Deep Field Campaign. *Astrophysical Journal*, 768:71, May 2013.

[671] B. E. Robertson, A. V. Kravtsov, J. Tinker, and A. R. Zentner. Collapse Barriers and Halo Abundance: Testing the Excursion Set Ansatz. *Astrophysical Journal*, 696:636–652, May 2009.

[672] A. J. Ross, W. J. Percival, A. Carnero, G.-b. Zhao, M. Manera, A. Raccanelli, E. Aubourg, D. Bizyaev, and et. al. The clustering of galaxies in the SDSS-III DR9 Baryon Oscillation Spectroscopic Survey: constraints on primordial non-Gaussianity. *Monthly Notices of the RAS*, 428:1116–1127, January 2013.

[673] E. Rozo, D. Nagai, C. Keeton, and A. Kravtsov. The Impact of Baryonic Cooling on Giant Arc Abundances. *Astrophysical Journal*, 687:22–38, November 2008.

[674] M. Ruszkowski and V. Springel. The role of dry mergers for the formation and evolution of brightest cluster galaxies. *ArXiv e-prints*, February 2009.

[675] Raphael Sadoun, Zheng Zheng, and Jordi Miralda-Escudé. On the Decreasing Fraction of Strong Lyα Emitters around z $\sim$ 6-7. *Astrophysical Journal*, 839(1):44, April 2017.

[676] V. Sahni, A. Shafieloo, and A. A. Starobinsky. Two new diagnostics of dark energy. *ArXiv e-prints*, July 2008.

[677] D. S. Salopek and J. R. Bond. Nonlinear evolution of long-wavelength metric fluctuations in inflationary models. *Physical Review D.*, 42:3936–3962, December 1990.

[678] R. Salvaterra, B. Ciardi, A. Ferrara, and C. Baccigalupi. Reionization history from coupled cosmic microwave background/21-cm line data. *Monthly Notices of the RAS*, 360:1063–1068, July 2005.

[679] R. Sánchez-Ramírez, S. L. Ellison, J. X. Prochaska, T. A. M. Berg, S. López, V. D'Odorico, G. D. Becker, L. Christensen, G. Cupani, K. D. Denney, I. Pâris, G. Worseck, and J. Gorosabel. The evolution of neutral gas in damped Lyman α systems from the XQ-100 survey. *Monthly Notices of the RAS*, 456:4488–4505, March 2016.

[680] M. G. Santos, A. Cooray, Z. Haiman, L. Knox, and C.-P. Ma. Small-Scale Cosmic Microwave Background Temperature and Polarization Anisotropies Due to Patchy Reionization. *Astrophysical Journal*, 598:756–766, December 2003.

[681] M. G. Santos, L. Ferramacho, M. B. Silva, A. Amblard, and A. Cooray. Fast large volume simulations of the 21-cm signal from the reionization and pre-reionization epochs. *Monthly Notices of the RAS*, 406:2421–2432, August 2010.

[682] Michael R. Santos. Probing reionization with Lyman α emission lines. *Monthly Notices of the RAS*, 349(3):1137–1152, April 2004.

[683] J. Schaye. Model-independent Insights into the Nature of the Lyα Forest and the Distribution of Matter in the Universe. *Astrophysical Journal*, 559:507–515, October 2001.

[684] J. Schaye, T. Theuns, M. Rauch, G. Efstathiou, and W. L. W. Sargent. The thermal history of the intergalactic medium*. *Monthly Notices of the RAS*, 318:817–826, November 2000.

[685] M. A. Schenker, B. E. Robertson, R. S. Ellis, Y. Ono, R. J. McLure, J. S. Dunlop, A. Koekemoer, R. A. A. Bowler, M. Ouchi, E. Curtis-Lake, A. B. Rogers, E. Schneider, S. Charlot, D. P. Stark, S. R. Furlanetto, and M. Cirasuolo. The UV Luminosity Function of Star-forming Galaxies via Dropout Selection at Redshifts z ˜ 7 and 8 from the 2012 Ultra Deep Field Campaign. *Astrophysical Journal*, 768:196, May 2013.

[686] M. A. Schenker, D. P. Stark, R. S. Ellis, B. E. Robertson, J. S. Dunlop, R. J. McLure, J.-P. Kneib, and J. Richard. Keck Spectroscopy of Faint $3<z<8$ Lyman Break Galaxies: Evidence for a Declining Fraction of Emission Line Sources in the Redshift Range $6<z<8$. *Astrophysical Journal*, 744:179, January 2012.

[687] M. A. Schenker, D. P. Stark, R. S. Ellis, B. E. Robertson, J. S. Dunlop, R. J. McLure, J.-P. Kneib, and J. Richard. Keck Spectroscopy of Faint 3 ¡ z ¡ 8 Lyman Break Galaxies: Evidence for a Declining Fraction of Emission Line Sources in the Redshift Range 6 ¡ z ¡ 8. *Astrophysical Journal*, 744:179, January 2012.

[688] F. Schmidt and M. Kamionkowski. Halo clustering with nonlocal non-Gaussianity. *Physical Review D.*, 82(10):103002, November 2010.

[689] K. B. Schmidt, T. Treu, M. Bradač, B. Vulcani, K. H. Huang, A. Hoag, M. Maseda, L. Guaita, L. Pentericci, G. B. Brammer, M. Dijkstra, A. Dressler, A. Fontana, A. L. Henry, T. A. Jones, C. Mason, M. Trenti, and X. Wang. The Grism Lens-Amplified Survey from Space (GLASS). III. A Census of Lyα Emission at z $\gtrsim$ 7 from HST Spectroscopy. *Astrophysical Journal*, 818(1):38, February 2016.

[690] P. Schneider. The cosmological lens equation and the equivalent single-plane gravitational lens. *Monthly Notices of the RAS*, 292:673, December 1997.

[691] P. Schneider, J. Ehlers, and E. E. Falco. *Gravitational Lenses*. 1992.

[692] A. Schulze, L. Wisotzki, and B. Husemann. Low redshift AGN in the Hamburg/ESO survey. I. The local AGN luminosity function. *Astronomy and Astrophysics*, 507:781–793, November 2009.

[693] Greg J. Schwarz, Jan-Uwe Ness, J. P. Osborne, K. L. Page, P. A. Evans, A. P. Beardmore, Frederick M. Walter, L. Andrew Helton, Charles E. Woodward, Mike Bode, Sumner Starrfield, and Jeremy J. Drake. Swift X-Ray Observations of Classical Novae. II. The Super Soft Source Sample. *Astrophysical Journals*, 197(2):31, Dec 2011.

[694] R. Scoccimarro, L. Hui, M. Manera, and K. C. Chan. Large-scale bias and efficient generation of initial conditions for nonlocal primordial non-Gaussianity. *Physical Review D.*, 85(8):083002, April 2012.

[695] R. Scoccimarro, E. Sefusatti, and M. Zaldarriaga. Probing primordial non-Gaussianity with large-scale structure. *Physical Review D.*, 69(10):103513, May 2004.

[696] D. Seery and J. E. Lidsey. Primordial non-Gaussianities in single-field inflation. *Journal of Cosmology and Astroparticle Physics*, 6:3, June 2005.

[697] E. Sefusatti. One-loop perturbative corrections to the matter and galaxy bispectrum with non-Gaussian initial conditions. *Physical Review D.*, 80(12):123002, December 2009.

[698] E. Sefusatti, M. Crocce, and V. Desjacques. The matter bispectrum in N-body simulations with non-Gaussian initial conditions. *Monthly Notices of the RAS*, 406:1014–1028, August 2010.

[699] E. Sefusatti, M. Crocce, and V. Desjacques. The Halo Bispectrum in N-body Simulations with non-Gaussian Initial Conditions. *ArXiv e-prints*, November 2011.

[700] E. Sefusatti and E. Komatsu. Bispectrum of galaxies from high-redshift galaxy surveys: Primordial non-Gaussianity and nonlinear galaxy bias. *Physical Review D.*, 76(8):083004, October 2007.

[701] Emiliano Sefusatti, Martin Crocce, Sebastian Pueblas, and Roman Scoccimarro. Cosmology and the bispectrum.

[702] S. Seitz, P. Schneider, and J. Ehlers. Light propagation in arbitrary spacetimes and the gravitational lens approximation. *Classical and Quantum Gravity*, 11:2345–2373, September 1994.

[703] U. Seljak. Large-scale structure effects on the gravitational lens image positions and time delay. *Astrophysical Journal*, 436:509–516, December 1994.

[704] U. Seljak. Analytic model for galaxy and dark matter clustering. *Monthly Notices of the RAS*, 318:203–213, October 2000.

[705] U. Seljak, A. Makarov, P. McDonald, and et al. Cosmological parameter analysis including SDSS Lyα forest and galaxy bias: Constraints on the primordial spectrum of fluctuations, neutrino mass, and dark energy. *Physical Review D.*, 71(10):103515–+, May 2005.

[706] E. Semboloni, Y. Mellier, L. van Waerbeke, H. Hoekstra, I. Tereno, K. Benabed, S. D. J. Gwyn, L. Fu, M. J. Hudson, R. Maoli, and L. C. Parker. Cosmic shear analysis with CFHTLS deep data. *Astronomy and Astrophysics*, 452:51–61, June 2006.

[707] L. Senatore, K. M. Smith, and M. Zaldarriaga. Non-Gaussianities in single field inflation and their optimal limits from the WMAP 5-year data. *Journal of Cosmology and Astroparticle Physics*, 1:28, January 2010.

[708] M. Sereno. Probing the dark energy with strong lensing by clusters of galaxies. *Astronomy and Astrophysics*, 393:757–764, October 2002.

[709] S. Shandarin, S. Habib, and K. Heitmann. Cosmic web, multistream flows, and tessellations. *Physical Review D.*, 85(8):083005, April 2012.

[710] S. Shandera, N. Dalal, and D. Huterer. A generalized local ansatz and its effect on halo bias. *Journal of Cosmology and Astroparticle Physics*, 3:17, March 2011.

[711] P. R. Shapiro and M. L. Giroux. Cosmological H II regions and the photoionization of the intergalactic medium. *Astrophysical Journal*, 321:L107–L112, October 1987.

[712] P. R. Shapiro, M. L. Giroux, and A. Babul. Reionization in a cold dark matter universe: The feedback of galaxy formation on the intergalactic medium. *Astrophysical Journal*, 427:25–50, May 1994.

[713] P. R. Shapiro, I. T. Iliev, and A. C. Raga. Photoevaporation of cosmological minihaloes during reionization. *Monthly Notices of the RAS*, 348:753–782, March 2004.

[714] P. R. Shapiro, Y. Mao, I. T. Iliev, G. Mellema, K. K. Datta, K. Ahn, and J. Koda. Will Nonlinear Peculiar Velocity and Inhomogeneous Reionization Spoil 21cm Cosmology from the Epoch of Reionization? *PRL*, 110:151301, November 2013.

[715] M. Sharma, T. Theuns, C. Frenk, R. Bower, R. Crain, M. Schaller, and J. Schaye. The brighter galaxies reionised the Universe. *Monthly Notices of the RAS*, February 2016.

[716] R. K. Sheth and G. Tormen. An excursion set model of hierarchical clustering: ellipsoidal collapse and the moving barrier. *Monthly Notices of the RAS*, 329:61–75, January 2002.

[717] R. K. Sheth and R. van de Weygaert. A hierarchy of voids: much ado about nothing. *Monthly Notices of the RAS*, 350:517–538, May 2004.

[718] Ravi K. Sheth and Giuseppe Tormen. Large-scale bias and the peak background split. *Monthly Notices of the RAS*, 308(1):119–126, September 1999.

[719] Takatoshi Shibuya, Masami Ouchi, Akira Konno, Ryo Higuchi, Yuichi Harikane, Yoshiaki Ono, Kazuhiro Shimasaku, Yoshiaki Taniguchi, Masakazu A. R. Kobayashi, Masaru Kajisawa, Tohru Nagao, Hisanori Furusawa, Tomotsugu Goto, Nobunari

Kashikawa, Yutaka Komiyama, Haruka Kusakabe, Chien-Hsiu Lee, Rieko Momose, Kimihiko Nakajima, Masayuki Tanaka, Shiang-Yu Wang, and Suraphong Yuma. SILVERRUSH. II. First catalogs and properties of ~2000 Lyα emitters and blobs at z ~ 6-7 identified over the 14-21 deg^2 sky*. *Publications of the ASJ*, 70:S14, January 2018.

[720] J. M. Shull, A. Harness, M. Trenti, and B. D. Smith. Critical Star Formation Rates for Reionization: Full Reionization Occurs at Redshift z $\approx$ 7. *Astrophysical Journal*, 747:100, March 2012.

[721] J. M. Shull, M. Stevans, and C. W. Danforth. HST-COS Observations of AGNs. I. Ultraviolet Composite Spectra of the Ionizing Continuum and Emission Lines. *Astrophysical Journal*, 752:162, June 2012.

[722] B. Siana, A. E. Shapley, K. R. Kulas, D. B. Nestor, C. C. Steidel, H. I. Teplitz, A. Alavi, T. M. Brown, C. J. Conselice, H. C. Ferguson, M. Dickinson, M. Giavalisco, J. W. Colbert, C. R. Bridge, J. P. Gardner, and D. F. de Mello. A Deep Hubble Space Telescope and Keck Search for Definitive Identification of Lyman Continuum Emitters at z˜3.1. *Astrophysical Journal*, 804:17, May 2015.

[723] B. Siana, H. I. Teplitz, J. Colbert, H. C. Ferguson, M. Dickinson, T. M. Brown, C. J. Conselice, D. F. de Mello, J. P. Gardner, M. Giavalisco, and F. Menanteau. New Constraints on the Lyman Continuum Escape Fraction at z˜1.3. *Astrophysical Journal*, 668:62–73, October 2007.

[724] E. Sirko. Initial Conditions to Cosmological N-Body Simulations, or, How to Run an Ensemble of Simulations. *Astrophysical Journal*, 634:728–743, November 2005.

[725] A. Slosar, C. Hirata, U. Seljak, S. Ho, and N. Padmanabhan. Constraints on local primordial non-Gaussianity from large scale structure. *Journal of Cosmology and Astroparticle Physics*, 8:31–+, August 2008.

[726] G. P. Smith, H. Ebeling, M. Limousin, J.-P. Kneib, A. M. Swinbank, C.-J. Ma, M. Jauzac, J. Richard, E. Jullo, D. J. Sand, A. C. Edge, and I. Smail. Hubble Space Telescope Observations of a Spectacular New Strong-Lensing Galaxy Cluster: MACS J1149.5+2223 at z = 0.544. *Astrophysical Journal*, 707:L163–L168, December 2009.

[727] K. M. Smith, S. Ferraro, and M. LoVerde. Halo clustering and g_{NL}-type primordial non-gaussianity. *Journal of Cosmology and Astroparticle Physics*, 3:32, March 2012.

[728] K. M. Smith and M. LoVerde. Local stochastic non-Gaussianity and N-body simulations. *Journal of Cosmology and Astroparticle Physics*, 11:9, November 2011.

[729] R. E. Smith, V. Desjacques, and L. Marian. Nonlinear clustering in models with primordial non-Gaussianity: The halo model approach. *Physical Review D.*, 83(4):043526, February 2011.

[730] R. E. Smith, J. A. Peacock, A. Jenkins, S. D. M. White, C. S. Frenk, F. R. Pearce, P. A. Thomas, G. Efstathiou, and H. M. P. Couchman. Stable clustering, the halo model and non-linear cosmological power spectra. *Monthly Notices of the RAS*, 341:1311–1332, June 2003.

[731] R. E. Smith and P. I. R. Watts. Triaxial haloes, intrinsic alignments and the dark matter power spectrum. *Monthly Notices of the RAS*, 360:203–215, June 2005.

[732] Geoffrey C. So, Michael L. Norman, Daniel R. Reynolds, and John H. Wise. Fully Coupled Simulation of Cosmic Reionization. II. Recombinations, Clumping Factors, and the Photon Budget for Reionization. *Astrophysical Journal*, 789(2):149, Jul 2014.

[733] E. Sobacchi and A. Mesinger. How does radiative feedback from a UV background impact reionization? *ArXiv e-prints*, January 2013.

[734] E. Sobacchi and A. Mesinger. How does radiative feedback from an ultraviolet background impact reionization? *Monthly Notices of the RAS*, 432:3340–3348, July 2013.

[735] E. Sobacchi and A. Mesinger. The depletion of gas in high-redshift dwarf galaxies from an inhomogeneous reionization. *Monthly Notices of the RAS*, 432:L51, May 2013.

[736] E. Sobacchi and A. Mesinger. Inhomogeneous recombinations during cosmic reionization. *Monthly Notices of the RAS*, 440:1662–1673, May 2014.

[737] E. Sobacchi and A. Mesinger. The clustering of Lyman alpha emitters at z=7: implications for reionization and host halo masses. *ArXiv e-prints*, May 2015.

[738] E. Sobacchi and A. Mesinger. The clustering of Lyman alpha emitters at z=7: implications for reionization and host halo masses. *ArXiv e-prints*, May 2015.

[739] A. Songaila, A. J. Barger, L. L. Cowie, E. M. Hu, and A. J. Taylor. The Evolution of Lyα Emitter Line Widths from z = 5.7 to z = 6.6. *Astrophysical Journal*, 935(1):52, August 2022.

[740] A. Songaila, E. M. Hu, A. J. Barger, L. L. Cowie, G. Hasinger, B. Rosenwasser, and C. Waters. Complex Lyα Profiles in Redshift 6.6 Ultraluminous Lyα Emitters. *Astrophysical Journal*, 859(2):91, June 2018.

[741] G. Soucail, J.-P. Kneib, and G. Golse. Multiple-images in the cluster lens Abell 2218: Constraining the geometry of the Universe? *Astronomy and Astrophysics*, 417:L33–L37, April 2004.

[742] D. N. Spergel, R. Bean, O. Doré, and et al. Three-Year Wilkinson Microwave Anisotropy Probe (WMAP) Observations: Implications for Cosmology. *Astrophysical Journals*, 170:377–408, June 2007.

[743] Benedetta Spina, Sarah E. I. Bosman, Frederick B. Davies, Prakash Gaikwad, and Yongda Zhu. Damping wings in the Lyman-Lyα forest: a model-independent measurement of the neutral fraction at 5.4¡z¡6.1. *arXiv e-prints*, page arXiv:2405.12273, May 2024.

[744] L. Spitzer. *Physical processes in the interstellar medium.* 1978.

[745] V. Springel. The cosmological simulation code GADGET-2. *Monthly Notices of the RAS*, 364:1105–1134, December 2005.

[746] V. Springel, J. Wang, M. Vogelsberger, A. Ludlow, A. Jenkins, A. Helmi, J. F. Navarro, C. S. Frenk, and S. D. M. White. The Aquarius Project: the subhaloes of galactic haloes. *Monthly Notices of the RAS*, 391:1685–1711, December 2008.

[747] V. Springel, S. D. M. White, A. Jenkins, C. S. Frenk, N. Yoshida, L. Gao, J. Navarro, R. Thacker, D. Croton, J. Helly, J. A. Peacock, S. Cole, P. Thomas, H. Couchman, A. Evrard, J. Colberg, and F. Pearce. Simulations of the formation, evolution and clustering of galaxies and quasars. *Nature*, 435:629–636, June 2005.

[748] D. P. Stark, R. S. Ellis, K. Chiu, M. Ouchi, and A. Bunker. Keck spectroscopy of faint 3 ¡ z ¡ 7 Lyman break galaxies - I. New constraints on cosmic reionization from the luminosity and redshift-dependent fraction of Lyman α emission. *Monthly Notices of the RAS*, 408:1628–1648, November 2010.

[749] D. P. Stark, R. S. Ellis, J. Richard, J.-P. Kneib, G. P. Smith, and M. R. Santos. A Keck Survey for Gravitationally Lensed Lyα Emitters in the Redshift Range 8.5¡z¡10.4: New Constraints on the Contribution of Low-Luminosity Sources to Cosmic Reionization. *Astrophysical Journal*, 663:10–28, July 2007.

[750] Daniel P. Stark, Richard S. Ellis, Stéphane Charlot, Jacopo Chevallard, Mengtao Tang, Sirio Belli, Adi Zitrin, Ramesh Mainali, Julia Gutkin, Alba Vidal-García, Rychard Bouwens, and Pascal Oesch. Lyα and C III] emission in z = 7-9 Galaxies: accelerated reionization around luminous star-forming systems? *Monthly Notices of the RAS*, 464(1):469–479, January 2017.

[751] Daniel P. Stark, Richard S. Ellis, Stéphane Charlot, Jacopo Chevallard, Mengtao Tang, Sirio Belli, Adi Zitrin, Ramesh Mainali, Julia Gutkin, Alba Vidal-García, Rychard Bouwens, and Pascal Oesch. Lyα and C III] emission in z = 7-9 Galaxies: accelerated reionization around luminous star-forming systems? *Monthly Notices of the RAS*, 464(1):469–479, January 2017.

[752] Charles C. Steidel, Milan Bogosavljević, Alice E. Shapley, Naveen A. Reddy, Gwen C. Rudie, Max Pettini, Ryan F. Trainor, and Allison L. Strom. The Keck Lyman Continuum Spectroscopic Survey (KLCS): The Emergent Ionizing Spectrum of Galaxies at z $\sim$ 3. *Astrophysical Journal*, 869(2):123, December 2018.

[753] M. Stiavelli et al. First light and reionization : open questions in the post-JWST era. In *astro2010: The Astronomy and Astrophysics Decadal Survey*, volume 2010 of *Astronomy*, page 287, 2009.

[754] R. A. Sunyaev and I. B. Zeldovich. The velocity of clusters of galaxies relative to the microwave background - The possibility of its measurement. *Monthly Notices of the RAS*, 190:413–420, February 1980.

[755] M. Takada and T. Hamana. Halo model predictions of the cosmic magnification statistics: the full non-linear contribution. *Monthly Notices of the RAS*, 346:949–962, December 2003.

[756] M. Takada and M. White. Tomography of Lensing Cross-Power Spectra. *Astrophysical Journal*, 601:L1–L4, January 2004.

[757] R. Takahashi and K. T. Inoue. Weak Lensing by Intergalactic Mini-Structures in Quadruple Lens Systems: Simulation and Detection. *ArXiv e-prints*, August 2013.

[758] R. Takahashi, M. Oguri, M. Sato, and T. Hamana. Probability Distribution Functions of Cosmological Lensing: Convergence, Shear, and Magnification. *Astrophysical Journal*, 742:15, November 2011.

[759] R. Takahashi, M. Sato, T. Nishimichi, A. Taruya, and M. Oguri. Revising the Halofit Model for the Nonlinear Matter Power Spectrum. *Astrophysical Journal*, 761:152, December 2012.

[760] Mengtao Tang, Daniel P. Stark, Zuyi Chen, Charlotte Mason, Michael Topping, Ryan Endsley, Peter Senchyna, Adèle Plat, Ting-Yi Lu, Lily Whitler, Brant Robertson, and Stéphane Charlot. JWST/NIRSpec Spectroscopy of $z = 7 - 9$ Star Forming Galaxies with CEERS: New Insight into Bright Lyα Emitters in Ionized Bubbles. *arXiv e-prints*, page arXiv:2301.07072, January 2023.

[761] Mengtao Tang, Daniel P. Stark, Michael W. Topping, Charlotte Mason, and Richard S. Ellis. JWST/NIRSpec Observations of Lyα Emission in Star Forming Galaxies at $6.5 \lesssim z \lesssim 13$. *arXiv e-prints*, page arXiv:2408.01507, August 2024.

[762] H. Tashiro and S. Ho. Constraining primordial non-Gaussianity with CMB-21cm cross-correlations? *ArXiv e-prints*, May 2012.

[763] H. Tashiro and N. Sugiyama. Ionized bubble number count as a probe of non-Gaussianity. *Monthly Notices of the RAS*, 420:441–446, February 2012.

[764] J. Taylor and A. Lidz. What do observations of the Lyman α fraction tell us about reionization? *Monthly Notices of the RAS*, 437:2542–2553, January 2014.

[765] J. E. Taylor and A. Babul. The evolution of substructure in galaxy, group and cluster haloes - II. Global properties. *Monthly Notices of the RAS*, 364:515–534, December 2005.

[766] Thorsten Tepper-García. Voigt profile fitting to quasar absorption lines: an analytic approximation to the Voigt-Hjerting function. *Monthly Notices of the RAS*, 369(4):2025–2035, July 2006.

[767] Thorsten Tepper-García. Voigt profile fitting to quasar absorption lines: an analytic approximation to the Voigt-Hjerting function. *Monthly Notices of the RAS*, 369(4):2025–2035, July 2006.

[768] T. Theuns, A. Leonard, G. Efstathiou, F. R. Pearce, and P. A. Thomas. P^3M-SPH simulations of the Lyalpha forest. *Monthly Notices of the RAS*, 301:478–502, December 1998.

[769] V. Tilvi, S. Malhotra, J. E. Rhoads, A. Coughlin, Z. Zheng, S. L. Finkelstein, S. Veilleux, B. Mobasher, J. Wang, R. Probst, R. Swaters, P. Hibon, B. Joshi, J. Zabl, T. Jiang, J. Pharo, and H. Yang. Onset of Cosmic Reionization: Evidence of an Ionized Bubble Merely 680 Myr after the Big Bang. *Astrophysical Journal*, 891(1):L10, March 2020.

[770] Jeremy L. Tinker, Charlie Conroy, Peder Norberg, Santiago G. Patiri, David H. Weinberg, and Michael S. Warren. Void Statistics in Large Galaxy Redshift Surveys: Does Halo Occupation of Field Galaxies Depend on Environment? *Astrophysical Journal*, 686(1):53–71, October 2008.

[771] Jeremy L. Tinker, David H. Weinberg, and Michael S. Warren. Cosmic Voids and Galaxy Bias in the Halo Occupation Framework. *Astrophysical Journal*, 647(2):737–752, August 2006.

[772] E. Torri, M. Meneghetti, M. Bartelmann, L. Moscardini, E. Rasia, and G. Tormen. The impact of cluster mergers on arc statistics. *Monthly Notices of the RAS*, 349:476–490, April 2004.

[773] H. Trac, R. Cen, and A. Loeb. Imprint of Inhomogeneous Hydrogen Reionization on the Temperature Distribution of the Intergalactic Medium. *Astrophysical Journal*, 689:L81–L84, December 2008.

[774] H. Trac, R. Cen, and P. Mansfield. SCORCH I: The Galaxy-Halo Connection in the First Billion Years. *Astrophysical Journal*, 813:54, November 2015.

[775] Hy Trac and Renyue Cen. Radiative Transfer Simulations of Cosmic Reionization. I. Methodology and Initial Results. *Astrophysical Journal*, 671(1):1–13, December 2007.

[776] Hy Trac, Renyue Cen, and Philip Mansfield. SCORCH. i. THE GALAXY–HALO CONNECTION IN THE FIRST BILLION YEARS. *The Astrophysical Journal*, 813(1):54, oct 2015.

[777] Hy Trac and Ue-Li Pen. A moving frame algorithm for high Mach number hydrodynamics. *New Astronomy*, 9(6):443–465, July 2004.

[778] Hy Trac and Ue-Li Pen. A moving frame algorithm for high Mach number hydrodynamics. *New Astronomy*, 9(6):443–465, July 2004.

[779] Hy Trac and Ue-Li Pen. A moving frame algorithm for high mach number hydrodynamics. *New Astronomy*, 9(6):443–465, 2004.

[780] M. Trenti, M. Stiavelli, R. J. Bouwens, P. Oesch, J. M. Shull, G. D. Illingworth, L. D. Bradley, and C. M. Carollo. The Galaxy Luminosity Function During the Reionization Epoch. *Astrophysical Journal*, 714(2):L202–L207, May 2010.

[781] M. Trenti, M. Stiavelli, R. J. Bouwens, P. Oesch, J. M. Shull, G. D. Illingworth, L. D. Bradley, and C. M. Carollo. The galaxy luminosity function during the reionization epoch. *The Astrophysical Journal*, 714(2):L202–L207, Apr 2010.

[782] D. Tseliakhovich and C. Hirata. Relative velocity of dark matter and baryonic fluids and the formation of the first structures. *Physical Review D.*, 82(8):083520, October 2010.

[783] H. TU, R. Gavazzi, M. Limousin, R. Cabanac, P. J. Marshall, B. Fort, T. Treu, R. Péllo, E. Jullo, J. . Kneib, and J. . Sygnet. The mass profile of early-type galaxies in overdense environments: the case of the double source plane gravitational lens SL2SJ02176-0513. *ArXiv e-prints*, February 2009.

[784] P. R. Upton Sanderbeck, A. D'Aloisio, and M. J. McQuinn. Models of the Thermal Evolution of the Intergalactic Medium After Reionization. *ArXiv e-prints*, November 2015.

[785] Phoebe R. Upton Sanderbeck, Anson D'Aloisio, and Matthew J. McQuinn. Models of the thermal evolution of the intergalactic medium after reionization. *Monthly Notices of the RAS*, 460(2):1885–1897, August 2016.

[786] Phoebe R. Upton Sanderbeck, Matthew McQuinn, Anson D'Aloisio, and Jessica K. Werk. The Sources of Extreme Ultraviolet and Soft X-Ray Backgrounds. *Astrophysical Journal*, 869(2):159, December 2018.

[787] P. Valageas. Mass function and bias of dark matter halos for non-Gaussian initial conditions. *Astronomy and Astrophysics*, 514:A46, May 2010.

[788] P. Valageas, A. Balbi, and J. Silk. Secondary CMB anisotropies from the kinetic SZ effect. *Astronomy and Astrophysics*, 367:1–17, February 2001.

[789] Stéfan van der Walt, Johannes L. Schönberger, Juan Nunez-Iglesias, François Boulogne, Joshua D. Warner, Neil Yager, Emmanuelle Gouillart, Tony Yu, and the scikit-image contributors. scikit-image: image processing in Python. *PeerJ*, 2:e453, 6 2014.

[790] L. Van Waerbeke, Y. Mellier, T. Erben, J. C. Cuillandre, F. Bernardeau, R. Maoli, E. Bertin, H. J. McCracken, O. Le Fèvre, B. Fort, M. Dantel-Fort, B. Jain, and P. Schneider. Detection of correlated galaxy ellipticities from CFHT data: first evidence for gravitational lensing by large-scale structures. *Astronomy and Astrophysics*, 358:30–44, June 2000.

[791] E. Vanzella, M. Giavalisco, A. K. Inoue, M. Nonino, F. Fontanot, S. Cristiani, A. Grazian, M. Dickinson, D. Stern, P. Tozzi, E. Giallongo, H. Ferguson, H. Spinrad, K. Boutsia, A. Fontana, P. Rosati, and L. Pentericci. The Great Observatories Origins Deep Survey: Constraints on the Lyman Continuum Escape Fraction Distribution of Lyman-break Galaxies at $3.4 < z < 4.5$. *Astrophysical Journal*, 725:1011–1031, December 2010.

[792] E. Vanzella, L. Pentericci, A. Fontana, A. Grazian, M. Castellano, K. Boutsia, S. Cristiani, M. Dickinson, S. Gallozzi, E. Giallongo, M. Giavalisco, R. Maiolino, A. Moorwood, D. Paris, and P. Santini. Spectroscopic Confirmation of Two Lyman Break Galaxies at Redshift Beyond 7. *Astrophysical Journal*, 730(2):L35, April 2011.

[793] L. Verde, R. Jimenez, M. Kamionkowski, and S. Matarrese. Tests for primordial non-Gaussianity. *Monthly Notices of the RAS*, 325:412–418, July 2001.

[794] L. Verde, L. Wang, A. F. Heavens, and M. Kamionkowski. Large-scale structure, the cosmic microwave background and primordial non-Gaussianity. *Monthly Notices of the RAS*, 313:141–147, March 2000.

[795] Anne Verhamme, Ivana Orlitová, Daniel Schaerer, and Matthew Hayes. Using Lyman-α to detect galaxies that leak Lyman continuum. *Astronomy and Astrophysics*, 578:A7, June 2015.

[796] M. Viel, E. Branchini, K. Dolag, M. Grossi, S. Matarrese, and L. Moscardini. Primordial non-Gaussianities in the Intergalactic Medium. *ArXiv e-prints*, November 2008.

[797] Matteo Viel, George D. Becker, James S. Bolton, and Martin G. Haehnelt. Warm dark matter as a solution to the small scale crisis: New constraints from high redshift Lyman-α forest data. *Physical Review D.*, 88(4):043502, Aug 2013.

[798] A. Vikhlinin, A. V. Kravtsov, R. A. Burenin, H. Ebeling, W. R. Forman, A. Hornstrup, C. Jones, S. S. Murray, D. Nagai, H. Quintana, and A. Voevodkin. Chandra Cluster Cosmology Project III: Cosmological Parameter Constraints. *Astrophysical Journal*, 692:1060–1074, February 2009.

[799] J.-M. Virey, D. Talon-Esmieu, A. Ealet, P. Taxil, and A. Tilquin. On the determination of curvature and dynamical dark energy. *Journal of Cosmology and Astro-Particle Physics*, 12:8–+, December 2008.

[800] Pauli Virtanen, Ralf Gommers, Travis E. Oliphant, Matt Haberland, Tyler Reddy, David Cournapeau, Evgeni Burovski, Pearu Peterson, Warren Weckesser, Jonathan Bright, Stéfan J. van der Walt, Matthew Brett, Joshua Wilson, K. Jarrod Millman, Nikolay Mayorov, Andrew R. J. Nelson, Eric Jones, Robert Kern, Eric Larson, C J Carey, İlhan Polat, Yu Feng, Eric W. Moore, Jake VanderPlas, Denis Laxalde, Josef Perktold, Robert Cimrman, Ian Henriksen, E. A. Quintero, Charles R. Harris, Anne M. Archibald, Antônio H. Ribeiro, Fabian Pedregosa, Paul van Mulbregt, and SciPy 1.0 Contributors. SciPy 1.0: Fundamental Algorithms for Scientific Computing in Python. *Nature Methods*, 17:261–272, 2020.

[801] E. Visbal, R. Barkana, A. Fialkov, D. Tseliakhovich, and C. M. Hirata. The signature of the first stars in atomic hydrogen at redshift 20. *Nature*, 487:70–73, July 2012.

[802] Frédéric P. A. Vogt, Michael A. Dopita, Lisa J. Kewley, Ralph S. Sutherland, Julia Scharwächter, Hassan M. Basurah, Alaa Ali, and Morsi A. Amer. Galaxy Emission Line Classification Using Three-dimensional Line Ratio Diagrams. *Astrophysical Journal*, 793(2):127, Oct 2014.

[803] C. Wagner, F. Schmidt, C. T. Chiang, and E. Komatsu. Separate universe simulations. *Monthly Notices of the RAS*, 448:L11–L15, Mar 2015.

[804] C. Wagner and L. Verde. N-body simulations with generic non-Gaussian initial conditions II: halo bias. *Journal of Cosmology and Astroparticle Physics*, 3:2, March 2012.

[805] C. Wagner, L. Verde, and L. Boubekeur. N-body simulations with generic non-Gaussian initial conditions I: power spectrum and halo mass function. *Journal of Cosmology and Astroparticle Physics*, 10:22–+, October 2010.

[806] Michael Walther, Jose Oñorbe, Joseph F. Hennawi, and Zarija Lukić. New Constraints on IGM Thermal Evolution from the Lyα Forest Power Spectrum. *Astrophysical Journal*, 872(1):13, February 2019.

[807] Michael Walther, Jose Oñorbe, Joseph F. Hennawi, and Zarija Lukić. New Constraints on IGM Thermal Evolution from the Lyα Forest Power Spectrum. *Astrophysical Journal*, 872(1):13, Feb 2019.

[808] J. Wambsganss, P. Bode, and J. P. Ostriker. Giant Arc Statistics in Concord with a Concordance Lambda Cold Dark Matter Universe. *Astrophysical Journal*, 606:L93–L96, May 2004.

[809] J. Wambsganss, P. Bode, and J. P. Ostriker. Gravitational Lensing in a Concordance ΛCDM Universe: The Importance of Secondary Matter along the Line of Sight. *Astrophysical Journal*, 635:L1–L4, December 2005.

[810] J. Wambsganss, J. P. Ostriker, and P. Bode. The Effect of Baryon Cooling on the Statistics of Giant Arcs and Multiple Quasars. *Astrophysical Journal*, 676:753–760, April 2008.

[811] Feige Wang, Frederick B. Davies, Jinyi Yang, Joseph F. Hennawi, Xiaohui Fan, Aaron J. Barth, Linhua Jiang, Xue-Bing Wu, Dale M. Mudd, Eduardo Bañados, Fuyan Bian, Roberto Decarli, Anna-Christina Eilers, Emanuele Paolo Farina, Bram Venemans, Fabian Walter, and Minghao Yue. A Significantly Neutral Intergalactic Medium Around the Luminous z = 7 Quasar J0252-0503. *Astrophysical Journal*, 896(1):23, June 2020.

[812] Feige Wang, Jinyi Yang, Xiaohui Fan, Xue-Bing Wu, Minghao Yue, Jiang-Tao Li, Fuyan Bian, Linhua Jiang, Eduardo Bañados, Jan-Torge Schindler, Joseph R. Findlay, Frederick B. Davies, Roberto Decarli, Emanuele P. Farina, Richard Green, Joseph F. Hennawi, Yun-Hsin Huang, Chiara Mazzuccheli, Ian D. McGreer, Bram Venemans, Fabian Walter, Simon Dye, Brad W. Lyke, Adam D. Myers, and Evan Haze Nunez.

Exploring Reionization-era Quasars. III. Discovery of 16 Quasars at $6.4 \lesssim z \lesssim 6.9$ with DESI Legacy Imaging Surveys and the UKIRT Hemisphere Survey and Quasar Luminosity Function at z ∼6.7. *Astrophysical Journal*, 884(1):30, Oct 2019.

[813] Feige Wang, Jinyi Yang, Joseph F. Hennawi, Xiaohui Fan, Fengwu Sun, Jaclyn B. Champagne, Tiago Costa, Melanie Habouzit, Ryan Endsley, Zihao Li, Xiaojing Lin, Romain A. Meyer, Jan-Torge Schindler, Yunjing Wu, Eduardo Bañados, Aaron J. Barth, Aklant K. Bhowmick, Rebekka Bieri, Laura Blecha, Sarah Bosman, Zheng Cai, Luis Colina, Thomas Connor, Frederick B. Davies, Roberto Decarli, Gisella De Rosa, Alyssa B. Drake, Eiichi Egami, Anna-Christina Eilers, Analis E. Evans, Emanuele Paolo Farina, Zoltan Haiman, Linhua Jiang, Xiangyu Jin, Hyunsung D. Jun, Koki Kakiichi, Yana Khusanova, Girish Kulkarni, Mingyu Li, Weizhe Liu, Federica Loiacono, Alessandro Lupi, Chiara Mazzucchelli, Masafusa Onoue, Maria A. Pudoka, Sofía Rojas-Ruiz, Yue Shen, Michael A. Strauss, Wei Leong Tee, Benny Trakhtenbrot, Maxime Trebitsch, Bram Venemans, Marta Volonteri, Fabian Walter, Zhang-Liang Xie, Minghao Yue, Haowen Zhang, Huanian Zhang, and Siwei Zou. A SPectroscopic Survey of Biased Halos in the Reionization Era (ASPIRE): JWST Reveals a Filamentary Structure around a z = 6.61 Quasar. *Astrophysical Journal*, 951(1):L4, July 2023.

[814] L. Wang and M. Kamionkowski. Cosmic microwave background bispectrum and inflation. *Physical Review D.*, 61(6):063504, March 2000.

[815] Y. Wang, D. E. Holz, and D. Munshi. A Universal Probability Distribution Function for Weak-lensing Amplification. *Astrophysical Journal*, 572:L15–L18, June 2002.

[816] N. N. Weinberg and M. Kamionkowski. Weak gravitational lensing by dark clusters. *Monthly Notices of the RAS*, 337:1269–1281, December 2002.

[817] Lewis H. Weinberger, Martin G. Haehnelt, and Girish Kulkarni. Modelling the observed luminosity function and clustering evolution of Ly α emitters: growing evidence for late reionization. *Monthly Notices of the RAS*, 485(1):1350–1366, May 2019.

[818] Lewis H. Weinberger, Girish Kulkarni, Martin G. Haehnelt, Tirthankar Roy Choudhury, and Ewald Puchwein. Lyman-α emitters gone missing: the different evolution of the bright and faint populations. *Monthly Notices of the RAS*, 479(2):2564–2587, September 2018.

[819] Lily R. Whitler, Charlotte A. Mason, Keven Ren, Mark Dijkstra, Andrei Mesinger, Laura Pentericci, Michele Trenti, and Tommaso Treu. The impact of scatter in the galaxy UV luminosity to halo mass relation on Ly α visibility during the epoch of reionization. *Monthly Notices of the RAS*, 495(4):3602–3613, July 2020.

[820] Claire E. Williams, William Lake, Smadar Naoz, Blakesley Burkhart, Tommaso Treu, Federico Marinacci, Yurina Nakazato, Mark Vogelsberger, Naoki Yoshida, Gen Chiaki, Yeou S. Chiou, and Avi Chen. The Supersonic Project: Lighting Up the Faint End of the JWST UV Luminosity Function. *The Astrophysical Journal Letters*, 960(2):L16, January 2024.

[821] C. J. Willott, P. Delorme, C. Reylé, L. Albert, J. Bergeron, D. Crampton, X. Delfosse, T. Forveille, J. B. Hutchings, R. J. McLure, A. Omont, and D. Schade. The Canada-France High-z Quasar Survey: Nine New Quasars and the Luminosity Function at Redshift 6. *Astronomical Journal*, 139:906–918, March 2010.

[822] Bayu Wilson, Vid Iršič, and Matthew McQuinn. A measurement of the Ly β forest power spectrum and its cross with the Ly α forest in X-Shooter XQ-100. *Monthly Notices of the RAS*, 509(2):2423–2442, January 2022.

[823] John H. Wise, Vasiliy G. Demchenko, Martin T. Halicek, Michael L. Norman, Matthew J. Turk, Tom Abel, and Britton D. Smith. The birth of a galaxy - III. Propelling reionization with the faintest galaxies. *Monthly Notices of the RAS*, 442(3):2560–2579, August 2014.

[824] D. M. Wittman, J. A. Tyson, D. Kirkman, I. Dell'Antonio, and G. Bernstein. Detection of weak gravitational lensing distortions of distant galaxies by cosmic dark matter at large scales. *Nature*, 405:143–148, May 2000.

[825] G. Worseck, J. X. Prochaska, J. F. Hennawi, and M. McQuinn. Early and Extended Helium Reionization Over More Than 600 Million Years of Cosmic Time. *ArXiv e-prints*, May 2014.

[826] G. Worseck, J. X. Prochaska, M. McQuinn, A. Dall'Aglio, C. Fechner, J. F. Hennawi, D. Reimers, P. Richter, and L. Wisotzki. The End of Helium Reionization at z ˜= 2.7 Inferred from Cosmic Variance in HST/COS He II Lyα Absorption Spectra. *Astrophysical Journal*, 733:L24, June 2011.

[827] Gábor Worseck, J. Xavier Prochaska, John M. O'Meara, George D. Becker, Sara L. Ellison, Sebastian Lopez, Avery Meiksin, Brice Ménard, Michael T. Murphy, and Michele Fumagalli. The Giant Gemini GMOS survey of z_{em} ¿ 4.4 quasars - I. Measuring the mean free path across cosmic time. *Monthly Notices of the RAS*, 445(2):1745–1760, December 2014.

[828] C. O. Wright and T. G. Brainerd. Gravitational Lensing by NFW Halos. *Astrophysical Journal*, 534:34–40, May 2000.

[829] Xiaohan Wu, Matthew McQuinn, Rahul Kannan, Anson D'Aloisio, Simeon Bird, Federico Marinacci, Romeel Davé, and Lars Hernquist. Imprints of temperature fluctuations on the z $\sim$ 5 Lyman-α forest: a view from radiation-hydrodynamic simulations of reionization. *Monthly Notices of the RAS*, 490(3):3177–3195, December 2019.

[830] J. S. B. Wyithe and J. S. Bolton. Near-zone sizes and the rest-frame extreme ultraviolet spectral index of the highest redshift quasars. *Monthly Notices of the RAS*, 412:1926–1936, April 2011.

[831] J. S. B. Wyithe and R. Cen. The Extended Star Formation History of the First Generation of Stars and the Reionization of Cosmic Hydrogen. *Astrophysical Journal*, 659:890–907, April 2007.

[832] J. S. B. Wyithe and A. Loeb. Was the Universe Reionized by Massive Metal-free Stars? *Astrophysical Journal*, 588:L69–L72, May 2003.

[833] J. S. B. Wyithe and M. F. Morales. Biased reionization and non-Gaussianity in redshifted 21-cm intensity maps of the reionization epoch. *Monthly Notices of the RAS*, 379:1647–1657, August 2007.

[834] J. S. B. Wyithe, H. Yan, R. A. Windhorst, and S. Mao. A distortion of very-high-redshift galaxy number counts by gravitational lensing. *Nature*, 469:181–184, January 2011.

[835] J.-Q. Xia, C. Baccigalupi, S. Matarrese, L. Verde, and M. Viel. Constraints on primordial non-Gaussianity from large scale structure probes. *Journal of Cosmology and Astroparticle Physics*, 8:33, August 2011.

[836] J.-Q. Xia, A. Bonaldi, C. Baccigalupi, G. De Zotti, S. Matarrese, L. Verde, and M. Viel. Constraining primordial non-Gaussianity with high-redshift probes. *Journal of Cosmology and Astroparticle Physics*, 8:13, August 2010.

[837] J.-Q. Xia and M. Viel. Early Dark Energy at High Redshifts: Status and Perspectives. *ArXiv e-prints*, January 2009.

[838] J.-Q. Xia, M. Viel, C. Baccigalupi, G. De Zotti, S. Matarrese, and L. Verde. Primordial Non-Gaussianity and the NRAO VLA Sky Survey. *Astrophysical Journal*, 717:L17–L21, July 2010.

[839] D. D. Xu, S. Mao, A. P. Cooper, L. Gao, C. S. Frenk, R. E. Angulo, and J. Helly. On the effects of line-of-sight structures on lensing flux-ratio anomalies in a ΛCDM universe. *Monthly Notices of the RAS*, 421:2553–2567, April 2012.

[840] N. Yahata, K. M. Lanzetta, H.-W. Chen, A. Fernández-Soto, S. M. Pascarelle, A. Yahil, and R. C. Puetter. Photometry and Photometric Redshifts of Faint Galaxies in the Hubble Deep Field South NICMOS Field. *Astrophysical Journal*, 538:493–504, August 2000.

[841] Huan Yang, Sangeeta Malhotra, Max Gronke, James E. Rhoads, Claus Leitherer, Aida Wofford, Tianxing Jiang, Mark Dijkstra, V. Tilvi, and Junxian Wang. Lyα Profile, Dust, and Prediction of Lyα Escape Fraction in Green Pea Galaxies. *Astrophysical Journal*, 844(2):171, August 2017.

[842] Jinyi Yang, Feige Wang, Xiaohui Fan, Joseph F. Hennawi, Frederick B. Davies, Minghao Yue, Eduardo Banados, Xue-Bing Wu, Bram Venemans, Aaron J. Barth, Fuyan Bian, Konstantina Boutsia, Roberto Decarli, Emanuele Paolo Farina, Richard Green, Linhua Jiang, Jiang-Tao Li, Chiara Mazzucchelli, and Fabian Walter. Pōniuā'ena: A Luminous z = 7.5 Quasar Hosting a 1.5 Billion Solar Mass Black Hole. *Astrophysical Journal*, 897(1):L14, July 2020.

[843] Jinyi Yang, Feige Wang, Xiaohui Fan, Joseph F. Hennawi, Frederick B. Davies, Minghao Yue, Anna-Christina Eilers, Emanuele P. Farina, Xue-Bing Wu, Fuyan Bian, Fabio Pacucci, and Khee-Gan Lee. Measurements of the z $\sim$ 6 Intergalactic Medium Optical Depth and Transmission Spikes Using a New z ¿ 6.3 Quasar Sample. *Astrophysical Journal*, 904(1):26, November 2020.

[844] M. Yashar, B. Bozek, A. Abrahamse, A. Albrecht, and M. Barnard. Exploring Parameter Constraints on Quintessential Dark Energy: the Inverse Power Law Model. *ArXiv e-prints*, November 2008.

[845] Jessica Y. C. Yeh, Aaron Smith, Rahul Kannan, Enrico Garaldi, Mark Vogelsberger, Josh Borrow, Rüdiger Pakmor, Volker Springel, and Lars Hernquist. The THESAN project: ionizing escape fractions of reionization-era galaxies. *Monthly Notices of the RAS*, 520(2):2757–2780, April 2023.

[846] S. Yokoyama and T. Matsubara. Scale-dependent bias with higher order primordial non-Gaussianity: Use of the Integrated Perturbation Theory. *ArXiv e-prints*, October 2012.

[847] J. Yoo. General relativistic description of the observed galaxy power spectrum: Do we understand what we measure? *Physical Review D.*, 82(8):083508, October 2010.

[848] J. Yoo, A. L. Fitzpatrick, and M. Zaldarriaga. New perspective on galaxy clustering as a cosmological probe: General relativistic effects. *Physical Review D.*, 80(8):083514, October 2009.

[849] L. Y. Aaron Yung, Rachel S. Somerville, Steven L. Finkelstein, Gergö Popping, and Romeel Davé. Semi-analytic forecasts for JWST - I. UV luminosity functions at z = 4-10. *Monthly Notices of the RAS*, 483(3):2983–3006, March 2019.

[850] L. Y. Aaron Yung, Rachel S. Somerville, Steven L. Finkelstein, Gergö Popping, Romeel Davé, Aparna Venkatesan, Peter Behroozi, and Harry C. Ferguson. Semi-analytic forecasts for JWST - IV. Implications for cosmic reionization and LyC escape fraction. *Monthly Notices of the RAS*, 496(4):4574–4592, August 2020.

[851] O. Zahn, A. Lidz, M. McQuinn, S. Dutta, L. Hernquist, M. Zaldarriaga, and S. R. Furlanetto. Simulations and Analytic Calculations of Bubble Growth during Hydrogen Reionization. *Astrophysical Journal*, 654:12–26, January 2007.

[852] O. Zahn, A. Mesinger, M. McQuinn, H. Trac, R. Cen, and L. E. Hernquist. Comparison of reionization models: radiative transfer simulations and approximate, seminumeric models. *Monthly Notices of the RAS*, 414:727–738, June 2011.

[853] O. Zahn, C. L. Reichardt, L. Shaw, A. Lidz, K. A. Aird, B. A. Benson, L. E. Bleem, J. E. Carlstrom, C. L. Chang, H. M. Cho, T. M. Crawford, A. T. Crites, T. de Haan, M. A. Dobbs, O. Doré, J. Dudley, E. M. George, N. W. Halverson, G. P. Holder, W. L. Holzapfel, S. Hoover, Z. Hou, J. D. Hrubes, M. Joy, R. Keisler, L. Knox, A. T. Lee, E. M. Leitch, M. Lueker, D. Luong-Van, J. J. McMahon, J. Mehl, S. S. Meyer,

M. Millea, J. J. Mohr, T. E. Montroy, T. Natoli, S. Padin, T. Plagge, C. Pryke, J. E. Ruhl, K. K. Schaffer, E. Shirokoff, H. G. Spieler, Z. Staniszewski, A. A. Stark, K. Story, A. van Engelen, K. Vanderlinde, J. D. Vieira, and R. Williamson. Cosmic Microwave Background Constraints on the Duration and Timing of Reionization from the South Pole Telescope. *Astrophysical Journal*, 756:65, September 2012.

[854] O. Zahn, M. Zaldarriaga, L. Hernquist, and M. McQuinn. The Influence of Nonuniform Reionization on the CMB. *Astrophysical Journal*, 630:657–666, September 2005.

[855] D. Zaritsky and A. H. Gonzalez. On the Incidence of Strong Gravitational Lensing by Clusters in the Las Campanas Distant Cluster Survey. *Astrophysical Journal*, 584:691–701, February 2003.

[856] A. R. Zentner. The Excursion Set Theory of Halo Mass Functions, Halo Clustering, and Halo Growth. *International Journal of Modern Physics D*, 16:763–815, 2007.

[857] J. Zhang and L. Hui. On Random Walks with a General Moving Barrier. *Astrophysical Journal*, 641:641–646, April 2006.

[858] J. Zhang, L. Hui, and Z. Haiman. A linear perturbation theory of inhomogeneous reionization. *Monthly Notices of the RAS*, 375:324–336, February 2007.

[859] Q.-J. Zhang, L.-M. Cheng, and Y.-L. Wu. Constraining Dark Energy From Splitting Angle Statistic of Strong Gravitational Lenses. *ArXiv e-prints*, August 2007.

[860] V. I. Zhdanov and G. Ivashchenko. Cosmological scalar fields that mimic the \$\Lambda CDM\$ cosmological model. *ArXiv e-prints*, June 2008.

[861] W. Zheng, L. D. Bradley, R. J. Bouwens, H. C. Ford, G. D. Illingworth, N. Benítez, T. Broadhurst, B. Frye, L. Infante, M. J. Jee, V. Motta, X. W. Shu, and A. Zitrin. Bright Strongly Lensed Galaxies at Redshift z $\sim$ 6-7 behind the Clusters Abell 1703 and CL0024+16. *Astrophysical Journal*, 697:1907–1917, June 2009.

[862] W. Zheng, M. Postman, A. Zitrin, J. Moustakas, X. Shu, S. Jouvel, O. Høst, A. Molino, and et. al. A magnified young galaxy from about 500 million years after the Big Bang. *Nature*, 489:406–408, September 2012.

[863] Zhen-Ya Zheng, Junxian Wang, James Rhoads, Leopoldo Infante, Sangeeta Malhotra, Weida Hu, Alistair R. Walker, Linhua Jiang, Chunyan Jiang, Pascale Hibon, Alicia Gonzalez, Xu Kong, XianZhong Zheng, Gaspar Galaz, and L. Felipe Barrientos. First Results from the Lyman Alpha Galaxies in the Epoch of Reionization (LAGER) Survey: Cosmological Reionization at z $\sim$ 7. *Astrophysical Journal*, 842(2):L22, June 2017.

[864] Zheng Zheng and Jordi Miralda-Escudé. Monte Carlo Simulation of Lyα Scattering and Application to Damped Lyα Systems. *Astrophysical Journal*, 578(1):33–42, October 2002.

[865] Yongda Zhu, George D. Becker, Sarah E. I. Bosman, Christopher Cain, Laura C. Keating, Fahad Nasir, Valentina D'Odorico, Eduardo Bañados, Fuyan Bian, Manuela Bischetti, James S. Bolton, Huanqing Chen, Anson D'Aloisio, Frederick B. Davies, Rebecca L. Davies, Anna-Christina Eilers, Xiaohui Fan, Prakash Gaikwad, Bradley Greig, Martin G. Haehnelt, Girish Kulkarni, Samuel Lai, Ewald Puchwein, Yuxiang Qin, Emma V. Ryan-Weber, Sindhu Satyavolu, Benedetta Spina, Fabian Walter, Feige Wang, Molly Wolfson, and Jinyi Yang. Damping wing-like features in the stacked Lyα forest: Potential neutral hydrogen islands at z ¡ 6. *Monthly Notices of the RAS*, June 2024.

[866] Yongda Zhu, George D. Becker, Sarah E. I. Bosman, Laura C. Keating, Holly M. Christenson, Eduardo Bañados, Fuyan Bian, Frederick B. Davies, Valentina D'Odorico, Anna-Christina Eilers, Xiaohui Fan, Martin G. Haehnelt, Girish Kulkarni, Andrea Pallottini, Yuxiang Qin, Feige Wang, and Jinyi Yang. Chasing the Tail of Cosmic Reionization with Dark Gap Statistics in the Lyα Forest over 5 ¡ z ¡ 6. *Astrophysical Journal*, 923(2):223, December 2021.

[867] Yongda Zhu, George D. Becker, Sarah E. I. Bosman, Laura C. Keating, Valentina D'Odorico, Rebecca L. Davies, Holly M. Christenson, Eduardo Bañados, Fuyan Bian, Manuela Bischetti, Huanqing Chen, Frederick B. Davies, Anna-Christina Eilers, Xiaohui Fan, Prakash Gaikwad, Bradley Greig, Martin G. Haehnelt, Girish Kulkarni, Samuel Lai, Andrea Pallottini, Yuxiang Qin, Emma V. Ryan-Weber, Fabian Walter, Feige Wang, and Jinyi Yang. Long Dark Gaps in the Lyβ Forest at z ¡ 6: Evidence of Ultra-late Reionization from XQR-30 Spectra. *Astrophysical Journal*, 932(2):76, June 2022.

[868] Yongda Zhu, George D. Becker, Holly M. Christenson, Anson D'Aloisio, Sarah E. I. Bosman, Tom Bakx, Valentina D'Odorico, Manuela Bischetti, Christopher Cain, Frederick B. Davies, Rebecca L. Davies, Anna-Christina Eilers, Xiaohui Fan, Prakash Gaikwad, Martin G. Haehnelt, Laura C. Keating, Girish Kulkarni, Samuel Lai, Hai-Xia Ma, Andrei Mesinger, Yuxiang Qin, Sindhu Satyavolu, Tsutomu T. Takeuchi, Hideki Umehata, and Jinyi Yang. Probing Ultra-late Reionization: Direct Measurements of the Mean Free Path over $5 < z < 6$. *arXiv e-prints*, page arXiv:2308.04614, August 2023.

[869] Adi Zitrin, Ivo Labbé, Sirio Belli, Rychard Bouwens, Richard S. Ellis, Guido Roberts-Borsani, Daniel P. Stark, Pascal A. Oesch, and Renske Smit. Lymanα Emission from a Luminous z = 8.68 Galaxy: Implications for Galaxies as Tracers of Cosmic Reionization. *Astrophysical Journal*, 810(1):L12, September 2015.

[870] Andrea Zonca, Leo Singer, Daniel Lenz, Martin Reinecke, Cyrille Rosset, Eric Hivon, and Krzysztof Gorski. healpy: equal area pixelization and spherical harmonics transforms for data on the sphere in python. *Journal of Open Source Software*, 4(35):1298, March 2019.